Impacts of interactions with soil organisms on the metabolome of ragwort (*Senecio jacobaea* L.)

Lynne Allison Robinson

A thesis submitted for the degree of Doctor of Philosophy

University of Sussex

September 2012

Abstract

Plants need to defend themselves against their natural enemies without compromising their interactions with beneficial organisms. Chemical mechanisms underpin many of these interactions and changes in plant metabolism are critical to both robust defences against antagonists and effective signals to mutualists. Further, such plant responses can be systemic, so mediating interactions between spatially separated organisms above and below ground. This thesis aimed to characterise the changes in the ragwort (*Senecio jacobaea* L.) metabolome caused by two different belowground organisms, an antagonistic herbivorous nematode (*Pratylenchus penetrans* (Cobb, 1917) Filipjev & Schuurmans Stekhoven, 1941) and a mutualist arbuscular mycorrhizal fungus (AMF) (*Glomus intraradices* Smith & Schenck). Initially, vegetative and reproductive stage ragwort plants were sampled in the field and the chemical composition of leaf and flower tissues was assessed using a metabolomic approach. Techniques for the identification of key ragwort secondary metabolites were trialled and results demonstrated that plants of different ages differed in their allocation of within plant defences such as flavanoids, pyrrolizidine alkaloids (PAs) and chlorogenic acids. Subsequent experiments with nematodes and AMF focussed on the analysis of leaf tissues from vegetative stage plants. Feeding by the nematode species *P. penetrans* resulted in increased concentrations of metabolites associated with plant defence, including the main class of ragwort defence compounds PAs. In contrast, colonisation of root material by AMF caused increases in the concentrations of metabolites associated with the maintenance of the beneficial interaction between plant and fungi, such as a number of apocarotenoids known as blumenols. The findings of both experimental studies detected unexpected and previously unreported changes in plant metabolism, highlighting the importance of an untargeted approach when examining the chemical ecology of plant interactions.

Declaration

I hereby declare that this thesis has not been submitted, either in the same or different form to this or any other University for a degree.

Signature:.....

Lynne Allison Robinson

September 2012

Acknowledgements

There are many people I would like to thank for their support, advice and help throughout my PhD. First, I would like to thank each of my supervisors Sue Hartley, Liz Hill and Adam Vanbergen for providing the essential expertise that underpinned the multidisciplinary approach required for this thesis. In addition, the help, support and encouragement provided by each of them throughout my PhD has been invaluable and very much appreciated.

The following people have provided assistance with field work and support in the laboratory - big thanks to you all: at CEH Edinburgh Fiona Grant, Chris Andrews and Niamh Britton all provided help collecting (vast) amounts of soil and extracting nematodes from it; Julia Horwood and all the members of Liz Hill's group for technical assistance and support in the laboratory; Raghad Al-Salhi and Ali Abdul-Sada for keeping the LC-MS machines in perfect working order when profiling, not to mention for answering my millions of, often very stupid, questions; Kate Storer and Angela Hodge for invaluable advice in all things AMF; and finally to Stefan Reidinger and Naomi Ewald, Sue's post-docs, for advice and help throughout my PhD.

Thanks go to the (many) members of the 5B1 office at the University of Sussex: Eric Lucas, David Fisher Barham, Stephanie Murphy, Jonathan Green, Claudia Harflett, Rosie Foster, Eduardo Medina Bárcenas, Citlalli Mj, Mike Clease and Claire Sanderson who have all given advice, supported and listened to me throughout the various high and low points. Extra thanks go to Rosie Foster and Claudia Harflett for their fantanstic home baked goods, sympathetic ear and excellent tea making skills!

I would like to thanks my friends, who have been so supportive and understanding of absences and last minute plan cancellations throughout my studies. Special thanks go to Matthew Lidiard and Clare Matheson for reading through drafts. Last, but certainly not least, I would like to thank my family, without their emotional and financial support, especially while writing up, I would not have been able to complete this thesis.

Table of contents

List of figures and tables

Chapter 1

Chapter 2

Chapter 3

Chapter 4

Chapter 1. Introduction

Plants underpin a complex web of species interactions in most terrestrial ecosystems. Plants directly provide energy to herbivores and mutualists, above and below ground, with approximately 40% of photosynthetic carbon allocated to below-ground tissues (Jones *et al.* 2009). Changes in plant community structure, stability and diversity can have repercussions for biodiversity both above (Haddad *et al.* 2011) and below ground (Wardle 2006). Many organisms attempt to utilise the nutrient resource represented by plants. Mutualist species, such as arbuscular mycorrhizal fungi (AMF), provide plants with essential macronutrients (Hodge *et al.* 2001, Javot *et al.* 2007) in exchange for plant photosynthates (Bago *et al.* 2000). Plant antagonists, such as phytophagous insects, are harmful to plants. Despite being attacked by at least 400,000 phytophagous insect species (Mitter *et al.* 1991), it has been estimated that on average 80% of plant biomass remains untouched by herbivores (Cyr and Pace 1993). While plants face a massive challenge from herbivores, it is clear that they are able to influence the outcome of many interspecific interactions.

Plants employ a range of defences to lessen or avoid the costs of interactions with antagonists (Marquis 1984, Belsky 1986). Those defences can be physical defensive structures such as trichromes and thorns, which hinder herbivore movement or feeding (Levin 1973, Hanley *et al.* 2007). For example, experimental removal of *Acacia* thorns resulted in a three-fold increase in herbivore leaf removal, demonstrating their important role for defence (Milewski *et al.* 1991). Chemical defences can also be deployed. This involves the synthesis of metabolites that reduce the performance (e.g. survival, development, growth and reproduction) of antagonists (van Dam and Vrieling 1994, Wittstock and Gershenzon 2002, Schaffner *et al.* 2003, Quintero and Bowers 2012). Metabolites produced by plants as a chemical defence have two modes of action. First, metabolite defences can indirectly protect a plant by attracting natural enemies, such as predators and parasitoids, to kill the attacking herbivore (Palmer *et al.* 2008, Yamawo *et al.* 2012). Through the production of extrafloral nectaries and pearl bodies, *Mallotus japonicus* Muell. Arg. attracts ant species that defend plant tissues against herbivory by lepidopteran larvae (Yamawo *et al.* 2012). Secondly, metabolite defences can directly affect antagonist performance via changes in plant nutritional quality or the production of toxic metabolites (Buskov *et al.* 2002, Macel *et al.* 2005, Arany *et al.* 2008). For example, the presence of alkaloids (Macel *et al.* 2005), flavonoids (Chen *et al.* 2004), glucosinolates (Arany *et al.* 2008) and chlorogenic acid (Leiss *et al.* 2009b) within plant tissues all have anti-herbivore properties. These defence mechanisms can be categorised as either induced (where the

defence is produced as a result of herbivory) or constitutive (where the defence is produced continuously).

1.1. Constitutive defensive traits that influence plant interactions

The constitutive production of defences is a relatively common and perhaps effective mechanism by which plants can influence interactions with an antagonistic organism. The precise nature of constitutive defence varies between plant species. For example, glucosinolates are plant-synthesised metabolites that serve as a chemical defence, protecting tissues against antagonistic organisms (Fahey *et al.* 2001, Buskov *et al.* 2002, Arany *et al.* 2008). Glucosinolates are, however, limited to a number of plant families, including the Brassicaceae (Halkier and Gershenzon 2006). Understanding the ecological and evolutionary processes driving such variation requires a fuller characterisation of patterns of defence from species to individual plant level. This remains a fundamental and challenging research area (Johnson 2011). A number of frameworks have been proposed to describe the allocation of resources to plant defence, both between species and within plant populations (Stamp 2003). These frameworks all recognise that plants do not have an infinite amount of available resources, and therefore should allocate resources according to a trade-off between costs and benefits in a dynamic environment.

Two frameworks used to explain between-species variations in plant constitutive defences are the Apparency Theory and the Growth Rate Hypothesis. Apparency Theory predicts that between-species variation in defences is a product of the likelihood that they will encounter herbivores (Feeny 1976, Rhodes and Cates 1976). Consequently, plant species that are long-lived, and hence apparent over time, would be expected to invest in defences because of a greater risk of herbivory (Feeny 1976, Rhodes and Cates 1976). Alternatively, the Growth Rate Hypothesis (GRH) suggests that between-species variation in defence is a result of differences in inherent growth rate (Coley *et al.* 1985). These authors hypothesise that the magnitude of the costs of damage due to herbivory, and the benefit of defence production, depends on the inherent growth rate of a plant (Coley *et al.* 1985). A recent meta-analysis found that between-species variations in growth rate better explained observed herbivory patterns than differences in plant apparency, leading to the conclusion that the GRH fitted the current evidence (Endara and Coley 2011).

Additional variation in constitutive plant defences exists between individual plants of the same species (e.g. de Boer 1999, Lambdon *et al.* 2003, Nuringtyas *et al.* 2012). Such variation within plant populations are perhaps at a spatial scale more relevant to many plant antagonists (Nuringtyas *et al.* 2012). A recent meta-analysis has identified Optimal Defence Theory (ODT) as a useful framework to examine the within-plant allocation to the production of defences (McCall and Fordyce 2010). The optimal distribution of defences will depend on the cost versus benefit of defending a particular tissue from herbivory (McKey 1974). This evolved trade-off required balancing the risk of herbivory, the costs of diverting metabolic resources away from essential physiology and towards defence, and the evolutionary value of a particular tissue (McKey 1974). Firstly, defences should be allocated in proportion to the risk of herbivory to a particular plant tissue (McKey 1974). Within wild parsnip plants (*Pastinaca sativa* L.), furanocoumarin defences are allocated in higher concentrations to flowers than leaves (Zangerl and Rutledge 1996). This variable allocation to within-plant parsnip defence is a reflection of the higher probability of flowers being attacked by herbivores (Zangerl and Rutledge 1996). Secondly, McKey (1974) theorised that the production, transport and storage of defences is costly, a prediction that has been corroborated by many empirical studies (reviewed by Koricheva 2002). Finally, it has been demonstrated that younger leaves have a higher photosynthetic potential than older leaves (Zangerl 1986). Therefore, ODT predicts that those younger tissues that contribute greatly to plant fitness should be the best protected (McKey 1974), a prediction supported by the current empirical evidence (reviewed by McCall and Fordyce 2010).

In contrast to affecting plant interactions with antagonists, constitutive defences can have a positive role in interactions with mutualist species. Plant metabolites associated with defence are present in nectar (Stephenson 1982, Adler 2000, Adler and Irwin 2012) and pollen (Boppre *et al.* 2005, Praz *et al.* 2008). The presence of defensive compounds in reproductive structures may have a number of functions (reviewed by Adler 2000). It has been suggested that the presence of toxic plant metabolites in pollen maintains the relationship between plants and pollinators (Rhoades and Bergdahl 1981). Indeed, the survival of specialist bee species is higher when reared on the pollen of their host (Praz *et al.* 2008). Defensive metabolites in nectar can also play a role in the outcome of plant and mutualist interactions. The presence of defensive metabolites in nectar has been shown to prevent nectar robbing by species that do not provide a pollinator function (Janzen 1977, Irwin *et al.* 2010). For example, toxic iridoid glycoside in the nectar of *Catalpa speciosa* (Warder ex Barney) Engel. protect the plant against nectar theft by ant species and lepidopteran larvae (*Poanes hobomok* (Harris, 1862))

(Stephenson 1982). In addition, the same defensive secondary metabolites have a role in the interaction with *Ceratomia catalpae*, a moth species that is one of the primary pollinators of *C. speciosa* (Langenheim 1994). The larval stages of *C. catalpae* are specialist herbivores of *C. speciosa* that sequester iridoid glycosides and use them for its own defence against predators (Bowers and Puttick 1986). This example demonstrates that constitutive defences can have complex beneficial effects on plant-mutualist interactions. Chemical defences may, however, also have adverse effects on mutualist interactions. The pollen of some plant species, and the defensive metabolites they contain, have been demonstrated to deter feeding by honey bee pollinators (Reinhard *et al.* 2009). Moreover, increased constitutive alkaloid defences in the nectar of *Gelsemium sempervirens* (L.) J. St.-Hil. reduced seed weight and an insect-vectored pollen donation (Adler and Irwin 2012). Clearly, constitutive production of defences does not always affect plant fitness positively. The complexity of ecological interactions may have favoured the evolution of induced chemical defences initiated by interactions with both mutualist and antagonistic organisms (Agrawal and Karban 1999).

1.2. Induced plant traits that influence plant interactions

Like constitutive defences, induced plant responses to interspecific interactions can involve the synthesis of physical (Milewski *et al.* 1991, Young *et al.* 2003) or metabolite (Karban and Myers 1989, van Dam *et al.* 1993, van Dam *et al.* 2000, Quintero and Bowers 2011) defences. Again, metabolite defences can have direct (Anderson and Agrell 2005, Kaplan *et al.* 2008, Gutbrodt *et al.* 2011) or indirect (Kessler and Baldwin 2001, Dicke *et al.* 2003, Ohgushi 2005, Gols *et al.* 2012) modes of action. The principal benefit of induced versus constitutive defence is that the costs to the plant are reduced because defences are only synthesised in response to the onset of an interspecific interaction (McKey 1974, Feeny 1976). Such tailoring of chemical induction to the identity of the other organism makes plant responses more effective (Adler and Karban 1994) and avoids the negative effects on mutualist species that can occur with constitutive defence (Agrawal and Karban 1999).

Effective induced defences are dependent on the ability of plants to recognise different organisms. Plants are able to recognise the specific challenges posed by different herbivore species, responding differently depending on the mode of herbivore feeding (Walling 2000) and degree of herbivore specialism (Ali and Agrawal 2012). It has been shown that herbivore oral secretions contain signals that elicit induced plant responses to herbivory (Bede *et al.*

2006, Delphia *et al.* 2006). There are a number of signals present in the oral secretions of different lepidopteran larvae that elicit plant responses including the production of fatty acid conjugates (Alborn *et al.* 1997), β-glucosidase (Mattiacci *et al.* 1995) and inceptins (Schmelz *et al.* 2006). The molecular mechanisms underpinning plant detection of these chemical signals remain unclear (e.g. fatty acid conjugates Wu and Baldwin 2010). The signals in oral secretions result in changes in both direct (Kahl *et al.* 2000, Schafer *et al.* 2011) and indirect (Mattiacci *et al.* 1995, Alborn *et al.* 1997, Delphia *et al.* 2006) defences. For instance, a well understood tri-trophic interaction is between corn plants (*Zea mays* L.), beet armyworm (*Spodoptera exigua* Hübner, 1808) caterpillars and the parasitoid species (*Cotesia marginiventris* Cresson). The fatty acid conjugate volicitin is present in the oral secretions of the beet armyworm (Alborn *et al.* 1997) and it induces the production of volatile metabolites by corn (Turlings *et al.* 1993). This change in the volatile profile of corn attracts *C. marginiventris* females which parasitizes the armyworms. This provides an induced, indirect benefit to the plant (Turlings *et al.* 1990).

In addition to herbivory, plants are also able to detect insect oviposition (Hilker and Meiners 2006). Plants can detect metabolites present either on the surface of herbivore eggs or the cement attaching it to the leaf (Hilker and Meiners 2006). Consequently, herbivore oviposition can, like herbivory, induce host-plant volatile emissions that attract parasitoid species (Meiners and Hilker 1997, Colazza *et al.* 2004, Hilker *et al.* 2005). Insect oviposition also induces a number of plant direct defences. Oviposition by the tomato fruitworm moth (*Helicoverpa zea* Boddie) on tomato plants (*Solanum lycopersicum* L.) result in changes in gene regulation that lead to increased concentrations of defensive metabolites which deter larval feeding (Kim *et al.* 2012). Plant direct defences in response to insect oviposition can also be physical (Shapiro and DeVay 1987, Doss *et al.* 2000). In response to pea weevil (*Bruchus pisorum* L.) oviposition, pea plants (*Pisum sativum* L.) create tumour-like growths beneath the egg that prevent larvae penetrating pea pods and damaging seeds (Doss *et al.* 2000). The insect metabolites responsible for this reaction are bruchins, mono- and bis 3-(hydroxypropanoyl) esters of long chain, unsaturated diols (Oliver *et al.* 2000). As yet, bruchins are the only group of insect metabolites that have been identified to induce such plant responses (Wu and Baldwin 2010).

Induced responses also influence the interactions between plants and mutualists. Indeed, induced responses that indirectly defend plants by attracting predators or parasitoids of herbivores are indirect mutualisms (Alborn *et al.* 1997, Meiners and Hilker 1997, Colazza *et al.* 2004, Delphia *et al.* 2006). Induced plant responses have been shown to have a role in the interactions between plants, AMF species (Strack *et al.* 2003) and mutualistic endophytic fungi

(Clay *et al.* 1993). Induced plant responses are sophisticated and allow plants to tailor their response based on the identity of the antagonist or mutualist. It should be noted that the evolution of constitutive defences does not prohibit the concomitant evolution of induced defences, indeed many plant species possess both modes of defence (e.g. van Dam *et al.* 1993, Kahl *et al.* 2000, Hol *et al.* 2004, Moreira *et al.* 2012).

1.3. Plant interactions with below-ground organisms

Plants represent a significant source of carbon in below-ground systems (Jones *et al.* 2009), and, as a result, interact with a range of below-ground herbivores and mutualists (van Dam 2009). An understanding of below-ground interactions is important because almost all plants have soil dwelling roots that will interact with the wider soil biota. Such below-ground interactions can have significant repercussions for above-ground interactions via changes in the shared plant host (discussed below in Section 1.4). Below-ground tissues are just as well defended as those above ground yet, compared to above ground situations, below-ground interactions are not well understood (Rasmann and Agrawal 2008, van Dam 2009). Technical limitations contribute to this lack of knowledge, for example, root defences are not measurable without destructive harvests. New technologies are beginning to provide novel insights, for instance, into root morphological changes caused by herbivory (Jahnke *et al.* 2009, Clark *et al.* 2011).

Like above-ground systems, both constitutive (Kaplan *et al.* 2008, Kabouw *et al.* 2010) and induced (Schmelz *et al.* 1999, van Dam *et al.* 2003b, Hol *et al.* 2004) defences occur below ground. Root defences can be physical (Care *et al.* 2000, Johnson *et al.* 2010) or via secondary metabolites with direct (Potter *et al.* 1999, Soriano *et al.* 2004) or indirect (van Tol *et al.* 2001, Aratchige *et al.* 2004, Rasmann *et al.* 2011) effects on other organisms. Physical defences of plant roots are considered in a limited number of studies. Root herbivory can increase root tissue density, a phenomenon that could be caused by the synthesis of physical root defences (Care *et al.* 2000). In addition, increased root toughness has been demonstrated to reduce herbivore feeding implying a defensive function (Johnson *et al.* 2010). Considered together these studies suggest a role for physical defences in the protection of root tissue, but further work to improve understanding is required.

Metabolite root defences are far better understood than physical defences. Root tissues have been shown to contain the same constitutive and induced defences as above-ground tissues.

Constitutive defences in roots include alkaloids in both *Senecio jacobaea* L. and *Nicotiana tabacum* L. (Hol *et al.* 2004, Kaplan *et al.* 2008), and glucosinolates in *Brassica* species (van Dam *et al.* 2003b, Kabouw *et al.* 2010). Increased concentrations of 2-phenylethyl glucosinolate are related to constitutive resistance to migratory endoparasitic nematodes (Potter *et al.* 1999). In addition, changes in the concentration of root alkaloids (Hol *et al.* 2004), glucosinolates (van Dam *et al.* 2003b) and phytoecdysteroids (Schmelz *et al.* 1999) are all induced by below-ground herbivory. For example, phytoecdysteroids are plant-derived mimics of ecdysteroid hormones that regulate growth and development in many arthropods (Dinan 2009). Many different plant species produce photoecdysteroids (Dinan 1995), and one of the best studied is 20-hydroxyecdysone found in spinach (*Spinacia oleracea* L.). Induction of 20-hydroxyecdysone in spinach roots following herbivory below ground (Schmelz *et al.* 1999) induces abnormal juvenile moulting of nematodes (Soriano *et al.* 2004). Therefore, increased concentrations of 20-hydroxyecdysone as a result of insect feeding thus provides a defensive function in spinach via reduced root damage (Schmelz *et al.* 2002).

The metabolites present in the exudates and volatiles released by roots also influence the below-ground interactions between plants and antagonists (Bais *et al.* 2006, Wenke *et al.* 2010, Hiltpold and Turlings 2012, Johnson and Nielsen 2012). It has been demonstrated that root exudates can have negative effects on microbial species (Bais *et al.* 2005). Root exudates have also been shown to contain metabolites that mimic bacterial signals (Teplitski *et al.* 2000) to affect bacterial cell-to-cell communication and quorum sensing (density dependant regulation of bacterial behaviour) (Givskov *et al.* 1996). As in above-ground tissues, volatiles emitted by roots play an important role in recruiting beneficial species that provide indirect defences against antagonists. Volatiles produced by plants following root herbivory attract natural enemies of below-ground herbivores (Aratchige *et al.* 2004, Rasmann *et al.* 2005, Ali *et al.* 2010, Rasmann *et al.* 2011).

Compared to root herbivore interactions, the chemical relationships between roots and mutualist organisms are far better understood (Perret *et al.* 2000, Akiyama *et al.* 2005, Horiuchi *et al.* 2005, Walter *et al.* 2010). The interactions between nitrogen-fixing bacterial species of the genus *Rhizobia* and leguminous species of plant are initiated by the presence in root exudates of species-specific metabolites known collectively as flavonoids (Kosslak *et al.* 1987, Caetano-Anollés *et al.* 1988, Pandya *et al.* 1999). These flavonoids differentially activate *nod* genes depending on the bacterial strain present (Kosslak *et al.* 1990). The activation of *nod* genes by the appropriate flavonoids induces the production of lipochitooligosaccharides called Nod factors, the structures of which are specific to different bacterial strains (Perret *et*

al. 2000). The Nod factors produced set in motion a complex set of events that result in root curling and the successful colonisation of roots by rhizobia (Perret *et al.* 2000, Riely *et al.* 2004). Furthermore, the plant-derived volatile metabolite dimethyl sulfide attracts the bacteriophagous nematode species *Caenorhabditis elegans* (Maupas, 1990) that transfers rhizobia on their skin and in their faeces, thereby mediating the rhizobia-legume interaction (Horiuchi *et al.* 2005). Plant-derived metabolites are also involved in at least two steps of the dialogue between plants and AMF. Firstly, plant-derived hormones (strigolactones) in root exudates stimulate AMF growth and increase the chance of establishing a connection with the plant host (Akiyama *et al.* 2005). Secondly, it is thought that the increased concentrations of C_{13} cyclohexenones associated with AMF colonisation (Peipp *et al.* 1997, Schliemann *et al.* 2006) are a mechanism by which the mutualism is maintained (Fester *et al.* 2002). All of these examples of below-ground interactions are complex, and, in the case of rhizobial interactions species-specific, demonstrating that plant reactions to below-ground interactions are just as sophisticated as those above ground.

1.4. Plant-mediated interactions between above- and below-ground ecosystems

While biologically important in their own right, below-ground interactions should not be considered in isolation, because plants provide an interface between above- and below-ground ecosystem components (van der Putten *et al.* 2001, Hol *et al.* 2004, Wardle *et al.* 2004, de Deyn and van der Putten 2005, van Dam and Heil 2011). Interactions between spatially separated herbivores have the potential to cascade in multiple directions. While many studies have demonstrated that below-ground organisms affect herbivores above ground (Gange and Brown 1989, Masters *et al.* 2001, Wackers and Bezemer 2003, Bezemer *et al.* 2005, Soler *et al.* 2005) fewer have studied above-ground to below-ground cascades (Bardgett *et al.* 1998, Wardle *et al.* 2005, Soler *et al.* 2007a). This relative dearth of information is probably due to the practical challenges associated with measuring the preferences and performance of below-ground organisms. Nonetheless, plants do mediate interactions between above- and below-ground systems. This has been shown between insect herbivore species (Gange and Brown 1989, Masters and Brown 1992, Soler *et al.* 2005) and between above-ground insect herbivores and AMF (Hartley and Gange 2009, Koricheva *et al.* 2009), nematodes (Bezemer *et al.* 2005, van Dam *et al.* 2005, Wurst and van der Putten 2007) and microbes (Wardle *et al.* 2005).

Masters *et al.* (1993) proposed a conceptual model enshrining the Stress Response Hypothesis to explain the interactions between above- and below-ground systems. This model suggested that because root herbivory leads to a decrease in the number of fine roots, a negative effect on water and nutrient uptake would be expected (Masters *et al.* 1993). The reduction in water and nutrient availability results in a plant stress response, leading to the accumulation of amino acids and carbohydrates in shoots (Masters *et al.* 1993). This increase in the availability of foliar nutrients due to below-ground stress would, it is predicted, increase above-ground herbivore performance, especially phloem feeders. The model also predicts that above-ground herbivores will cause a limitation in root growth with negative repercussions for root herbivores (Masters *et al.* 1993).

An alternative mechanism that has been suggested to underpin the interactions between above- and below-ground systems is the Induced Defence Hypothesis (Bezemer *et al.* 2003, van Dam *et al.* 2003a). This states that herbivory in one part of a plant system will induce a defence response that will be echoed in, or at the expense of, defences in other parts of the system (Bezemer *et al.* 2003, van Dam *et al.* 2003a). The Induced Defence Hypothesis thus predicts that below-ground feeding by herbivores can have a negative effect on above-ground herbivores (Bezemer *et al.* 2003, van Dam *et al.* 2003a). Support has been found for both the Stress Response (Gange and Brown 1989, Moran and Whitham 1990, Masters 1995) and the Induced Defence (Bezemer and van Dam 2005, van Dam *et al.* 2005, Kaplan *et al.* 2008) hypotheses. In addition, some studies have found that changes in both primary and secondary metabolism influence the performance of above- and below-ground interactions (Bezemer *et al.* 2005, Soler *et al.* 2005), demonstrating that both hypotheses have a role in influencing interactions between above-ground and below-ground ecosystems.

Most studies of above- and below-ground interactions consider relatively simple combinations of organisms at one trophic level. It has, however, been demonstrated that above- and below-ground interactions have repercussions at higher trophic levels (Soler *et al.* 2012). One of the best understood examples of this is provided by a series of experiments examining the above- and below-ground multi-trophic interactions centred on black mustard plants (*Brassica nigra* L.). The butterfly *Pieris brassicae* L. and the parasitoid species *Cotesia glomerata* L. avoid *B. nigra* plants that have been fed on below-ground by larvae of the fly *Delia radicum* L. (Soler *et al.* 2007c). Decreased performance of the hyperparasitoid species *Lysibia nana* Gravenhorst is also observed as a result of below-ground herbivory (Soler *et al.* 2005), demonstrating that fly root herbivory significantly affects performance of above-ground insects over three trophic levels. By performing reciprocal experiments with the same study system, the presence of

above-ground herbivores was found to more than half the survival of the root herbivore (Soler *et al.* 2007a). This effect was reflected by a concomitant decrease in the survival of the parasitoid species *Trybliographa rapae* (Westwood) that utilises *D. radicum* as a host (Soler *et al.* 2007a). Examination of above- and below-ground interactions using this system has demonstrated that higher trophic levels above (Soler *et al.* 2005) and below (Soler *et al.* 2007a) ground can be affected by herbivory in different regions of the shared host plant. Therefore, the outcomes of plant-mediated above- and below-ground interactions have implications for the structure of communities both above and below ground (van der Putten *et al.* 2001, Wardle *et al.* 2004).

1.5. Ragwort (*Senecio jacobaea* L.) as a study system

Ragwort (*Senecio jacobaea* L.) is a biennial plant native to the British Isles. It is a pioneer species, thriving in highly disturbed environments with low concentrations of plant available nitrogen (Suter *et al.* 2007). Typically, plants form a low-lying rosette during the first year of growth. A period of winter vernalisation (although not essential) increases the chances of bolting and flowering the following year. Ragwort effectively negates the detrimental effect of defoliation on plant biomass via the mechanism of compensatory growth (van der Meijden *et al.* 1988, van der Meijden *et al.* 2000), and, if damaged, can persist in a vegetative stage for a number of years (Harper and Wood 1957). Compensatory regrowth can, however, have negative repercussions for reproduction depending on the severity of damage experienced (Islam and Crawley 1983).

Ragwort is distributed throughout the British Isles and has established in many temperate regions worldwide (Cameron 1935, Roberts and Pullin 2007). Different morphological adaptations in ragwort ray and disc achenes (McEvoy 1984) allow short and long distance seed dispersal for successful colonisation of, and persistence in, environments (Wardle 1987). Agricultural intensification has increased the likelihood of ragwort occurrence through more frequent soil disturbance (McEvoy *et al.* 1993, Suter *et al.* 2007). The occurrence of ragwort in agricultural landscapes is a problem because of its toxicity to humans (World Health Organisation 1988), avian species (Cheeke and Pierson-Goeger 1983), cows (Johnson 1978, Johnson and Smart 1983), horses (Mendel *et al.* 1988), bees (Reinhard *et al.* 2009) and soil microbes (Hol and van Veen 2002, Kowalchuk *et al.* 2006, Joosten and van Veen 2011). It is also toxic to generalist above-ground insect herbivores (Macel *et al.* 2005, Narberhaus *et al.*

2005) and herbivorous nematodes (Thoden *et al.* 2009a). Due to its noxious effect, ragwort is listed as a specified weed in the United Kingdom under the 1959 Weeds Act (Anon 2004). The Ragwort Control Act 2003 provides a guideline for the control of ragwort and failure of a landowner to adhere to this legislation can lead to legal proceedings (Anon 2004). According to the 1959 Weeds Act, a landowner must take management actions when ragwort occurs within 100 metres of land used for the grazing of animals or the production of forage (Anon 2004); the plants remain toxic after the drying process (Candrian *et al.* 1984). As a result, the focus of much scientific literature has been to determine successful practices for the control of ragwort (reviewed by Roberts and Pullin 2007, Leiss 2011).

The toxicity of ragwort and other *Senecio* species is caused by pyrrolizidine alkaloids (PAs), a group of nitrogen-containing plant secondary metabolites. Each PA can be found in two forms, the reduced parent PA and the oxidised PA N-oxide (Figure 1.1.) (Joosten *et al.* 2011). A total of 17 retrorsine type PAs have been recorded in ragwort (Figure 1.2.) (Macel *et al.* 2004, Joosten *et al.* 2010, Kostenko *et al.* 2012). In *Senecio* species, PAs are synthesised exclusively in root tissues (Hartmann *et al.* 1989) as senecionine N-oxide (Hartmann and Toppel 1987, Toppel *et al.* 1987). After synthesis, senecionine N-oxide is transferred in the phloem (Hartmann *et al.* 1989) to their site of diversification (root or shoot), where they are transformed into the species-specific profile observed across the *Senecio* genus (Hartmann and Dierich 1998).

a) b)

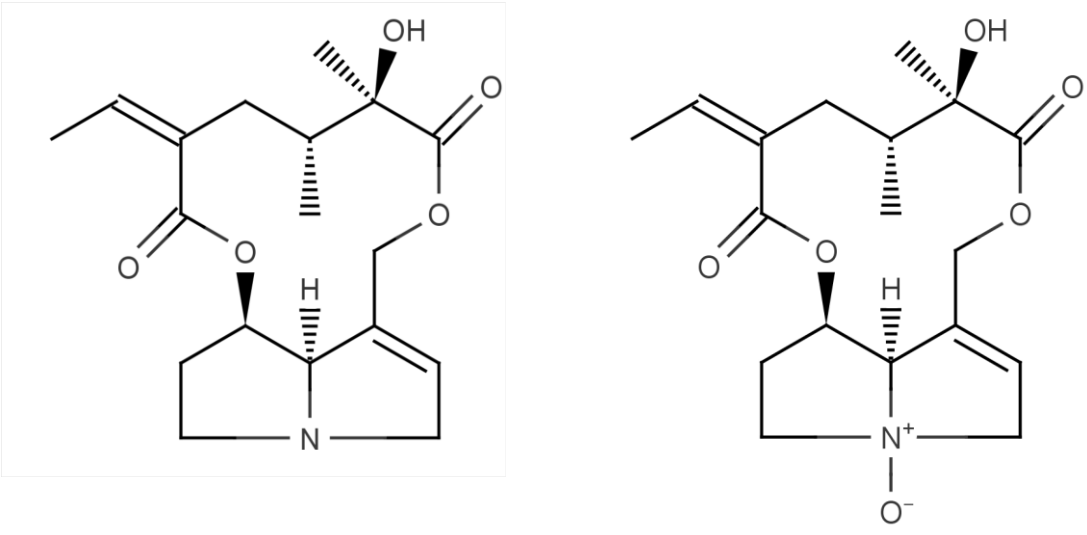

Figure 1.1. The pyrrolizidine alkaloid senecionine in its a) parent and b) N-oxide forms.

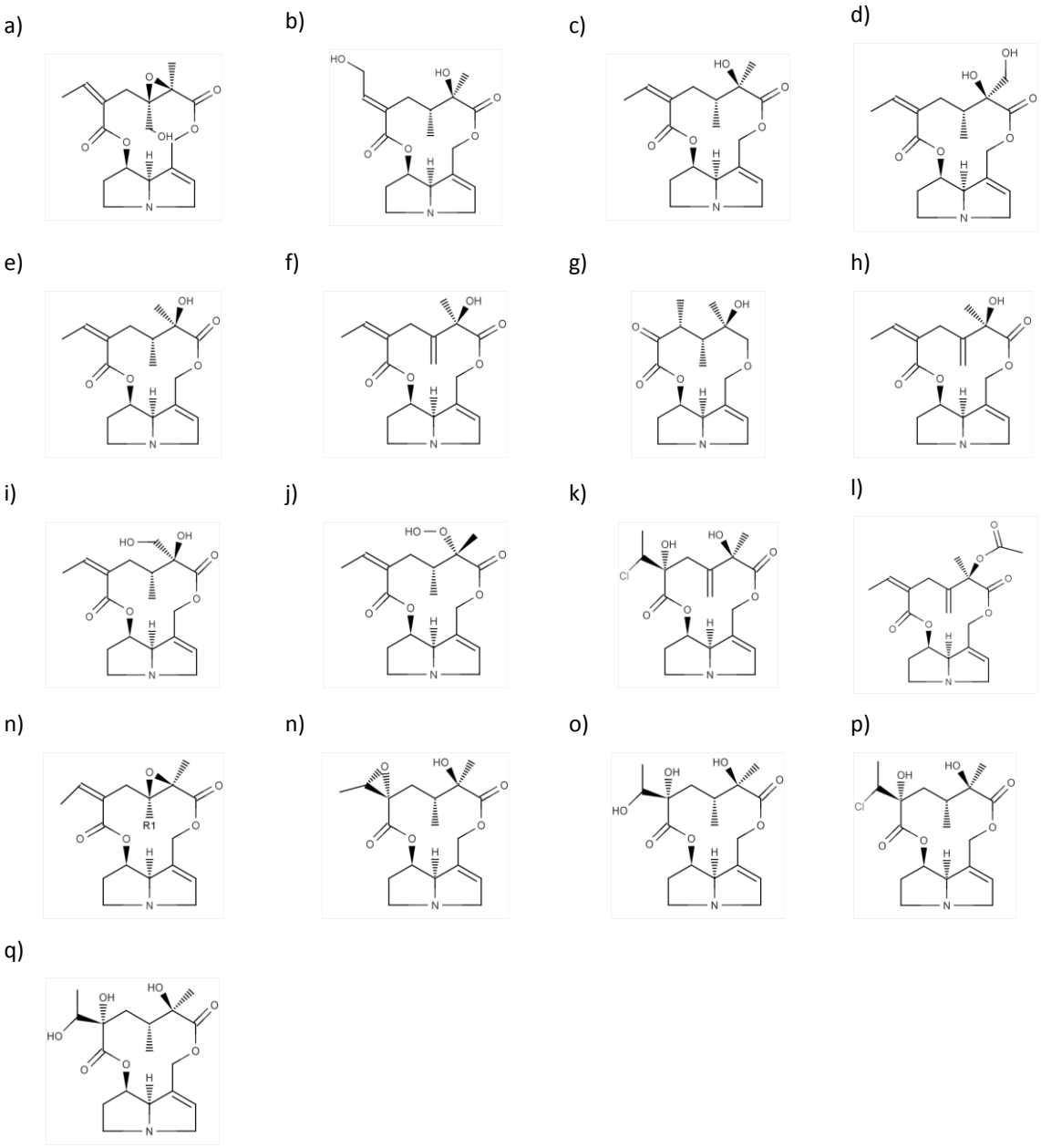

Figure 1.2. The parent pyrrolizidine alkaloids (PAs) recorded in ragwort: a) erucifoline, b) eruciflorine, c) integerrimine, d) retrorsine, e) senecionine, f) seneciphylline, g) senecivernine, h) spartioidine, i) riddelline, j) ursaramine, k) dehydrojaconine, l) acetylseneciphylline, m) acetylerucifoline, R1=CH_2OAc, n) jacobine, o) jacoline, p) jaconine and q) jacozine (Macel *et al.* 2004, Joosten *et al.* 2010, Kostenko *et al.* 2012).

PAs are a constitutive defence present on the surface of, and within, ragwort tissues (Vrieling and Derridj 2003). No developmental stage of ragwort is left undefended by PAs (Schaffner *et al.* 2003). Differences in PA species-specific profile are found between clonal and half-sib plants but variation is greater between half-sibs, demonstrating that the species-specific profile of PAs found within a plant has a strong genetic element (Macel *et al.* 2004). Indeed, Vrieling *et al.* (1993) estimated that that genetic differences between individual ragwort plants accounted for almost half of the variation in PAs. The proportion of parent PA versus N-oxides observed in a plant is also genetically controlled (Joosten *et al.* 2011). An investigation of the PA composition of flowering plants sourced from over 100 ragwort populations across Europe led Witte *et al.* (1992) to propose that two chemotypes can be defined. The first 'jacobine chemotype' was characterised by high levels of jacobine, jacoline, jaconine and jacozine, but no erucifoline. The 'erucifoline chemotype' typically contained high levels of erucifoline and acetylerucifoline, and low or undetectable levels of PAs indicative of the 'jacobine chemotype. Macel *et al.* (2004) analysed the PA composition of vegetative ragwort plants sourced from ten different European populations, and suggested two additional ragwort chemotypes. Those plants that contained both 'jacobine chemotype' and 'erucifoline chemotype' PAs in equal amounts were described as 'mixed chemotypes', while those with trace amounts of 'jacobine chemotype' and 'erucifoline chemotype' PAs were termed 'senecionine chemotypes'.

Diurnal (van Dam *et al.* 1993) and seasonal (Johnson *et al.* 1985) variations in PA concentrations have also been observed. Moreover, additional variation in PA concentration and composition can be caused by different abiotic environmental conditions. Increased nutrient availability results in decreased concentrations of foliar PAs in ragwort (Hol *et al.* 2003, Hol 2011). This phenomenon was hypothesised to be caused by the inability to increase the production of defences at a rate proportional to the increase in biomass observed following fertilisation (Koricheva 1999). Furthermore, increased nutrient availability shifts relative PA composition: while concentrations of other PAs decrease, the levels of jacobine remain constant regardless of nutrient availability (Hol *et al.* 2003, Macel and Klinkhamer 2010). Although the effect of soil type on PA concentrations is small, it has been demonstrated to affect PA composition of both above- and below-ground ragwort tissues (Joosten *et al.* 2009). Constitutive levels of PAs can also be influenced by biotic interactions. Vrieling *et al.* (1991) demonstrated that variations in PA concentrations could be maintained by the multi-trophic interactions between ragwort, aphids (*Aphis jacobaeae* Schrank), various ant species and cinnabar moths (*Tyria jacobaeae* L.). Ragwort plants with low PA concentrations are more likely to host an aphid-ant mutualism. The presence of ants defends

ragwort against defoliation by the cinnabar moth (Vrieling *et al.* 1991), thus providing a fitness benefit of reduced defence allocation, and so a potential mechanism for the maintenance of a low PA genotype (Vrieling *et al.* 1991).

Changes in PA concentrations and composition can be induced by artificial leaf damage (van Dam *et al.* 1993) and by interactions with biotic agents. For example, alterations to PA composition (increased proportion of erucifoline) in shoots were observed because of feeding by a generalist caterpillar (*Mammestra brassicae* L.) (Hol *et al.* 2004). No influences of shoot herbivores on above-ground PA concentrations were observed (Hol *et al.* 2004). In the same experiment, Hol *et al.* (2004) also demonstrated that below-ground artificial damage both increased root PA concentration and altered PA composition. Soil microorganisms have also been demonstrated to affect PA concentration and composition in roots (Joosten *et al.* 2009). An induced decrease in PA concentrations and alterations to PA composition were observed in roots as a result of above-ground feeding (Hol *et al.* 2004). Soil-borne microorganisms have been demonstrated to induce changes in the PA concentration and composition of shoot material (Joosten *et al.* 2009). Considered together, these studies identify variations in the PA profile of ragwort as a possible mechanism for reciprocal above- and below-ground interspecific interactions.

A wide range of generalist and specialist insect herbivores occur on natural populations of ragwort (Harrison and Thomas 1991, Kunin 1999, Bezemer *et al.* 2006). While PAs detrimentally affect generalist herbivores (Narberhaus *et al.* 2005), they do not have the same effect on specialist herbivores. The best understood ragwort-herbivore interactions are with the cinnabar moth (*T. jacobaeae*, Arctiidae), which utilises PA containing *Senecio* species as a larval food plant (Dempster 1982), and the ragwort flea beetle (*Longitarsus jacobaeae* Waterhouse), a chrysomelid beetle that feeds on ragwort in both adult and larval life-stages. Cinnabar moth larvae are obvious on the host plant due to their bright yellow and black aposematic colouration. At all stages of development (van Zoelen and van der Meijden 1991), cinnabar moths contain alkaloids in their body tissues (Aplin *et al.* 1968) called callimorphines (Edgar *et al.* 1980); these are synthesised using PAs sequestered from their host (Beuerle *et al.* 2007). Many aspects of the interaction between ragwort and the cinnabar moth have been studied: the population dynamics of both the plant and insect (Myers 1980, Crawley and Gillman 1989, Bonsall *et al.* 2003), plant chemistry effects on larvae (Crawley and Nachapong 1984, van der Meijden *et al.* 1984, Wilcox and Crawley 1988, Macel *et al.* 2002) and adult oviposition (Wilcox and Crawley 1988, van der Meijden *et al.* 1989, Vrieling and de Boer 1999, Macel and Vrieling 2003). Ragwort flea beetles also sequester plant PAs, and to a lesser

degree, alter their structure (Dobler *et al.* 2000) for defensive purposes (Narberhaus *et al.* 2003). Those studies that consider ragwort flea beetle-ragwort interactions investigate their ecology (Windig 1991) with a view to using them as a bio-control agent for invasive ragwort populations (Windig 1993). The effect of specialist insect herbivory on PA concentration or composition in ragwort has never been examined. Artificial damage of approximately half of the leaf area of ragwort resulted in decreased PA concentrations (van Dam *et al.* 1993). Total defoliation of ragwort by cinnabar moths is common (van der Meijden *et al.* 1988). Thus, a similar reduction in PA concentrations in response to specialist herbivory might be an effective defence response against specialist herbivores that utilise PAs for host recognition (Macel and Vrieling 2003) and their own defence (Dobler *et al.* 2000, Beuerle *et al.* 2007). It is clear that variation in PA concentration and composition are caused by interspecific interactions, but the direction of the response is likely to depend on herbivore identity.

Due to their importance to ragwort defence, PAs have been the focus of the majority of studies that consider the metabolites of ragwort. Many different methods have been used to catalogue and quantify the PA species-specific profiles of *Senecio* species including: spectrophotomic methods that measure the Ehrlich's reagent (Mattocks 1986), micellar electrokinetic chromatography (Yu *et al.* 2005, Qi *et al.* 2009a), nuclear magnetic resonance (NMR) (Johnson *et al.* 1985), gas chromatography-mass spectrometry (GC-MS) (Luthy *et al.* 1981, Candrian *et al.* 1984) and liquid chromatography-mass spectrometry (LC-MS) (Parker *et al.* 1990, Boppre *et al.* 2005, Colegate *et al.* 2005). NMR is useful for structural identification, whereas GC-MS and LC-MS are the most commonly used techniques for PA profiling (Crews *et al.* 2010). Due to high sensitivity, GC-MS analysis is a useful tool to examine PAs at trace concentrations (Roeder 1999). Sample preparation procedures are, however, complicated by the inability of GC-MS to detect PA N-oxides without derivatization (Beales *et al.* 2003). This is because oxidised PAs are unstable at the high temperatures required for analysis (Crews *et al.* 2010). As N-oxides can account for a significant proportion of the PA content of ragwort (Joosten *et al.* 2011), it is essential to consider N-oxides when the PA profile of *Senecio* species is determined (Cao *et al.* 2008). A method traditionally used to reduce N-oxides to their parent form is the application of an excess of zinc oxide dust (Koekemoer and Warren 1951, Hartmann and Zimmer 1986). The use of zinc oxide has been demonstrated to be inconsistent (Beales *et al.* 2003), thus an analytical method that can determine both parent PAs and N-oxides is preferable for improved reliability and reduced processing times. LC-MS provides such a technique, as PAs can be detected regardless of their form (Wuilloud *et al.* 2004).

Despite the focus of many studies on PAs, other secondary metabolites associated with defence against generalist insect herbivores have also been observed in ragwort tissues. All are reported in foliar tissues; non-PA secondary metabolite defences in flowers, bolting leaves or roots have never been examined. A number of phenylpropanoids, including chlorogenic acid, have been observed in ragwort tissues (Kirk *et al.* 2005, Nuringtyas *et al.* 2012). Phenylpropanoids are widely distributed across many plant species (Clifford 2000), and convey resistance against generalist herbivore feeding (Leiss *et al.* 2009b). Flavanoids, such as kaempferol (Kirk *et al.* 2005), found in the foliar tissues of ragwort, have been demonstrated to have herbivore deterrent properties (Thoison *et al.* 2004). Jacaranone analogues (benzoquinoids) have also been detected in ragwort tissues (Kirk *et al.* 2005, Nuringtyas *et al.* 2012). The inclusion of jacaranone analogues in herbivore diet has been shown to inhibit the growth of a generalist insect herbivore (Lajide *et al.* 1996). All of these non-PA secondary metabolites were discovered in ragwort using a metabolomic approach, demonstrating the importance of adopting a non-targeted approach.

One reason why ragwort was chosen as the focal plant for this study is related to the movement of PAs from root to shoot tissues between plant tissues during biosynthesis. In addition, as outlined above, biotic environmental conditions have significant effects on ragwort chemistry, both above- and belowground. This plastic response of ragwort to biotic conditions meant that it was an ideal focal plant to study how the interactions between plant roots and below-ground mutualists or antagonists could influence the wider plant metabolome.

1.6. Metabolomics as a tool to examine plant interactions

The metabolome of an organism refers to the array of small organic biosynthetic molecules (metabolites <1000 Da) present in tissues or fluids (Oliver *et al.* 1998). The number of different metabolites across all plant species is likely to number hundreds of thousands (Pichersky and Gang 2000) and only a small proportion of primary metabolites (e.g. amino acids and sugars) are shared. The remaining secondary metabolites (e.g. flavonoids and alkaloids) tend to be restricted in their distribution among plant species. Metabolomics is the unbiased attempt to characterise an organism's metabolome (Fiehn 2002). Despite the diversity of the plant metabolome being known, traditional analyses have been used to target certain classes of plant secondary metabolites depending on the plant species studied, for example PAs in

Senecio species (Joosten *et al.* 2009) and glucosinolates in *Brassica* species (Kabouw *et al.* 2010). Although no existing technique can truly measure the whole metabolome of an organism (Macel *et al.* 2010), relatively recent advances in analytical techniques have much improved the analytical coverage of different metabolite classes (Hall 2006).

Metabolomic analyses have been applied to a wide range of interactions between plants and mutualistic AMF (Schliemann *et al.* 2008a, Fester *et al.* 2011); above-ground insect herbivores (Widarto *et al.* 2006, Arany *et al.* 2008, Jansen *et al.* 2009, Leiss *et al.* 2009a, Leiss *et al.* 2009b, Mirnezhad *et al.* 2010, Steinbrenner *et al.* 2011); parasitic nematode species (Hofmann *et al.* 2010, Baldacci-Cresp *et al.* 2012); nitrogen fixing bacteria (Colebatch *et al.* 2004, Desbrosses *et al.* 2005) and bacterial pathogens (Depuydt *et al.* 2009). Metabolomics is a relatively flexible approach and by applying the same analytical technique to plant and herbivore tissues, the presence of plant-derived compounds in the tissues of insect herbivores can be assessed (Schroeder *et al.* 2006, Jansen *et al.* 2009). The same method of metabolomic analysis can be applied to shoot and root tissues (e.g. Desbrosses *et al.* 2005). This allows the concomitant examination of the local and systemic effects of biotic interactions on the plant metabolome. This makes metabolomics a useful tool when examining interactions between above- and below-ground ecosystems. Another real strength of the metabolomic technique is that it is an unbiased analysis that can highlight metabolites important in plant interactions that would not have been identified using traditional targeted analyses. For example, Leiss *et al* (2009a) found, on examining the metabolites of *Senecio* F_2 hybrids, that increased levels of jacaranone (a benzoquinoid) and kaempferol glycoside (a flavonoid glycoside) were associated with resistance to thrip herbivory. Targeted analysis of *Senecio* species may only have considered PAs, and would have missed the differences in other defensive metabolites associated with thrip resistance in *Senecio* F_2 hybrids. Another benefit of a metabolomic approach is that the simultaneous examination of both precursor and product metabolites can be used to examine the signalling systems underpinning the interspecific interactions between plants and other organisms. For example, using a metabolomic examination of the interaction between a thistle (*Cirsium arvense* (L.) Scop.) and an endophytic fungus (*Chaetomium cochlioides* (Wallr.) S. Hughs, (1958)), Hartley *et al.* (2012) revealed that the jasmonic signalling pathway was involved in the initiation of a defence response. These authors demonstrated that endophytic fungi infection was associated with a decrease in precursor metabolites of the jasmonic acid pathway (Hartley *et al.* 2012). Concomitantly, increased concentrations of product metabolites associated with jasmonic acid signalling were observed, demonstrating a role for

the jasmonic acid pathway in mediating the *C. arvense* defence response to *C. cochliolides* infection (Hartley *et al.* 2012).

The different techniques used in metabolomic analyses include NMR, LC-MS and GC-MS. The sample preparation techniques used for each analytical method follow some broadly similar principles. Enzymatic processes in tissues need to be halted as soon as possible, which can be achieved using liquid nitrogen, acid treatment or freeze clamping (Fiehn 2002). To maintain metabolite integrity, samples should be kept as cold as possible throughout sample preparation and should be ideally stored at -80°C. The techniques used vary depending on the volume and type of tissue, but to ensure a representative sample is analysed, plant tissues need to be homogenised prior to extraction (Fiehn 2002). Metabolites are then solvent extracted from plant tissues. Solvent choice will unavoidably introduce bias into the analytical process (Hall 2006). For example, extraction with methanol will better represent semi-polar metabolites than polar and non-polar ones. Extraction of plant tissues with a solvent mixture should help maximise the classes of metabolites represented and the metabolomic range covered (Sana *et al.* 2010). Whichever approach is adopted, sample preparation techniques should aim to be consistent so that the variation introduced during the error prone preparation process is reduced (Fiehn 2002).

The choice of analytical technique introduces bias into metabolomic analyses as no one technique covers the whole metabolome, and as such is a considered compromise between the available methods (Hagel and Facchini 2008). All of the analytical techniques commonly used in metabolomic studies, NMR, LC-MS and GC-MS, provide reproducible analyses. Each technique has advantages and disadvantages depending on metabolite class. NMR is a non-destructive analysis that detects a broad range of metabolites (primary and secondary) present in high concentrations (Kim *et al.* 2011). It is an excellent technique to quantify metabolites of interest because the concentration of a metabolite is proportional to the number of nuclear spins recorded (Pauli 2001). In addition, structural information can be obtained using NMR spectra allowing the detailed determination of a metabolite's structure and the discrimination between any isomeric metabolites (Kim *et al.* 2011). It is because of this that NMR is considered one of the best tools for metabolite identification (Moco *et al.* 2007). The main disadvantage of adopting an NMR metabolomic approach is low sensitivity (10^{-6}mol) when compared to GC-MS (10^{-12}mol) and LC-MS (10^{-15}mol) techniques (Sumner *et al.* 2003). As a result, fewer metabolites are observed during NMR analyses, typically 30-150 metabolites (Kim *et al.* 2011), when compared to more sensitive MS based metabolomic approaches which result in the detection of thousands of metabolites.

GC-MS and LC-MS are analytical methods that combine the metabolite separation qualities of chromatography and the sensitivity of mass spectrometry (MS) technologies. Both techniques provide information about metabolite identity based on their chemical nature by using the time they take to elute from the analytical column (retention time (r.t.)) and their mass by using mass-to-charge ratio (*m/z*) (Hagel and Facchini 2008). One of the biggest disadvantages of adopting MS techniques to examine an organism's metabolome is related to the difficult process of metabolite quantification, meaning that the abundance of metabolites tends to be expressed in relative terms (Macel *et al.* 2010). GC-MS principally analyses primary and volatile metabolites, but is less suited to the analysis of polar metabolites or those with a relatively high molecular weight (Hagel and Facchini 2008). One of the main disadvantages of adopting a GC-MS metabolomic approach is increased sample preparation time. This is caused by the need to derivatize many metabolite groups, such as organic acids and PA N-oxides, to enable their detection (Beales *et al.* 2003, Halket *et al.* 2005). LC-MS, on the other hand, overcomes many of the disadvantages of the two techniques already outlined: sample preparation is relatively simple and analyses are highly sensitive. LC-MS analyses are suited to the detection of semi-polar metabolites, including many groups of secondary metabolites (Allwood and Goodacre 2010). One of the main disadvantages of adopting an LC-MS metabolomic approach is that detection is restricted to those metabolites that can be ionised (Hall 2006), a problem that can be partially overcome by employing different ionisation modes (for instance both negative and positive electrospray ionisation) to analyse the same sample to increase metabolome coverage.

1.7. Thesis objectives and outline

The overall aim of this study was to characterise the distribution of secondary metabolites among ragwort foliar and root tissues; and then to assess how this changed through interspecific interactions with a below-ground antagonist and mutualist, namely the herbivorous nematode *Pratylenchus penetrans* (Cobb, 1917) Filipjev & Schuurmans Stekhoven, 1941 and the mutualistic arbuscular mycorrhizal fungi *Glomus intraradices* (Smith & Schenck). Chapter 2 examines the 'Within plant variation in the above-ground secondary chemistry of ragwort' in relation to optimal defence theory. In addition, this chapter demonstrates the successful application of a UPLC-TOFMS metabolomic approach to ragwort tissues. Therefore, the same technique was used to examine the interactions between ragwort and two soil biotic agents. Chapter 3 investigates the effect of migratory endoparasitic nematode herbivory by

Pratylenchus penetrans on the above- and below-ground secondary chemistry of ragwort. Chapter 4 aims to characterise the chemical changes caused above- and below-ground by colonisation of ragwort by a mutualist arbuscular mycorrhizal fungi (AMF) *Glomus intraradices*. Finally, in chapter five, the key themes identified by the studies presented in the preceding chapters are discussed.

Chapter 2. Within-plant variation in the above-ground secondary chemistry of ragwort

2.1. Abstract

To protect against herbivore attack plants must distribute limited defence resources optimally. Optimal Defence Theory (ODT) predicts that plant tissues of high nutritional value to herbivores should be best defended. Using a metabolomic approach, variation in plant secondary chemistry was quantified in the flowering and vegetative tissues of a ragwort population. Multivariate statistical analysis revealed significant differences in the metabolomic profiles of the leaf and flower tissues and, to a lesser extent, between leaves of different ages. The metabolites driving the observed metabolomic differences between plant tissues included pyrrolizidine alkaloids, flavonoids, fatty acids, phospholipids, chlorogenic acids and steriods. As predicted by ODT, around two thirds of the metabolites identified were allocated in higher concentrations to tissues more valuable to plants. This study is one among few to have demonstrated that a metabolomic approach can be employed to characterise the spatial heterogeneity of secondary chemical allocation of a plant under field conditions.

2.2. Introduction

Plants deploy a range of physical and chemical defence mechanisms to limit or prevent herbivore damage. These plant defences can be indirect by attracting mutualists (Palmer *et al.* 2008, Yamawo *et al.* 2012) or natural enemies (Vos *et al.* 2001, Gols *et al.* 2012) that can alleviate herbivore damage. Alternatively, plant defences can directly reduce the impact of herbivory by influencing herbivore feeding preference and/or performance (Onyilagha *et al.* 2004, Macel *et al.* 2005, Blüthgen and Metzner 2007, Johns *et al.* 2009, Kimball *et al.* 2012). One mechanism by which plants directly reduce herbivory is through the production of defensive secondary metabolites that reduce the palatability or digestibility of tissues or increase toxicity to herbivores. The term 'secondary metabolite' encompasses a huge diversity of chemicals, both in terms of the number of chemicals produced (Pichersky and Gang 2000) and the numerous combinations in which they can be mixed (Gershenzon *et al.* 2012). Another major source of heterogeneity in secondary metabolite profiles is their unequal distribution within individual plants (de Boer 1999, Lambdon *et al.* 2003, Gutbrodt *et al.* 2011).

This variation in the diversity, form, function and distribution of defensive secondary metabolites provides a major challenge for herbivores.

A number of hypotheses have been suggested to explain the variation in the levels of defence observed between and within individual plants (Stamp 2003). The Optimal Defence Theory (ODT) is one of the most prominent hypotheses used to explain within-plant allocation to different tissues (McKey 1974). To optimise defence, a plant should allocate resources according to the costs of defence, the value of the tissue to the plant and the probability that the tissue will be attacked by herbivores (McKey 1974). The ODT assumes that the production, transport and maintenance of defences are costly. Therefore, the allocation of resources is the result of a trade-off between defence and other essential processes such as growth and reproduction.

The optimal outcome from this trade-off will depend on the costs versus benefits of defending particular tissues. For instance, plant tissues of a high physiological or fitness value to the plant should be the most defended as their loss would have the greatest negative impact. In support of the ODT, Zangerl (1986) demonstrated that fully expanded, younger leaves were of the highest value to a plant due to an increased photosynthetic potential. The removal of young leaves has also been shown to have a cost by reducing plant reproduction (Ohnmeiss and Baldwin 2000). The importance of different tissues to the plant is dynamic with the relative value of tissues changing with plant ontogeny (Boege and Marquis 2005, Barton and Koricheva 2010). For instance, as they develop, flowers and fruiting bodies are typically better defended than leaves due to their more direct link to plant reproduction and ultimately fitness (Strauss *et al.* 2004).

A recent meta-analysis concluded that the ODT is a useful framework to study within-plant variations in defence (McCall and Fordyce 2010). ODT predicts that the allocation of secondary chemical defences will be greatest in reproductive tissues (e.g. flowers) and physiologically crucial younger leaves should be more heavily defended than older ones. There is substantial empirical support for the key prediction of this theory that chemical defence allocation decreases with increasing leaf age (van Dam *et al.* 1994, Ohnmeiss and Baldwin 2000, Lambdon *et al.* 2003, Barton and Koricheva 2010, Gutbrodt *et al.* 2011, Yamawo *et al.* 2012). Similarly, concentrations of defensive metabolites are much higher in plant tissues directly associated with reproduction (Hartmann and Zimmer 1986, Zangerl and Rutledge 1996, Brown *et al.* 2003, Strauss *et al.* 2004, Smallegange *et al.* 2007).

The allocation of secondary defence metabolites within the plant is highly plastic and is determined by the probability of, and reaction to, herbivory. If the likelihood of herbivore attack is high, it should be reflected in the concentrations of metabolite defences in that particular plant tissue. The nutrient status of a given tissue governs the probability of herbivore attack (Mattson 1980, Jacobsen 1992), with younger, more nutritious leaves preferred by herbivores over older leaves (Lambdon *et al.* 2003, Gutbrodt *et al.* 2011). Herbivore food choice is thus a trade-off between limiting exposure to harmful chemical defences and maximising nutritional gain. Herbivore specialisation arising from co-evolutionary processes can further predict feeding selectivity of different insect species. Generalist insect herbivores tend to avoid well-defended new leaves, whereas specialists with evolved abilities to circumvent defences (e.g. detoxification and sequestration) can feed on the more nutritious younger foliage (Cates 1980, de Boer 1999, Blüthgen and Metzner 2007, Gutbrodt *et al.* 2011). In addition, specialist insect species in the later stages of development can feed preferentially on reproductive organs, which can improve herbivore performance (Dempster 1982, Smallegange *et al.* 2007).

Although there is much evidence supporting the predictions of the ODT, it should be noted that many studies have been limited by focusing on particular metabolite classes (e.g. de Boer 1999, Lambdon *et al.* 2003). This targeted approach to the study of plant defences may not accurately portray the total allocation and composition of defensive metabolites across all metabolites present in the plant system (Goodger *et al.* 2006). A focussed approach examining a particular group of defence metabolites will not provide the most meaningful test of the ODT. This study set out to test robustly the predictions of the ODT by using a metabolomic approach to quantify simultaneously the allocation of plant secondary metabolites.

Ragwort (*Senecio jacobaea* L.) as a model plant species. Most studies that have examined within-plant variation in ragwort secondary chemistry have focused on pyrrolizidine alkaloids (PAs), the main defence metabolites of *Senecio* species (Hartmann and Zimmer 1986, de Boer 1999). A thorough study of PA distribution in the leaves of vegetative ragwort plants showed that total PA concentrations decreased with increasing leaf age (de Boer 1999). This led the author to conclude that ragwort was optimally defended against generalist herbivores (de Boer 1999). In flowering ragwort, PA concentrations are greater in flowers than leaves (Hartmann and Zimmer 1986). This difference between flowers and leaves is thought to be driven by increased concentrations of erucifoline (Joshi and Vrieling 2005), a PA found in numerous *Senecio* species (da Silva *et al.* 2006). In addition, trade-offs between growth and PA production have been detected in ragwort grown in light-limited laboratory conditions

(Vrieling and van Wijk 1994). This suggests PA production has a physiological cost and consequently they cannot be ubiquitously distributed within a plant. Ragwort is attacked by a range of generalist (e.g. *Chromatomyia syngenesiae* Hardy and *Melanagromyza aeneiventris* Fallen) and specialist (e.g. *Tyria jacobaeae* L. and *Longitarsus jacobaeae* Waterhouse) herbivores (Harper and Wood 1957, Harrison and Thomas 1991, Kunin 1999). Ragwort is therefore likely to require a number of metabolite classes, varying in form and function, to defend itself against multiple herbivore species. Hence, a metabolomic approach, allowing the concomitant examination of a wide range of metabolite classes (including PAs) in different plant tissues, was used to test the predictions of the ODT in this plant species. Variation in metabolite profiles were compared in samples collected from plants at two ontogenetic stages (flowering and vegetative). Optimal Defence Theory predicts that those metabolites associated with defence will be found in greater concentrations in those plant tissues of more value to the plant (McKey 1974). Hence, flowers were expected to contain the highest concentrations of metabolites associated with defence. Moreover, it was predicted that across both ontogenetic stages, new leaves would be better defended than older leaves.

2.3. Methods

2.3.1. Sample collection

Plant material was collected in October 2008 from a wild ragwort population on the University of Sussex campus (Grid ref: TQ 3484 0941). Fifteen flowering plants and 15 plants in the vegetative growth stage were sampled (Figure 2.1.). Composite samples of flowers, new and old leaves were collected from flowering plants (mean height: 61.1 c.m. ± 4.1 S.E.). Five flowers were selected from different positions around the ragwort corymb (Figure 2.1.c). Leaf samples were collected from the plant's bolting stem (Figure 2.1.a). New leaves were defined as the top three fully opened leaves on the bolting stem. Old leaves were classified as the three bottom-most leaves that showed no visible signs of senescence. Leaves were not collected from two of the flowering plants sampled as all leaves on the bolting structure were senescing. New and old leaves were collected from the rosettes of vegetative plants (Figure 2.1.b). An abundance of plants in this growth-stage allowed selection of plants of similar size (mean width: 33.3 cm ± 1.8 S.E.). New leaves were defined as the three fully opened leaves that were closest to the centre of the rosette. Old leaves were determined as three on the outside of the rosette that showed no visible signs of senescence. All plant tissues were snap frozen in liquid nitrogen immediately after removal from the plant; this halted enzymatic processes. Samples were kept on dry ice before being transferred to the laboratory where they were stored at -80°C until analysed.

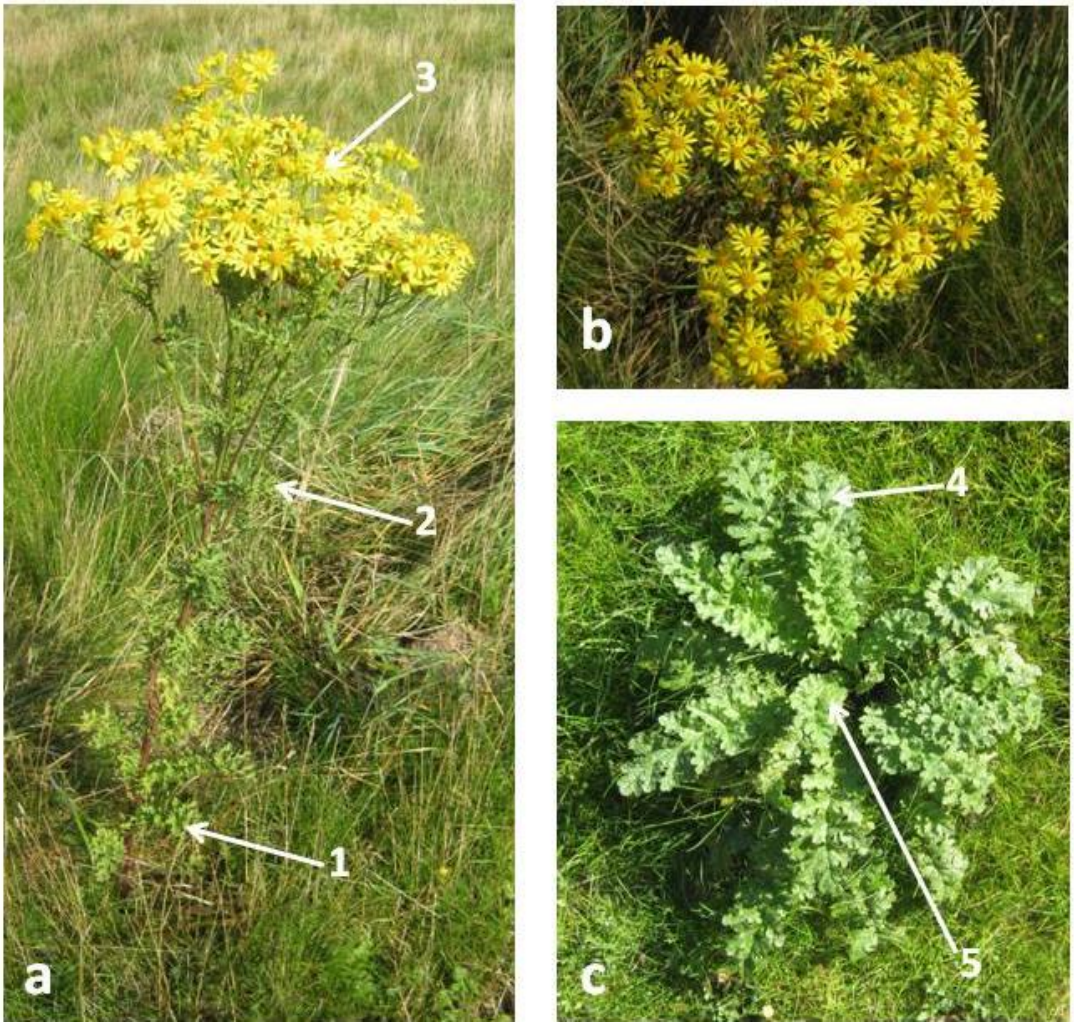

Figure 2.1. Samples taken from ragwort at different ontogenetic stages. a) A flowering ragwort plant used in this study. An indication of the samples taken for metabolomic analysis is given: old leaves (1), new leaves (2) and flowers (3). b) The corymb of the same flowering plant. Flowers for metabolomic analysis are taken from different areas around the corymb to ensure a respresentative sample. c) The low-lying rosette that ragwort forms during the vegetative ontogenetic stage. Samples taken for metabolomic analysis are indicated: old leaves (4) and new leaves (5).

2.3.2. Chemicals and Standards

A mixed standard of two PAs, seneciphylline and senecionine, was purchased from Carl Roth, GmbH & Co (Karlsruhe, Germany). All other standards, including formic acid, were purchased from Sigma-Aldrich Company, Ltd (Dorset, UK). All remaining chemical reagents were purchased from Rathburn Chemicals Ltd (Walkerburn, UK). Sirocco protein precipitation plates were purchased from Waters (Manchester, UK).

2.3.3. Sample preparation and solvent extraction

Extraction of all plant material were performed using a double solvent method. The first solvent was a mixture of isopropanol, acetonitrile and water in a ratio of 3:3:2. This solvent mixture has been shown to extract both polar (carbohydrates, amino acids) and non-polar (lipids) metabolites present in the metabolome of plants (Sana *et al.* 2010) . A new mix was made daily to prevent a change in the ratio caused by differential rates of evaporation between the solvents. The solvent used for the second extraction of plant material was 100% methanol. Preliminary experimental work indicated that most of the plant metabolome detected by the mass spectrometry techniques used in this study were extracted using this method.

All stages of the extraction process were kept cold using liquid nitrogen, dry and wet ice. Frozen plant material was homogenised using a pestle and mortar in the presence of liquid nitrogen. Once finely ground, 0.1g ± 0.01g of plant material was weighed into a ball mill crucible. After adding 500µl of the first solvent, samples were pulverised at 50 oscillations/second for 30 seconds using a ball mill (Pulverisette 23. Fritsch, Germany) and pipetted into a glass tube. An additional 1500µl of the first solvent was used to rinse the crucible and was added to the same tube. After capping, the sample tubes were vortexed for 30 seconds and immediately placed in to a -20°C freezer for overnight extraction.

The following day, samples were brought back up to ice temperature before being centrifuged at 2000g for five minutes. The supernatant was collected and stored at -80°C until the next stage of the extraction process. The remaining pellet was re-suspended in 2ml of methanol, vortexed and placed back in the -20°C freezer overnight for the second extraction. The next morning the methanol supernatant was removed and stored as described above. A representative 250µl aliquot of each of the two supernatants was mixed and evaporated under vacuum. The residue was then resuspended in 240µl methanol water (3:1 ratio). The samples

were then passed through protein precipitation plates under vacuum, and the filtrate stored in amber HPLC vials to prevent photodegradation of metabolites. Samples were stored at -80°C until analysed by mass spectrometry (MS).

2.3.4. Chemical profiling of ragwort material

The metabolome of each sample was profiled using ultra performance liquid chromatography (UPLC) coupled to a time of flight mass spectrometer (TOFMS) that used an electrospray ionisation (ESI) interface. This technique was chosen for a number of reasons. NMR was not used because it is a less sensitive metabolomic approach (Sumner *et al.* 2003) and some PAs, as well as many other metabolites such as flavanoids, have been shown to be present in ragwort at low concentrations (Joosten *et al.* 2010). A GC-MS metabolomic approach was not adopted because N-oxides and other polar metabolites cannot be observed without a derivatization step (Beales *et al.* 2003). Instead, LC-MS was used because most polar metabolites, including N-oxide and parent PAs, can be detected simultaneously without derivatization steps (Wuilloud *et al.* 2004) and at low concentrations (Joosten *et al.* 2010). Ultra-high performance liquid chromatography (UPLC) was chosen for the metabolomic analysis in this study, because increased LC pressures used in this technique improve chromatographic quality and decrease analytical run times (Moco *et al.* 2007). The MS used was a time of flight (TOF) mass analyser. This analyser applies the same amount of energy to each metabolite and measures the time they each take to reach the detector; it is this information that is used to determine a metabolites *m/z* (Ardrey 2003). TOF analyses enable high resolution analyses of each mass spectral signal, and this allows for differentiation between masses of the same nominal value which increases the number of metabolite signals that can be detected in a sample. ESI measures metabolites in two different ionisation modes: positive where a proton is gained, and negative where a proton is lost (Allwood and Goodacre 2010). Different classes of plant secondary metabolites are observed depending on the ionisation mode used. For example, glucosinolates are best detected in negative ESI mode (Lee *et al.* 2006) and PAs are observed in positive ESI mode (Lin *et al.* 1998), thus using ESI increases the coverage of the metabolome. More specifically to the analysis of ragwort, UPLC also allows the simultaneous analysis of both parent PAs and their N-oxides, without the potentially complicated and unreliable derivatization steps required for gas-chromatography (GC) (Beales *et al.* 2003). ESI was used because it is the best ionisation method for many polar metabolites, including parent PAs and their N-oxides; this ensures greater reliability of analysis, especially for those PAs found in lower quantities (Beales *et al.* 2003). In a recent review, Crews *et al.* (2010) noted that LC-MS was the most common ionisation method used to measure PAs.

Extraction aliquots of 10µl were injected on to an Acquity UPLC BEH C18 column (1.7µm particle size, 1.0 x 100mm, Waters, UK). The column was maintained at 30°C. In both positive and negative ESI, the mobile phase consisted of 100% water (A) and 100% acetonitrile (ACN) (B), and both solvents contained 0.1% formic acid. A flow rate of 0.085mL min^{-1} was maintained throughout the following UPLC program: 0.0-3.0 min maintained at 100% A; 3.0-12.0 min, from 0% to 30.0% B; 12.0-20.0 min, from 30.0% to 100% B; 20.0 to 25.0 min, 100% B. At the end of the programme, the column was equilibrated for four minutes in 100% A prior to the next injection.

Metabolites were detected using a Micromass TOF-MS system (Waters, Manchester, UK). The mass spectrometer was tuned to 9000 mass resolution and data collected in full scan mode from 100 to 1200 *m/z*. Argon was used as the collision at a constant collision energy of 10eV and the TOF penning pressures ranged from 4.53 x 10^{-7} to 5.15 x 10^{-7} mbar. Capillary voltage was -2.70 and 2.50 in negative and positive mode, respectively. Cone voltage was set at 35V and multiplier voltage was set at 550V. The source and desolvation temperatures were 100°C and 250°C, respectively. Desolvation nitrogen flow was set at 300 L h^{-1} in positive ESI and 600 L h^{-1} in negative ESI mode. To account for calibration drift within a run, an internal lockmass was used. Sulfadimethoxine (5pg μL^{-1} in methanol water, 1:1, with 0.1% formic acid added for positive ESI mode) was infused at 50µL min^{-1} using a lockspray interface (baffling frequency, 0.2s^{-1}). Ions were obtained at *m/z* 311.0814 in negative mode and *m/z* 309.0658 in positive mode. Standard solutions were prepared to monitor MS performance prior to analysis of experimental samples. A mixed standard solution was made containing senecionine, seneciphylline, naringenin, quercertin and gibberellic acid at 1ng/µl in methanol:water (1:1). The first three of the standards were detected in positive electrospray ionisation (ESI) mode, the final three in negative ESI mode. At the start and end of every analytical batch, 3µl of the standard mixture was analysed and the MS response and retention time of the standards checked to examine MS sensitivity and any significant drift in chromatography performance.

2.3.5. Statistical analysis of ragwort metabolomic profiles

2.3.5.1. Pre-processing of profiling datasets

The four datasets created from UPLC-TOFMS profiling were analysed as follows. The chromatograms generated were aligned in MarkerLynx (Version 4.1, Waters, UK) using signals common to all samples that arose from plastic contamination during the workup (in positive ESI mode these had a *m/z* ion of 453.3382, and retention time 10.60 min; negative ESI mode

m/z: 265.1472, retention time: 17.19 min). After isotopic peaks of all the metabolite signals were removed, the data were binned into 0.03 Da mass and 0.20 retention time (r.t.) windows. Finally, the area of each mass signal in the datasets was normalised using the total area under each chromatogram. The processed data set was now consisted of the suite of metabolite signals found in each sample. Each metabolite signal was the description of an analyte using its specific r.t. and mass-to-charge ratio (*m/z*). The complete metabolite dataset was then imported into the statistical programme SIMCA-P+ (Version 12.0.1, Umetrics, Sweden), where it was transformed and scaled prior to analysis. Log transformations were performed so that the data roughly approximated to a normal distribution. The data were pareto-scaled to prevent large metabolite signals dominating the dataset. Pareto-scaling up-weights small and medium metabolite signals without inflating the level of background noise observed within the dataset (Wiklund *et al.* 2008).

2.3.5.2. Principle component analysis (PCA) of ragwort datasets

After pre-processing, the metabolite datasets generated had relatively few observations of individual plants (n=15) and many thousands of measures of different metabolites. The most appropriate approach to the analysis of such datasets was to use multivariate data analysis, such as principle component analysis (PCA). PCA is an unsupervised analysis that does not consider information on the data structure, such as plant tissue identity. This multivariate technique was used to identify outliers (explained in detail below) and examine trends within the data. PCA reduced each dataset to a number of components by taking 'cuts' through the multivariate space; these 'cuts' were angled so that the amount of variation explained by each was maximised. Typically, the most informative separations of the dataset were provided in the first few components (Liland 2011). Each principle component calculated using the datasets can be described using scores (t) and loadings (p). The scores calculated allowed simplified two-dimensional representations of the datasets to be visualised in plots. Score plots allow any groupings of profiles to be observed, for example groupings of different tissues of ragwort plants can be investigated at this stage. Loadings relate the calculated scores back to the original data set, and suggest which metabolites have a strong effect on each component of the model.

Two measures of a PCA model can be used to evaluate the reliability of the PCA model, R^2X and Q^2. R^2X is a measure, based on residuals, of the variation within the dataset that is explained by the model. Q^2 measures the predictive ability of the model and is ascertained by

several cross validation (CV) rounds. During a CV round, a seventh of the data were excluded and re-plotted based on the predictions of the remaining dataset. It is the performance of these predictions that the Q^2 represents. Both R^2X and Q^2 range from zero to one, with one indicating a model of a better quality.

2.3.5.3. Outlier detection using principle component analysis

PCA allowed the visualisation of outlier data points that represented anomalous UPLC-TOFMS profiles. Outliers can highlight any differences in profiling data caused by extraction problems and analytical errors. In this study, all strong outliers (if present) were excluded and moderate outliers monitored to ensure they did not negatively affect the model. If a data point was a strong outlier it is considerably closer to, or further from, the 'cut' taken through multivariate space than all the other observations. This was problematic because it was an indication that the outlier data point had disproportionately influenced the angle of the 'cut' taken through the data. Moderate outliers are those that are far from the 'cut', but do not affect the angle it takes. Two outlier detection tools were used in this study: Hotelling's T^2 and DModX. Hotelling's T^2 generate 95% confidence intervals using a multivariate generalisation of the Student's t-distribution. These generated values were visualised by plotting them on scores' plots, and Hotelling's T^2 ellipses are seen on all of the scores plots displayed in this study. Exceptions to the Hotelling's T^2 were classified as strong outliers and always excluded from further analyses. DModX is a measure of the distance of each data point from the model plane created by each 'cut' through the data set, and was a method used to confirm strong outliers and identify moderate ones. Once all the outliers were identified and appropriately dealt with, the datasets were re-modelled using supervised analyses. Supervised analysis considers class information, such as plant tissue identity (e.g. flower, old leaf, new leaf) during the analysis of the data. If more than two plant tissues were profiled from each plant, as was the case for flowering plants, datasets were analysed using first partial least squared-discriminate analysis (PLS-DA) and then orthogonal partial least-squared discriminate analysis (OPLS-DA) (both are described below). If two plant tissues were profiled per plant, as was the case for vegetative plants, then only OPLS-DA was used.

2.3.5.4. Supervised multivariate analyses of ragwort datasets

Supervised analyses allow separations between different plant tissues to be maximised, so that the models created are more informative when visualised. PLS-DA, a supervised analysis that

considers information about plant tissue identity, was used to examine profile clustering of more than two plant tissues. PLS-DA was a method of analysis that maximised covariance between the metabolites and the known response variable, in this case plant tissue identity (Liland 2011). By considering plant tissue identity when taking 'cuts' through the dataset the amount of variation explained by each 'cut' was maximised. Unlike PCA, PLS-DA models are characterised by latent variables rather than principle components, but like PCA these are described using scores and loadings. The model diagnostics of PLS-DA are broadly similar to those of the PCA models.

PLS-DA was used to describe the maximum variation within a dataset. The maximum amount of variation may not, however, coincide with the maximum separation between plant tissues in the first, second or even third latent variable. By using OPLS-DA, this problem can be overcome through a rotation of the dataset, so that the first component explains the maximum separation between plant tissue types (Trygg and Wold 2002). Pair-wise comparisons of plant tissues, using OPLS-DA, were made for all plant tissues collected within the same ontogenetic stage. In this case, OPLS-DA used information about plant tissue identity to classify the profiled metabolites into those that correlate with this classification, and those that are orthogonal to it (Bylesjo *et al.* 2006). The diagnostics and interpretation of the models is similar to PCA, but where R^2Y measures the amount of data modelled and Q^2 the predictive power of the model.

Metabolites that vary with, and are correlated to, plant tissue identity that were examined further. The metabolites that correlated with the orthogonal component explained variation between the same plant tissues collected from different plants (within class variation), and as such were not useful for this study. The main advantage of rotating the dataset with OPLS-DA is that it allows easier identification of the metabolites driving class differences. The method used to identify metabolites of interest was the 'S'-plot (Figure 2.2.). By plotting two of the loadings calculated during OPLS-DA, the influence of the metabolites on each model can be observed. This plot displayed the contribution of a metabolite to the separation of samples according to class, against the magnitude of the difference in metabolite concentration observed between classes (Wiklund *et al.* 2008). By examining the 'S'-plot, those metabolites that greatly influence the OPLS-DA model can be identified. The metabolites located at the end of the plotted curve are those that differ greatly in concentration and drive the significant separations observed between plant tissues (Figure 2.2.). These metabolites were investigated further to examine the differences among plant tissues.

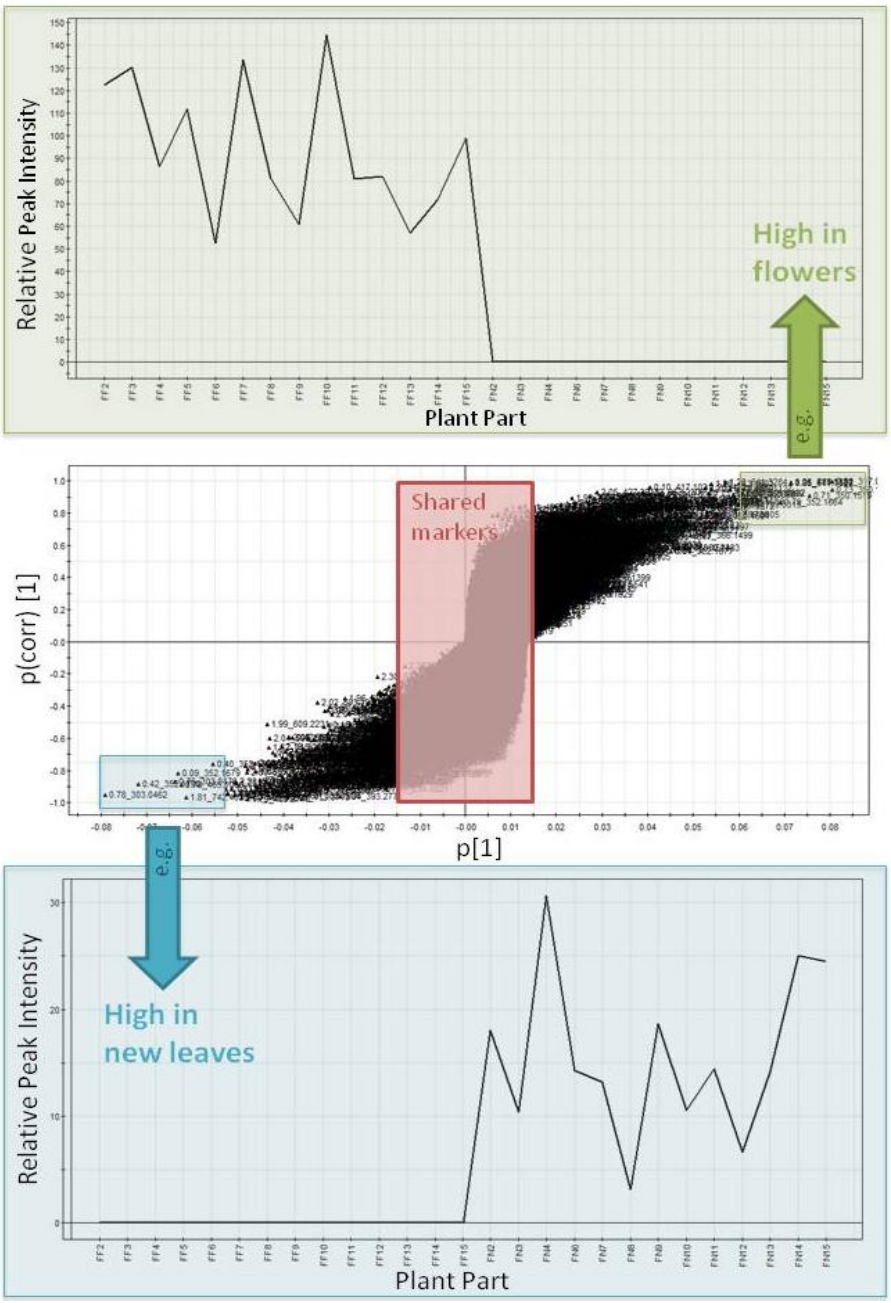

Figure 2.2. An example of an 'S'-plot, highlighting the typical patterns of the metabolites at either extreme. The middle graph is the 'S'-plot of the OPLS-DA model comparing the negative ESI metabolomic profiles flowers and new leaves. 'S'-plots identify those metabolites that contribute greatly to class separation and account for large differences between plant tissues. The metabolites in the green shaded area are those that are high in flowers, those in the blue shaded area are high in new leaves. These are the metabolites of interest that are investigated further. Those at the centre of the plot are shared in, and do not differ between, flowers and new leaves and are not examined in further detail.

2.3.5.5. Quantification and statistical testing of metabolites of interest

Metabolites of interest were identified using 'S'-plots of OPLS-DA models and quantified using normalised values obtained from MarkerLynx binning. These gave values of relative concentrations of the metabolite signal per unit of fresh weight of plant material. Signals of PA metabolites often tailed in the analysis and so their concentrations were manually quantified using the peak integration function in MassLynx software (Version 4.1, Waters, UK). Concentration differences in metabolite concentrations between plant tissues were compared using t-tests when the assumptions of normality (Kolmogorov-Smirnov tests) and equality of variances (Levene's test) were met. If the assumptions for parametric testing could not be satisfied, either before or following transformations, the non-parametric Mann-Whitney test was used (SPSS Version 17.0). The conservative Bonferroni correction term was applied to account for false discovery rates (Type I error) due to multiple testing (Broadhurst and Kell 2006). Those metabolites detected in positive ESI were statistically significant if $P < 1.70 \times 10^{-6}$, and the metabolites detected in negative ESI were statistically significant if $P < 2.43 \times 10^{-6}$. Metabolite concentrations that remained significant after Bonferroni correction represented substantial differences between plant tissues. The elemental compositions, and where possible structures, of these metabolites were determined using QTOF-MS CID (collision induced dissociation) and UPLC-NanoSpray (as described below).

2.3.6. Pyrrolizidine alkaloid (PA) identification and quantification

PAs were detected in positive ESI mode, as in previous studies (Crews *et al.* 2009). The chromatograms of all plant tissues analysed were investigated using the masses of the ragwort PAs recently reported by Joosten *et al.* (2010), and by comparisons with commercial standard PAs. Chromatogram peaks that eluted at a similar retention time and with a similar mass spectrum as the standard PAs were identified as probable PA structures. This was because a similar reaction to the mobile and stationary phases suggested homogeneity in chemical structure. In some chromatograms, the parent ion of the PA metabolite was saturated, and thus could not be quantified accurately. If this was the case, the C^{13} or O^{18} isotopes of the PA parent ions were quantified in all the samples of the dataset. Once quantified, the relative concentrations of PAs in leaves and flowers were tested using t-tests when the assumptions of normality (Kolmogorov-Smirnov tests) and equality of variances (Levene's test) were met. If the assumptions for parametric testing could not be satisfied, either before or following transformations, the non-parametric Mann-Whitney test was used. No differences in PA concentrations between new and old leaves collected from flowering plants meant that data

were pooled to compare overall PA concentrations in leaves with the flower extracts. After the application of Bonferroni corrections for metabolites detected in positive mode, differences in PA concentrations were considered statistically significant if $P < 1.70x10^{-6}$. Further information on the structural identity of PAs that varied significantly between plant tissues was determined using QTOF-MS CID (as described below).

2.3.7. Further structural identification of the plant metabolites associated with within-plant variations in ragwort

Composite samples of each plant tissue were prepared by combining some of the extracts used for initial metabolomic profiling. This allowed enough plant extract for further MS analyses. Metabolites were assigned putative identities using their accurate mass composition and isotopic fit as determined by MassLynx software. Putative metabolite identities were also confirmed using data collected using a UPLC-NanoSpray system. The UPLC-NanoSpray system obtained a more accurate mass measurement than the previously used UPLC-TOFMS, resulting in a more reliable likely elemental composition. The UPLC-NanoSpray system used was a UPLC Xevo G2-TOF (Waters, Manchester, UK) fitted with a Nano Acquity UPLC BEH 300 C18 column (1.7µm particle size, 100µm x 100mm, Waters, Manchester, UK). A 0.5µl aliquot of the composite sample was injected onto the column maintained at 30°C. In both positive and negative ESI, the mobile phase consisted of 100% water (A) and 100% methanol (B), and both solvents contained 0.1% formic acid. A flow rate of 0.70µL min^{-1} was maintained throughout the following UPLC program: 0.0-4.0 min, from 10% to 30% B; 4.0-18.0 min, from 30% to 50% B; 18.0-30.0 min, from 50% to 100% B. After each injection finished running, the solvent washing the column was stepped to 90% A and the column allowed to equilibrate for five minutes prior the next injection. A fused-silica emitter tip with the internal diameter 10µm was used. To account for calibration drift within a run, an internal lockmass was used. Leucine (purchased from Waters, Manchester, UK and diluted to 1ng μL^{-1}) was infused at 0.5µL min^{-1} using a lockspray interface (baffling frequency, $0.2s^{-1}$). Lockspray ions were obtained at *m/z* 554.2615 in negative mode and *m/z* 556.2771 in positive mode. Where possible, additional structural information was also elucidated using fragmentation data obtained from collision induced dissociated (CID) using quadrupole-ESI TOFMS (Q-TOFMS). Several metabolomic databases were queried using the information obtained on elemental composition and fragmentation patterns to obtain putative identities. These included KEGG Ligand: http://www.genome.jp/ kegg/ligand.html, KNApSAcK: http://kanaya.naist.jp/knapsack_jsp

/top.html, Scripps Center for Metabolomics, METLIN: http://metlin.scripps.edu/metabo_search_alt2.php, ChemSpider: http://www.chemspider.com/Search.aspx, and PubChem: http://www.ncbi.nlm.nih.gov/pccompound. Where possible, metabolites were classified into broad classes (e.g. flavonoids, fatty acids and steroids), and the likely composition of any conjugate was also determined.

2.4. Results

Profiling of the extracts of leaves and flowers by UPLC-TOFMS revealed that the overall profile of the different plant tissues were broadly similar (Figure 2.3.). In positive ESI mode, PAs were detected in all extracts and eluted in highly aqueous conditions when the mobile phase consisted of 100-70% water (0-12 minutes). The PA standards, senecionine and seneciphylline, eluted within this retention time window at a retention time of 8.31 and 7.47 minutes, respectively. The profiles revealed that a number of highly abundant lipophilic metabolites, likely to be phospholipids, eluted later in the LC program between 20-25 minutes when the mobile phase was 100% acetonitrile. Unconjugated flavonoids were likely to elute between 11-14 minutes as the standards quercetin and naringenin eluted at 12.0 and 13.15 minutes respectively. These initial observations are, however, based on the measurement of the intensity of the base peak (ion) of any metabolite, and therefore will only show the most abundant metabolites in the plant extracts. Further work based on the multivariate analyses of the many thousands of ions in the chromatograms were needed to explore the data in detail.

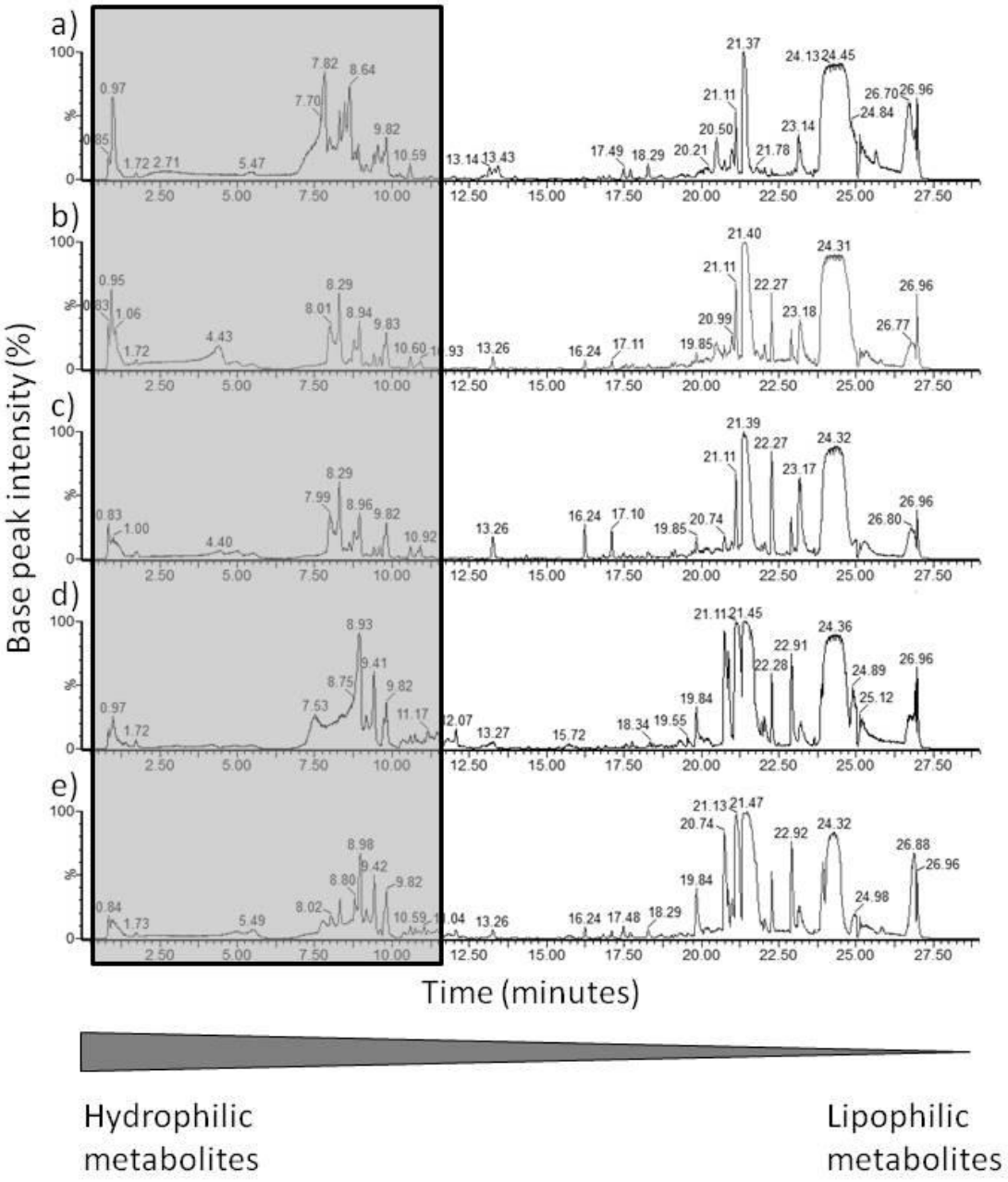

Figure 2.3. Representative chromatograms from UPLC-TOFMS in positive ESI mode profiling of extracts of ragwort a) flowers, b) new leaves and c) old leaves from flowering plants, and d) new leaves and e) old leaves from vegetative plants. The chromatogram region in which pyrrolizidine alkaloids (PAs) elute is marked in grey. Hydrophobic metabolites elute early in the program, when the mobile phase has a high water content. Lipophilic metabolites elute later when the mobile phase contains mainly acetonitrile. Chromatograms are normalised to the highest intensity of the base peak (ion) in metabolites eluting from the UPLC-TOFMS profile.

2.4.1. Flowering plants

2.4.1.1. Multivariate modelling of variation between flowering plant tissues

Data from UPLC-TOFMS profiling of the extracts of the leaves and flowers from flowering ragwort plants were analysed by PCA. Initial PCA of the positive ESI dataset identified one flower sample as an outlier (data not shown), it was thus excluded from subsequent analyses. No outliers were identified in negative ESI using PCA modelling. Despite explaining relatively small amounts of the variation observed (positive ESI: $R^2X = 0.235$, $Q^2 = 0.142$; negative ESI: $R^2X = 0.213$, $Q^2 = 0.124$), PCA modelling of both datasets revealed separations between flowers and leaf material in the first principle component (Figure 2.4.). The second principle component was unable to discriminate between old and new leaves. Supervised PLS-DA modelling of all three tissues collected from ragwort flowering plants demonstrated a clear separation between plant tissues, in both ESI modes (Figure 2.5.). The PLS-DA models of both datasets explained a high level of variation ($R^2Y > 0.987$ in both cases) and predictability (for all significant components, total $Q^2 > 0.790$). In both models, flowers were separated from leaves in the first latent variable, leaves of different ages were separated by the second latent variable. To identify metabolites responsible for the differences observed, supervised OPLS-DA modelling was performed. Every pair-wise combination of different plant tissues was performed for the datasets collected in both ESI modes. All of these models account for a high amount of the variation within the datasets ($R^2Y > 0.865$) and have a high predictive ability ($Q^2 > 0.461$, for the total of all latent variables) (Table 2.1.).

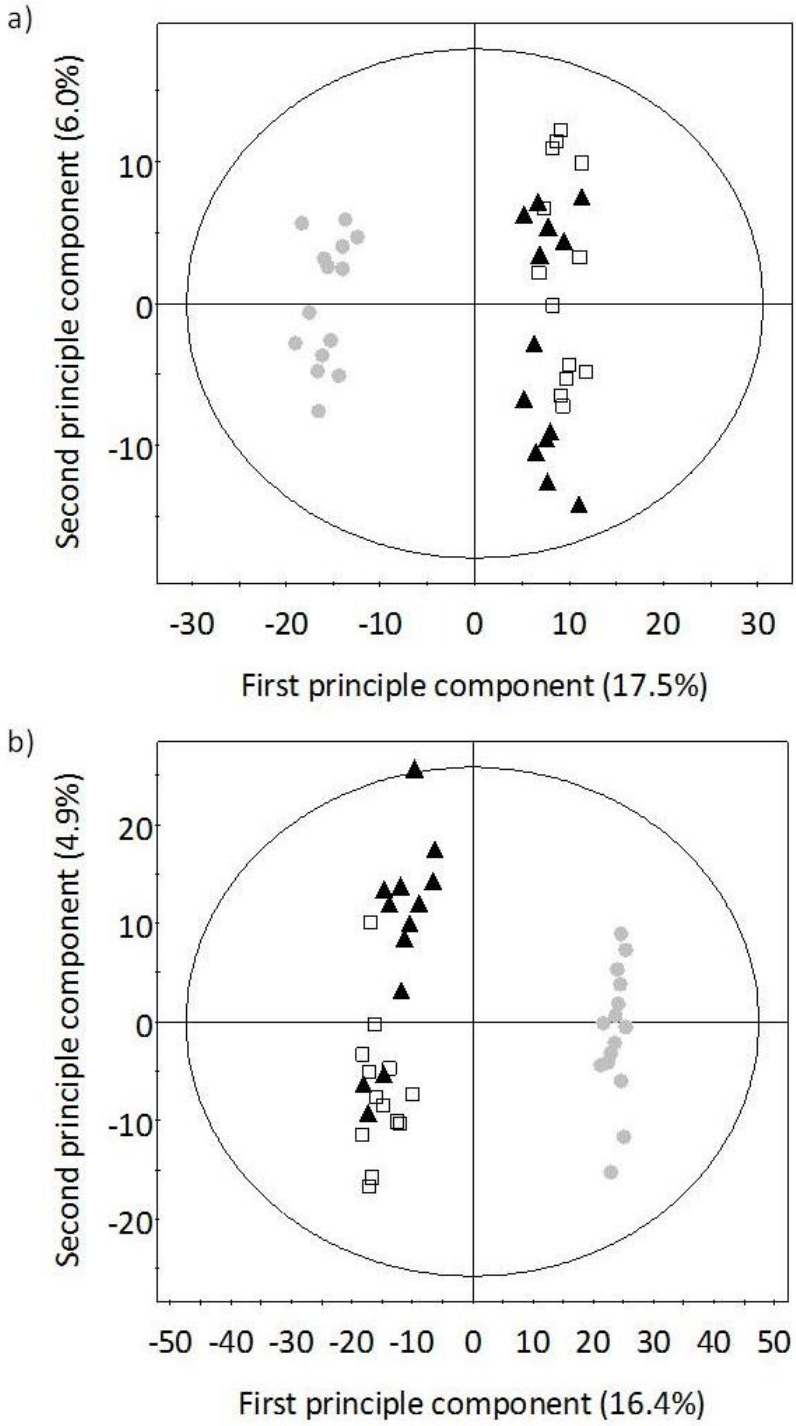

Figure 2.4. Principle component analysis (PCA) scores plots of the chemical profiles of ragwort flowering plants. Datasets were collected using UPLC-TOFMS in a) positive and b) negative ESI MS modes. The percentages of explained variation (R^2X) modelled for the first two principle components are displayed on the axes. Grey circles represent flowers, new leaves are black triangles and old leaves are unfilled squares.

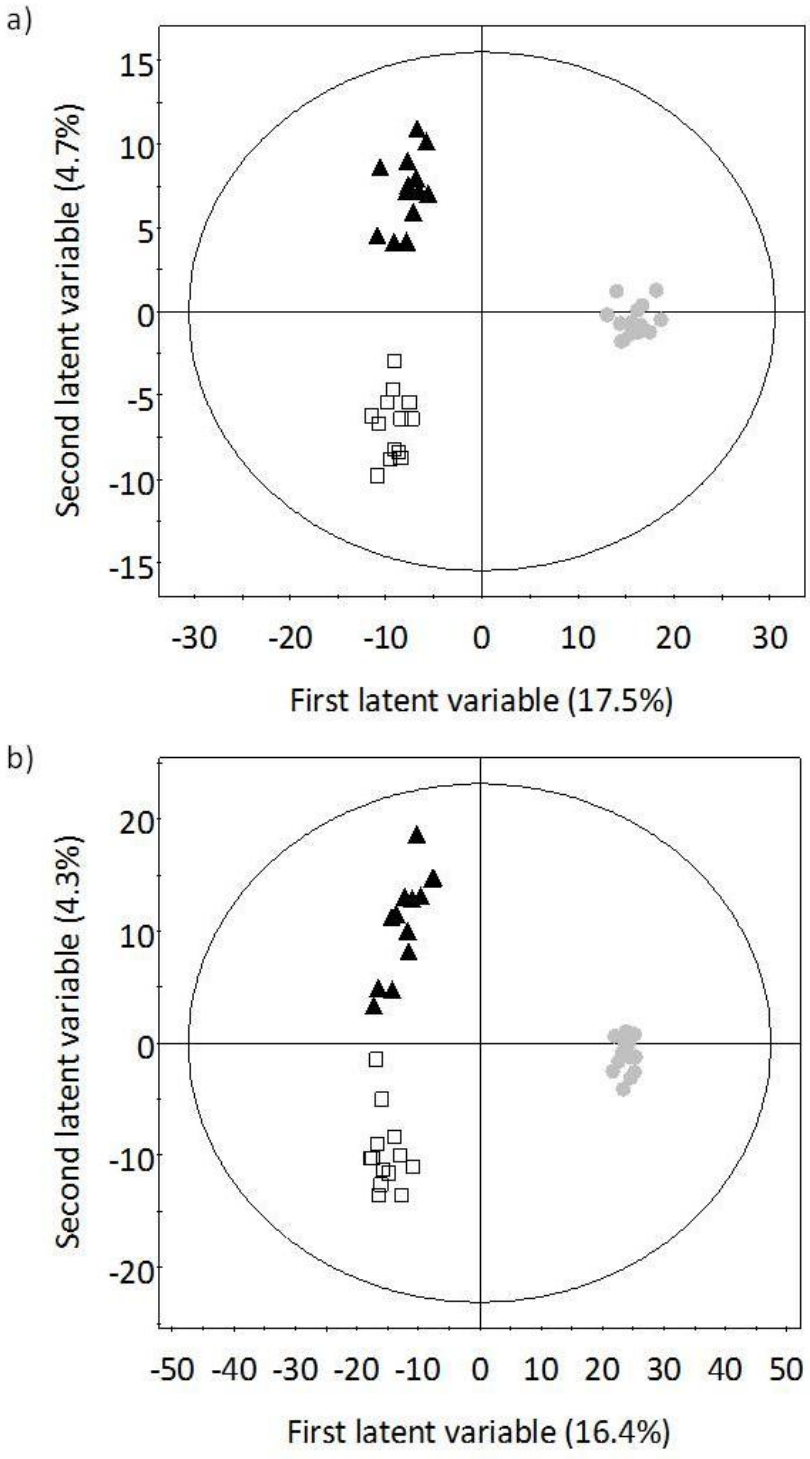

Figure 2.5. Partial least squared-discriminate analysis (PLS-DA) score plots of the chemical profiles of ragwort flowering plants. Datasets were collected using UPLC-TOFMS in a) positive and b) negative ESI MS modes. The percentages of explained variation (R^2Y) modelled by the first two latent variables are displayed on the axes. Grey circles represent flowers, new leaves are black triangles and old leaves are unfilled squares.

Table 2.1. Model diagnostics of the OPLS-DA models performed to compare the different tissues of flowering and vegetative ragwort plants. R^2Y is a measure of the variability of the data explained by the model and Q^2 indicates the predictability of the model.

Plant type	Tissue type	ESI mode	R^2Y	Q^2
Flowering	Flowers versus new leaves	Positive	0.987	0.956
		Negative	0.922	0.954
Flowering	Flowers versus old leaves	Positive	0.988	0.960
		Negative	0.994	0.961
Flowering	New leaves versus old leaves	Positive	0.990	0.690
		Negative	0.865	0.461
Vegetative	New leaves versus old leaves	Positive	0.981	0.746
		Negative	0.990	0.780

The OPLS-DA models were further analysed to determine which metabolite signals contributed to the separations of the different plant tissues in the model. Examination of the positive and negative ESI data revealed a total of 33 and 36 discriminatory metabolites at high concentrations in flowers compared to new and old leaves, respectively (Table 2.2.). Of those metabolites, 24 were shared and reflected the general differences between flowers and leaves of any age. Conversely, 54 and 56 discriminatory metabolites were detected in both new and old leaves, respectively, when compared to flowers (Table 2.2.). Of those metabolites, 22 were shared and reflected the differences between leaves of any age and flowers. Finally, when comparing new and old leaves of the flowering plant five metabolites were increased in new leaves (Table 2.2.).

Table 2.2. Summary of the metabolites of interest that differ significantly between the tissues of flowering ragwort plants. Plant extracts were analysed using UPLC-TOFMS in both positive and negative ESI modes. Results displayed represented those that remain significant after applying a Bonferroni correction.

		High in		
		Flowers	New leaves	Old leaves
Low in	Flowers	x	56	54
	New leaves	33	x	0
	Old leaves	36	5	x

2.4.1.2. Variation in pyrrolizidine alkaloids between flowering plant tissues

A total of 18 PAs were observed within the chromatograms of flowering plant material (Table 2.3.). Only 17 peaks were quantified. The peak shape of one PA signal (*m/z*: 352.1760; r.t.: 8.48 & 8.66) suggested it was likely to correspond to two different PAs, but was not separated by the UPLC program utilised. No variation between the PA concentrations of old and new leaves from flowering plants were observed after applying a Bonferroni correction ($P < 1.70x10^{-6}$) (Table 2.3.). Therefore, new and old leaf data were pooled to provide one dataset of PA concentrations in leaves, and was compared to PA concentrations in flowers. After applying a Bonferroni correction ($P < 1.70x10^{-6}$), nine variations in flowering plant material were observed when comparing flowers to leaves, eight were observed in higher concentration in flowers (metabolites 1, 2, 4, 5, 8, 9, 10 and 14) and one (metabolite 7) was higher in leaf material (Table 2.3.). The remaining nine PAs observed did not vary significantly within material collected from flowering plants.

Table 2.3. Concentrations (mean ±S.E., determined in 10µl injections, equivalent to 0.26mg of fresh leaf material) of PA type structures observed in the different tissues of ragwort flowering plants. PAs were detected using UPLC-TOFMS in positive ESI mode. Seventeen signals, corresponding to 18 PAs, were observed. Leaf fold changes were calculated by dividing average PA concentrations in new leaves with old leaves. Differences between plant tissues were tested using t-tests if marked with a ^, unmarked P-values were obtained using the non-parametric Mann-Whitney test. The tests that remained significant after Bonferroni corrections were applied ($P < 1.70 \times 10^{-6}$) are in **bold**.

Metabolite number	*m/z*	UPLC-TOFMS r.t.	flowers	new leaves	old leaves	new versus old leaves		flowers versus leaves	
						fold dif.	P-value	fold dif.	P-value
1	334.1654	7.47	64.02 (±12.62)	3.67 (±1.16)	9.22 (±3.40)	0.398	0.135^	9.926	**2.39×10^{-8}^**
2	336.181	8.31	100.07 (±24.28)	5.50 (±1.82)	19.12 (±6.36)	0.288	0.049^	8.129	**2.56×10^{-7}^**
3	350.1604	3.86	300.99 (±85.41)	14.09 (±4.05)	9.79 (±4.12)	1.439	0.465^	25.272	2.55×10^{-5}
4		5.96	198.08 (±55.51)	0.86 (±0.26)	2.95 (±1.20)	0.292	0.070^	104.253	**2.10×10^{-9}**
5		7.82	944.67 (±176.59)	20.79 (±10.71)	59.12 (±27.70)	0.352	0.209^	23.640	**2.10×10^{-9}**
6	352.1760	0.94	19.38 (±14.30)	243.47 (±57.96)	145.89 (±38.00)	1.669	0.172^	0.100	9.64×10^{-6}
7		4.47	11.24 (±5.42)	517.41 (±121.23)	296.50 (±66.21)	1.745	0.123^	0.028	**5.61×10^{-9}^**
8		8.48 & 8.66	728.18 (±253.87)	24.53 (±9.99)	100.61 (±34.85)	0.244	0.043^	11.638	**1.13×10^{-7}^**
9	366.1550	0.93	694.26 (±271.16)	39.94 (±22.00)	39.43 (±26.99)	1.013	0.545	17.492	**1.27×10^{-6}**
10		5.28	615.03 (±131.57)	68.62 (±33.44)	75.25 (±49.40)	0.899	0.664^	8.550	**3.57×10^{-7}**
11		8.50	12.94 (±3.93)	30.94 (±6.20)	9.96 (±1.97)	3.106	8.82×10^{-3}^	0.633	0.207^
12	368.1709	1.05	173.98 (±23.60)	108.23 (±30.60)	167.93 (±57.65)	0.644	0.370^	1.260	0.445^
13		5.47	1745.32 (±327.54)	1070.55 (±316.79)	1739.33 (±614.62)	0.615	0.756^	1.242	0.516^
14		7.21	247.22 (±48.52)	32.18 (±10.07)	59.34 (±17.97)	0.542	0.200^	5.403	**6.12×10^{-7}^**
15	386.1815	2.21	13.37 (±3.54)	30.54 (±12.04)	53.67 (±15.71)	0.569	0.254^	0.318	0.221
16	388.1527	5.14	1.81 (±0.42)	59.57 (±14.63)	28.08 (±8.57)	2.121	0.076^	0.041	2.77×10^{-6}
17	392.1709	11.03	51.75 (±17.11)	4.24 (±0.97)	9.84 (±2.24)	0.431	0.021^	7.351	2.81×10^{-6}^

The PAs that vary as a result of within plant variation in flowering ragwort plants were Metabolites 1, 2, 4, 5, 7, 8, 9, 10 and 14. These PAs were identified using exact mass information to calculate the empirical formula followed by fragmentation of the molecule using Q-TOFMS CID (collision induced dissociation) at 30eV (Table 2.4.). Metabolites 1 and 2 were identified as seneciphylline ($C_{18}H_{24}NO_5$) and senecionine ($C_{18}H_{26}NO_5$), respectively (Table 2.4.). Seneciphylline and senecionine are the only PAs with this elemental compositions that have been reported in ragwort (da Silva *et al.* 2006, Joosten *et al.* 2010). The seneciphylline and senecionine standards also eluted at the same time as Metabolites 1 and 2. In addition, fragmentation of both structures gave rise to two ion characteristic of retronecine PAs which were ± 5ppm of the calculated *m/z* 138.0919 ($C_8H_{12}NO$) and 120.0813 ($C_8H_{10}N$) (Rösemann 2006). The structure of Metabolite 4 was tentatively identified as seneciphylline N-oxide ($C_{18}H_{24}NO_6$) (Table 2.4.). Q-TOFMS CID fragmentation was not performed on this metabolite, but the presence in full scan of the dimer ($C_{36}H_{47}N_2O_{12}$) suggested that the PA was most likely to be an N-oxide (Qi *et al.* 2009b). As seneciphylline N-oxide was the only N-oxide of this elemental composition, its identity was tentatively confirmed. Metabolite 5 was identified as erucifoline ($C_{18}H_{24}NO_6$), the presence of characteristic fragment ions of this structure rules out other potential PAs (Table 2.4.). Q-TOFMS CID revealed fragment ions ± 5ppm of the calculated *m/z* 209.1178 ($C_{12}H_{17}O_3$), 174.1256 ($C_9H_{18}O_3$) and 146.0943 ($C_7H_{14}O_3$), and ensured it could not be jacozine, riddelline and seneciphylline N-oxide respectively. Q-TOFMS CID of Metabolite 7 identified it as either retrorsine or usaramine ($C_{18}H_{26}NO_6$), however the observed fragments were unable to differentiate between the two PA isomers (Table 2.4.). The elemental composition of Metabolite 8 was confirmed as $C_{18}H_{26}NO_6$. However, Metabolite 8 was not identified because, as previously mentioned, it is thought to represent two PAs that had not separated using the LC program employed. Of the PAs previously reported in ragwort tissues, Metabolite 8 could be retrorsine, usaramine or jacobine. The analyses of Metabolites 9 and 10 were unable to determine their identity (Table 2.4.). As the only PAs with the elemental composition $C_{18}H_{24}NO_7$ reported in ragwort were N-oxides, it was assumed that they were N-oxides. Of the PA N-oxides previously reported in ragwort, metabolites 9 and 10 could be erucifoline N-oxide, riddelline N-oxide or jacobine N-oxide. Metabolite 14 was identified as either retrorsine N-oxide or usaramine N-oxide (Table 2.4.). Q-TOFMS CID revealed a characteristic fragment ion of ± 5ppm of the calculated *m/z* 178.1232 ($C_{11}H_{16}NO$) that demonstrated that Metabolite 14 was not jacobine. However, the fragmentation pattern was unable to determine between the isomeric structures of retrorsine N-oxide and usaramine N-oxide.

Table 2.4. Identification of PAs that significantly vary between the different tissues of ragwort flowering plants. Metabolites were detected using UPLC-TOFMS in positive ionisation mode. Fragments were obtained using Q-TOF MS CID. ^ Unidentified PA options include retrorsine, usaramine and jacobine. * PA N-oxide options include erucifoline, riddelline and jacozine.

Metabolite number	*m/z* of observed ion	UPLC-TOFMS r.t.	Putative formula	Δ PPM	Theoretical mass of ion	*m/z* of additional ions and fragments	Formula of additional and fragment ion	Identity
1	334.1660	7.47	$C_{18}H_{24}NO_5$	1.8	334.1654	138.0919 120.0813	$C_8H_{12}NO$ $C_8H_{10}N$	Seneciphylline
2	336.1812	8.31	$C_{18}H_{26}NO_5$	0.3	336.1811	138.0919 120.0813	$C_8H_{12}NO$ C8H10N	Senecionine
4	350.1591	5.96	$C_{18}H_{24}NO_6$	-3.7	350.1604	699.3219	$C_{36}H_{47}N_2O_{12}$	Seneciphylline N-oxide
5	350.1605	7.82	$C_{18}H_{24}NO_6$	0.3	350.1604	322.1654 288.1600 209.1178 174.1256 146.0943 138.0919 120.0813	$C_{17}H_{24}NO_5$ $C_{17}H_{22}NO_3$ $C_{12}H_{17}O_3$ $C_9H_{18}O_3$ $C_7H_{14}O_3$ $C_8H_{12}NO$ $C_8H_{10}N$	Erucifoline
7	352.1760	4.47	$C_{18}H_{26}NO_6$	0.0	352.1760	308.1498 280.1549 262.1443 234.1494 194.1545 162.0892 155.1072 120.0813	$C_{16}H_{22}NO_5$ $C_{15}H_{22}NO_4$ $C_{15}H_{20}NO_3$ $C_{14}H_{20}NO_2$ $C_{12}H_{20}NO$ $C_7H_{14}O_4$ $C_9H_{15}O_2$ $C_8H_{10}N$	Retrorsine or Usaramine

Table 2.4. continued....

Metabolite number	*m/z* of observed ion	UPLC-TOFMS r.t.	Putative formula	Δ PPM	Theoretical mass of ion	*m/z* of additional ions and fragments	Formula of additional and fragment ion	Identity
8	352.1765	8.48 & 8.66	$C_{18}H_{26}NO_6$	1.4	352.1760	324.1881 246.1494 220.1338 202.1205 190.1232 178.1232 164.1075 153.0916 138.0919 136.0762 119.0735	$C_{17}H_{26}NO_5$ $C_{15}H_{20}NO_2$ $C_{13}H_{18}NO_2$ $C_{10}H_{18}O_4$ $C_{12}H_{16}NO$ $C_{11}H_{16}NO$ $C_{10}H_{14}NO$ $C_9H_{13}O_2$ $C_8H_{12}NO$ $C_8H_{10}NO$ C_8H_9N	Unidentified PA^
9	366.1554	0.93	$C_{18}H_{24}NO_7$	0.3	366.1553	-	-	unknown N-oxide*
10	366.1552	5.28	$C_{18}H_{24}NO_7$	-0.3	366.1553	294.1341 164.1049	$C_{15}H_{20}NO_5$ $C_7H_{16}O_4$	unknown N-oxide*
14	368.1710	7.21	$C_{18}H_{26}NO_7$	0.3	368.1709	246.1494 220.1338 178.1232 136.0762	$C_{15}H_{20}NO_2$ $C_{13}H_{18}NO_2$ $C_{11}H_{16}NO$ $C_8H_{10}NO$	Retrorsine N-oxide or Usaramine N-oxide

2.4.1.3. Identification of other metabolites that varied within flowering plant tissues

Nine of the 138 discriminatory metabolites observed in the comparisons of extracts of flowers with leaves were identified as PAs. An additional 15 metabolites (not PAs) were assigned putative identities (metabolites 18-32, Table 2.5.), so that in total 17% of all discriminatory metabolites were identified into metabolite types or classes. Metabolite 18, a metabolite observed at high concentrations in leaves of both ages when compared to flowers was identified as caffeoylquinic acid (a chlorogenic acid) (Table 2.5.). Q-TOFMS CID analysis of the $[M-H]^-$ ion resulted in an ion corresponding to quinic acid (*m/z* 191.0556) which corresponded to the loss of caffeic acid ($C_9H_8O_3$). This fragmentation pattern is consistent with the identity of Metabolite 18 being caffeoylquinic acid (Treutter 2005).

Table 2.5. Identified metabolites that significantly varied between the different tissues of ragwort flowering plants. Metabolites were detected using UPLC-TOFMS in positive and negative ionisation modes. Fragmentation patterns were determined using Q-TOFMS CID. Fold changes were calculated by dividing average metabolite concentration (determined in 10µl injections, equivalent to 0.26mg of fresh leaf material) in the plant tissue with the highest concentration with the tissue with the lower average value. Differences between plant tissues were tested using t-tests if marked with a ^, unmarked P-values were obtained using the non-parametric Mann-Whitney test. * Indicates that LOD values were used to calculate fold changes, this occurred when the concentration of a metabolite was below levels that could be detected.

Metabolite number	Observed ion (*m/z*)	Charge of observed ion	UPLC-TOFMS r.t.	Putative formula	Theoretical mass of ion	Δ PPM	*m/z* of additional ions and fragments	Formula of fragment ion	Fold change	P-value	Putative identity
High in both new and old leaves compared to flowers											
18	353.0871	$[M-H]^-$	8.21	$C_{16}H_{17}O_9$	353.0873	-0.6	191.0556	$C_7H_{11}O_6$	9.96	5.38×10^{-14}^	Caffeoylquinic acid
19	751.2078	$[M+H]^+$	9.01	$C_{34}H_{39}O_{19}$	751.2086	1.2	589.1557 465.1033 287.0913	$C_{28}H_{29}O_{14}$ $C_{21}H_{21}O_{12}$ $C_{16}H_{15}O_5$	4.72	1.21×10^{-15}^	Flavonoid diglycoside
High in old leaves compared to flowers											
20	565.3024	$[M+H]^+$	14.31	$C_{30}H_{45}O_{10}$	565.3013	1.9	317.2481 299.2375 281.2269	$C_{21}H_{33}O_2$ $C_{21}H_{31}O$ $C_{21}H_{29}$	130.15	5.34×10^{-8}	C21 steroid malonylglyco-side
21	317.2486	$[M+H]^+$	16.22	$C_{21}H_{33}O_2$	317.2481	1.6	299.2375 281.2269 255.2113 241.1956 203.1800 109.0659 97.0655	$C_{21}H_{31}O$ $C_{21}H_{29}$ $C_{19}H_{27}$ $C_{18}H_{25}$ $C_{15}H_{23}$ C_7H_9O C_6H_9O	74.07	5.34×10^{-8}	C21 steroid

Table 2.5. continued...

Metabolite number	Observed ion (*m/z*)	Charge of observed ion	UPLC-TOFMS r.t.	Putative formula	Theoretical mass of ion	Δ PPM	*m/z* of additional ions and fragments	Formula of fragment ion	Fold change	P-value	Putative identity
High in old leaves compared to flowers											
22	315.2315	$[M+H]^+$	17.17	$C_{21}H_{31}O_2$	315.2324	-2.9	297.2218 279.2113 255.2113 239.1800 177.1279	$C_{21}H_{29}O$ $C_{21}H_{27}$ $C_{19}H_{27}$ $C_{18}H_{23}$ $C_{12}H_{17}O$	42.08	2.03×10^{-8}^	C21 steroid
High in new leaves compared to flowers											
23	645.2182	$[M-H]^-$	12.65	$C_{32}H_{37}O_{14}$	645.2183	-0.2	601.2285	$C_{31}H_{37}O_{12}$	1.67	5.34×10^{-8}	Flavonoid diglycoside
24	213.1495	$[M-H]^-$	14.36	$C_{12}H_{21}O_3$	213.1491	1.9	-	-	2.13	5.34×10^{-8}	Oxododecanoic acid
High in flowers compared to new and old leaves											
25	463.0872	$[M-H]^-$	9.58	$C_{21}H_{19}O_{12}$	463.0877	-1.1	301.0346 271.0243 255.0293 178.9980 151.0031	$C_{15}H_9O_7$ $C_{14}H_7O_6$ $C_{14}H_7O_5$ $C_8H_3O_5$ $C_7H_3O_4$	18.77	3.15×10^{-11}	Flavonoid glycoside
26	477.1031	$[M-H]^-$	10.26	$C_{22}H_{21}O_{12}$	477.1033	-0.4	545.0907 955.2144 357.0610 315.0505 285.0399 271.0243 257.0450 243.0293	$C_{23}H_{22}O_{14}Na$ $C_{44}H_{43}O_{24}$ $C_{18}H_{13}O_8$ $C_{16}H_{11}O_7$ $C_{15}H_9O_6$ $C_{14}H_7O_6$ $C_{14}H_9O_5$ $C_{13}H_7O_5$	227.84	3.15×10^{-11}	Flavonoid glycoside

Table 2.5. continued...

Metabolite number	Observed ion (*m/z*)	Charge of observed ion	UPLC-TOFMS r.t.	Putative formula	Theoretical mass of ion	Δ PPM	*m/z* of additional ions and fragments	Formula of fragment ion	Fold change	P-value	Putative identity
High in flowers compared to new and old leaves											
27	563.1040	$[M-H]^-$	10.94	$C_{25}H_{23}O_{15}$	563.1037	1.4	-	-	14.15*	3.15×10^{-11}	Flavonoid malonyglycoside
27	565.1195	$[M+H]^+$	10.94	$C_{25}H_{25}O_{15}$	565.1193	0.4	317.0661 302.0428 245.0450 217.0504 203.0341 153.0188	$C_{16}H_{13}O_7$ $C_{15}H_{10}O_7$ $C_{13}H_9O_5$ $C_{12}H_9O_4$ $C_{11}H_7O_4$ $C_7H_5O_4$	18.18	1.26×10^{-10}	Flavonoid malonyglycoside
28	327.2173	$[M-H]^-$	13.85	$C_{18}H_{31}O_5$	327.2171	0.6	395.2046 229.1440 211.1334	$C_{19}H_{32}O_7Na$ $C_{12}H_{21}O_4$ $C_{12}H_{19}O_3$	28.41	6.02×10^{-23}^	Trihydroxyocta-decadienoic acid
29	329.2326	$[M-H]^-$	14.36	$C_{18}H_{33}O_5$	329.2328	-0.6	329.2202 229.1440 211.1334	$C_{19}H_{34}O_7Na$ $C_{12}H_{21}O_4$ $C_{12}H_{19}O_3$	55.91	3.15×10^{-11}	Trihydroxyocta-decenoic acid
30	295.2274	$[M-H]^-$	18.13	$C_{18}H_{31}O_3$	295.2273	0.3	277.2168	$C_{18}H_{29}O_2$	14.52	2.58×10^{-14}^	Hydroxyocta-decadienoic acid
High in flowers compared to old leaves											
31	611.1614	$[M+H]^+$	8.90	$C_{27}H_{31}O_{16}$	465.1033	-1.7	751.2078 465.1025 303.0505	$C_{34}H_{39}O_{19}$ $C_{21}H_{21}O_{12}$ $C_{15}H_{11}O_7$	3.03	8.74×10^{-10}^	Flavonoid diglycoside

Table 2.5. continued...

Metabolite number	Observed ion (*m/z*)	Charge of observed ion	UPLC-TOFMS r.t.	Putative formula	Theoretical mass of ion	Δ PPM	*m/z* of additional ions and fragments	Formula of fragment ion	Fold change	P-value	Putative identity
High in flowers compared to new leaves											
32	433.2352	$[M-H]^-$	18.30	$C_{21}H_{38}O_7P$	433.2355	-0.7	501.2229 279.2324 171.0058 152.9953	$C_{22}H_{39}O_9PNa$ $C_{18}H_{31}O_2$ $C_3H_8O_6P$ $C_3H_6O_5P$	6.86	1.86×10^{-11}^	Octadecadienoyl-glycero-phosphate

Many of the metabolites in the comparisons of leaves and flowers from flowering plants were identified as conjugated flavonoids. Metabolites 19 and 23 were at higher concentration in leaves compared to flowers, whereas Metabolites 25, 26, 27, and 31 were high in flowers compared to leaves (Table 2.5.). Some flavonoids were detected in both positive and negative ESI modes, e.g. metabolite 27. Metabolites 25, 26 and 27 were identified as flavonoids conjugated with one sugar group (Table 2.5.). For instance, Q-TOFMS CID of the $[M-H]^-$ ion of Metabolite 25 resulted in the observation of the unconjugated flavonoid ± 5ppm of the *m/z* 301.0346 and elemental composition $C_{15}H_9O_7$, by examining the corresponding losses the conjugate was identified as a glycoside (loss of $C_6H_{10}O_5$). Analysis of the $[M-H]^-$ ion of Metabolite 26 using Q-TOFMS CID gave rise to a flavonoid fragment ± 5ppm of the *m/z* 315.0505 and elemental composition $C_{16}H_{11}O_7$, which corresponded to the loss of a glycoside from the parent ion. Metabolite 27 was identified as a flavonoid malonylglycoside, and was observed in positive and negative ESI MS modes. In negative ESI the $[M-H]^-$ ion was observed ± 5ppm of the *m/z* 563.1037 and elemental composition $C_{25}H_{23}O_{15}$. Q-TOFMS CID of the $[M+H]^+$ ion revealed the flavonoid fragment ± 5ppm of the *m/z* 317.0661 ($C_{16}H_{13}O_7$), which corresponded to the loss of a malonylglycoside ($C_9H_{12}O_8$). Metabolites 19, 23 and 31 were identified as flavonoids conjugated with two sugar groups (Table 2.5.). Metabolite 19 was identified as a flavonoid conjugated with both a glycoside and possibly an alkylglycoside sugar ($C_{34}H_{39}O_{19}$). Q-TOFMS CID of the $[M+H]^+$ ion revealed fragments corresponding to the loss of a glycoside (*m/z* 589.1557) and a possible loss of an alkylglycoside (*m/z* 465.1033) sugar. The $[M-H]^-$ of Metabolite 23 was identified as a flavonoid diglycoside ± 5ppm of the *m/z* 645.2183 and elemental composition $C_{32}H_{37}O_{14}$ using UPLC-TOFMS. Q-TOFMS CID of the $[M+H]^+$ ion of Metabolite 31 revealed a fragment ± 5ppm of the *m/z* 465.1025 corresponding to the loss of sugar group of the elemental composition ($C_6H_{10}O_4$). Further fragmentation of the metabolite revealed the flavonoid fragment ± 5ppm of the *m/z* 303.0505 ($C_{15}H_{11}O_7$), which corresponded to the loss of an additional glycoside conjugate ($C_6H_{10}O_5$). Thus, the basic structure of Metabolite 31 was confirmed as a flavonoid diglycoside. The observation of a related ion ± 5ppm of the *m/z* 751.2078 (elemental composition: $C_{34}H_{39}O_{19}$) revealed further conjugation of the flavonoid diglycoside that could not be determined.

In old leaf material, two free plant C21 steroids were detected as the $[M+H]^+$ ions and were ± 5ppm of the *m/z* 317.2481 and 315.2324 (Metabolites 21 & 22, Table 2.5.). Q-TOFMS CID fragmentation gave rise to ions consistent with loss of one (*m/z* 299.2375 and 297.2218) and two water molecules (*m/z* 281.2269 and 279.2113). In addition, analyses of both metabolites gave rise to a fragment ion ± 5ppm of the *m/z* 255.2113 ($C_{19}H_{27}$). The observation of this

fragment ion corresponded to the steroid backbone which suggested that Metabolites 21 and 22 were free plant steroids. Also observed in old leaves, Metabolite 20 was identified as the malonylglycoside conjugate of a similar C21 steroid (Table 2.5.). Q-TOFMS CID fragmentation gave rise to a steroid fragment ± 5ppm of the *m/z* 317.2481, which corresponded to the loss of a malonylglycoside conjugate ($C_9H_{12}O_8$).

Using accurate mass and likely elemental composition measured using UPLC NanoSpray, Metabolite 24 was identified as the saturated fatty acid oxododecanoic acid (Table 2.5.). Metabolites 28, 29 and 30 were identified as unsaturated hydroxy fatty acids (Table 2.5.). Metabolites 28 and 29 were identified as trihydroxyoctadecadienoic acid and trihydroxyoctadecenoic acid, respectively. The structures of Metabolites 28 and 29 differ only in the degree of saturation, but clear chromatography separations were still observed; Metabolite 29 was more saturated with only a single double bond, whereas Metabolite 28 had two. This similarity in structure was reflected in their chromatography behaviour, both metabolites formed a sodium formate adduct in Q-TOF analyses (*m/z* 395.2046 and 329.2202). Q-TOFMS CID of both $[M-H]^-$ ions gave rise to two fragments in common ± 5ppm of the *m/z* 229.1440 and 211.1334. Metabolite 30 was identified as hydroxyoctadecadienoic acid. Q-TOFMS CID revealed a fragmentation ion ± 5ppm of the *m/z* 277.2168 that corresponded to the loss of water, a loss commonly observed when hydroxyoctadecadienoic acids are fragmented (Guo *et al.* 2012). Metabolite 32 was identified as octadecadienoyl-glycero-phosphate, a phospholipid (Table 2.5.). Q-TOFMS CID gave rise to ions ± 5ppm of *m/z* 279.2324 and 171.0058 which corresponded to the fatty acid and the phospholipid head respectively.

In summary, higher concentrations of eight PAs (Metabolites 1, 2, 4, 5, 8, 9, 10 & 14) and three unsaturated fatty acids (Metabolites 28-30) were observed in flowers when compared with leaves of any age (see summary Table 2.6.). In addition, the phospholipid octadecadienoyl-glycero-phosphate (Metabolite 32) was observed in higher levels in flowers than new leaves. When the leaves of flowering plants were compared to flowers, concentrations of one PA (Metabolite 7) and caffeoylquinic acid (a chlorogenic acid, Metabolite 18) increased regardless of leaf age. Old leaves contained higher concentrations of plant steroids when compared to flowers (Metabolites 20-22). Higher concentrations of oxododecanoic acid (Metabolite 24) were observed in new leaves when compared to flowers. No clear flavonoid pattern was observed between the tissues of flowering plants, both in terms of broad classification and level of conjugation. Many other concentration differences of unidentified structures were

also detected between plant tissues, and the mass spectrometry information is given in the supplementary material (Tables S2.1. & S2.2.).

Table 2.6. Summary of the metabolites identified in the different plant tissues of ragwort plants. Unless indicated ([a] = compared to new leaves, [b] = compared to flowers and [c] = compared to old leaves) comparisons were made between all other tissues from the same ontogenetic-stage. The magnitude of the fold change between tissues was indicated as follows 2-5 fold increase (+), 5-10 fold increase (++), 10-50 fold increase (+++) and a greater than 50 fold increase (++++).

Metabolite number	Putative identity	Metabolite class	High in flowering plant tissue			High in vegetative plant tissue	
			Flowers	New leaves	Old leaves	New leaves	Old leaves
1	Seneciphylline	Pyrrolizidine alkaloid	++				
2	Senecionine	Pyrrolizidine alkaloid	++				
4	Seneciphylline N-oxide	Pyrrolizidine alkaloid	++++				
5	Erucifoline	Pyrrolizidine alkaloid	+++				
7	Retrorsine or Usaramine	Pyrrolizidine alkaloid		+++[b]	+++[b]		
8	Unidentified PA	Pyrrolizidine alkaloid	+++				
9	Unidentified N-oxide	Pyrrolizidine alkaloid	+++				
10	Unidentified N-oxide	Pyrrolizidine alkaloid	++				
14	Retrorsine or Usaramine N-oxide	Pyrrolizidine alkaloid	++				
28	Trihydroxyoctadecadienoic acid	Hydroxy-unsaturated fatty acid	+++				
29	Trihydroxyoctadecenoic acid	Hydroxy-unsaturated fatty acid	++++			++	
30	Hydroxyoctadecadienoic acid	Hydroxy-unsaturated fatty acid	+++			++	
24	Oxododecanoic acid	Saturated fatty acid		+[b]			
32	Octadecadienoylglycero-phosphate	Phospholipid	++[a]				
18	Caffeoylquinic acid	Chlorogenic acid		++[b]	++[b]		
20	C21 steroid malonylglycoside	Steroid			++++[b]		
21	C21 steroid	Steroid			++++[b]		++++
22	C21 steroid	Steroid			++++[b]		+++

Table 2.6. continued...

Metabolite number	Putative identity	Metabolite class	High in flowering plant tissue			High in vegetative plant tissue	
			Flowers	New leaves	Old leaves	New leaves	Old leaves
19	Flavonoid diglycoside	Flavonoid		+[b]	+[b]		
23	Flavonoid diglycoside	Flavonoid		+[b]			
25	Flavonoid glycoside	Flavonoid	+++				
26	Flavonoid glycoside	Flavonoid	++++				
27	Flavonoid malonylglycoside	Flavonoid	+++				
31	Flavonoid diglycoside	Flavonoid	+[c]				

2.4.2. Vegetative plants

2.4.2.1. Multivariate modelling of variation between vegetative plant tissues

Initial PCA modelling of the positive and negative datasets revealed no outliers, therefore all samples were included in the analyses. Clear separations were observed in the positive and negative datasets using a combination of the first two principle components (Figure 2.6.). A small amount of the datasets' variation were explained by the models (positive ESI: R^2X= 0.203, negative ESI: R^2X= 0.182). Clear separations were observed using supervised OPLS-DA modelling of both the positive and negative datasets (Figure 2.7.). For the analyses of the datasets of both ESI modes, a high amount of variation was described (in both cases R^2Y > 0.980) as was the predictive ability of the models (for all variables of both models Q^2 > 0.745) (Table 2.1.). Metabolites responsible for the observed separations were extracted from the models using 'S'-plots. A total of 26 metabolites of interest were identified in the positive and negative datasets, 13 were found in higher concentrations in new leaves and the remaining 13 were higher in old leaves.

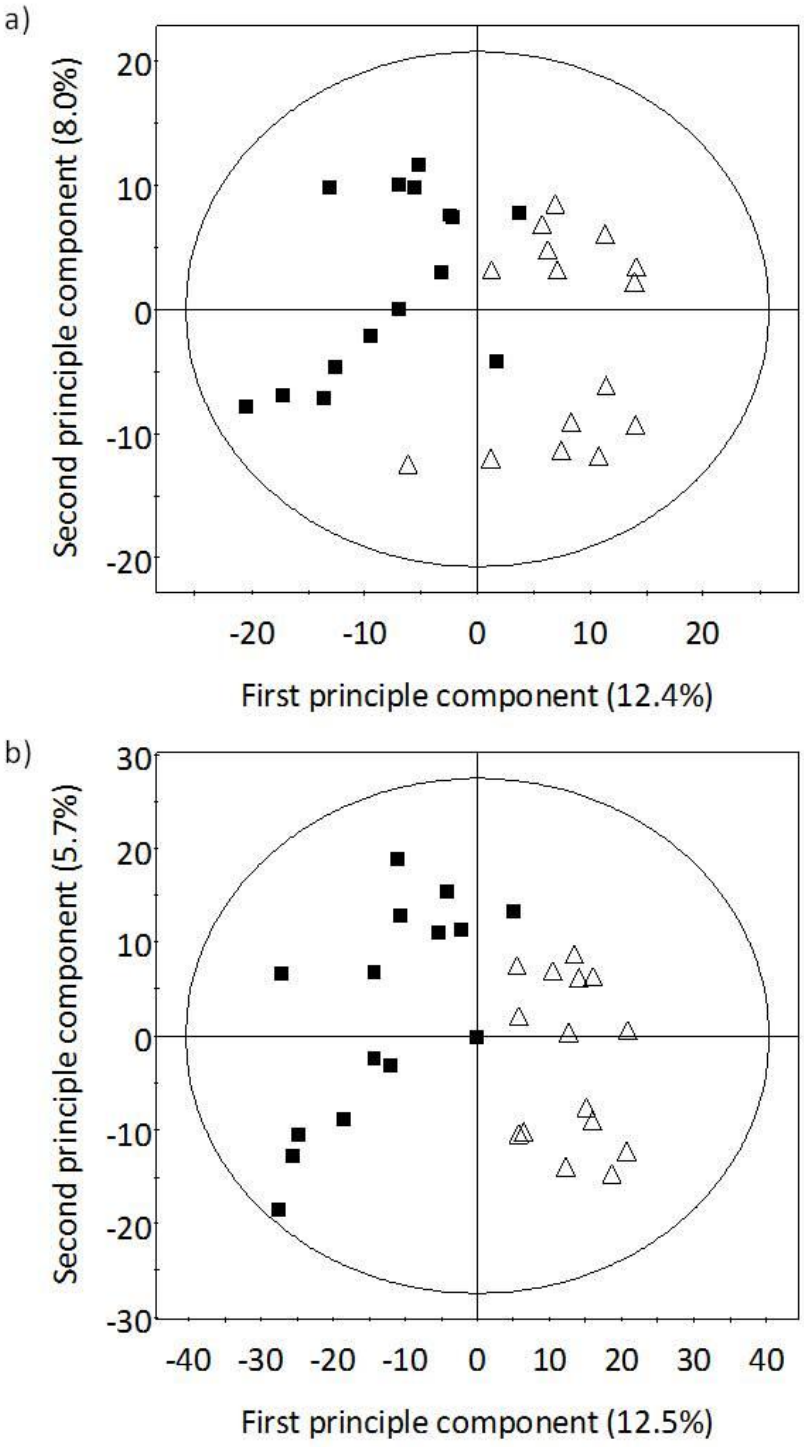

Figure 2.6. Principle component analysis (PCA) scores plots of the chemical profiles of ragwort vegetative plants. Datasets were collected using UPLC-TOFMS in a) positive and b) negative ESI MS modes. The percentages of explained variation (R^2X) modelled for the first two principle components are displayed on the axes. New leaves are unfilled triangles and old leaves are black squares.

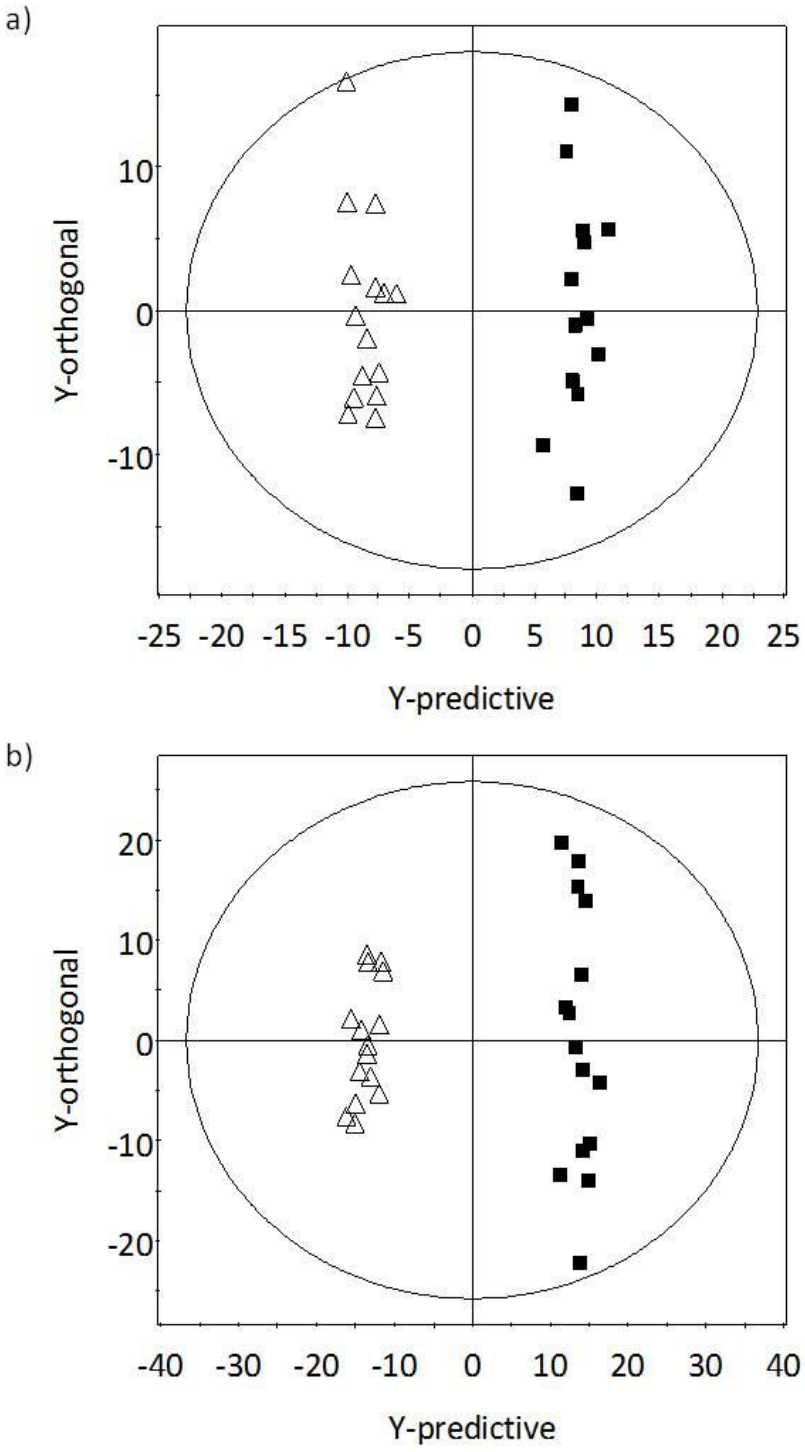

Figure 2.7. Orthogonal partial least squared-discriminate analysis (OPLS-DA) score plots of the chemical profiles of ragwort vegetative plants. Datasets were collected using UPLC-TOFMS in a) positive and b) negative ESI MS modes. New leaves are unfilled triangles and old leaves are black squares.

2.4.2.2. Identification metabolites that varied within vegetative plant tissues

Of the 26 metabolite signals of interest observed in comparisons of vegetative plant material, four (15%) were assigned putative identities (Table 2.7.). The information regarding the unidentified metabolites observed in negative and positive mode is displayed in the supplementary material (Tables S2.3. & S2.4.). None of the Metabolites of interest were identified as PAs, a conclusion corroborated by manual quantification of the PA signals in vegetative ragwort material (Table 2.8.). Like flowering plant material, 18 PAs were observed but 17 peaks were quantified due to poor separation of two PA signals (*m/z*: 352.1760; r.t.: 8.48 & 8.66 minutes). In negative ESI MS mode, high concentrations of two unsaturated hydroxy fatty acids were observed as the $[M-H]^-$ ions in new leaf material (metabolites 29 & 30, Tables 2.6. & 2.7.). Fragmentation of these fatty acids revealed that they were the same as those already identified in the comparison of flowering plants. Two free plant C21 steroids were found in significantly higher concentrations in old leaf material (Metabolites 21 & 22, Tables 2.6. & 2.7.). These free steroids were detected in positive ESI MS mode as $[M+H]^+$ ions. Q-TOFMS CID fragmentation revealed that these metabolites were the same free plant steroids that were observed in previous comparisons made between flowering plant tissues, and were identified using the same characteristic fragment ion ± 5ppm of *m/z* 255.2113.

Table 2.7. Identified metabolites that significantly varied between the different tissues of ragwort vegetative plants. Metabolites were detected using UPLC-TOFMS in positive and negative ionisation modes. Fold changes were calculated by dividing average metabolite concentration (determined in 10µl injections, equivalent to 0.26mg of fresh leaf material) in the plant tissue with the highest concentration with the tissue with the lower average value. Differences between plant tissues were tested using t-tests if marked with a ^, unmarked P-values were obtained using the non-parametric Mann-Whitney test.

Metabolite number	Observed ion (*m/z*)	Charge of observed ion	UPLC-TOFMS r.t.	Putative formula	Theoretical mass of ion	Δ PPM	*m/z* of additional ions and fragments	Formula of fragment ion	Fold change	P-value	Putative identity
High in new leaves compared to old leaves											
29	329.2331	$[M-H]^-$	14.36	$C_{18}H_{33}O_5$	329.2328	0.9	229.1440 211.1334 171.1021	$C_{12}H_{21}O_4$ $C_{12}H_{19}O_3$ $C_9H_{15}O_3$	5.18	3.11×10^{-9}^	Trihydroxyocta-decenoic acid
30	295.2273	$[M-H]^-$	18.13	$C_{18}H_{31}O_3$	295.2273	0.0	363.2147 277.2168 195.1385	$C_{19}H_{32}O_5Na$ $C_{18}H_{29}O_2$ $C_{12}H_{19}O_2$	5.85	5.33×10^{-7}^	Hydroxyocta-decadienoic acid
High in old leaves compared to new leaves											
21	317.2483	$[M+H]^+$	16.22	$C_{21}H_{33}O_2$	317.2481	0.6	299.2375 281.2269 255.2113 241.1956 203.1800 109.0659 97.0655	$C_{21}H_{31}O$ $C_{21}H_{29}$ $C_{19}H_{27}$ $C_{18}H_{25}$ $C_{15}H_{23}$ C_7H_9O C_6H_9O	74.34	2.50×10^{-7}	C21 steroid
22	315.2326	$[M+H]^+$	17.17	$C_{21}H_{31}O_2$	315.2324	0.6	297.2218 279.2113 255.2113 239.1800 177.1279	$C_{21}H_{29}O$ $C_{21}H_{27}$ $C_{19}H_{27}$ $C_{18}H_{23}$ $C_{12}H_{17}O$	14.29	1.25×10^{-6}	C21 steroid

Table 2.8. Concentrations (mean ±S.E., determined in 10µl injections, equivalent to 0.26mg of fresh leaf material) of PA type structures observed in the different tissues of ragwort vegetative plants. PAs were detected using UPLC-TOFMS in positive ionisation mode. Seventeen signals, corresponding to 18 PAs, were observed. Fold changes were calculated by dividing average PA concentration in new leaves with old leaves. Differences between plant tissues were tested using t-tests if marked with a ^, unmarked P-values were obtained using the non-parametric Mann-Whitney test. No tests remained significant after Bonferroni corrections were applied.

m/z	UPLC-TOFMS r.t.	new leaves	old leaves	new versus old leaves	
				fold dif.	P-value
334.1654	7.47	38.30 (±16.24)	11.46 (±4.81)	3.342	0.239^
336.181	8.31	14.04 (±11.77)	15.76 (±9.12)	0.891	0.239^
350.1604	3.86	158.59 (±98.55)	8.46 (±3.64)	18.746	0.961^
	5.96	20.51 (±6.93)	25.24 (±24.49)	0.813	0.202^
	7.82	466.66 (±227.36)	117.97 (±55.35)	3.956	0.137^
352.1760	4.47	8.29 (±4.72)	91.62 (±46.28)	0.090	0.066^
	8.48 & 8.66	154.89 (±132.87)	101.86 (±53.91)	1.521	0.659^
366.155	0.93	245.69 (±104.55)	116.72 (±79.16)	2.105	0.046^
	5.28	330.75 (±83.41)	134.75 (±73.42)	2.455	2.67×10^{-3}^
	8.50	32.37 (±4.20)	25.51 (±6.27)	1.269	0.371^
368.1709	1.05	26.55 (±5.89)	70.13 (±18.82)	0.379	0.294^
	5.47	246.70 (±55.26)	788.96 (±224.09)	0.313	0.226^
	7.21	135.34 (±55.87)	94.54 (±37.85)	1.432	0.550^
386.1815	2.21	0.81 (±0.29)	9.62 (±2.78)	0.084	0.010^
388.1527	5.14	1.27 (±0.41)	19.01 (±14.44)	0.067	0.233

2.5. Discussion

In flowering ragwort, the concentrations of PAs (an important class of ragwort defensive metabolites), chlorogenic acid, fatty acids, a phospholipid, flavonoids and steroids varied substantially between leaves (old and new) and flowers. To a lesser extent, the metabolome of old and new leaves from vegetative ragwort similarly differed. These differences were mainly associated with variations in fatty acid and steroid concentrations, and no differences in PA concentrations were detected. Most of these differences followed the patterns predicted by ODT, although there were some exceptions, which highlight potential limitations of this theory.

As predicted by ODT, and in agreement with previous studies that have focused on PAs (e.g. Hartmann and Zimmer 1986), the concentrations of eight PAs were hugely elevated in flower tissues. One of these was ericufoline, a PA previously observed in ragwort to be at higher concentrations in flowers than leaves (Joshi and Vrieling 2005). The similarity between the current study and the findings of Joshi and Vrieling (2005), who examined plants from a number of different populations (but not including Southern England), suggests an important role for erucifoline in the defence of ragwort flowers irrespective of plant genotype and location. Contrary to the prediction of ODT, that tissues more valuable to the plant are the most defended, a single PA was found in lower concentrations in flowers than in leaves. It could be that an increased concentration of this PA in leaves was a function of its effectiveness against folivore insect herbivores specifically. It has been shown that the deterrent effect of PAs differs depending on the identity of both PA and insect herbivore (Macel *et al.* 2005).

ODT predicts that increased defences should be observed in new leaf material when compared to old leaves. In the current study however, no differences in PA composition or concentration were observed between the leaf material of different ages collected over both ontogenetic-stages. This contrasts with the results of a laboratory experiment that found highest concentrations of PAs in younger leaves, leading to a conclusion that the PAs of ragwort are optimally distributed (de Boer 1999). It is possible that the ragwort population in this study does not exhibit great heterogeneity in within-plant allocation of PAs: PA profiles differ greatly between ragwort populations (Macel *et al.* 2004) and environmental conditions also alter PA concentrations (Hol *et al.* 2003, Joosten *et al.* 2009). It is also possible that additional differences in PA concentrations would have been detected if the data were treated as paired points. By treating the data as paired points statistical power would have been increased,

perhaps allowing any more subtle differences in PA variation to be detected between leaf tissues. This methodological detail applies to all the analyses of PA and marker concentrations.

A total of six metabolites were identified as flavonoids in the comparisons made between the flowers and leaves of flowering plants. Significant differences in both free and conjugated flavonoids were detected, but no clear pattern in distribution was observed. Flavonoids have a range of functions in plants (Treutter 2005). They have been demonstrated to have a role in the interaction between plants and the abiotic environment (Dolzhenko *et al.* 2010, Pawlak-Sprada *et al.* 2011, Ballizany *et al.* 2012). Flavonoids also play a role in the interactions between plants and herbivores (Chapter 3, Haribal and Feeny 2003, Chen et al. 2004, Thoison et al. 2004), pathogens (Grayer and Harborne 1994), microbes (Treutter 2005) and other plant species (Chang-Hung 1999). This wide range of flavonoid function in plants is likely to give rise to a variable allocation across plant tissues. Consequently, interpreting their observed distribution in ragwort will require further identification work to pinpoint specific structures and their likely role in interspecific interactions. In this study those flavonoids observed in higher concentration in flowers may imply a role in the defence of tissues of high value to the plant.

Caffeoylquinic acid is a chlorogenic acid, a group of phenolic metabolites widely distributed across many plant species (Clifford 2000) that has been observed in the flowers of other plant species (Banos *et al.* 2012). The presence of chlorogenic acids in their food has been shown to reduce nutritional quality to Lepidoptera larvae (Felton *et al.* 1992), and is associated with plant resistance to leaf herbivores (Leiss *et al.* 2009b) and bacterial infection (Niggeweg *et al.* 2004). It might be expected therefore that chlorogenic acid would have a similar role in ragwort defence, with highest concentrations in the more valuable flowers as predicted by ODT. In contrast to this prediction, in this study the highest levels of caffeoylquinic acid were observed in the leaves of flowering ragwort plants. It could be that chlorogenic acids are effective defences against leaf feeding herbivores. Alternatively, chlorogenic acids may have a different function in leaf tissues, for example, they are known to have a regulatory role in preventing premature cell death in leaves (Tamagnone *et al.* 1998). If this was the case, higher concentrations of chlorogenic acids might be expected in old leaves. No differences in chlorogenic acid concentrations were observed between old and new leaves in this study. To determine the role of chlorogenic acids in ragwort tissues their effect on herbivores needs to be examined.

The phospholipid octadecadienoyl-glycero-phosphate was found in higher concentrations in flowers than either young or old leaves. Phospholipids are associated with seed production (Zlatanov *et al.* 2009) and this is likely to explain their higher concentrations in flowers. Increased concentrations of C21 steroids were observed in the old leaves of ragwort when compared to new leaves. This was a consistent pattern observed across both flowering and vegetative ontogenetic-stages. C21 steroids can be important precursors of cardenolides (Heasley 2012) which are toxic defensive agents detected across 12 plant families (Agrawal *et al.* 2012). If C21 steroids have a role in the defensive chemistry of ragwort, they do not follow the distribution predicted by ODT. Unsaturated hydroxy fatty acids, including two trihydroxy fatty acids, were found in higher concentrations in flowers compared to young and old leaves. In addition, increased concentrations were detected in the new leaves of vegetative plants when compared to old leaves. In other plant species, hydroxy fatty acids have been shown to play a role in plant defence against pathogenic fungi (Hou and Forman 2000). The observed distribution of hydroxy fatty acids across both ontogenetic-stages of ragwort is in accordance with the predictions made by ODT, and is consistent a with them having a defensive role.

Of those defensive metabolites that vary between ragwort tissues (n=27), 17 were distributed as predicted by ODT. This high proportion of metabolites that follow ODT (63%) gives significant support to the predictions of this theory. Thus reinforcing the conclusions of a recent meta-analysis (McCall and Fordyce 2010) which suggested that ODT had wide generality. The results presented here do not, however, represent a complete test of the predictions of the ODT. Herbivore feeding trials testing the anti-herbivore properties of the metabolites identified in this study are required to confirm their defensive role in ragwort. Moreover, a large number of metabolites were not recorded in the online databases and remained unidentified, therefore their distribution in relation to ODT could not be examined. Regardless of the identities of the unknown metabolites in the present study, some metabolites do not follow the distribution predicted by ODT. Other studies (Moreira *et al.* 2012) have noted that within-plant defence allocation patterns may depend on the metabolite class measured, with not all types of defences following the distribution predicted by ODT. This may also explain the deviations from the predictions made by ODT in this study. Alternatively, those metabolites which have within-plant distribution which contradict ODT may provide a function in ragwort that does not relate to plant defence.

In conclusion, significant metabolomic differences were detected between the above-ground tissues of flowering and vegetative ragwort plants. These differences were caused by metabolites belonging to a wide range of classes including flavonoids, unsaturated hydroxy

fatty acids and PAs. The majority, but not all, of the metabolites identified were allocated to different tissues as predicted by ODT. To understand fully the distribution of the defences present in ragwort further work is needed to characterise those currently unidentified metabolites. Continued improvements in the database resources and certified standards available to plant chemists will aid future metabolomic investigations. This study is one of the first to apply a metabolomic approach to characterise the allocation of secondary metabolite classes across plant tissues and ontogenetic stages. This study also illustrates the potential of metabolomics for studying chemical interactions between plants and other species. In the remainder of this study, metabolomic approaches have been used to characterise fully the metabolite changes that underpin the interactions between ragwort plants and other organisms, specifically nematode herbivores and arbuscular mycorrhizal fungi.

2.6. Supplementary material

Table S2.1. Unidentified metabolites that significantly varied between the different tissues of ragwort flowering plants. Metabolites were detected using UPLC-TOFMS in negative ionisation mode. Fold changes were calculated by dividing average metabolite concentration (determined in 10µl injections, equivalent to 0.26mg of fresh leaf material) in the plant tissue with the highest concentration with the tissue with the lower average value. Differences between plant tissues were tested using t-tests if marked with a ^, unmarked P-values were obtained using the non-parametric Mann-Whitney test. * Indicates that LOD values were used to calculate fold changes, this occurred when the concentration of a metabolite was below the levels that could be detected.

Observed ion (*m/z*)	Charge of observed ion	UPLC-TOFMS r.t.	Putative formula	Theoretical mass of ion	Δ PPM	*m/z* of additional ions and fragments	Formula of fragment ion	Fold change	P-value	Putative Identity
High in new and old leaves compared to flowers										
563.2278	$[M-H]^-$	8.21	$C_{32}H_{35}O_9$	563.2278	-0.5	445.2015 189.1270 173.0422	$C_{28}H_{29}O_5$ $C_{13}H_{17}O$ $C_7H_9O_5$	22.44	3.15×10^{-11}	-
649.2279	$[M-H]^-$	9.41	$C_{35}H_{37}O_{12}$	649.2285	-0.9	-	-	20.31	3.15×10^{-11}	-
373.1496	$[M-H]^-$	11.46	$C_{17}H_{24}O_9$	373.1499	-0.8	769.2895 329.1600 287.1495 269.1389 225.1491 209.1178 207.1385	$C_{34}H_{50}O_{18}Na$ $C_{16}H_{25}O_7$ $C_{14}H_{23}O_6$ $C_{14}H_{21}O_5$ $C_{13}H_{21}O_3$ $C_{12}H_{17}O_3$ $C_{13}H_{19}O_2$	14.66	3.15×10^{-11}	-

Table S2.1. continued....

Observed ion (*m/z*)	Charge of observed ion	UPLC-TOFMS r.t.	Putative formula	Theoretical mass of ion	Δ PPM	*m/z* of additional ions and fragments	Formula of fragment ion	Fold change	P-value	Putative Identity
High in new and old leaves compared to flowers										
653.3231	$[M-H]^-$	13.17	$C_{26}H_{53}O_{18}$	653.3232	-0.2	721.3106	$C_{27}H_{54}O_{20}Na$	27.91	3.15×10^{-11}	-
						535.2966	$C_{22}H_{47}O_{14}$			
						477.2911	$C_{20}H_{45}O_{12}$			
						175.0242	$C_6H_7O_6$			
739.3170	$[M-H]^-$	13.85	$C_{35}H_{51}O_{16}$	739.3177	-0.9	695.3279	$C_{35}H_{51}O_{14}$	16.16	3.67×10^{-16}^	Malonyl-glycoside conjugate
						591.3169	$C_{32}H_{47}O_{10}$			
						477.2852	$C_{27}H_{41}O_7$			
						459.2747	$C_{27}H_{39}O_6$			
						315.2324	$C_{21}H_{31}O_2$			
						175.0243	$C_6H_7O_6$			
						161.0450	$C_6H_9O_5$			
						113.0236	$C_5H_5O_3$			
481.2581	$[M-H]^-$	17.78	$C_{29}H_{37}O_6$	481.2581	-1.9	549.2464	$C_{30}H_{38}O_8Na$	6.76	3.02×10^{-14}^	-
						253.2172	$C_{16}H_{29}O_2$			
						245.0455	$C_{13}H_9O_5$			
785.3902	$[M-H]^-$	18.47	$C_{46}H_{57}O_{11}$	785.3901	0.1	-	-	19.98	6.27×10^{-22}^	-
929.4738	$[M-H]^-$	18.64	$C_{46}H_{73}O_{19}$	929.4746	-0.9	997.4620	$C_{46}H_{74}O_{21}Na$	10.45	1.00×10^{-14}^	-
						883.4691	$C_{45}H_{71}O_{17}$			
						865.4586	$C_{45}H_{69}O_{16}$			
						675.3533	$C_{40}H_{51}O_9$			
						605.2328	$C_{41}H_{33}O_5$			
						587.2222	$C_{41}H_{31}O_4$			
						397.1346	$C_{15}H_{25}O_{12}$			

Table S2.1. continued....

Observed ion (*m/z*)	Charge of observed ion	UPLC-TOFMS r.t.	Putative formula	Theoretical mass of ion	Δ PPM	*m/z* of additional ions and fragments	Formula of fragment ion	Fold change	P-value	Putative Identity
High in new and old leaves compared to flowers										
767.4146	$[M-H]^-$	19.67	$C_{47}H_{59}O_9$	767.4159	-1.7	835.4033	$C_{48}H_{60}O_{11}Na$	6.14	1.31×10^{-11}^	-
						721.4104	$C_{46}H_{57}O_7$			
689.3625	$[M-H]^-$	19.87	$C_{48}H_{49}O_4$	689.3631	-0.9	-	-	10.01	7.58×10^{-16}^	-
High in new leaves compared to flowers										
933.2264	$[M-H]^-$	8.89	$C_{24}H_{53}O_{37}$	933.2266	-0.2	595.1358	$C_{19}H_{31}O_{21}$	4.16	3.18×10^{-13}^	-
						337.0923	$C_{16}H_{17}O_8$			
						191.0556	$C_7H_{11}O_6$			
417.2122	$[M-H]^-$	10.77	$C_{20}H_{33}O_9$	417.2125	-0.7	485.1999	$C_{21}H_{34}O_{11}Na$	23.76	6.49×10^{-18}^	Glycoside conjugate
						237.1491	$C_{14}H_{21}O_3$			
						179.0556	$C_6H_{11}O_6$			
						161.0450	$C_6H_9O_5$			
721.3643	$[M-H]^-$	16.76	$C_{34}H_{57}O_{16}$	721.3647	-0.6	789.3521	$C_{35}H_{58}O_{18}Na$	5.59	1.21×10^{-12}^	Glycoside conjugate
						675.3592	$C_{33}H_{55}O_{14}$			
						415.1452	$C_{15}H_{55}O_{14}$			
						397.1346	$C_{15}H_{27}O_{13}$			
						305.0873	$C_{12}H_{17}O_9$			
						287.0767	$C_{12}H_{15}O_8$			
						277.2168	$C_{18}H_{29}O_2$			
						235.0818	$C_9H_{15}O_7$			
						179.0556	$C_6H_{11}O_6$			
						161.0450	$C_6H_9O_5$			
787.3958	$[M-H]^-$	17.96	$C_{35}H_{63}O_{19}$	787.3964	-0.8	855.3838	$C_{36}H_{64}O_{21}Na$	20.68	5.34×10^{-8}	-
						509.1659	$C_{24}H_{29}O_{12}$			
						225.0035	$C_9H_5O_7$			

Table S2.1. continued....

Observed ion (*m/z*)	Charge of observed ion	UPLC-TOFMS r.t.	Putative formula	Theoretical mass of ion	Δ PPM	*m/z* of additional ions and fragments	Formula of fragment ion	Fold change	P-value	Putative Identity
High in new leaves compared to flowers										
481.2537	$[M-H]^-$	18.13	$C_{22}H_{35}N_5O_7$	481.2336	0.2	253.2168 245.0450 227.0331	$C_{16}H_{29}O_2$ $C_{13}H_9O_5$ $C_{11}H_5N_3O_3$	7.07	3.82×10^{-13}^	-
803.3974	$[M-H]^-$	18.13	$C_{39}H_{64}O_{15}P$	803.3983	-1.1	-	-	4.58	2.55×10^{-7}^	-
885.4866	$[M-H]^-$	18.13	$C_{45}H_{73}O_{17}$	885.4848	2.0	931.4903	$C_{46}H_{75}O_{19}$	10.70	1.04×10^{-10}^	-
947.4855	$[M-H]^-$	18.30	$C_{46}H_{75}O_{20}$	947.4852	0.3	883.4691	$C_{45}H_{71}O_{17}$	4.38	2.28×10^{-9}^	-
943.4895	$[M-H]^-$	18.98	$C_{47}H_{75}O_{19}$	943.4903	-0.8	-	-	3.71	8.65×10^{-14}^	-
691.3777	$[M-H]^-$	19.15	$C_{30}H_{59}O_{17}$	691.3752	3.6	-	-	1.84	1.95×10^{-11}^	-
723.4266	$[M-H]^-$	19.15	$C_{46}H_{59}O_7$	723.4261	0.7	769.4316 705.4155 513.3005 445.2015 277.2168 227.1283 209.1178	$C_{47}H_{61}O_9$ $C_{46}H_{57}O_6$ $C_{34}H_{41}O_4$ $C_{28}H_{29}O_5$ $C_{18}H_{29}O_2$ $C_{12}H_{19}O_4$ $C_{12}H_{17}O_3$	2.00	9.14×10^{-9}^	-
765.4098	$[M-H]^-$	19.32	$C_{33}H_{65}O_{19}$	765.4120	-2.9	537.3273	$C_{26}H_{49}O_{11}$	1.94	5.97×10^{-9}^	-
739.4282	$[M-H]^-$	19.32	$C_{39}H_{63}O_{13}$	739.4269	1.8	785.4323 721.4163 513.3064	$C_{40}H_{65}O_{15}$ $C_{39}H_{61}O_{12}$ $C_{27}H_{45}O_9$	9.88	5.34×10^{-8}	-
801.4636	$[M-H]^-$	19.32	$C_{41}H_{69}O_{15}$	801.4636	0.0	445.2015 277.2168 253.0923 227.1283 209.1178	$C_{28}H_{29}O_5$ $C_{18}H_{29}O_2$ $C_9H_{17}O_8$ $C_{12}H_{19}O_4$ $C_{12}H_{17}O_3$	5.81	5.34×10^{-8}	-

Table S2.1. continued....

Observed ion (*m/z*)	Charge of observed ion	UPLC-TOFMS r.t.	Putative formula	Theoretical mass of ion	Δ PPM	*m/z* of additional ions and fragments	Formula of fragment ion	Fold change	P-value	Putative Identity
High in new leaves compared to flowers										
869.5112	$[M-H]^-$	19.32	$C_{42}H_{77}O_{18}$	869.5110	0.2	-	-	1.72	1.62×10^{-7}^	-
707.3781	$[M-H]^-$	19.49	$C_{41}H_{55}O_{10}$	707.3795	-2.0	-	-	8.39	7.43×10^{-11}^	-
723.4247	$[M-H]^-$	19.49	$C_{46}H_{59}O_{7}$	723.4261	-1.9	-	-	6.39	3.68×10^{-9}^	-
797.4314	$[M-H]^-$	19.67	$C_{41}H_{65}O_{15}$	797.4323	-1.1	-	-	8.46	3.41×10^{-10}^	-
763.3846	$[M-H]^-$	19.84	$C_{47}H_{55}O_{9}$	763.3846	0.3	-	-	10.27	7.95×10^{-13}^	-
907.4868	$[M-H]^-$	20.18	$C_{44}H_{75}O_{19}$	907.4903	-3.9	975.4777	$C_{45}H_{76}O_{21}Na$	1.77	7.03×10^{-11}^	-
777.4157	$[M-H]^-$	20.52	$C_{52}H_{57}O_{6}$	777.4155	0.3	-	-	1.95	5.34×10^{-8}	-
865.4930	$[M-H]^-$	20.69	$C_{46}H_{73}O_{15}$	865.4949	-2.2	-	-	1.55	3.97×10^{-10}^	-
771.4460	$[M-H]^-$	21.38	$C_{41}H_{68}O_{11}Cl$	771.4450	1.3	-	-	4.27	4.78×10^{-11}^	-
High in old leaves compared to flowers										
287.0766	$[M-H]^-$	3.59	$C_{12}H_{15}O_{8}$	287.0767	-0.3	171.0657	$C_{8}H_{11}O_{4}$	200.03	$5.34 \times 10^{-8-}$	-
545.2231	$[M-H]^-$	9.23	$C_{25}H_{37}O_{13}$	545.2234	-0.6	337.0771 235.0454 193.0348	$C_{12}H_{17}O_{11}$ $C_{8}H_{11}O_{8}$ $C_{6}H_{9}O_{7}$	31.84	8.81×10^{-22}^	-
453.1968	$[M-H]^-$	9.58	$C_{19}H_{33}O_{12}$	453.1972	-0.9	277.1651 175.0243	$C_{13}H_{25}O_{6}$ $C_{6}H_{7}O_{6}$	39.45*	5.34×10^{-8}	-
965.6415	$[M-H]^-$	10.43	$C_{50}H_{93}O_{17}$	965.6416	0.2	-	-	81.70	5.34×10^{-8}	
287.1494	$[M-H]^-$	10.60	$C_{14}H_{23}O_{6}$	287.1495	-0.3	269.1389 227.1283 209.1178	$C_{14}H_{21}O_{5}$ $C_{12}H_{19}O_{4}$ $C_{12}H_{17}O_{3}$	15.38	3.42×10^{-10}^	-
369.1181	$[M-H]^-$	10.77	$C_{17}H_{21}O_{9}$	369.1186	-1.4	240.9984 198.9879	$C_{9}H_{5}O_{8}$ $C_{7}H_{3}O_{7}$	62.86	6.57×10^{-13}^	-

Table S2.1. continued....

Observed ion (*m/z*)	Charge of observed ion	UPLC-TOFMS r.t.	Putative formula	Theoretical mass of ion	Δ PPM	*m/z* of additional ions and fragments	Formula of fragment ion	Fold change	P-value	Putative Identity
High in old leaves compared to flowers										
417.2119	$[M-H]^-$	10.77	$C_{20}H_{33}O_9$	417.2125	-1.4	485.1999	$C_{21}H_{34}O_{11}Na$	18.90	2.45×10^{-13}^	Glycoside conjugate
						835.4327	$C_{40}H_{67}O_{18}$			
						237.1491	$C_{14}H_{21}O_3$			
						179.0556	$C_6H_{11}O_6$			
357.1197	$[M-H]^-$	10.94	$C_{16}H_{21}O_9$	357.1186	3.1	241.9984	$C_9H_5O_8$	14.97	1.24×10^{-13}^	-
539.1912	$[M-H]^-$	10.94	$C_{29}H_{31}O_{10}$	539.1917	-0.9	495.2019	$C_{28}H_{31}O_8$	20.31	1.90×10^{-13}^	Glycoside conjugate
						277.1651	$C_{13}H_{25}O_6$			
						161.0450	$C_6H_9O_5$			
805.2861	$[M-H]^-$	11.29	$C_{46}H_{45}O_{13}$	805.2860	0.1	643.2332	$C_{40}H_{35}O_8$	26.51	3.74×10^{-7}	
631.2233	$[M-H]^-$	12.83	$C_{28}H_{39}O_{16}$	631.2238	-0.8	-	-	39.45*	5.34×10^{-8}	-
525.1978	$[M-H]^-$	13.51	$C_{25}H_{33}O_{12}$	525.1972	1.1	353.1236	$C_{17}H_{21}O_8$	123.79	5.34×10^{-8}	
739.3183	$[M-H]^-$	13.68	$C_{36}H_{51}O_{16}$	739.3177	0.8	695.3279	$C_{35}H_{51}O_{14}$	32.02	3.75×10^{-21}^	Malonylglyco-side conjugate
						677.3173	$C_{35}H_{49}O_{13}$			
						653.3172	$C_{33}H_{49}O_{13}$			
						635.3068	$C_{33}H_{47}O_{12}$			
						591.3169	$C_{32}H_{47}O_{10}$			
						577.3013	$C_{31}H_{45}O_{10}$			
						477.2852	$C_{27}H_{41}O_7$			
						459.2747	$C_{27}H_{39}O_6$			
						315.2324	$C_{21}H_{31}O_2$			
						175.0243	$C_6H_7O_6$			
						161.0450	$C_6H_9O_5$			
						113.0239	$C_5H_5O_3$			
581.2962	$[M-H]^-$	13.85	$C_{30}H_{45}O_{11}$	581.2962	0.0	-	-	44.51	1.60×10^{-14}^	-

Table S2.1. continued....

Observed ion (*m/z*)	Charge of observed ion	UPLC-TOFMS r.t.	Putative formula	Theoretical mass of ion	Δ PPM	*m/z* of additional ions and fragments	Formula of fragment ion	Fold change	P-value	Putative Identity
High in old leaves compared to flowers										
839.2358	$[M-H]^-$	13.85	$C_{23}H_{51}O_{32}$	839.2363	-0.6	-	-	10.61*	5.34×10^{-8}	-
519.2961	$[M-H]^-$	14.71	$C_{29}H_{43}O_8$	519.2958	0.6	565.3013 587.2832	$C_{30}H_{45}O_{10}$ $C_{30}H_{44}O_{10}Na$	53.02	5.98×10^{-14}^	-
869.4165	$[M-H]^-$	14.88	$C_{43}H_{65}O_{18}$	869.4171	-0.7	-	-	595.01	5.34×10^{-8}	-
293.2115	$[M-H]^-$	18.81	$C_{18}H_{29}O_3$	289.2117	-0.7	361.1991	$C_{19}H_{30}O_5Na$	76.48	5.34×10^{-8}	-
763.3990	$[M-H]^-$	20.18	$C_{51}H_{55}O_6$	763.3999	-1.2	-	-	10.81	5.36×10^{-10}^	-
849.4941	$[M-H]^-$	20.69	$C_{53}H_{69}O_9$	849.4942	2.4	917.4816	$C_{54}H_{70}O_{11}Na$	5.56	5.34×10^{-8}	-
845.4688	$[M-H]^-$	21.72	$C_{46}H_{59}O_{14}$	845.4687	0.1	-	-	77.32	5.34×10^{-8}	-
High in flowers compared to new and old leaves										
991.2156	$[M-H]^-$	10.26	$C_{47}H_{43}O_{24}$	991.2144	1.2	-	-	21.66*	3.15 x 10-^{11}	-
909.1663	$[M-H]^-$	12.31	$C_{49}H_{33}O_{18}$	909.1667	-0.4	313.0348	$C_{33}H_{24}O_{11}$	26.15*	3.15 x 10-^{11}	-
947.4066	$[M-H]^-$	12.48	$C_{51}H_{63}O_{17}$	947.4065	0.1	785.3537	$C_{45}H_{53}O_{12}$	44.95	3.15 x 10-^{11}	-
785.3536	$[M-H]^-$	13.85	$C_{45}H_{53}O_{12}$	785.3537	-0.1	853.3411	$C_{46}H_{54}O_{14}Na$	69.32	3.15 x 10-^{11}	-
831.3595	$[M-H]^-$	14.01	$C_{46}H_{55}O_{14}$	831.3592	0.4	-	-	23.07	3.15 x 10-^{11}	-
815.3643	$[M-H]^-$	14.08	$C_{46}H_{55}O_{13}$	815.3643	0.0	883.3517	$C_{47}H_{56}O_{15}Na$	41.23	3.15 x 10-^{11}	-
555.2585	$[M-H]^-$	16.07	$C_{31}H_{39}O_9$	555.2597	-1.6	623.2468	$C_{32}H_{40}O_{11}Na$	6.97	6.47×10^{-11}^	-
683.2642	$[M-H]^-$	16.25	$C_{43}H_{39}O_8$	555.2597	-1.6	751.2518	$C_{44}H_{40}O_{10}Na$	159.33	3.15 x 10-^{11}	-
293.2117	$[M-H]^-$	18.30	$C_{18}H_{29}O_3$	293.2117	0.0	-	-	13.88	6.31×10^{-11}	Acid

Table S2.1. continued....

Observed ion (*m/z*)	Charge of observed ion	UPLC-TOFMS r.t.	Putative formula	Theoretical mass of ion	Δ PPM	*m/z* of additional ions and fragments	Formula of fragment ion	Fold change	P-value	Putative Identity
High in flowers compared to new leaves										
377.0871	$[M-H]^-$	12.31	$C_{18}H_{17}O_9$	377.0873	-0.5	-	-	14.52*	5.34×10^{-8}	-
High in flowers compared to old leaves										
743.2176	$[M-H]^-$	11.80	$C_{36}H_{39}O_{17}$	743.2187	-1.5	811.2061 611.1401 321.0974 167.0344	$C_{37}H_{40}O_{19}Na$ $C_{30}H_{27}O_{14}$ $C_{16}H_{17}O_7$ $C_8H_7O_4$	24.77	8.79×10^{-12}^	-
582.2453	$[M-H]^-$	13.00	$C_{41}H_{32}N_3O$	582.2454	-0.3	-	-	32.78*	5.34×10^{-8}	-
815.3071	$[M-H]^-$	15.56	$C_{48}H_{47}O_{12}$	815.3068	0.4	883.2942 797.2962 593.1084 503.2070 485.1964 299.0192	$C_{49}H_{48}O_{14}Na$ $C_{48}H_{45}O_{11}$ $C_{33}H_{21}O_{11}$ $C_{30}H_{31}O_7$ $C_{30}H_{29}O_6$ $C_{15}H_7O_7$	11.32	5.76×10^{-10}^	-
573.2644	$[M-H]^-$	16.59	$C_{38}H_{37}O_5$	573.2641	0.5	641.2515 555.2535 351.0657 215.0556	$C_{39}H_{38}O_7Na$ $C_{38}H_{35}O_4$ $C_{23}H_{11}O_4$ $C_9H_{11}O_6$	9.68	3.52×10^{-10}^	-
703.4270	$[M-H]^-$	18.47	$C_{36}H_{63}O_{13}$	703.4269	0.1	483.2747	$C_{29}H_{39}O_6$	26.56*	5.34×10^{-8}	-
687.4328	$[M-H]^-$	21.20	$C_{36}H_{36}O_{12}$	687.4320	1.2	-	-	48.54	2.15×10^{-12}^	-

Table S2.2. Unidentified metabolites that significantly varied between the different tissues of ragwort flowering plants. Metabolites were detected using UPLC-TOFMS in positive ionisation mode. Fold changes were calculated by dividing average metabolite concentration (determined in 10µl injections, equivalent to 0.26mg of fresh leaf material) in the plant tissue with the highest concentration with the tissue with the lower average value. Differences between plant tissues were tested using t-tests if marked with a ^, unmarked P-values were obtained using the non-parametric Mann-Whitney test. * Indicates that LOD values were used to calculate fold changes, this occurred when the concentration of a metabolite was below the levels that could be detected.

Observed ion (*m/z*)	Charge of observed ion	UPLC-TOFMS r.t.	Putative formula	Theoretical mass of ion	Δ PPM	*m/z* of additional ions and fragments	Formula of fragment ion	Fold change	P-value	Putative Identity
High in new and old leaves compared to flowers										
419.2285	$[M+H]^+$	10.18	$C_{20}H_{35}O_9$	419.2281	1.0	441.2101	$C_{20}H_{34}O_9Na$	40.52	4.38×10^{-9}	glycoside conjugate
						279.1572	$C_{14}H_{24}O_4Na$			
						257.1753	$C_{14}H_{25}O_4$			
						203.0532	$C_6H_{12}O_6Na$			
375.1649	$[M+H]^+$	10.92	$C_{17}H_{27}O_9$	375.1655	-0.6	397.1475	$C_{17}H_{26}O_9Na$	17.65	3.15×10^{-11}	-
						392.1921	$C_{17}H_{30}NO_9$			
						357.1549	$C_{17}H_{25}O_8$			
						353.1576	$C_{16}H_{26}O_7Na$			
						311.1471	$C_{14}H_{24}O_6Na$			
						293.1365	$C_{14}H_{24}O_6Na$			
						271.1545	$C_{14}H_{23}O_5$			
						253.1440	$C_{14}H_{21}O_4$			
						249.1467	$C_{13}H_{22}O_3Na$			
						235.1334	$C_{14}H_{19}O_3$			
797.2633	$[M+H]^+$	13.25	$C_{34}H_{50}O_{19}Cl$	797.2635	-0.3	-	-	69.99	3.15×10^{-11}	-

Table S2.2. continued...

Observed ion (*m/z*)	Charge of observed ion	UPLC-TOFMS r.t.	Putative formula	Theoretical mass of ion	Δ PPM	*m/z* of additional ions and fragments	Formula of fragment ion	Fold change	P-value	Putative Identity
High in new and old leaves compared to flowers										
779.2756	$[M+H]^+$	13.25	$C_{37}H_{47}O_{18}$	779.2762	-0.8	693.2758	$C_{34}H_{45}O_{15}$	85.02	3.15×10^{-11}	-
						633.2547	$C_{32}H_{42}O_{13}$			
						605.2598	$C_{31}H_{41}O_{12}$			
						517.2438	$C_{28}H_{37}O_9$			
						317.2481	$C_{21}H_{33}O_2$			
741.3263	$[M+H]^+$	13.25	$C_{43}H_{49}O_{11}$	741.3275	-1.6	758.3540	$C_{43}H_{52}NO_{11}$	45.71	3.15×10^{-11}	-
						763.3094	$C_{43}H_{48}O_{11}Na$			
						587.2832	$C_{30}H_{44}O_{10}Na$			
						543.2934	$C_{29}H_{44}O_8Na$			
409.2745	$[M+H]^+$	18.97	$C_{27}H_{37}O_3$	407.2743	0.5	391.2637	$C_{27}H_{35}O_2$	18.12	6.55×10^{-18}^	-
						300.2089	$C_{20}H_{28}O_2$			
						287.2011	$C_{19}H_{27}O_2$			
						234.1620	$C_{15}H_{22}O_2$			
						221.1542	$C_{14}H_{21}O_2$			
						203.1436	$C_{14}H_{19}O$			
						175.1123	$C_{12}H_{15}O$			
						165.0916	$C_{10}H_{13}O_2$			
742.4643	$[M+H]^+$	19.19	$C_{41}H_{64}N_3O_9$	472.4643	0.0	545.3802	$C_{28}H_{53}N_2O_8$	6.12	2.21×10^{-10}	-
						382.2018	$C_{23}H_{28}NO_4$			
745.4206	$[M+Na]^+$	19.72	$C_{32}H_{66}O_{17}Na$	745.4198	1.1	740.4644	$C_{32}H_{70}NO_{17}$	4.48	2.95×10^{-15}^	-
						519.2934	$C_{27}H_{44}O_8Na$			
						467.1893	$C_{21}H_{32}O_{10}Na$			
705.4177	$[M+H]^+$	19.82	$C_{37}H_{62}O_{11}Na$	705.4190	-1.8	687.4084	$C_{37}H_{60}O_{10}Na$	5.96	1.47×10^{-16}^	Glycoside conjugate
						543.3662	$C_{31}H_{52}O_6Na$			

Table S2.2. continued...

Observed ion (*m/z*)	Charge of observed ion	UPLC-TOFMS r.t.	Putative formula	Theoretical mass of ion	Δ PPM	*m/z* of additional ions and fragments	Formula of fragment ion	Fold change	P-value	Putative Identity
High in new and old leaves compared to flowers										
717.4253	$[M+Na]^+$	20.25	$C_{44}H_{58}N_2O_5Na$	717.4243	1.5	712.4689	$C_{44}H_{63}N_3O_5$	1.87	1.51×10^{-11}^	-
High in new leaves compared to flowers										
597.1434	$[M+H]^+$	8.27	$C_{26}H_{29}O_{16}$	597.1456	-3.7	619.1273 465.1040 435.0939 303.0500	$C_{26}H_{28}O_{16}Na$ $C_{21}H_{21}0_{12}$ $C_{20}H_{19}0_{11}$ $C_{15}H_{11}O_7$	2.39	8.87×10^{-7}^	Glycoside conjugate
581.1509	$[M+H]^+$	8.90	$C_{26}H_{29}O_{15}$	581.1506	0.5	449.0931 287.0556 133.0501	$C_{17}H_{21}O_{14}$ $C_{15}H_{11}O_6$ $C_5H_9O_4$	3.43	2.94×10^{-11}^	-
677.3729	$[M+H]^+$	16.64	$C_{33}H_{57}O_{14}$	677.3748	-2.8	694.4014 699.3568 537.3040	$C_{33}H_{60}NO_{14}$ $C_{33}H_{56}O_{14}Na$ $C_{27}H_{46}O_9Na$	5.62	9.34×10^{-10}^	Glycoside conjugate
515.3241	$[M+H]^+$	17.81	$C_{27}H_{47}O_9$	515.3220	4.1	532.3486 537.3064	$C_{27}H_{50}NO_9$ $C_{27}H_{46}O_9Na$	8.26	4.05×10^{-12}^	-
909.4697	$[M+Na]^+$	18.13	$C_{59}H_{66}O_7Na$	909.4706	-1.0	904.5152 689.4182 545.3818 463.2249	$C_{59}H_{70}NO_7$ $C_{44}H_{58}O_5Na$ $C_{31}H_{54}O_6Na$ $C_{30}H_{32}O_3Na$	10.83	5.34×10^{-8}	-
725.4418	$[M+H]^+$	19.19	$C_{46}H_{61}O_7$	725.4417	0.1	747.4237 385.2015	$C_{46}H_{60}O_7Na$ $C_{23}H_{29}O_5$	6.03	3.02×10^{-13}^	-
759.4240	$[M+Na]^+$	20.03	$C_{47}H_{60}O_7Na$	759.4237	0.4	754.4683	$C_{47}H_{64}NO_7$	2.11	6.07×10^{-7}^	-
583.4109	$[M+H]^+$	20.25	$C_{35}H_{55}N_2O_5$	583.4111	-0.3	-	-	3.47	1.43×10^{-10}^	-
409.3780	$[M+H]^+$	22.15	$C_{25}H_{49}N_2O_2$	409.3794	-3.1	-	-	12.11	1.92×10^{-7}	-

Table S2.2. continued...

Observed ion (*m/z*)	Charge of observed ion	UPLC-TOFMS r.t.	Putative formula	Theoretical mass of ion	Δ PPM	*m/z* of additional ions and fragments	Formula of fragment ion	Fold change	P-value	Putative Identity
High in old leaves compared to flowers										
409.1810	$[M+H]^+$	9.65	$C_{28}H_{25}O_3$	409.1804	1.5	-	-	13.94	8.65×10^{-12}^	-
547.3475	$[M+H]^+$	10.71	$C_{28}H_{51}O_{10}$	547.3482	-1.3	363.3110 345.3005	$C_{20}H_{43}O_5$ $C_{20}H_{40}O_4$	12.00*	5.34×10^{-8}	-
577.2130	$[M+Na]^+$	11.34	$C_{23}H_{38}O_{15}Na$	577.2108	3.8	572.2554 533.2210 401.1788 357.1889 315.1784 271.0430 227.0532	$C_{23}H_{42}NO_{15}$ $C_{22}H_{38}O_{13}Na$ $C_{17}H_{30}O_9Na$ $C_{16}H_{30}O_7Na$ $C_{14}H_{28}O_6Na$ $C_9H_{12}O_8Na$ $C_8H_{12}O_6Na$	6.00	2.66×10^{-13}^	-
655.3334	$[M+H]^+$	12.61	$C_{33}H_{51}O_{13}$	655.3330	0.6	677.3149 479.3009 317.2481 299.2375 281.2269 163.0606 145.0501	$C_{33}H_{50}O_{13}Na$ $C_{27}H_{43}O_7$ $C_{21}H_{33}O_2$ $C_{21}H_{31}O$ $C_{21}H_{29}$ $C_6H_{11}O_5$ $C_6H_9O_4$	21.90*	5.34×10^{-8}	-
769.2801	$[M+H]^+$	13.25	$C_{50}H_{41}O_8$	769.2825	2.3	-	-	826.76	5.34×10^{-8}	-
741.3408	$[M+H]^+$	13.25	$C_{29}H_{57}O_{21}$	741.3392	2.2	763.3212 758.3658 723.3287 299.2375	$C_{29}H_{56}O_{21}Na$ $C_{29}H_{60}NO_{21}$ $C_{29}H_{55}O_{20}$ $C_{21}H_{31}O$	229.95	5.34×10^{-8}	
425.0938	$[M+H]^+$	13.25	$C_{15}H_{21}O_{14}$	425.0931	1.6	-	-	34.49*	5.34×10^{-8}	-
393.2798	$[M+H]^+$	19.50	$C_{27}H_{37}O_2$	393.2794	1.0	-	-	7.20	7.76×10^{-13}^	-

Table S2.2. continued...

Observed ion (*m/z*)	Charge of observed ion	UPLC-TOFMS r.t.	Putative formula	Theoretical mass of ion	Δ PPM	*m/z* of additional ions and fragments	Formula of fragment ion	Fold change	P-value	Putative Identity
High in flowers compared to new and old leaves										
611.1619	$[M+H]^+$	9.01	C27H31O16	611.1612	1.1	633.1432 338.0427 317.0849 185.0450 173.0450	C27H30O16Na C18H10O7 C11H18O9Na C8H9O5 C7H9O5	67.81	3.39×10^{-27}^	-
346.1286	$[M+H]^+$	10.39	C18H20NO6	346.1291	-1.4	-	-	17.97	6.64×10^{-13}^	-
787.3750	$[M+H]^+$	13.36	$C_{38}H_{59}O_{17}$	787.3752	-0.3	809.3572 641.3173 623.3068 521.2598 478.2625 421.2074 572.1800 204.0998	$C_{38}H_{58}O_{17}Na$ $C_{32}H_{49}O_{13}$ $C_{32}H_{47}O_{12}$ $C_{24}H_{41}O_{12}$ $C_{19}H_{42}O_{13}$ $C_{19}H_{33}O_{10}$ $C_{21}H_{23}$ $C_9H_{16}O_5$	97.26	3.15 x 10-^{11}	-
353.2308	$[M+Na]^+$	13.99	$C_{18}H_{34}O_5Na$	353.2304	1.1	-	-	320.94	3.15 x 10-^{11}	-
323.2065	$[M+H]^+$	20.56	$C_{15}H_{31}O_7$	323.2070	-1.5	281.1964	$C_{13}H_{29}O_6$	9.73	4.80×10^{-16}^	-
296.2012	$[M+H]^+$	20.56	$C_{20}H_{26}NO$	296.2014	-0.7	-	-	9.44	5.39×10^{-16}^	-
451.3776	$[M+H]^+$	23.00	$C_{28}H_{51}O_4$	451.3787	-2.4	473.3607	$C_{28}H_{50}O_4Na$	226.73	5.34×10^{-8}	Steroidal structure?
479.4103	$[M+H]^+$	23.53	$C_{30}H_{55}O_4$	479.4100	0.6	501.3920	$C_{30}H_{54}O_4Na$	5.23	8.92×10^{-9}^	-

Table S2.2. continued...

Observed ion (*m/z*)	Charge of observed ion	UPLC-TOFMS r.t.	Putative formula	Theoretical mass of ion	Δ PPM	*m/z* of additional ions and fragments	Formula of fragment ion	Fold change	P-value	Putative Identity
High in flowers compared to new leaves										
422.1450	$[M+H]^+$	13.36	$C_{20}H_{24}NO_9$	422.1452	-0.2	-	-	30.51	4.27×10^{-18}^	-
413.1600	$[M+H]^+$	13.36	$C_{23}H_{25}O_7$	413.1600	0.0	-	-	34.75	2.18×10^{-22}^	-
316.2849	$[M+H]^+$	16.64	$C_{18}H_{38}NO_3$	316.2852	-0.9	298.2745 280.2640 262.2526 250.2537	$C_{18}H_{36}NO_2$ $C_{18}H_{34}NO$ $C_{18}H_{32}N$ $C_{17}H_{32}N$	5.31	3.13×10^{-11}^	-
718.4590	$[M+H]^+$	20.56	$C_{44}H_{65}NO_5P$	718.4600	-1.4	-	-	3.34	2.43×10^{-8}^	
676.4180	$[M+H]^+$	20.56	$C_{36}H_{58}N_3O_9$	676.4173	1.0	-	-	5.63	5.34×10^{-8}	-
282.1867	$[M+H]^+$	20.56	$C_{19}H_{24}NO$	282.1858	3.2	-	-	8.75	5.34×10^{-8}	-
625.4257	$[M+H]^+$	21.20	$C_{42}H_{57}O_4$	625.4257	1.4	-	-	20.45*	1.60×10^{-6}	-
High in flowers compared to old leaves										
631.1597	$[M+H]^+$	8.16	$C_{37}H_{27}O_{10}$	631.1604	-1.1	487.1182 445.1076 427.1029 337.0923 277.0712 259.0606 255.0657 229.0712 193.0501 187.0606 169.0501 149.0239	$C_{31}H_{19}O_6$ $C_{29}H_{17}O_5$ $C_{22}H_{19}O_9$ $C_{16}H_{17}O_8$ $C_{14}H_{13}O_6$ $C_{14}H_{11}O_5$ $C_{15}H_{11}O_4$ $C_{10}H_{13}O_6$ $C_{10}H_9O_4$ $C_8H_{11}O_5$ $C_8H_9O_4$ $C_8H_5O_3$	3.97	9.52×10^{-11}^	-
595.1931	$[M+H]^+$	10.18	$C_{17}H_{39}O_{22}$	595.1933	-0.3	-	-	11.25	1.28×10^{-9}^	-

Table S2.2. continued...

Observed ion (*m/z*)	Charge of observed ion	UPLC-TOFMS r.t.	Putative formula	Theoretical mass of ion	Δ PPM	*m/z* of additional ions and fragments	Formula of fragment ion	Fold change	P-value	Putative Identity
High in flowers compared to old leaves										
617.1778	$[M+H]^+$	10.28	$C_{19}H_{37}O_{22}$	617.1776	0.3	-	-	9.81	1.68×10^{-7}^	-
745.2285	$[M+H]^+$	11.55	$C_{43}H_{37}O_{12}$	745.2285	0.0	767.2104 762.2551 641.1694	$C_{43}H_{36}O_{12}Na$ $C_{43}H_{40}NO_{12}$ $C_{26}H_{34}O_{17}Na$	17.70	1.07×10^{-7}	-
270.1706	$[M+H]^+$	13.25	$C_{14}H_{24}NO_4$	270.1705	0.4	292.1525	$C_{14}H_{23}NO_4Na$	5.47	1.98×10^{-7}^	-
High in new leaves compared to old leaves										
493.4219	$[M+H]^+$	21.84	$C_{26}H_{57}N_2O_6$	493.4217	0.4	-	-	17.26	2.50×10^{-11}^	-
507.4375	$[M+H]^+$	22.15	$C_{27}H_{59}N_2O_6$	507.4373	0.4	-	-	24.69	4.49×10^{-12}^	-
515.4105	$[M+H]^+$	23.21	$C_{33}H_{55}O_4$	515.4100	1.0	537.3920 532.4366	$C_{33}H_{58}NO_4$ $C_{33}H_{54}O_4Na$	6.08	7.56×10^{-11}^	-
634.5314	$[M+H]^+$	23.32	$C_{41}H_{68}N_3O_2$	634.5312	0.3	-	-	27.91	2.71×10^{-9}^	-
507.4374	$[M+H]^+$	23.64	$C_{27}H_{59}N_2O_6$	507.4373	0.2	-	-	25.23	1.77×10^{-14}^	-

Table S2.3. Unidentified metabolites that significantly varied between the different tissues of vegatative flowering plants. Metabolites were detected using UPLC-TOFMS in negative ionisation mode. Fold changes were calculated by dividing average metabolite concentration (determined in 10µl injections, equivalent to 0.26mg of fresh leaf material) in the plant tissue with the highest concentration with the tissue with the lower average value. Differences between plant tissues were tested using t-tests if marked with a ^, unmarked P-values were obtained using the non-parametric Mann-Whitney test.

Observed ion (*m/z*)	Charge of observed ion	UPLC-TOFMS r.t.	Putative formula	Theoretical mass of ion	Δ PPM	*m/z* of additional ions and fragments	Formula of fragment ion	Fold change	P-value	Putative identity
High in new leaves compared to old leaves										
213.1491	$[M-H]^-$	14.36	$C_{12}H_{21}O_3$	213.1491	0.0	281.1365	$C_{13}H_{22}O_5Na$	8.95	7.37×10^{-8}^	Oxo-dodecanoic acid?
663.3016	$[M-H]^-$	14.54	$C_{34}H_{47}O_{13}$	663.3017	-0.2	471.2383	$C_{27}H_{35}O_7$	7.05	6.70×10^{-7}^	-
545.2757	$[M-H]^-$	15.90	$C_{30}H_{41}O_9$	545.2751	1.1	353.2117 309.2218 191.0556	$C_{23}H_{29}O_3$ $C_{22}H_{29}O$ $C_7H_{11}O_6$	8.14	5.80×10^{-7}	-
327.2176	$[M-H]^-$	17.27	$C_{18}H_{31}O_5$	327.2171	-1.2	395.2046 209.1178	$C_{19}H_{32}O_7Na$ $C_{12}H_{17}O_3$	5.38	1.09×10^{-7}^	Trihydroxyocta-decadienoic acid?
385.2584	$[M-H]^-$	17.61	$C_{21}H_{37}O_6$	385.2590	-1.6	431.2645	$C_{22}H_{39}O_8$	5.89	8.38×10^{-7}^	-
513.3064	$[M-H]^-$	17.96	$C_{27}H_{45}O_9$	513.3046	-3.5	559.3118 277.2168 253.0923 179.0556 161.0450	$C_{28}H_{47}O_{11}$ $C_{18}H_{29}O_2$ $C_9H_{17}O_8$ $C_6H_{11}O_6$ $C_6H_9O_5$	4.54	5.58×10^{-7}^	Glycoside conjugate
311.2229	$[M-H]^-$	21.38	$C_{18}H_{31}O_4$	311.2222	2.2	293.2117	$C_{18}H_{29}O_3$	7.75	8.38×10^{-9}	Dihydroxyocta-decadienoic acid?

Table S2.3. continued...

Observed ion (*m/z*)	Charge of observed ion	UPLC-TOFMS r.t.	Putative formula	Theoretical mass of ion	Δ PPM	*m/z* of additional ions and fragments	Formula of fragment ion	Fold change	P-value	Putative identity
High in old leaves compared to new leaves										
563.2324	$[M-H]^-$	8.21	$C_{25}H_{39}O_{14}$	563.2340	-2.8	-	-	7.17	1.03×10^{-6}^	-
649.2332	$[M-H]^-$	9.06	$C_{28}H_{41}O_{17}$	649.2344	-1.8	605.2445 487.2179 191.0556 173.0450	$C_{27}H_{41}O_{15}$ $C_{23}H_{35}O_{11}$ $C_7H_{11}O_6$ $C_7H_9O_5$	5.80	5.05×10^{-8}^	-
357.1183	$[M-H]^-$	10.26	$C_{16}H_{21}O_9$	357.1186	-0.8	-	-	47.80	9.03×10^{-8}	-
417.2073	$[M-H]^-$	10.77	$C_{27}H_{29}O_4$	417.2066	1.7	485.1940	$C_{28}H_{30}O_6Na$	7.48	9.51×10^{-9}^	-
329.1599	$[M-H]^-$	11.46	$C_{16}H_{25}O_7$	329.1600	-0.3	225.1491	$C_{13}H_{21}O_3$	10.76	2.15×10^{-12}^	-
689.3326	$[M-H]^-$	14.54	$C_{40}H_{49}O_{10}$	689.3326	-0.1	757.3200	$C_{41}H_{50}O_{12}Na$	965.25	1.29×10^{-8}	-
519.2947	$[M-H]^-$	14.71	$C_{29}H_{43}O_8$	519.2958	-2.1	565.3013 587.2832	$C_{30}H_{45}O_{10}$ $C_{30}H_{44}O_{10}Na$	59.07	5.16×10^{-8}	-

Table S2.4. Unidentified metabolites that significantly varied between the different tissues of vegetative flowering plants. Metabolites were detected using UPLC-TOFMS in positive ionisation mode. Fold changes were calculated by dividing average metabolite concentration (determined in 10µl injections, equivalent to 0.26mg of fresh leaf material) in the plant tissue with the highest concentration with the tissue with the lower average value. Differences between plant tissues were tested using t-tests if marked with a ^, unmarked P-values were obtained using the non-parametric Mann-Whitney test.

Observed ion (*m/z*)	Charge of observed ion	QToF r.t.	Putative formula	Theoretical mass of ion	Δ PPM	*m/z* of additional ions and fragments	Formula of fragment ion	Fold change	P-value	Putative identity
High in new leaves compared to old leaves										
409.2550	$[M+H]^+$	17.49	$C_{18}H_{37}N_2O_8$	409.2550	0.0	391.2444 351.2495 321.1662	$C_{18}H_{35}N_2O_7$ $C_{16}H_{35}N_2O_6$ $C_{13}H_{25}N_2O_7$	7.34	3.08×10^{-7}^	-
353.2690	$[M+H]^+$	17.60	$C_{21}H_{37}O_4$	353.2692	-0.6	-	-	4.28	4.71×10^{-8}^	-
277.2165	$[M+H]^+$	18.34	$C_{18}H_{29}O_2$	277.2168	-1.1	-	-	6.27	1.10×10^{-7}^	-
317.2117	$[M+H]^+$	18.34	$C_{20}H_{29}O_3$	317.2117	0.0	-	-	6.23	6.87×10^{-8}^	-
High in old leaves compared to new leaves										
751.2078	$[M+H]^+$	9.22	$C_{34}H_{39}O_{19}$	751.2086	1.2	589.1557 465.1033 303.0505 287.1131 251.0919 155.0708	$C_{28}H_{29}O_{14}$ $C_{21}H_{21}O_{12}$ $C_{15}H_{11}O_7$ $C_{13}H_{19}O_7$ $C_{13}H_{15}O_5$ $C_8H_{11}O_3$	2.84	9.09×10^{-7}	Flavonoid glycoside and an unknown conjugate
375.1657	$[M+H]^+$	10.92	$C_{17}H_{27}O_9$	375.1622	0.5	392.1921 397.1475 357.1549 353.1576 311.1471 293.1365 249.1467	$C_{17}H_{30}NO_9$ $C_{17}H_{26}O_9Na$ $C_{17}H_{25}O_8$ $C_{16}H_{26}O_7Na$ $C_{14}H_{22}O_6Na$ $C_{14}H_{22}O_5Na$ $C_{13}H_{22}O_3Na$	118.85	1.29×10^{-8}	-

Table S2.4. continued...

Observed ion (*m/z*)	Charge of observed ion	QToF r.t.	Putative formula	Theoretical mass of ion	Δ PPM	*m/z* of additional ions and fragments	Formula of fragment ion	Fold change	P-value	Putative identity
High in old leaves compared to new leaves										
253.1444	$[M+H]^+$	10.92	$C_{14}H_{21}O_4$	253.1440	1.6	235.1338	$C_{14}H_{19}O_3$	284.79	1.29×10^{-8}	-
317.2481	$[M+H]^+$	13.25	$C_{21}H_{33}O_2$	317.2481	0.0	299.2375	$C_{21}H_{31}O$	74.33	2.45×10^{-7}	-

Chapter 3. The effect of *Pratylenchus penetrans* herbivory on the above- and below-ground secondary chemistry of ragwort

3.1. Abstract

Nematode herbivores are ubiquitous to all soil ecosystems and can significantly modify above- and below-ground plant chemistry. Combining an experimental and metabolomic approach, the effects of root infection by the migratory endoparasitic nematode *Pratylenchus penetrans* on ragwort (*Senecio jacobaea*) secondary chemistry was examined. To investigate the effects of timing and longevity of nematode infection, plants were destructively harvested seven and 28 days post *P. penetrans* infection. The metabolome of root and shoots were analysed using UPLC-TOFMS. Supervised multivariate OPLS-DA models revealed significant metabolomic differences between *P. penetrans* and control treatments in roots, but not shoots, over both infection durations. Nematode infection increased the root concentrations of 20 metabolites that belonged to at least four different metabolite classes. The root concentrations of the pyrrolizidine alkaloid retrorsine N-oxide increased initially (seven days post-infection), but this waned as the interaction progressed (28 days post-infection). This temporary-induced response implied that migratory endoparasitic nematodes may be able to suppress the induced defence response by the plant host.

3.2. Introduction

Plants are exposed to a wide range of herbivores both above and below ground. Herbivores vary in mode of feeding (e.g. chewers versus piercers) and host specificity (e.g. monophagy versus polyphagy) resulting in contrasting host-plant chemical responses (Wurst and van der Putten 2007, Ali and Agrawal 2012, Zvereva and Kozlov 2012). Induction of plant chemical defence by herbivory provides a mechanism for plant-mediated interactions between spatially-separated herbivores (van der Putten *et al.* 2001). Below-ground herbivory can affect above-ground herbivore performance (Gange and Brown 1989, Masters *et al.* 2001, Bezemer *et al.* 2005, Soler *et al.* 2005). Yet, the impacts of below-ground herbivory on plant chemical defences are less well understood than those of above-ground herbivores (van Dam 2009).

Nematodes are an abundant and diverse taxon, including below-ground herbivores that are important drivers of plant succession and diversity in semi-natural ecosystems (de Deyn *et al.* 2003). Certain nematode species are major pests of agriculture, causing reduced plant yield with global economic losses exceeding US$100 billion per annum (Castillo and Vovlas 2007, Fuller *et al.* 2008). Herbivorous nematodes can be classified by feeding mode: sedentary or migratory endoparasites, and ectoparasites. Due to their specialised and intimate host-plant associations, studies have focussed on the effects of sedentary endoparasites (*Heterodera* spp., *Globodera* spp. and *Meloidogyne* spp.) that establish permanent feeding sites within roots (Williamson and Gleason 2003). Consequently, the effect of sedentary endoparasitic nematodes on plant gene expression (reviewed by Williamson and Gleason 2003) and chemistry (reviewed by Zinov'eva *et al.* 2004) are better understood than plant responses to migratory endoparasitic or ectoparasitic nematodes. Migratory endoparasitic nematodes tunnel through root tissues to feed (Oyekan *et al.* 1972), whereas ectoparasitic nematodes remain in the rhizosphere feeding externally on roots. Comparatively fewer studies have examined the genetic (Williams et al. 2002, Williamson and Kumar 2006) or chemical (Acedo and Rohde 1971, Epstein and Cohn 1971, Epstein 1972, 1974, Baldridge *et al.* 1998, Collingborn *et al.* 2000) plant responses to mobile, migratory endoparasitic and ectoparasitic nematodes.

A recent meta-analysis revealed that below-ground herbivory can induce changes in root secondary chemistry (Kaplan *et al.* 2008). For example, nematode herbivory leads to increased levels of root alkaloids in *Nicotiana tabacum* L. (Kaplan *et al.* 2008), phenols in *Bidens tripartita* L. (Epstein 1972), glucosinolates in *Brassica nigra* L. (van Dam 2012) and condensed tannins and flavonoids in *Musa* cultivars (Collingborn *et al.* 2000). Pyrrolizidine alkaloids (PAs) synthesised in the roots of *Senecio* spp. (Hartmann *et al.* 1989) have been shown to repel nematodes and reduce worm mobility, vitality and reproduction (Thoden *et al.* 2009a). Nevertheless, plant species containing PAs have been recorded as a suitable host for the migratory endoparasitic nematode *Pratylenchus penetrans* (Cobb, 1917) Filipjev & Schuurmans Stekhoven, 1941 (Kutywayo and Been 2006). Nematode herbivory can drive changes in above-ground secondary chemistry (Friedman and Rohde 1976, van Dam *et al.* 2005, Kaplan *et al.* 2008, Lohmann *et al.* 2009). For example, increased concentrations of shoot glucosinolates are associated with nematode herbivory (van Dam *et al.* 2005). Kaplan *et al.* (2008) suggested that the site of metabolite synthesis within the plant predicts the effect of nematode herbivory. For example, in *N. tabacum*, chemicals synthesised in roots tended to decrease in foliar tissues in response to nematode root herbivory, whereas those synthesised in shoots tended to increase (Kaplan *et al.* 2008). Such changes in above-ground chemistry induced by

below-ground herbivory will have repercussions for above-ground herbivores. Indeed, nematode infestation, despite differences in feeding guild and specialism, has been shown to affect the growth and reproduction of above-ground invertebrate herbivores negatively (Bezemer *et al.* 2005, van Dam *et al.* 2005, Wurst and van der Putten 2007).

Plant resistance to nematode herbivory is genetically controlled, with a degree of congruence in resistance mechanisms between feeding guilds (Williams *et al.* 2002, Williamson and Kumar 2006, Sharma *et al.* 2011). It is known that the timing and longevity of plant responses to nematode herbivory varies depending on the resistance genes present in the host-plant (Williamson and Kumar 2006). Initiation of plant-responses to nematode infection, measured using mRNA and enzyme activity associated with plant defence-related genes, took between 6 (Baldridge *et al.* 1998) and 96 hours (Edens *et al.* 1995). A rapid induced plant defence response to herbivory may reduce the overall cost of defence (Agrawal and Karban 1999) and induced defences can persist for weeks following attack. For example, enhanced glucosinolate levels were observed in *Brassica nigra* L. shoots 19 days after nematode root infection (van Dam *et al.* 2005).

In the present study, a model plant (ragwort, *Senecio jacobaea* L.) that synthesises PAs in its roots was challenged with an experimental infection of the migratory endoparasitic nematode *P. penetrans.* *Pratylenchus* species are the most common plant feeding nematodes found within the rhizosphere of wild ragwort (Bezemer *et al.* 2006). Using a metabolomic approach, the effect of this nematode herbivore on above- and below-ground ragwort chemistry was investigated. It was predicted that *P. penetrans* root damage would: 1) increase below-ground concentrations of PAs and other root synthesised plant metabolites (Hol *et al.* 2004, Kaplan *et al.* 2008); 2) decrease above-ground concentrations of PAs and other root-synthesised plant metabolites (Kaplan *et al.* 2008); and, 3) elicit a rapid induced response that would increase in magnitude with *P. penetrans* densities.

3.3. Methods

3.3.1. Nematode study species

Pratylenchus species have six life-history stages: egg, four juvenile stages and adult, with all, apart from the eggs and first juvenile stage, able to infect plants (Vovlas and Troccoli 1990). Abiotic soil conditions such as pH, moisture and temperature can cause variations in life-cycle length (Castillo and Vovlas 2007) but under laboratory conditions the life-cycle averages four weeks from egg to adult. While *P. penetrans* can feed ectoparasitically, they are primarily migratory endoparasites feeding on the fluids of cortical root cells. To enter and travel through plant cells *P. penetrans* pierces the cell several times in a row with its stylet, then opens the cell wall by pressing against these openings and thrashing their head in a sideways motion (Kurppa and Vrain 1985). Once the cell wall has been penetrated, the damaged area becomes attractive to other nematodes and extended feeding can lead to the shrinking of the vacuole membrane resulting in cell death (Zunke 1990). *P. penetrans* feeding and movement causes root necrosis, which can be identified by characteristic root-lesions (Oyekan *et al.* 1972). These root lesions are caused by oxidised phenols, either synthesised by the plant or caused by the breakdown of roots by nematode saliva, and do not affect *P. penetrans* negatively (Acedo and Rohde 1971). The phenols are transformed into tannins, melanins and lignins that cause the browning observed in infested roots (Rohde 1972).

3.3.2. Plant microcosms

Ragwort seeds were collected on October 2008 from a single plant on the University of Sussex campus (Grid Ref: TQ 348 098), dried at ambient temperature, and stored with silica gel in sealed containers at 4°C until required. Seeds were germinated on damp vermiculite (29/06/10). After two weeks, one three-leaf seedling, per replicate, was transferred to a 1.7L plastic pot filled with a 3:1 mixture of silver sand and John Innes No. 2 potting compost. Prior to use in the experiment, the growth media was double-autoclaved (75 minutes at 121°C) to standardise the microbial community in each microcosm and twice flushed to saturation with water to remove the nutrient pulse following sterilisation (Troelstra *et al.* 2001). Nematodes were directly applied to the root system via two lengths of drinking straws (7cm long) inserted into the growth media either side of the seedling at the time of transfer (van Dam *et al.* 2005). For the duration of the experiment, each replicate plant received 35ml of Hoagland's solution weekly. The experiment was performed in a greenhouse maintained at 15-25°C with

supplementary lighting (400W, high pressure sodium lamps) on a 16:8 L:D photoperiod. Plants were watered with tap water *ad libitum*.

3.3.3. Below-ground treatments

Thirty ragwort plants were randomly assigned to each soil treatment (control or *P. penetrans* infection) which was applied two weeks after the seedlings were transferred to individual pots. Sixty plants were arranged in 30 randomised blocks in the greenhouse, each block contained one replicate of each experimental treatment. Each replicate received at total of 165ml of liquid when the treatments were applied to account for any possible effect of liquid volume on plant metabolism.

All plant microcosms were inoculated with a microbial wash prior to the application of the experimental treatment to standardise the microbial community. The microbial wash was sourced from an area heavily infested with wild ragwort at Castle Hill Nature Reserve, Sussex (Grid ref: TQ 365 065). Using a Dutch soil auger, 10kg of soil was randomly collected from the rhizosphere of ragwort plants across the site to form a single bulk sample stored at 4°C for 2 days until extraction. Nematodes and other soil microfauna were excluded from the microbial wash using the Cobb nematode extraction method (van Bezooijen 2006). Firstly, the soil was homogenised by hand-mixing and weighed to five 2kg batches. These batches were each mixed thoroughly with 6 litres of water. The water was then decanted and passed through a series of progressively finer sieves (500µm, 180µm, 75µm and 3 x 45µm). This process only left microbes in the soil water that passed through the final 45µl sieve. Every replicate received 65ml of the microbial wash applied to the surface of the growth media.

A *P. penetrans* inoculate containing juvenile nematodes was obtained from HZPC Research and Development (The Netherlands). The inoculate volume was made up to 450ml using tap water, allowing it to be easily divided between *P. penetrans* replicates. An initial count using a dissecting microscope (x400) determined that there were on average 71.7 nematodes per millilitre of inoculate. Each replicate in this treatment received 10ml of the *P. penetrans* inoculate, 5ml down each straw, equating to an average 717 nematodes per replicate. To keep the amount of liquid applied on each treatment constant an additional 90ml of reverse osmosis (RO) water was applied to the *P. penetrans* replicates. Controls received 100ml of RO water (5ml down each straw, 90ml on the surface of the growth media).

3.3.4. Harvesting

3.3.4.1. Plant material

Plant replicates were randomly harvested at 7 and 28 days post-infection to follow the progression of nematode-induced secondary chemistry (Table 3.1.). At each time point 30 plants were harvested, comprising 15 replicates of each treatment. For logistical reasons five randomly chosen blocks, equating to five replicates from each treatment, were harvested each day over three days. Each day individual plants were harvested in a random order.

Table 3.1. Experimental overview that notes key dates in the experiment. The experiment ran just over eight weeks from 29/06/10 to 26/08/10. Thirty replicates were destructively harvested over a three day period, equating to five replicates of each treatment per harvest day.

Day	Event
0	Seeds germinated on vermiculite
14	Seedlings potted into sterilised growth medium
28	Nematodes and microbes applied
35-37	First plant harvest, seven days post-infection (n=30)
56-58	Second plant harvest, 28 days post-infection (n=30)

Before any leaves were harvested, the number of leaves was recorded per plant replicate. For each plant harvested seven days post-infection a composite sample of three new leaves, mature leaves closest to the centre of the rosette, were excised and fresh weight determined (g). These leaves were immediately snap-frozen in liquid nitrogen to stop enzymatic processes and preserve the samples for analysis of the metabolome. All samples for metabolomic analyses were stored in foil on dry ice before transfer to the -80°C freezer at the end of the day for long-term storage. Plants harvested 28 days post-infection were large enough to allow an additional composite sample of three old leaves (on the outside of the rosette) per plant to be collected, processed and stored as described above. Senescent leaves were not collected. The leaves (from both sampling periods) remaining following sampling were removed and fresh weight (g) determined. This biomass was then dried at 60°C for three days and a dry weight (g) obtained. Dry weight was positively related to fresh weight (Pearson product-moment correlation coefficient: r^2 = 0.940, P <0.001), so the weight of the removed leaves were included in the final fresh weight and only fresh weight was tested for treatment effects on shoot biomass.

The root mass of each replicate was freed from the growth media and halved, with one sample for nematode extraction (see below) and the other for metabolomic analysis. Where the root mass was too small no root samples were collected for nematode extraction. The root metabolome sample was washed for 12 minutes, patted dry with paper towels and weighed (g) then a representative sub-sample of root material (approx. 0.2g) was excised, weighed (g), snap frozen in liquid nitrogen and stored in a -80°C freezer.

3.3.4.2. Nematode extraction, fixing and counting

The root section that was to be used for nematode extraction was weighed (g) and stored at 4°C until processed. A sample of the soil was also removed from the root mass. This was homogenised to ensure a representative 100g sub-sample (± 1g) was collected and stored at 4°C until extracted. The roots that remained after nematode and metabolome sampling were dried at 60°C for three days before weighing again to determine a dry weight (g). After determining that dry weight was significantly related to fresh weight (Pearson product-moment correlation coefficient: r^2 = 0.952, P <0.001), the weight of the removed roots was included in the final fresh weight, and only fresh weight was tested for treatment effects on root biomass. Nematodes were extracted from both soil and plant roots for 48 hours using a modified Baermann funnel method (van Bezooijen 2006). The extraction substrate (roots or soil) was placed into a plastic mesh sieve, (13cm diameter, 1mm mesh size) lined with a KimTech delicate wipe (Kimberly-Clark™, UK), and lowered into a water filled plastic funnel (300ml volume) attached to a 4ml glass vial by rubber tubing. The water level of the funnel was maintained to keep the sample wet throughout the extraction period. This encouraged nematode movement out of the substrate and into the water column where they gravitate into the collection vial. Vials containing the nematode extracts were stored temporarily (maximum 24 hours) in a 4°C cold room until nematodes were killed and fixed using a formalin-glycerine solution (F.G. 4:1) heated to 60°C for three minutes (van Bezooijen 2006). These extracted samples were stored in the F.G. 4:1 until the total number of nematodes per vials could be counted under a stereomicroscope at x400 magnification to quantify the *P. penetrans* infection of ragwort roots and soil. To account for differences in the root mass per replicate, *P. penetrans* root counts were adjusted to represent the number per 0.1g of fresh weight of root.

3.3.5. Metabolomic Profiling

3.3.5.1. Chemicals and Standards

Two deuterated standards, 17β-estradiol 2,4,16,16-d_4 sodium 3-sulfate (E2-d_4-S, >99% D atom) and progesterone-2,2,4,6,6,17α,21,21,21-d_9 (P-d_9, 98% D atom), were purchased from Cambridge Isotope Laboratories Inc. (MA) and CDN isotopes (Quebec, Canada), respectively. A retrorsine N-oxide standard was purchased from PhytoLab GmbH & Co. KG (Nürnberg, Germany). Strata Impact protein precipitation plates were purchased from Phenomenex Ltd (Macclesfield, UK). Centrifuge Anopore VectaSpin Micro filters (0.2µl pore sire, 2ml volume) were purchased from Whatmann (United Kingdom). All remaining chemicals, standards and equipment used were purchased from the suppliers listed in Chapter 2.

The deuterated steroids were used as internal standards (IS); E2-d_4-S was used for analysis in negative ESI mode and P-d_9 for analysis in positive mode. These were made up in ethanol and were added to each sample of plant material during solvent extraction. The IS was used to monitor the efficiency of extraction, mass spectrometry (MS) sensitivity and for use in chromatogram alignment. The concentration of IS added to each extract was adjusted as the analysis progressed (Table 3.2.). The initial concentrations of IS added (32µl of both E2-d_4-S and P-d_4 at 100ng/µl) during the analysis of root and new leaves harvested 28 days post-infection resulted in IS responses that were saturated in both ESI modes. IS concentrations in subsequent analyses were, therefore, decreased (24µl of P-d_4 at 1ng/µl and 12µl of E2-d_4-S at 10ng/µl) (Table 3.2.).

Table 3.2. Summary of the sample preparation for different plant materials. The details of the different volumes (vol. added) and concentrations (conc. added) of the two standards 17β-estradiol 2,4,16,16-d_4 sodium, 3-sulfate (E2-d_4-S) and progesterone-2,2,4,6,6,17α,21,21,21-d_9 (P-d_9) added to material of different plant parts and harvest. The vol. speed vac'd relates to the volume of the extract that was evaporated down and then resuspended in 3:1 methanol:water, the volume of which is indicated by vol. resuspended. The volumes injected on to the columns is noted in both positive and negative ESI MS modes.

Days in treatment	Plant material	P-d_9		E2-d_4-S		Vol. speed vac'd	Vol. resuspended	Vol. injected - post	Vol. injected - neg
		Vol. added	Conc. added	Vol. added	Conc. added				
7	Root	12µl	10ng/µl	24µl	1ng/µl	2ml	120µl	20µl & 1µl	20µl
7	Shoot	12µl	10ng/µl	24µl	1ng/µl	2ml	160µl	20µl & 1µl	20µl
28	Root	32µl	100ng/µl	32µl	100ng/µl	1ml	240µl	5µl	20µl
28	New leaves	32µl	100ng/µl	32µl	100ng/µl	1ml	240µl	1µl	10µl
28	Old leaves	12µl	10ng/µl	24µl	1ng/µl	2ml	160µl	20µl & 1µl	20µl

3.3.5.2. Solvent Extraction

As described in Chapter 2, a double solvent extraction of plant material was performed. The differences between the methods used previously and this experiment are outlined below. The IS solutions were added to the plant material during the first solvent extraction prior to vortexing and extraction in the freezer. Throughout the experiment 0.1g (±0.01g) of plant material was extracted using a total of 4ml of solvent. As described in Chapter 2, a 1ml sub-sample of the root and new leaf extract from material harvested 28 days post-infection was evaporated down and the residue was resuspended in 240µl 3:1 methanol:water (Table 3.2.). The analysis of these samples revealed that the metabolite changes characteristic of nematode infection were observed, but these metabolites were present at low concentrations. To increase the signal of these metabolites by four-fold, when root samples harvested seven days post-infection were prepared, a 2ml sub-sample was evaporated down and resuspended in 120µl of 3:1 methanol:water (Table 3.2.). As expected, the analysis of these samples revealed an increased concentration of metabolites associated with nematode infection. Similarly, to increase the concentration of leaf extracts by 3.5-fold for subsequent metabolite identification analyses, the extraction of shoots harvested seven days post-infection and old leaves harvested 28 days post-infection were prepared so that a 2ml sub-sample was evaporated down and resuspended in 160µl of 3:1 methanol:water (Table 3.2.). After resuspension of all extracts in 3:1 methanol: water, samples were passed through a Strata protein precipitation plate under vacuum, and the filtrate stored in amber HPLC vials to prevent any photodegradation. Samples were stored at -80°C until analysed.

3.3.5.3. UPLC-TOFMS conditions

Aliquots of plant extracts were injected on to an Acquity UPLC BEH C18 column (1.7µm particle size, 2.1 x 100mm, Waters, UK) (injection volumes given in Table 3.2.). The injection volumes analysed ranged from 1-20µl. The first analyses of root (5µl injection volume) and new leaves (1µl injection volume) harvested 28 days post-infection revealed that the metabolite changes characteristic of nematode infection were observed at low concentrations. Injections of subsequent sample extracts for analyses were increased to 20µl, with an additional injection of 1µl in positive ESI mode. This allowed large metabolite signals of PAs to be examined in the low volume injections and small metabolite signals to be measured in the high volume injections. Samples and column were maintained at 4°C and 30°C, respectively. In both ionisation modes the mobile phase consisted of 100% water (A) and 100% acetonitrile (ACN) (B), and both solvents contained 0.1% formic acid. A flow rate of 0.2mL min^{-1} was maintained

throughout the following UPLC program: 0-9.0 min, from 0 to 30.0% B; 9.0-15.0 min, from 30.0 to 100% B; 15.0 to 23.0 min, 100% B. At the end of each run, the column was equilibrated in 100% A for four minutes prior the next injection.

Metabolites were detected using a Micromass TOF-MS system (Waters, Manchester, UK). The conditions of the MS in this experiment were broadly similar to previous experiments (Chapter 2). There were, however, some differences, all condition details are therefore described below. The mass spectrometer was tuned to 9000 mass resolution and data collected in full scan mode from 100 to 1200 *m/z*. The collision gas used was argon; constant collision energy of 10eV was used for all experiments and the TOF penning pressures ranged from 4.34×10^{-7} to 4.94×10^{-7} mbar. Capillary voltage ranged from -2.70 in negative mode and 2.6 in positive mode. Cone voltage was set at 35V, and multiplier voltage was set at 550V. The source and desolvation temperatures were 100°C and 250°C, respectively. Desolvation nitrogen flow was set at 300L h^{-1} in negative ESI and ranged from 310 L h^{-1} in positive mode. To account for instrumental drift within a run an internal lockmass was used. Sulfadimethoxine (5pg μL^{-1} in methanol water, 1:1, with 0.1% formic acid for positive mode) was infused at 50µL min^{-1} using a lockspray interface (baffling frequency, $0.2s^{-1}$). Ions are obtained at *m/z* 311.0814 in negative mode and 309.0658 in positive mode.

3.3.5.4. Analysis of datasets from UPLC-TOFMS analyses of plant extracts

Spectral peaks were aligned using the retention time of the internal standard using the MarkerLynx V 4.1 software package. Using SIMCA-P multivariate analysis software (Umetrics UK Ltd, Windsor, UK) the data were pareto-scaled, log transformed, and modelled using PCA, PLS-DA and OPLS-DA, as outlined in Chapter 2. Discriminatory metabolites associated with *P. penetrans* infection were extracted from 'S'-plots and quantified using peak integration of the responses on the original chromatograms. In addition, the mass sign ($[M+H]^+$ ion) of PAs known to occur in ragwort were examined in each chromatogram (as described previously in Chapter 2), and the peaks quantified manually using MassLynx peak integration software. Before statistically testing discriminatory metabolites and PAs, peak areas were adjusted to account for a number of differences between analytical runs. First, to account for different sample preparation procedures and injection volumes, peak areas were adjusted to standardise all responses to the equivalent of 10mg of wet plant material. Secondly, peak areas were adjusted for losses during work-up and changes in analytical sensitivity of the MS between samples using the peak area of the IS.

3.3.5.5. Structural analysis of metabolites associated with *P. penetrans* infection

To obtain structural identification of the metabolites associated with nematode infection, composite samples of roots infested with *P. penetrans* harvested seven and 28 days post-infection were prepared. Composite samples were prepared by combining the extracts that remained after the profiling analyses. Where possible, structural information was obtained using Q-TOFMS CID, as described in Chapter 2. Accurate mass measurements were obtained using a UPLC Xevo G2-TOF nanospray system (Chapter 2). Additional structural information was obtained using the UPLC Xevo G2-TOF nanospray system through the full scan analysis of multiple injections at a range of collision energies (10-40eV, at 10eV intervals).

3.3.6. Statistical analysis

All statistical analyses were performed in SPSS V11. The residuals of the nematode count data did not meet the assumptions of normality and homogeneity of variance (even after transformations), so non-parametric tests were used. To compare across all combinations of treatments and infection durations Kruskal-Wallis tests were performed. When comparisons of the same treatment over different infection durations were made, Mann-Whitney U tests were used. All plant parameter data (e.g. number of leaves, biomass) satisfied the assumptions of normality and equal variance required for parametric analysis. Dry weight was significantly related to fresh weight (Pearson product-moment correlation coefficient: 28 days post-infection, roots: r^2 = 0.952, P <0.001, shoots: r^2 = 0.940, P <0.001), thus only total fresh weights were fitted to ANOVA models. In all cases the response variable was not affected significantly by experimental block (one-way ANOVA with block as a random factor) or sampling date (two-way ANOVA), thus they were eliminated from all analyses. Shoot fresh weight (g), root fresh weight (g), shoot:root ratio (fresh weight-dry weight)/(fresh weight *100) and number of leaves for each treatment were compared for each harvest (seven and 28 days post-infection) using a one-way ANOVA. Concentration differences for both discriminatory metabolites and PAs were compared between treatment groups using t-tests when the assumptions of normality (Kolmogorov-Smirnov tests) and equality of variances (Levene's test) were met. If the assumptions for parametric testing could not be satisfied, either before or following transformations, the non-parametric Mann-Whitney test was used. Due to the large amount of metabolites measured there was a high likelihood of Type I statistical error. Consequently Bonferroni corrections were applied to the P-values obtained.

Fold changes were calculated for each discriminatory metabolite and PA by dividing the *P. penetrans* concentrations with those observed in the controls: values greater than one indicate higher concentrations are observed in the *P. penetrans* plants and those less than one represent concentrations higher in the controls.

3.4. Results

3.4.1. Nematode densities and plant growth

Counts of nematode density (per 0.1g root or 100g soil) revealed that nematode densities were greatest in *P. penetrans* treated plants, with very low densities in the roots (Figure 3.1.a, Kruskal-Wallis: $\chi^2_{(3)} = 36.929$, $P < 0.001$) and soil (Figure 3.1.b, Kruskal-Wallis: $\chi^2_{(3)} = 40.141$, $P < 0.001$) of the control plants. These low densities in control replicates either represent a degree of contamination by *P. penetrans* or failure to exclude indigenous nematodes by sieving. Nonetheless the differences between the nematode counts between treatments were substantial (Figure 3.1.). In addition, a maximum level of *P. penetrans* infestation of roots was reached after only seven days in treatment; no increase in root nematode numbers was seen after an additional 21 days in treatment (Figure 3.1.a, Mann-Whitney U test: $z = -0.306$; $P = 0.800$, not significant). While the root nematode count did not differentiate between samples from different infection durations, *P. penetrans* densities per 100g of soil increased over time (Figure 3.1.b, Mann-Whitney U test: $z = -4.493$; $P < 0.001$).

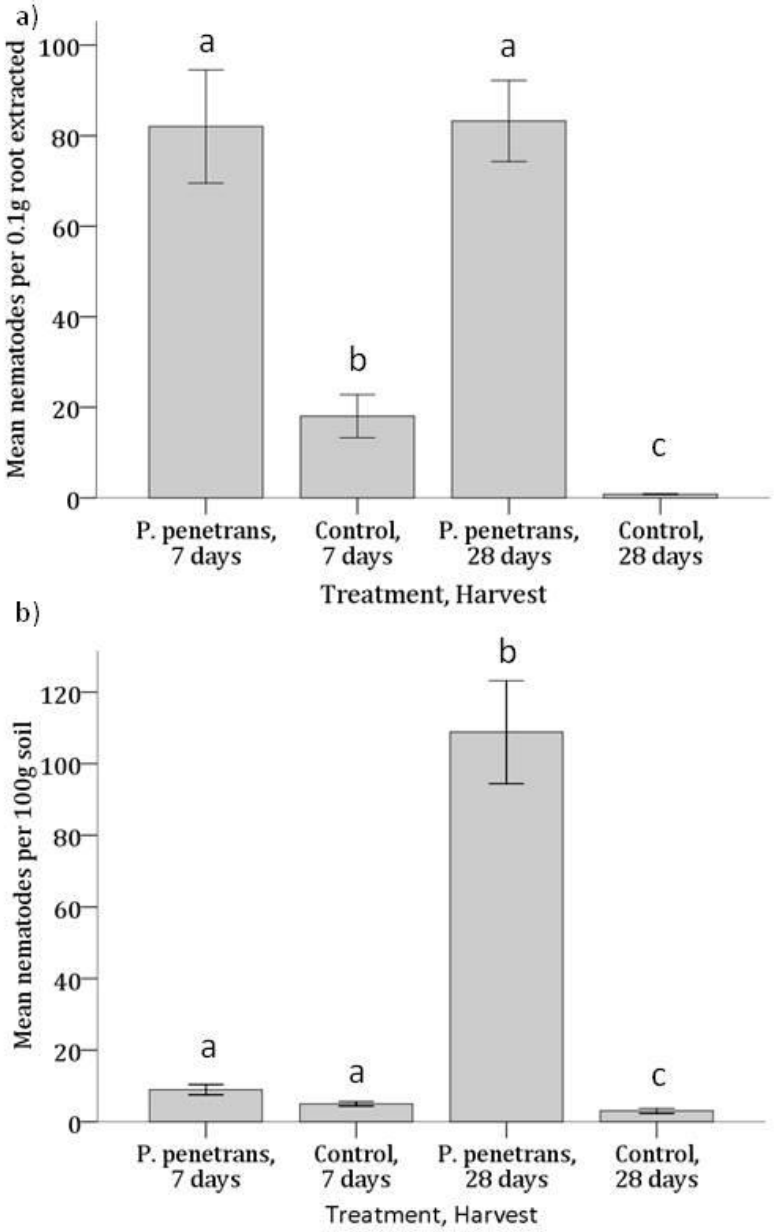

Figure 3.1. Measures of nematode population in the roots and soil of experimental plants. Mean (± standard error) nematode numbers extracted a) per 0.1g of roots (Kruskal Wallis: $\chi^2_{(3)}$ = 36.929, P < 0.001) and b) from 100g soil (Kruskal Wallis: $\chi^2_{(3)}$ = 40.141, P < 0.001). Plants were grown with *Pratylenchus penetrans* nematodes or with no added nematodes (control plants). Data are presented from plants harvested seven and 28 days post-infection. Letters represent significant differences between classes following post-hoc Mann Whitney U testing.

P. penetrans infection did not affect any of the plant growth parameters measured over either harvest period (Table 3.3.). During the final harvest (28 days post-infection), however, it was noted that the roots of *P.* penetrans infested plants had more root necrosis (12/15) than plants in the control (1/15) treatment ($\chi^2_{(1)}$ =20.484, P < 0.001). Previous studies have observed similar root necrosis following *Pratylenchus* spp. feeding (Vovlas and Troccoli 1990). These data strongly suggest that *P. penetrans* feeding was damaging ragwort roots 28 days post-infection.

Table 3.3. The effect of nematode infection on ragwort growth. Mean (± S.E.) shoot fresh weight (g), root fresh weight (g) and shoot:root ratio of ragwort plants grown 1) with *Pratylenchus penetrans* nematodes and 2) no added nematodes (control). Plants were harvested seven and 28 days post-infection. $F_{2,41}$ for plants harvested seven days post-infection and $F_{2,42}$ for plants harvested 28 days post-infection.

Plant measure	*P. penetrans*	Control	F ratio	P-value
Shoot fresh weight				
7 days post-infection	0.244 (± 0.021)	0.257 (± 0.020)	0.236	0.791
28 days post-infection	3.394 (± 0.290)	3.656 (± 0.289)	0.305	0.739
Root fresh weight				
7 days post-infection	0.135 (± 0.011)	0.130 (± 0.015)	0.026	0.974
28 days post-infection	1.243 (± 0.164)	1.336 (± 0.125)	0.331	0.720
Shoot:root ratio				
7 days post-infection	0.571 (± 0.031)	0.507 (± 0.055)	0.574	0.568
28 days post-infection	0.354 (± 0.030)	0.366 (± 0.026)	0.340	0.714

3.4.2. Metabolomic analysis of *P. penetrans* infection

PAs elute relatively early in the LC program, when the mobile phase comprised of 93-70% water, between two and nine minutes (Figure 3.2.). The positive internal standard, P-d_9, was observed 13.4±0.2 minutes into the program; the negative internal standard, E2-d_4, eluted after 9.0±0.2 minutes. The retention times and peak areas of the internal standard were consistent in all samples in the same analytical run, indicating reliable extraction methodology and MS performance.

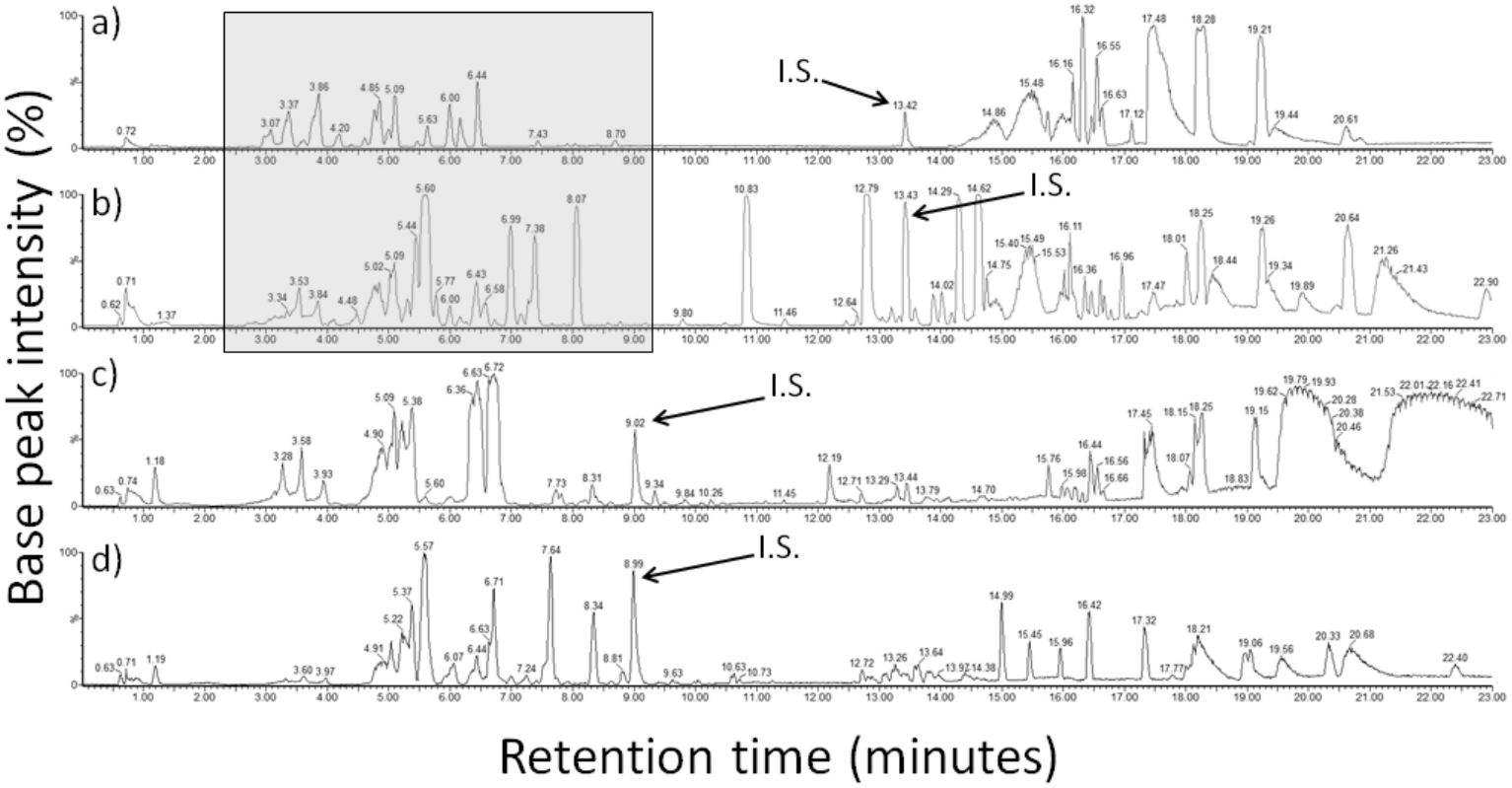

Figure 3.2. Typical metabolomic profiles of ragwort a) new leaf (1µl injection, equivalent to 0.104mg of new leaves) and b) roots (5µl injection, equivalent to 0.521mg of new leaves) as measured by UPLC-TOFMS in positive ESI mode. The I.S. was the deuterated steroid standard progesterone-d_9. Pyrrolizidine alkaloids (PAs) eluted during the retention time window are shaded grey. Typical metabolomic profiles of ragwort c) new leaf (10µl injection, equivalent to 1.042mg of new leaves) and d) roots (20µl injection, equivalent to 2.083mg of new leaves) as measured by UPLC-TOFMS in negative ESI mode. The I.S. was the deuterated steroid standard 17β-estradiol-d_4 sodium, 3-sulfate.

3.4.3.1. *Pratylenchus penetrans* effects on ragwort chemistry (UPLC-TOFMS) seven days post-infection

PCA of the root UPLC-TOFMS datasets revealed two (one control, and one *P. penetrans* infected plant) outliers in the positive dataset and one (a *P. penetrans* infected plant) outlier and negative dataset that were excluded from all subsequent analyses (as defined in Chapter 2). After remodelling, the PCA model diagnostics for both positive and negative ESI were poor (positive ESI: R^2X = 0.166, Q^2 = -0.009; negative ESI: R^2X = 0.177, Q^2 = -0.016), and no separations of the two treatment groups were apparent (Figure 3.3.c & d). A supervised OPLS-DA resulted in models that explained a large amount of the variation (for both OPLS-DA models the total R^2Y was > 0.984) (Table 3.4.) but had poor predictability (Q^2 < 0.200 for the Y predictive component) (Table 3.4.). Clear separations between the metabolomes of *P. penetrans* and control ragwort roots can, however, be observed (Figure 3.4.a and b). Nonetheless, it was possible to extract from the 'S'-plots metabolites that discriminated between *Pratylenchus* and control plant roots. For all of the metabolites of interest, higher concentrations of discriminatory metabolites were observed in *P. penetrans* infested plants. Poor predictability of the model is observed when discriminatory variables are observed in very low concentrations compared to other metabolite signals, and examination of the discriminatory metabolites associated with *P. penetrans* feeding revealed that this was the case. Eleven metabolites of interest were extracted from the modelling of the positive ESI dataset (Table 3.5.) and 14 were obtained from the negative ESI dataset (see Table 3.6.). One discriminatory metabolite was common to both ionisation modes (according to retention time and likely elemental composition). Following correction for the false discovery rate associated with multivariate data using a Bonferroni correction, 17 metabolites (eight in positive and nine in negative ESI mode) differed between *P. penetrans* and control plants (Bonferroni threashold: positive ESI: $P < 4.58 \times 10^{-7}$; negative ESI: $P < 6.57 \times 10^{-7}$, Tables 3.5. & 3.6.).

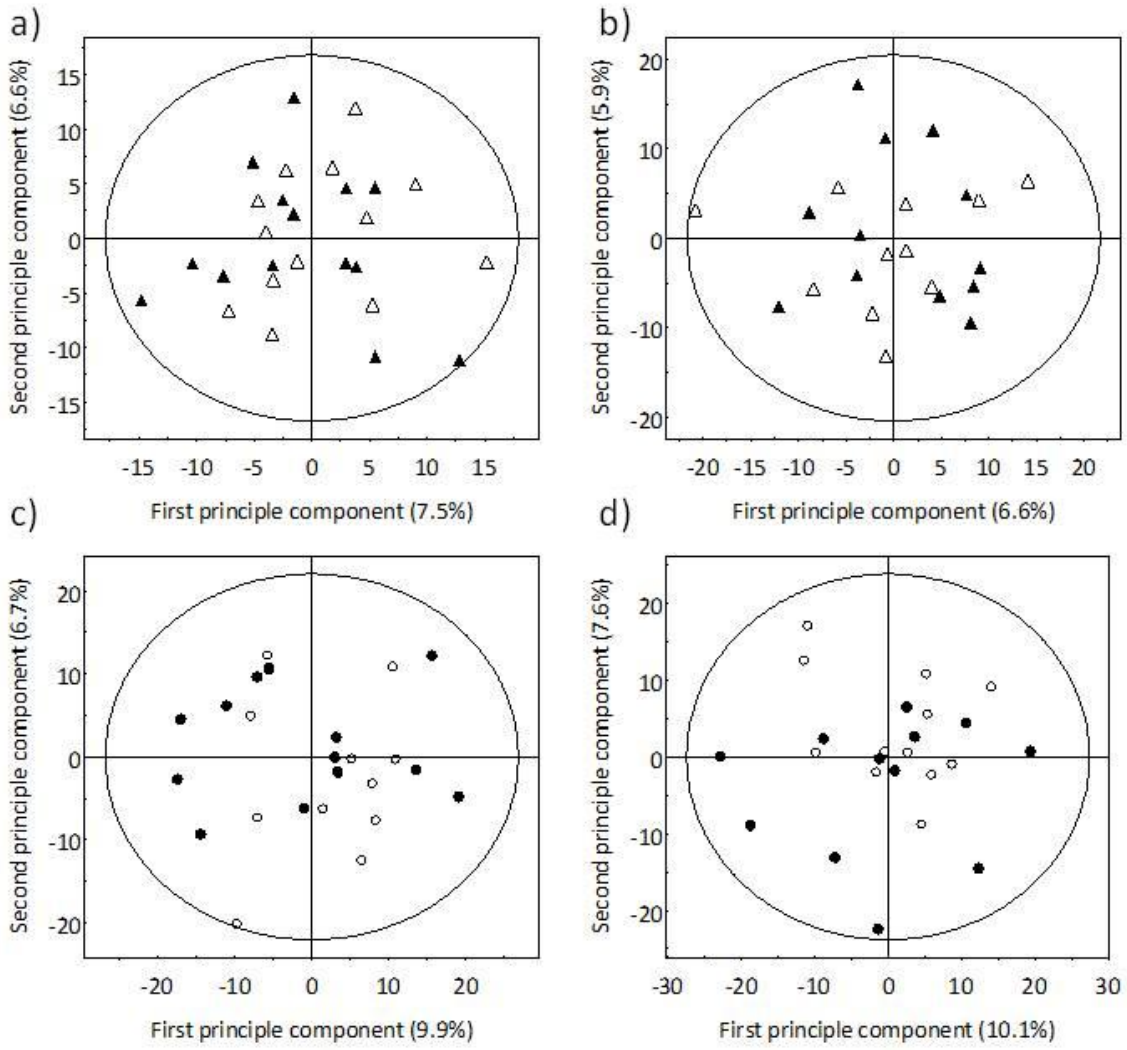

Figure 3.3. Results of the PCA modelling of plant material harvested seven days post-infection and analysed using UPLC-TOFMS in positive (a and c) and negative (b and d) ESI modes. Plots display the first two principle components of the models of ragwort shoots (triangles - a and b) and roots (circles - c and d). Black symbols represent plants treated with a *Pratylenchus penetrans* inoculate and open symbols are control plants.

Table 3.4. Summary of the OPLS-DA modelling that compared roots and shoots of ragwort collected using UPLC-TOFMS in positive and negative ESI modes. These models consider control and *P.penetrans* infested plants harvested seven and 28 days post-infection. Adding additional orthogonal projections of these models did not improve the Q^2 values. Those models which resulted in the detection of metabolites associated with nematode infection are shown in **bold**.

Days post-infection	Plant material	Ionisation mode	R^2Y	Q^2
7	Root	**Positive**	**0.984**	**0.175**
		Negative	**0.990**	**0.199**
	Shoots	Positive	0.928	-0.194
		Negative	0.978	-0.049
28	Root	**Positive**	**1.000**	**0.138**
		Negative	**0.894**	**0.435**
	New shoots	Positive	0.817	0.046
		Negative	0.906	-0.271
	Old shoots	Positive	0.984	-0.104
		Negative	0.965	-0.018

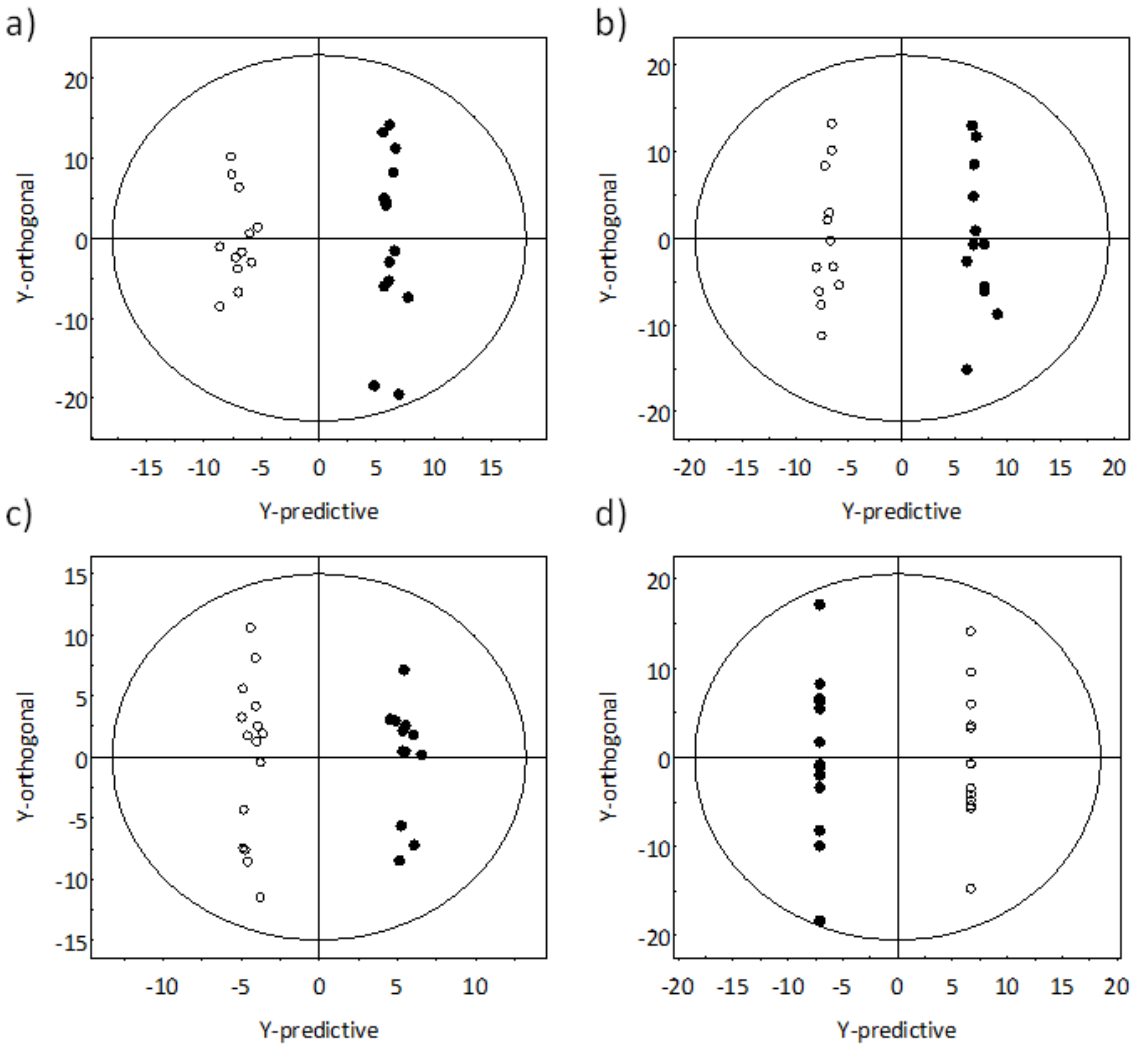

Figure 3.4. Results of the OPLS-DA modelling of plant roots harvested seven days (a and b) and 28 days (c and d) post-infection and analysed using UPLC-TOFMS in positive (a and c) and negative (b and d) ESI modes. Black symbols represent plants treated with a *Pratylenchus penetrans* inoculate and open symbols are control plants.

Table 3.5. Relative concentrations (equivalent to 0.01g fresh material, mean ±S.E.) of discriminatory root metabolites associated with *Pratylenchus penetrans* infection of ragwort seven and 28 days post-infection. Data were collected using UPLC-TOFMS in positive ESI mode and are displayed in early to late retention time (r.t.) order. Fold difference values >1 indicate higher concentrations are observed in the *P.penetrans* plant. Within each harvest discriminatory root metabolites were compared using t-tests (^) or a Mann-Whitney U tests (unmarked). Those comparisons that remained significant after Bonferroni correction (seven days post-infection: $P < 4.58 \times 10^{-7}$, 28 days post infection: $P < 1.28 \times 10^{-6}$) are in **bold**.

Metabolite number	*m/z*	UPLC-TOFMS r.t.	7 days post-infection				28 days post-infection			
			P. penetrans	Control	Fold dif.	P-value	*P. penetrans*	Control	Fold dif.	P-value
1	435.1630	3.43	Not detected	Not detected	n/a	n/a	215.90 (±65.05)	14.37 (±4.44)	15.02	7.12×10^{-5}
2	448.1357	3.57	**718.62 (±93.12)**	**118.37 (±20.51)**	**6.07**	**1.47×10^{-7}^**	1020.56 (±264.72)	322.86 (±72.59)	3.16	3.47×10^{-3}^
3	390.1531	4.50	**159.26 (±29.42)**	**25.36 (±4.66)**	**6.28**	**1.22×10^{-7}^**	332.76 (±42.68)	105.63 (±13.41)	3.15	1.59×10^{-5}^
4	419.1711	5.34	Not detected	Not detected	n/a	n/a	57.90 (±9.37)	13.73 (±4.28)	4.22	3.23×10^{-5}^
5	413.0400	5.68	21.93 (±4.16)	8.46 (±1.25)	2.95	1.02×10^{-3}^	**64.40 (±9.82)**	**12.97 (±2.83)**	**4.97**	**8.64×10^{-7}**
6	251.0919	5.92	43.30 (±4.63)	27.69 (±4.72)	1.56	1.70×10^{-2}	105.31 (±18.94)	44.71 (±6.97)	2.36	3.75×10^{-3}^
7	390.1915	6.32	**383.42 (± 1.22)**	**7.12 (±2.45)**	**53.85**	**6.37×10^{-9}^**	**2259.55 (±514.53)**	**82.08 (±30.34)**	**27.53**	**4.06×10^{-8}^**
8	499.1217	6.68	Not detected	Not detected	n/a	n/a	163.14 (±35.03)	31.98 (±9.27)	5.10	3.74×10^{-5}^
9	489.1972	7.65	**24.96 (±3.71)**	**0.31 (±0.31)**	**80.52**	**1.07×10^{-7}**	55.41 (±10.69)	1.20 (±1.05)	46.18	4.81×10^{-6}
10	499.2178	8.39	40.98 (±9.36)	9.86 (±2.03)	4.16	3.58×10^{-6}	242.19 (±69.72)	36.09 (±9.66)	6.71	4.26×10^{-5}^
11	555.1393	8.38	**22.56 (±3.13)**	**3.99 (±0.97)**	**5.65**	**5.76×10^{-8}^**	199.95 (±48.26)	26.92 (±7.97)	7.43	3.50×10^{-5}^
12	269.0815	8.39	11.48 (±1.95)	0.76 (±0.41)	15.11	7.01×10^{-7}^	84.95 (±20.98)	12.15 (±4.45)	6.99	1.12×10^{-4}^
13	609.1359	8.39	**29.40 (±4.47)**	**0.69 (±0.47)**	**42.61**	**1.63×10^{-11}^**	**58.77 (±11.21)**	**1.48 (±0.95)**	**39.71**	**5.16×10^{-8}**
14	575.1949	8.38	**11.89 (±20.09)**	**1.62 (±0.59)**	**7.34**	**2.62×10^{-13}^**	**216.31 (±43.23)**	**8.81 (±3.50)**	**24.55**	**4.63×10^{-11}^**
15	399.1655	10.43	**27.81 (±5.50)**	**0.03 (±0.02)**	**927.00**	**5.34×10^{-8}**	24.05 (±6.65)	0.17 (±0.16)	141.47	6.96×10^{-4}

Table 3.6. Relative concentrations (equivalent to 0.01g fresh material, mean ±S.E.) of discriminatory root metabolites associated with *Pratylenchus penetrans* infection of ragwort seven and 28 days post-infection. Data were collected using UPLC-TOFMS in negative ESI mode and are displayed in early to late retention time (r.t.) order. Fold difference values >1 indicate higher concentrations are observed in the *P.penetrans* plant. Within each harvest discriminatory root metabolites were compared using t-tests (^) or a Mann-Whitney U tests (unmarked). Those comparisons that remained significant after Bonferroni correction (seven days post-infection: $P < 6.57 \times 10^{-7}$, 28 days post-infection: $P < 6.85 \times 10^{-7}$) are in **bold**.

Metabolite number	*m/z*	UPLC-TOFMS r.t.	7 days post-infection				28 days post-infection			
			P. penetrans	Control	Fold dif.	P-value	*P. penetrans*	Control	Fold dif.	P-value
2	446.1201	3.57	**162.91 (±22.55)**	**20.19 (±3.90)**	**8.069**	**3.60×10^{-8}^**	48.65 (±9.21)	17.60 (±2.95)	2.764	9.97×10^{-4}
16	231.087	4.15	**121.02 (±18.63)**	**21.80 (±2.31)**	**5.551**	**1.49×10^{-8}^**	38.92 (±6.90)	7.62 (±1.17)	5.108	3.02×10^{-5}^
17	321.0607	4.16	**35.25 (±7.10)**	**7.08 (±1.05)**	**4.979**	**1.92×10^{-7}**	6.28 (±0.95)	1.30 (±0.36)	4.831	2.00×10^{-5}^
18	683.1829	5.56	40.39 (±4.82)	19.41 (±2.84)	2.081	5.53×10^{-4}^	18.48 (±3.60)	3.98 (±0.54)	4.643	9.62×10^{-6}^
19	423.0936	5.94	17.48 (±1.48)	5.87 (±1.37)	2.978	5.96×10^{-6}^	7.10 (±1.01)	1.97 (±0.44)	3.604	1.43×10^{-5}^
20	465.1967	7.56	**35.09 (±6.06)**	**0.15 (±0.05)**	**233.933**	**1.92×10^{-7}**	**13.46 (±2.88)**	**0.18 (±0.11)**	**74.778**	**8.70×10^{-10}^**
21	601.1714	7.61	5.06 (±1.18)	0.03 (±0.02)	168.667	2.97×10^{-4}	Not detected	Not detected	n/a	n/a
22	529.1868	8.63	18.25 (±3.51)	4.33 (±0.56)	4.215	1.78×10^{-3}^	**6.45 (±1.14)**	**0.97 (±0.26)**	**6.649**	**4.66×10^{-7}^**
23	641.1636	8.63	16.51 (±3.14)	0.18 (±0.16)	91.722	1.30×10^{-4}	4.42 (±0.87)	0.14 (±0.08)	31.571	7.12×10^{-5}
24	551.1976	8.71	**46.45 (±7.54)**	**6.26 (±0.56)**	**7.420**	**1.92×10^{-7}**	**20.68 (±3.71)**	**2.42 (±0.46)**	**8.545**	**7.44×10^{-8}^**
25	709.1596	8.71	**9.15 (±1.56)**	**0.02 (±0.01)**	**457.500**	**1.92×10^{-7}**	3.29 (±0.64)	0.08 (±0.07)	41.125	1.79×10^{-6}
26	453.2126	8.73	**22.60 (±3.78)**	**2.63 (±0.75)**	**8.593**	**1.23×10^{-7}^**	40.22 (±9.02)	4.84 (±1.38)	8.310	4.13×10^{-6}^
27	541.138	8.96	3.11 (±0.70)	0.05 (±0.04)	62.200	6.03×10^{-3}	**3.18 (±0.49)**	**0.11 (±0.06)**	**28.909**	**6.16×10^{-9}^**
28	405.1553	8.97	**29.07 (±4.22)**	**2.14 (±0.64)**	**13.584**	**1.88×10^{-8}^**	**12.41 (±1.85)**	**0.81 (±0.28)**	**15.321**	**5.40×10^{-10}^**
29	509.216	9.49	**16.62 (±3.72)**	**1.34 (±0.35)**	**12.403**	**1.37×10^{-8}^**	3.94 (±1.39)	0.28 (±0.10)	14.071	3.67×10^{-3}

PCA of the shoot data revealed one outlier (representing a control plant) from the positive dataset and six from the negative dataset (four controls, and two *P. penetrans* infected plants) that were excluded from all further analyses. After exclusion of the outliers, PCA resulted in shoot models with poor diagnostics (positive ESI: $R^2X = 0.141$, $Q^2 = -0.040$; negative ESI: $R^2X = 0.125$, $Q^2 = -0.073$) and revealed no separations between the treatment groups (Figure 3.3.a & b). Supervised OPLS-DA explained a large amount of variation in shoot chemistry in both the positive and negative datasets (total R^2Y was > 0.927) (Table 3.4.). The predictability OPLS-DA, however, was very poor for both the positive ($Q^2 = -0.049$) and negative ($Q^2 = -0.194$) data. Consequently, it was not possible to detect in the 'S'-plots any metabolites that discriminated between shoots of *P. penetrans* infected and control plants.

3.4.3.2. *Pratylenchus penetrans* effects on ragwort chemistry (UPLC-TOFMS) 28 days post-infection

PCA of roots revealed five outliers in the positive (one control, and four *P. penetrans* infected plants) and one in the negative (a *P. penetrans* infected plant) dataset that were excluded from additional analyses. After exclusion of the outliers, PCA resulted in root models with poor diagnostics (positive ESI: $R^2X = 0159$, $Q^2 = -0.022$; negative ESI: $R^2X = 0.139$, $Q^2 = -0.061$). Control and *P. penetrans* treated plants were not separated along the ordination axes (Figure 3.5.e and f). Supervised OPLS-DA revealed clear metabolome differences between control and *Pratylenchus* treated plants (Figure 3.4.c and d), and explained a large amount of the root variance (for both positive and negative models R^2Y of the predictive component > 0.894) (Table 3.4.). Despite poor predictability (Table 3.4.), the models and resulting 'S'-plots of the datasets obtained in both positive and negative ESI MS modes revealed metabolites that discriminated between control and *Pratylenchus* treated plants. As observed in models of roots harvested seven days post-infection, the low concentrations of discriminatory metabolites may have explained the poor model predictability. A total of 14 discriminatory metabolites were extracted from the datasets collected in positive ESI (see Table 3.5.) and 13 for the data collected in negative ESI (see Table 3.6.); all increased in *P. penetrans* infected plants. One metabolite (Metabolite 2) was observed in both positive and negative ESI MS modes. Of these, nine discriminatory metabolites remained significant (Tables 3.5. & 3.6.) after Bonferroni adjustment (Bonferroni threshold: positive: $P < 1.28 \times 10^{-6}$; negative: $P < 6.85 \times 10^{-7}$).

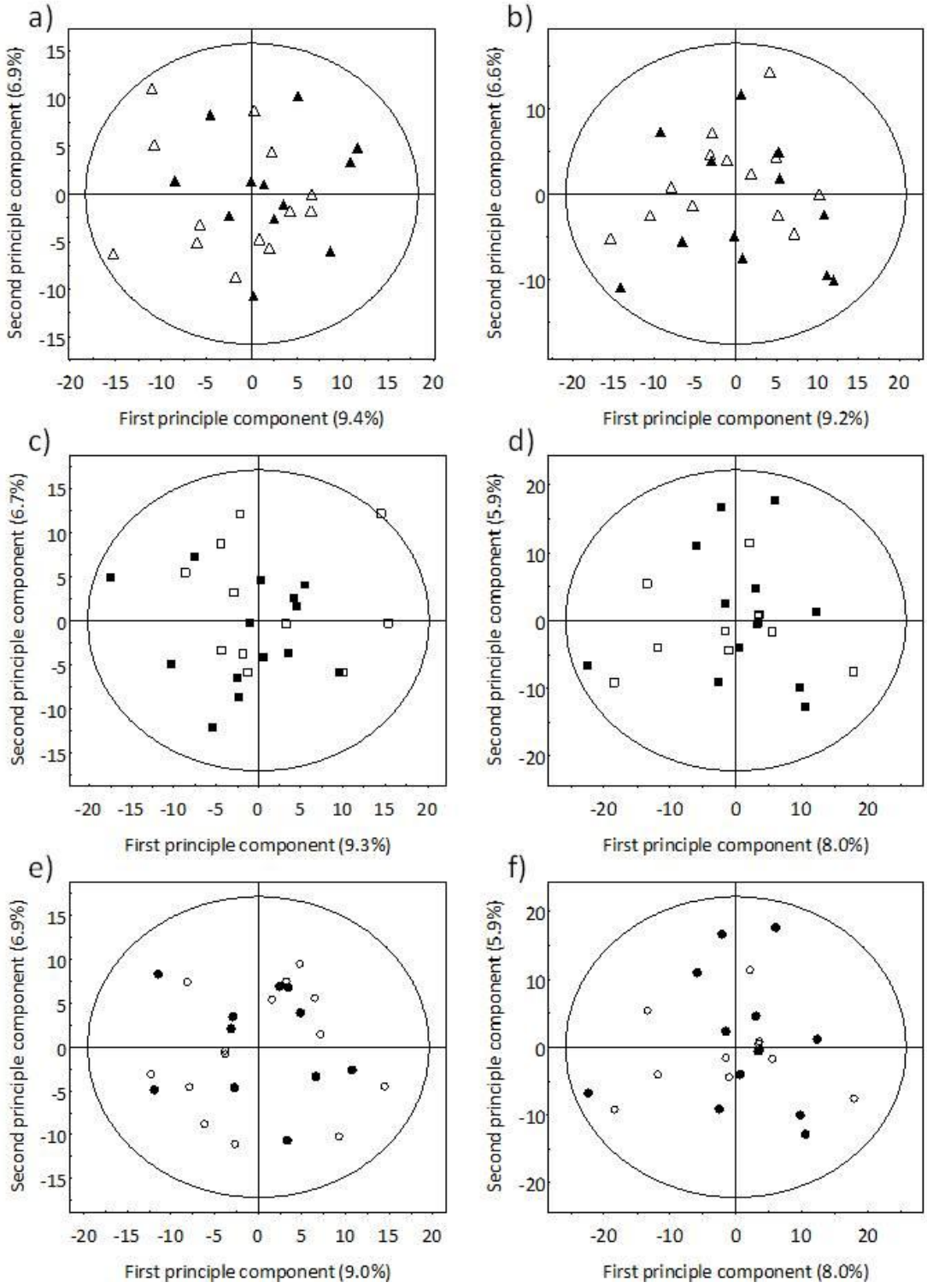

Figure 3.5. Results of the PCA modelling of plant material harvested 28 days post-infection and analysed using UPLC-TOFMS in positive (a, c and e) and negative (b, d and f) ESI modes. Plots display the first two principle components of the models of ragwort new shoots (triangles - a and b), old shoots (squares - c and d) and roots (circles - e and f). Black symbols represent plants treated with a *Pratylenchus penetrans* inoculate and open symbols are control plants.

The PCA of the new shoots harvested 28 days post-infection revealed four outliers originating from the positive dataset (one control, and three *P. penetrans* infected plants) and five from negative dataset (two controls, and three *P. penetrans* infected plants) that were excluded from all further analyses. The PCA of the new shoot data did not separate control and *P. penetrans* treated plants (positive ESI: $R^2X = 0.164$, $Q^2 = -0.017$; negative ESI: $R^2X = 0.158$, $Q^2 = -0.025$) (Figure 3.5.a and b). Supervised OPLS-DA explained a high amount of variation (for both the positive and negative datasets $R^2Y > 0.816$), but had very poor predictability ($Q^2 < 0.045$ for both datasets) (Table 3.4.). Consequently, no metabolites associated with the discrimination of treatment groups could be extracted using the 'S'-plots of these models.

PCA of the old shoot analyses revealed four outliers in the positive (three controls, and one *P. penetrans* infected plant) and five in the negative (two controls, and three *P. penetrans* infected plants) datasets. These outliers were excluded from subsequent analysis. PCA did not separate old shoot chemistry of control and *P. penetrans* treated plants (positive ESI: $R^2X = 0.160$, $Q^2 = -0.024$; negative ESI: $R^2X = 0.140$, $Q^2 = -0.061$) (Figure 3.5.c and d). Supervised OPLS-DA produced models that explained a high amount of variation ($R^2Y > 0.964$ for the models of both positive and negative datasets) (Table 3.4.) but with poor predictability (for both ESI MS modes $Q^2 < -0.017$). Consequently, no metabolites associated with the control and *P. penetrans* treatments could be extracted from the 'S'-plots.

3.4.3.3. Effect of *P. penetrans* infection duration on the chemistry of ragwort

The effect of infection duration on the concentrations of discriminatory metabolites in ragwort roots infected with *P. penetrans*, required the results of both infection durations to be compared. The analyses of the positive and negative ESI datasets obtained from plants harvested seven and 28 days post-infection led to a total of 29 metabolites of interest being identified in 'S'-plots (Tables 3.5. & 3.6.). After Bonferroni correction, the number of metabolites of interest that significantly increased as a result of *P. penetrans* infection was, however, 19 (Tables 3.5. & 3.6.). One of those metabolites (Metabolite 2) was observed in both ionisation modes. One metabolite observed in roots harvested seven days post-infection was not observed in plants harvested 28 days post-infection (Metabolite 21, Table 3.6.), whereas, the concentrations of three metabolites were only increased in roots harvested 28 days post-infection (Metabolites 1, 4 and 8, Table 3.5.). Across both ESI datasets, more metabolite differences between treatments were observed in plants harvested seven days post-infection (17 metabolites), than after 28 days (nine metabolites) (Tables 3.5. & 3.6.).

Regardless of infection duration, the concentrations of six metabolites (Metabolites 7, 13, 14, 20, 24 & 28) were significantly greater in *P. penetrans* infected plants than controls (Tables 3.5. & 3.6.).

3.4.4. Identification of root metabolites associated with *P. penetrans* infection

3.4.4.1. Pyrrolizidine alkaloid (PA) variation associated with *P. penetrans* infection

One metabolite signal (Metabolite 3, Table 3.5.) observed in positive ESI analysis of roots was identified as a $[M+Na]^+$ ion of a PA (Table 3.7.). The parent PA ion was calculated to be *m/z* 368.1708 (± 5ppm) with an elemental composition $C_{18}H_{25}NO_7$ (r.t. = 4.50 in Tables 3. 8., 3.9. & 3.10.). This PA was observed in all plant material from all harvests, but concentrations increased significantly only in *P. penetrans* infected roots harvested seven days post-infection (Tables 3.8., 3.9. & 3.10.). Previous studies of the PAs in ragwort (da Silva *et al.* 2006, Joosten *et al.* 2010, Kostenko *et al.* 2012) suggested that the PA (*m/z*: 368.1708; elemental composition: $C_{18}H_{25}NO_7$) could be either retrorsine N-oxide, usaramine N-oxide or jacobine N-oxide (Figure 3.6.). In an attempt to determine the unknown PA identity, the compound was analysed using Q-TOFMS CID. This produced a characteristic fragment ion (± 5ppm of the calculated *m/z*: 178.1232; elemental composition: $C_{11}H_{16}NO$) that cannot be produced by fragmentation of the jacobine N-oxide structure (Figure 3.7.). To determine if the unknown PA was retrorsine N-oxide or usaramine N-oxide an authentic retrorsine N-oxide standard was analysed using UPLC-TOFMS. This retrorsine N-oxide standard eluted at the same time as the unknown PA (Figure 3.8.). In addition clear separations are seen between the peak of interest and other peaks of the same *m/z* (Figure 3.8.). It was concluded that the unknown PA was retrorsine N-oxide.

Table 3.7. Identification of the PA discriminatory metabolite detected in ragwort roots infected with of *Pratylenchus* penetrans. The metabolites was detected using UPLC-TOFMS, additional ions and fragments were determined using UPLC-TOFMS and Q-TOFMS CID.

Metabolite number	*m/z* of observed ion	Charge of observed ion	UPLC-TOFMS r.t.	Putative formula	Δ PPM	Theoretical mass of ion	*m/z* of additional ions and fragments	Formula of additional and fragment ion	Identity
3	390.1531	$[M+Na]^+$	4.50	$C_{18}H_{25}NO_7Na$	0.5	390.1529	368.1708 220.1338 178.1232 136.0762 120.0813	$C_{18}H_{26}NO_7$ $C_{13}H_{18}NO_2$ $C_{11}H_{16}NO$ $C_8H_{10}NO$ $C_8H_{10}N$	Retrorsine N-oxide

Table 3.8. Relative concentrations (equivalent to 0.01g fresh material, mean ±S.E.) of pyrrolizidine alkaloids (PAs) in control and *Pratylenchus penetrans* ragwort roots seven and 28 days post-infection. Data were collected using UPLC-TOFMS in positive ESI mode and are displayed in ascending *m/z* order. When the PA response was saturated the C_{13} and O_{18} isotope responses of the PA were used for quantification, these are indicated by [a] and [b] respectively. Fold differences >1 indicate higher concentrations are observed in the *P.penetrans* plant and those <1 represent higher concentrations in control plants. Within each harvest, P-values marked with a ^ are from t-tests, unmarked P-values are from Mann-Whitney U tests.. Those comparisons that remained significant after Bonferroni correction (seven days post-infection: $P < 4.58 \times 10^{-7}$, 28 days post-infection: $P < 1.28 \times 10^{-6}$) are in **bold**.

		7 days post-infection				28 days-post infection			
m/z	UPLC-TOFMS r.t.	*P. penetrans*	Control	Fold dif	P-value	*P. penetrans*	Control	Fold dif	P-value
334.1650	4.90	1293.71 (±308.91)	1511.78 (±455.91)	0.86	0.696^	398.64 (±62.04)	332.38 (±44.45)	1.20	0.392^
	5.21	128.24 (±20.84)	125.54 (±21.65)	1.02	0.929^	89.96 (±9.60)	75.13 (±7.40)	1.20	0.231^
336.1811	5.70	7996.24 (±972.17)	9521.38 (±958.61)	0.84	0.275^	2252.45 (±392.06)	2790.72 (±336.40)	0.81	0.306^
	6.80	792.70 (±80.40)	739.49 (±71.32)	1.07	0.625^	423.84 (±55.07)	563.50 (±60.39)	0.75	0.098^
	7.37	1061.71 (±133.19)	1006.64 (±127.03)	1.06	0.767^	459.47 (±47.28)	636.12 (±44.94)	0.72	0.011^
350.1604	5.22	6146.92 (±971.83)	6184.38 (±1025.78)	0.99	0.979 [a]^	6145.05 (±826.56)	5204.56 (±591.94)	1.18	0.363 [a]^
352.1760	3.75	4229.27 (±283.12)	4335.56 (±384.23)	0.98	0.826^	3332.24 (±915.87)	3883.64 (±1417.87)	0.86	0.746^
	4.30	593.75 (±207.22)	705.57 (±209.07)	0.84	0.707^	592.77 (±202.90)	320.95 (±46.34)	1.85	0.202^
	4.40	47.73 (±47.73)	101.57 (±19.09)	0.47	1.55×10^{-3}	895.75 (±87.25)	764.61 (±64.65)	1.17	0.237^
	4.77	645.83 (±150.82)	431.42 (±57.12)	1.50	0.832^	1271.79 (±143.52)	1247.36 (±87.54)	1.02	0.885^
	5.93	2319.63 (±346.11)	1747.30 (±188.58)	1.33	0.159 [b]^	4963.03 (±833.19)	3809.44 (±211.26)	1.30	0.348 [b]^
366.1553	3.38	1250.91 (±348.01)	1279.08 (±256.34)	0.98	0.949^	171.35 (±31.30)	136.60 (±26.92)	1.25	0.407^
	3.96	958.94 (±278.15)	561.41 (±168.74)	1.71	0.234^	500.81 (±190.66)	264.73 (±67.75)	1.89	0.253^
368.1709	4.10	965.56 (±331.85)	1910.31 (±742.93)	0.51	0.872 [a]^	1171.03 (±220.43)	805.08 (±246.93)	1.46	0.278 [a]^
	4.50	**17121.91 (±2363.77)**	**2561.62 (±390.67)**	**6.69**	**4.18×10^{-8}** [a]^	1134.14 (±163.92)	301.62 (±44.64)	3.76	1.73×10^{-5} [a]^
	4.99	2689.28 (±524.06)	2103.63 (±319.35)	1.28	0.568 [a]^	421.82 (±41.72)	325.87 (±44.13)	1.29	0.151 [a]^
	5.27	4482.82 (±655.14)	3508.65 (±354.52)	1.28	0.203 [a]^	717.30 (±68.85)	595.97 (±54.40)	1.20	0.178 [a]^

Table 3.8. continued...

m/z	UPLC-TOFMS r.t.	7 days post-infection				28 days post-infection			
		P. penetrans	Control	Fold dif	P-value	*P. penetrans*	Control	Fold dif	P-value
370.1866	4.87	2597.01 (±343.07)	1879.16 (±284.45)	1.38	0.120^	1797.31 (±286.53)	1639.23 (±280.91)	1.10	0.697^
376.1760	8.24	286.20 (±42.63)	224.15 (±40.36)	1.28	0.301^	186.55 (±24.34)	329.52 (±67.65)	0.57	0.047^
	8.44	112.45 (±18.50)	78.43 (±15.75)	1.43	0.174^	91.12 (±11.00)	114.53 (±12.20)	0.80	0.165^
386.1815	4.68	469.86 (±53.99)	455.58 (±61.64)	1.03	0.863^	179.99 (±25.30)	124.92 (±20.24)	1.44	0.100^
	5.75	247.99 (±20.36)	236.35 (±18.56)	1.05	0.676^	102.19 (±7.98)	79.96 (±8.16)	1.28	0.061^
392.1709	8.45	4388.77 (±879.84)	3570.95 (±862.20)	1.23	0.513 [a]^	3784.95 (±561.30)	6167.12 (±1002.66)	0.61	0.057 [a]^

Table 3.9. Relative concentrations (equivalent to 0.01g fresh material, mean ±S.E.) of pyrrolizidine alkaloids (PAs) in control and *Pratylenchus penetrans* ragwort new shoots seven and 28 days post-infection. Data were collected using UPLC-TOFMS in positive ESI mode and are displayed in ascending *m/z* order. Fold difference values >1 indicate higher concentrations are observed in the *P.penetrans* plant and those <1 represent concentrations higher in the control plants. Within each harvest, P-values marked with a ^ are from t-tests, unmarked P-values are from Mann-Whitney U tests.. No comparisons remained significant after Bonferroni correction (seven days post-infection: $P < 1.80 \times 10^{-6}$, 28 days post-infection: $P < 1.30 \times 10^{-6}$).

m/z	UPLC-TOFMS r.t.	7 days post-infection				28 days post-infection			
		P. penetrans	Control	Fold dif	P-value	*P. penetrans*	Control	Fold dif	P-value
334.1650	4.90	117.97 (±22.95)	119.13 (±18.92)	0.99	0.969^	5.97 (±1.26)	9.12 (±1.58)	0.66	0.128^
336.1811	5.80	160.57 (±20.98)	152.65 (±25.62)	1.05	0.817^	10.57 (±2.67)	16.34 (±2.80)	0.65	0.147^
350.1604	5.29	1833.52 (±210.97)	2010.46 (±208.83)	0.91	0.559^	699.28 (±134.67)	1118.53 (±159.70)	0.63	0.054^
352.1760	3.97	723.74 (±280.37)	973.17 (±250.49)	0.74	0.966^	63.84 (±35.70)	32.74 (±21.61)	1.95	0.152^
	4.25	446.53 (±34.71)	349.24 (±43.49)	1.28	0.866^	9.91 (±1.15)	14.32 (±1.69)	0.69	0.120^
	4.50	584.88 (±43.11)	574.74 (±41.36)	1.02	0.866^	23.82 (±4.32)	34.66 (±4.42)	0.69	0.091^
	4.87	304.56 (±41.38)	307.43 (±49.44)	0.99	0.513^	89.47 (±19.31)	125.44 (±14.42)	0.71	0.084^
	6.07	2749.71 (±426.67)	2876.00 (±576.22)	0.96	0.092^	490.65 (±133.14)	800.36 (±139.96)	0.61	0.038^
366.1553	3.50	129.01 (±24.62)	133.63 (±24.36)	0.97	0.895^	46.42 (±6.54)	68.24 (±15.14)	0.68	0.549^
	4.10	206.39 (±81.59)	113.85 (±28.68)	1.81	0.294^	58.53 (±13.85)	111.39 (±27.10)	0.53	0.075^
	6.53	146.72 (±22.99)	116.21 (±15.85)	1.26	0.281^	5.18 (±0.89)	8.25 (±1.32)	0.63	0.060^
	7.81	226.16 (±30.78)	201.87 (±26.61)	1.12	0.556^	8.24 (±1.91)	11.35 (±2.35)	0.73	0.311^
	8.77	88.60 (±13.50)	76.61 (±11.07)	1.16	0.498^	2.50 (±0.57)	3.32 (±0.73)	0.75	0.380^
368.1709	3.84	110.27 (±30.22)	219.78 (±84.01)	0.50	0.261^	625.58 (±172.78)	514.66 (±185.80)	1.22	0.665^
	4.50	249.84 (±45.66)	134.69 (±36.58)	1.86	0.058^	174.17 (±28.24)	394.30 (±103.39)	0.44	0.017^
	5.02	41.07 (±4.08)	44.74 (±3.79)	0.92	0.516^	16.67 (±2.63)	21.73 (±2.46)	0.77	0.173^
	5.40	96.64 (±9.49)	101.60 (±8.89)	0.95	0.706^	29.84 (±4.03)	43.80 (±5.20)	0.68	0.042^
376.1760	8.34	39.37 (±9.09)	38.60 (±13.70)	1.02	0.963^	Not detected	Not detected	n/a	n/a
386.1815	5.16	4.43 (±1.57)	12.31 (±5.33)	0.36	0.168^	2.36 (±1.01)	1.52 (±0.65)	1.55	0.497^
392.1709	8.54	246.74 (±62.51)	197.01 (±69.12)	1.25	0.598^	0.31 (±0.10)	1.02 (±0.28)	0.30	0.077

Table 3.10. Relative concentrations (equivalent to 0.01g fresh material, mean ±S.E.) of pyrrolizidine alkaloids (PAs) in control and *Pratylenchus penetrans* ragwort old shoots harvested 28 days post-infection. Data were collected using UPLC-TOFMS in positive ESI mode and are displayed in ascending *m/z* order. Fold difference values >1 indicate higher concentrations are observed in the *P.penetrans* plant and those <1 represent concentrations higher in the control plants. P-values marked with a ^ are from t-tests, unmarked P-values are from Mann-Whitney U tests. No comparisons remained significant after Bonferroni correction (28 days post-infection: $P < 1.30 \times 10^{-6}$).

m/z	UPLC-TOFMS r.t.	28 days post-infection			
		P. penetrans	Control	Fold dif	P-value
334.1650	4.90	505.66 (±123.83)	334.69 (±54.23)	1.511	0.416^
336.1811	5.80	591.19 (±138.88)	479.68 (±117.41)	1.232	0.545^
350.1604	5.29	813.86 (±151.88)	633.95 (±125.83)	1.284	0.389^
352.1760	3.97	2963.00 (±543.02)	2515.95 (±969.23)	1.178	0.950^
	4.25	301.19 (±49.36)	424.12 (±124.18)	0.710	0.721^
	4.50	278.15 (±37.12)	225.61 (±32.56)	1.233	0.297^
	4.87	33.36 (±5.99)	32.84 (±5.24)	1.016	0.691^
	6.07	702.01 (±137.52)	630.36 (±139.50)	1.114	0.769
366.1553	3.50	7.99 (±2.13)	6.50 (±1.76)	1.229	0.595^
	4.10	188.14 (±68.45)	414.89 (±229.22)	0.453	0.388^
	6.53	55.24 (±9.79)	57.70 (±10.16)	0.957	0.863^
	7.81	100.62 (±19.03)	100.88 (±19.11)	0.997	0.993^
	8.77	32.34 (±6.74)	32.85 (±6.42)	0.984	0.957^
368.1709	3.84	292.02 (±79.49)	230.66 (±73.34)	1.266	0.585^
	4.50	156.56 (±26.69)	227.09 (±103.68)	0.689	0.471^
	5.02	25.01 (±3.48)	25.40 (±4.47)	0.985	0.945^
	5.40	45.23 (±4.89)	55.20 (±6.99)	0.819	0.214^
376.1760	8.34	18.80 (±2.01)	16.80 (±1.70)	1.119	0.452^
386.1815	5.16	64.07 (±20.27)	53.65 (±17.63)	1.194	0.701^
392.1709	8.54	27.57 (±13.70)	20.75 (±6.23)	1.329	0.654^

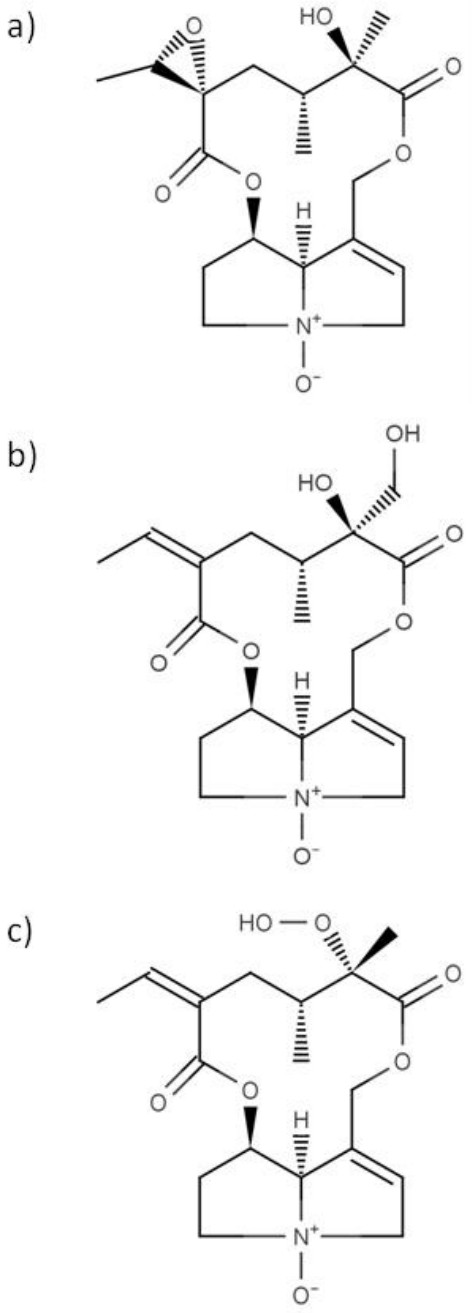

Figure 3.6. Structures of the pyrrolizidine alkaloids a) jacobine N-oxide, b) retrorsine N-oxide and c) usaramine N-oxide. These isomers share the same molecular ion (*m/z*: 368.1709) and elemental composition ($C_{18}H_{25}NO_7$).

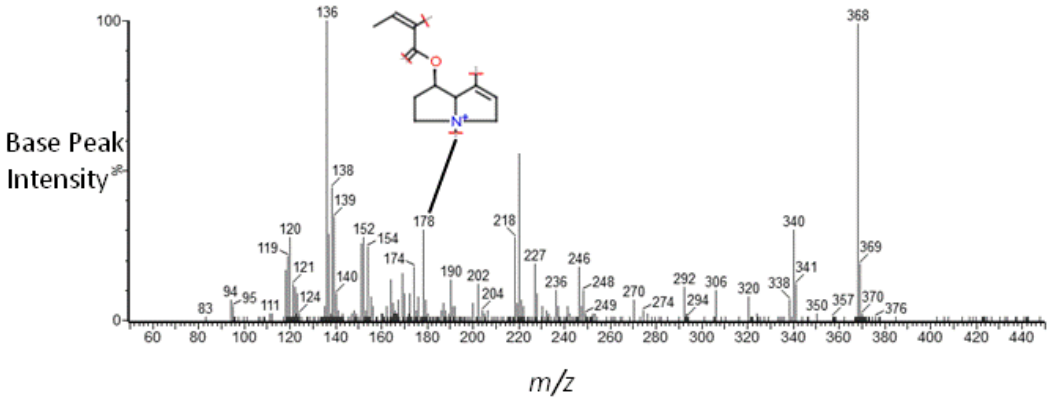

Figure 3.7. Identification of the root PA that was significantly increased in *Pratylenchus penetrans* infected plants harvested seven days post-infection. This characteristic fragment of mass 178.1232 cannot be formed by fragmentation of the jacobine N-oxide structure. The observation of this diagnostic fragment means that the unknown root PA, that significantly differs as a result of *Pratylenchus penetrans* infection, cannot be jacobine N-oxide. However, this fragment (or any others observed) were able to distinguish between retrorsine N-oxide and usaramine N-oxide.

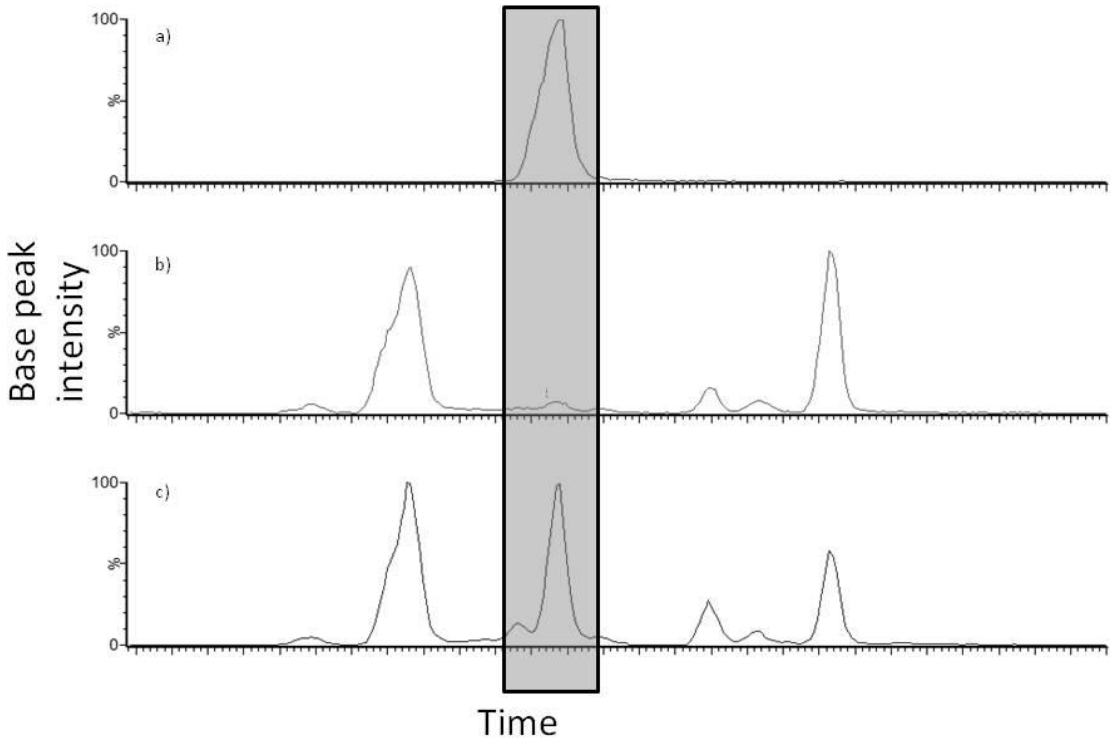

Figure 3.8. Identification of the root PA, retrorsine N-oxide, that increased in *Pratylenchus penetrans* infected plants harvested seven days post-infection. The top BPI trace **a)** displays a 5µl injection of a retrorsine N-oxide standard (1ng/µl). The bottom two BPI traces are representative samples from this experiment (in both cases, 1µl injection, equivalent to 0.104mg of plant wet weight, was analysed), **b)** shows the response for plants grown without nematodes and **c)** represent plants grown with nematodes. The difference between traces b) and c) was clearly visible (highlighted in grey). A greater response, and thus larger concentration, of the PA *m/z* 368.1709 was seen in plants colonised by *P. penetrans*. In addition, by comparing traces a) and c) it was demonstrated that clear separations are obtained between peaks of *m/z* 368.1709 and that the PA peak of interest has the same retention time as the retrorsine N-oxide standard.

All other PAs were manually quantified to ensure that they were not discriminatory chemicals associated with *P. penetrans* infection (Tables 3.8., 3.9. & 3.10.). Including the PA identified as retrorsine N-oxide, 23 root (Table 3.8.) and 20 new shoot (Table 3.9.) PAs were identified over both harvests. Old shoots harvested 28 days post-infection yielded 20 PAs (Table 3.10.). Other than the one previously described, no previously reported variations in ragwort PA concentrations were observed in this experiment following infection by *P. penetrans* (Tables 3.8., 3.9. & 3.10.).

3.4.4.2. Other metabolite variation associated with *P. penetrans* infection

In addition to the PA retrorsine N-oxide discussed above, eight root metabolites associated with *P. penetrans* were assigned putative identities (Tables 3.11. and 3.12.). Analysis of the $[M+H]^+$ parent ion using UPLC Xevo G2-TOF revealed that Metabolite 7 was an alkaloid (Table 3.11.) with the elemental composition $C_{21}H_{28}NO_6$ ±5ppm of the *m/z* 390.1917, which does not correspond to any of the PAs previously observed in ragwort (da Silva *et al.* 2006, Joosten *et al.* 2010, Kostenko *et al.* 2012). Metabolite 10 (Table 3.11.) was identified as a terpenoid malonylglycoside. Fragmentation of the $[M+H]^+$ ion by UPLC Xevo G2-TOF at 20eV gave rise to a fragment ion corresponding to the terpenoid aglycone $C_{15}H_{23}O_3$ (*m/z* 251.1652) indicating loss of a malonylglycoside moiety (*m/z* 248, $C_9H_{12}O_8$) from the parent ion. Metabolite 2 was identified as a tryptophan conjugate of an unidentified C9 metabolite which was not present in any plant databases. In positive ESI mode ions of m/z 205.0977 and 188.0712 corresponded to protonated tryptophan and its major CID fragment respectively. As with many of these metabolites, further material was required for structural analysis, and their low concentrations in the plant root samples precluded further mass spectrometry or NMR analyses. Five metabolites were identified as flavonoids, unconjugated (metabolites 17 and 22), glycoside (Metabolite 8) and diglycoside (Metabolites 18 and 25) flavonoids were observed. Flavonoids were detected in both positive and negative ESI MS modes. Both unconjugated flavonoids (Metabolites 17 and 22, Table 3.12.) were observed as $[M-H]^-$ ions in negative ESI MS mode. Accurate mass measurement using UPLC Xevo G2-TOF confirmed the likely elemental compositions as $C_{15}H_{13}O_8$ and $C_{31}H_{29}O_8$ for Metabolites 17 and 22, respectively. Metabolite 8 was identified as a flavonoid glycoside (Table 3.11.). The sodium adduct, $[M+Na]^+$, of Metabolite 8 was identified as a flavonoid glycoside ±5ppm of the *m/z* 499.1216 and elemental composition $C_{23}H_{24}O_{11}Na$ using UPLC Xevo G2-TOF. Both diglycoside flavonoids (Metabolites 18 and 25, Table 3.12.) were observed as $[M-H]^-$ ions in negative ESI MS mode. The parent ion, $[M-H]^-$, of Metabolites 18 and 25 were identified as a flavonoid diglycoside ± 5ppm of the *m/z*

683.1823 and 709.1616 and elemental compositions $C_{30}H_{35}O_{18}$ and $C_{31}H_{33}O_{19}$, respectively, using UPLC Xevo G2-TOF.

Table 3.11. Putative identification of the discriminatory metabolites detected in the roots of ragwort infected with *Pratylenchus penetrans*. All metabolites were detected using UPLC-TOFMS in positive ESI mode. Additional ions and fragments were observed using UPLC-TOFMS and UPLC Xevo G2-TOF, both in positive ESI mode.

Metabolite number	*m/z* of observed ion	Charge of observed ion	UPLC-TOFMS r.t.	Putative formula	Δ PPM	Theoretical mass of ion	*m/z* of additional ions and fragments	Formula of additional and fragment ion	Putative identity
1	435.1630	$[M+Na]^+$	3.43	$C_{20}H_{28}O_9Na$	-0.2	435.1631	-	-	-
2	448.1357	$[M+H]^+$	3.57	$C_{20}H_{22}N_3O_9$	-0.4	448.1356	430.1248 244.1909 205.0977 188.0712	$C_{20}H_{20}N_3O_8$ $C_9H_{11}NO_7$ $C_{11}H_{13}N_2O_2$ $C_{11}H_{10}NO_2$	Tryptophan conjugate
4	419.1711	$[M+H]^+$	5.34	$C_{22}H_{27}O_8$	-1.6	419.1706	-	-	-
5	413.0400	-	5.68	-	-	-	-	-	-
6	251.0919	$[M+H]^+$	5.92	$C_{13}H_{15}O_5$	0.0	251.0919	-	-	-
7	390.1915	$[M+H]^+$	6.32	$C_{21}H_{28}NO_6$	-0.5	390.1917	330.1704	$C_{19}H_{24}NO_4$	Alkaloid
8	499.1217	$[M+Na]^+$	6.68	$C_{23}H_{24}O_{11}Na$	0.2	499.1216	163.0396	$C_9H_7O_3$	Flavonoid glycoside
9	489.1972	$[M+H]^+$	7.65	$C_{22}H_{33}O_{12}$	-0.4	489.1972	-	-	-
10	499.2178	$[M+H]^+$	8.39	$C_{24}H_{35}O_{11}$	-0.2	499.2178	521.1998 251.1652 203.1437	$C_{24}H_{34}O_{11}Na$ $C_{15}H_{23}O_3$ $C_{14}H_{19}O$	Terpenoid malonyglycoside
11	555.1393	$[M+H]^+$	8.38	$C_{17}H_{31}O_{20}$	-2.9	555.1409	-	-	-
12	269.0815	$[M+H]^+$	8.39	$C_{16}H_{13}O_4$	0.4	269.0814	-	-	-
13	609.1359	$[M+H]^+$	8.39	$C_{16}H_{33}O_{24}$	-0.5	609.1362	-	-	-
14	575.1949	$[M+Na]^+$	8.38	$C_{23}H_{36}O_{15}Na$	-0.5	575.1952	570.2401 399.1631	$C_{23}H_{40}NO_{15}$ $C_{17}H_{28}O_9Na$	-
15	399.1655	$[M+H]^+$	10.43	$C_{19}H_{27}O_9$	0.0	399.1655	421.1483	$C_{19}H_{26}O_9Na$	-

Table 3.12. Putative identification of the discriminatory metabolites detected in the roots of ragwort infected with *Pratylenchus penetrans*. All metabolites were detected using UPLC-TOFMS in negative ESI mode. Additional ions and fragments were observed using UPLC-TOFMS and UPLC Xevo G2-TOF, both in negative ESI mode.

Metabolite number	*m/z* of observed ion	Charge of observed ion	UPLC-TOFMS r.t.	Putative formula	Δ PPM	Theoretical mass of ion	*m/z* of additional ions and fragments	Formula of additional and fragment ion	Putative identity
2	446.1201	$[M-H]^-$	3.57	$C_{20}H_{20}N_3O_9$	0.2	446.1200	514.1063	$C_{21}H_{21}N_3O_{11}Na$	Tryptophan conjugate
16	231.0869	$[M-H]^-$	4.15	$C_{10}H_{15}O_6$	0.0	231.0869	265.0927 215.0925 171.1021 153.0916	$C_{10}H_{17}O_8$ $C_{10}H_{15}O_5$ $C_9H_{15}O_3$ $C_9H_{13}O_2$	-
17	321.0607	$[M-H]^-$	4.16	$C_{15}H_{13}O_8$	-0.9	321.0610	-	-	Flavonoid
18	683.1829	$[M-H]^-$	5.56	$C_{30}H_{35}O_{18}$	0.9	683.1823	329.0873	$C_{14}H_{17}O_9$	Flavonoid diglycoside
19	423.0936	$[M-H]^-$	5.94	$C_{19}H_{19}O_{11}$	0.9	423.0927	-	-	-
20	465.1967	$[M-H]^-$	7.56	$C_{20}H_{33}O_{12}$	-1.1	465.1972	-	-	-
21	601.1714	$[M-H]^-$	7.61	$C_{33}H_{29}O_{11}$	0.7	601.1710	-	-	-
22	529.1868	$[M-H]^-$	8.63	$C_{31}H_{29}O_8$	1.1	529.1862	-	-	Flavonoid
23	641.1636	$[M-H]^-$	8.63	$C_{17}H_{37}O_5$	1.9	641.1624	-	-	-
24	551.1976	$[M-H]^-$	8.71	$C_{23}H_{35}O_{15}$	0.0	551.1976	573.1793 507.2072	$C_{23}H_{34}O_{15}Na$ $C_{22}H_{35}O_{13}$	-
25	709.1596	$[M-H]^-$	8.71	$C_{31}H_{33}O_{19}$	-2.8	709.1616	777.1488	$C_{32}H_{34}O_{21}Na$	Flavonoid diglycoside
26	453.2126	$[M-H]^-$	8.73	$C_{23}H_{33}O_9$	0.2	453.2125	521.2008 161.0453 101.0242	$C_{24}H_{34}O_{11}Na$ $C_6H_9O_5$ $C_4H_5O_3$	Glycoside conjugate

Table 3.12. continued...

Metabolite number	*m/z* of observed ion	Charge of observed ion	UPLC-TOFMS r.t.	Putative formula	Δ PPM	Theoretical mass of ion	*m/z* of additional ions and fragments	Formula of additional and fragment ion	Putative identity
27	541.138	$[M+CHO_2Na]^-$	8.96	$C_{25}H_{26}O_{12}Na$	3.9	541.1322	473.1477	$C_{24}H_{25}O_{10}$	-
28	405.1553	$[M-H]^-$	8.97	$C_{21}H_{25}O_8$	1.0	405.1549			-
29	509.216	$[(M-H)-CO_2]^-$	9.49	$C_{22}H_{37}O_{13}$	-1.0	509.2234	553.2129	$C_{23}H_{37}O_{15}$	-

3.5. Discussion

This study details the first metabolomic assessment of the effect of migratory endoparasitic nematode herbivory on the secondary chemistry of host-plant roots and shoots. Nineteen metabolites, including the PA retrorsine N-oxide, increased in concentration in nematode infected roots irrespective of infection duration. We did not, however, detect any change in the concentrations of other previously reported ragwort PAs. Our second prediction was unsupported with no evidence of concomitant changes in shoot metabolome with nematode herbivory. As predicted, nematode herbivory elicited a rapid plant metabolomic response with 17 metabolomic differences (11 specific to this harvest) detected in roots seven days post-infection. Contrary to prediction, however, this effect diminished as the nematode infection proceeded. Despite similar nematode root densities, and greater soil densities, only seven metabolite concentrations increased 28 days post-infection, with only three metabolites unique to that harvest. Six metabolites, including a suspected alkaloid, consistently increased in concentration with *P. penetrans* infection irrespective of harvest time.

The induction of plant root metabolites in response to nematode feeding is observed in numerous study systems (Kaplan *et al.* 2008, Hofmann *et al.* 2010, Baldacci-Cresp *et al.* 2012, van Dam 2012). This study is the first to use a metabolomic approach to detect changes in plant secondary metabolism as a result of infection by a migratory endoparasitic nematode. Two previous studies have adopted a metabolomic approach to examine the interaction between sedentary endoparasitic nematodes and plant metabolism. Hofmann *et al.* (2010) showed with a GC-MS metabolomic approach that infection by *Heterodera schachtii* (a cyst nematode) increased root concentrations of amino acids, phosphates and six unidentified metabolites likely to be trisaccharides or disaccharides with similar sized conjugates. Similarly, using NMR Baldacci-Cresp *et al.* (2012) observed increased concentrations of amino acids and sugars, but decreased levels of glycoxylate, in roots infected by the root knot nematode *Meloidogyne incognita*.

In contrast to studies that have shown nematode root feeding to affect above-ground secondary chemistry (Friedman and Rohde 1976, van Dam *et al.* 2005, Kaplan *et al.* 2008, Lohmann *et al.* 2009, Hofmann *et al.* 2010), this study did not detect *P. penetrans* induced changes in shoot metabolome. Below-ground herbivory is known to affect plant-volatile profiles (Soler *et al.* 2007c), with repercussions for insect behaviour at higher trophic levels (Soler *et al.* 2007b). In the current study neither primary metabolism nor plant-volatiles were measured. Above-ground responses to below-ground mechanical damage in ragwort are

known to be highly genotype dependant (Hol *et al.* 2004). It could be that the genotype of the half-sibs examined in the current study do not respond above ground to nematode herbivory below ground.

The induction of increased concentrations of retrorsine N-oxide and unidentified alkaloid (metabolite 7) by *P. penetrans* infection of roots is consistent with other alkaloid-containing plant species (Kaplan *et al.* 2008). Unfortunately, the identity of this unknown alkaloid could not be confirmed due to low concentrations of the metabolite being available. It is likely that *P. penetrans* encountered PAs when they fed on ragwort because PAs of *Senecio* species are synthesised in roots (Hartmann *et al.* 1989) and stored in cell vacuoles (Ehmke *et al.* 1988). PAs are known to have nematacidal effects on migratory endoparasitic nematodes *in vitro* (Thoden *et al.* 2009a). When tested *in planta*, the PAs of *Senecio bicolor* Tod. did not, however, kill the root knot nematode species *Meloidogyne hapla* Chitwood 1949 (Thoden *et al.* 2009b) but arrested development so that the worms remained juvenile and unable to reproduce (Thoden *et al.* 2009b). The effect of retrorsine N-oxide on nematodes has never been investigated. The magnitude of the negative effects of retrorsine N-oxide on nematodes cannot be understood from studies of other PAs because small differences in chemical structures have different effects on herbivores (van Leur *et al.* 2008, Thoden *et al.* 2009a).

In addition to increased concentrations of the unidentified alkaloid (Metabolite 7) and retrorsine N-oxide, 17 other root metabolites increased as a result of *P. penetrans* infection. Consistent with the findings of Collingborn *et al.* (2000), five were identified as flavonoids. Flavonoids are known to have nematoxic activity (Begum *et al.* 2000). Unfortunately, the identities of the flavonoids could not be confirmed in the present study due to their occurrence at low concentrations. Further work examining the host-plant response to migratory endoparasitic nematode feeding should consider the use of a targeted flavonoid analysis to obtain additional structural information allowing their role in the interaction to be examined. Some of the hitherto unknown metabolites may also be effective nematode biocontol agents. While likely elemental compositions were determined for all metabolites, and fragmentation ions obtained for some, a lack of information on the online plant metabolomic databases hampered the identification and thus application of nine metabolites. This emphasises the need for improved online metabolomic resources, to understand better the plant metabolome and its interaction with other biota.

Metabolomic responses to *P. penetrans* infection were noted in roots harvested seven and 28 days post-infection. Twice as many metabolite differences were observed in roots from the

earlier harvest. Many plant-responses would not have been observed if an early harvest was not undertaken, emphasising the importance of multiple harvest events when investigating plant-nematode interactions. Sedentary endoparasitic nematodes manipulate their plant-host, and are known to alter plant primary metabolism for their own gain (Hofmann *et al.* 2010, Baldacci-Cresp *et al.* 2012). A recent study by Kyndt *et al.* (2012) was the first that examined the expression of defence-related genes as a result of migratory endoparasitic nematode infection. Genes responsible for the regulation of the general defence response in rice (*Oryza sativa* L.) initially increased three days after infection with *Hirshmanniella oryzae*, an effect that was completely reversed four days later (Kyndt *et al.* 2012). The results of the current study observed a similar PA induction seven days post *P. penetrans* infection, an effect that had waned 21 days later. This, coupled with the increase in total *P. penetrans* populations as the present study progressed, supports the findings of Kyndt *et al.* (2012) that concluded that migratory endoparasitic nematodes are very effective manipulators of the plant-host defence response.

Although relatively short lived, the induced changes in root PA chemistry caused by *P. penetrans* may have wider implications for the interactions between ragwort and its root herbivores. Increases in PA root concentrations may have indirect negative effects on ragwort by attracting specialist root herbivores (Robert *et al.* 2012). *Longitarsus* beetles sequester *Senecio* PAs in their root feeding larval stage (Dobler *et al.* 2000). Although hosts are selected by the adult beetle based on above-ground cues (Potter *et al.* 2004), perhaps PAs have a role for larvae when locating suitable below-ground parts of the host-plant. In addition, increased concentrations of root PAs induced by *P. penetrans* feeding could have a negative effect on other generalist herbivore species sharing the same plant-host. The presence of endoparasitic nematodes has been shown to affect the development of ectoparasitic nematodes sharing a plant-host negatively (Brinkman *et al.* 2004). PA containing plants have been suggested as potential biocontrol tools for controlling nematode populations (Thoden and Boppre 2010). The results of the current study suggested that future applied work should focus on the effect retrorsine N-oxide has on multiple aspects of nematode biology. It is possible that retrorsine N-oxide affects nematodes in more subtle ways than by merely reducing numbers (Baldacci-Cresp *et al.* 2012). Tests of nematode mobility, vitality, development, reproduction, chemotaxis, root locating and invasion ability are all possible *in vitro*, as is the effect of metabolites as a nematode repellent (Wuyts *et al.* 2006, Thoden *et al.* 2007, 2009a). In addition, to ensure the biological relevance of the results they should be performed at concentrations relevant to those observed *in planta* (Chitwood 2002).

In summary, using a metabolomic approach the secondary chemistry of the interaction between *P. penetrans* and ragwort was examined. Significant metabolomic differences were observed including the induction of the PA retrorsine N-oxide, an effect that waned as the interaction progressed. This suggested that, like sedentary nematodes, migratory endoparasitc nematodes are very effective manipulators of the plant-host metabolism. The results of this study emphasise the need to consider secondary metabolism when studying the interactions between nematodes and their host-plant. Future work should focus on identifying the secondary metabolites that increased as a result of *P. penetrans* feeding, and testing their multiple effects on *P. penetrans* behaviour at concentrations relevant to those found in plants.

Chapter 4. The effect of the arbuscular mycorrhizal fungus *Glomus intraradices* on the secondary chemistry of ragwort

4.1. Abstract

Arbuscular mycorrhizal fungi (AMF) colonisation of plant roots alters plant chemistry with consequences for AMF-host communication and host defence against herbivory. The consequences of colonisation by the AMF species, *Glomus intraradices*, for ragwort (*Senecio jacobaea*) were examined using a metabolomic approach. This enabled the concomitant observation of the communication and defensive metabolites involved in this chemical interaction. *G. intraradices* colonisation changed secondary chemistry in ragwort roots but not shoots. Increased concentrations of seven blumenol apocarotenoids, a class of metabolites associated with communication in AMF-plant interactions, were observed in roots. Changes in the main class of secondary metabolite defences in ragwort (pyrrolizidine alkaloids) were not induced by *G. intraradices* colonisation, implying that this interaction with AMF is indeed beneficial to the ragwort host. This study demonstrates that if AMF colonisation of ragwort affects plant interactions with above-ground herbivores, it is not via an AMF induced shift in constitutive shoot chemistry.

4.2. Introduction

Plant-mycorrhizal associations are a widespread phenomenon across many ecosystems (Helgason *et al.* 2007). Arbuscular mycorrhizal fungi (AMF) of the Glomeromycota are obligate symbionts that form mutualistic connections with host plant roots that enhance root uptake of macronutrients, such as phosphorus and nitrogen, from the soil (Hodge *et al.* 2001, Javot *et al.* 2007). In return, AMF are dependent on the provision of plant primary metabolites (up to 20% of host plant photosynthate) (Bago *et al.* 2000). In addition to mutualistic nutrient exchange, AMF can help host plants resist environmental stresses such as drought (Ruiz-Sanchez *et al.* 2011) and heavy metal pollution (Vivas *et al.* 2003). The secondary chemical composition of plants can also be altered through the process of initiating and maintaining AMF colonisation (Schliemann *et al.* 2008a, Fester *et al.* 2011). One key group of AMF induced metabolites are the apocarotenoids: a suite of metabolites derived from the cleavage of C_{40} carotenoids that are thought to be involved in the chemical signalling underpinning the plant-AMF interaction (Walter *et al.* 2010). The apocarotenoids involved in AMF colonisation fall in to three main

groups: strigolactones, C_{14} polyenes and C_{13} cyclohexenones (Figure 4.1.). Strigolactones are plant hormones present in root exudates that stimulate the branching and growth of AMF, thereby increasing the chance of establishing the hyphal-root connection (Akiyama *et al.* 2005). Root strigolactone concentrations decrease with increasing AMF colonisation, suggesting the host plant can avoid any physiological cost by regulating this stimulus to AMF colonisation (Lopez-Raez *et al.* 2011).

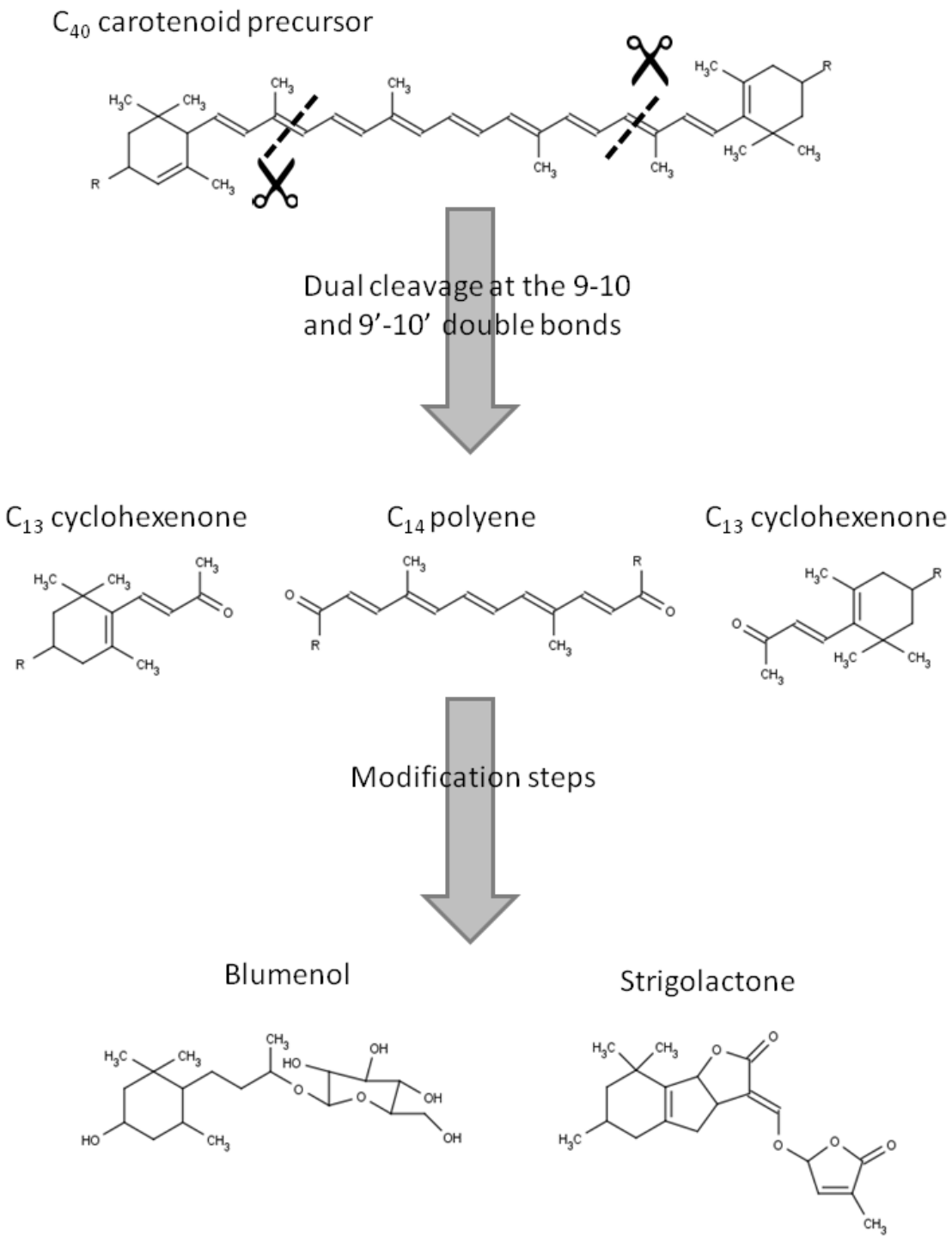

Figure 4.1. Cleavage of the C_{40} carotenoid precursor resulting in the apocarotenoids thought to be associated with the establishment and maintenance of AMF-plant interactions (adapted from Walter *et al.* 2010).

As the plant-AMF interaction progresses the concentrations of C_{14} polyenes and C_{13} cyclohexenones in roots tend to increase (for example, see Peipp *et al.* 1997, Schliemann *et al.* 2006, Schliemann *et al.* 2008b). These apocarotenoids accumulate in root cells hosting AMF structures, which may imply a role for them in maintaining plant-AMF interactions once they are established (Fester *et al.* 2002). C_{14} polyenes are one group of metabolites implicated in the yellowing roots seen in many plant taxa following AMF colonisation (Klingner *et al.* 1995a, Fester *et al.* 2002), their precise function in the plant-AMF interaction remains unknown (Walter and Strack 2011). AMF colonisation is also associated with increased concentrations of a variety of C_{13} cyclohexenones (e.g. blumenin) produced by the host plant (Maier *et al.* 1995, Strack and Fester 2006). There is some evidence that C_{13} cyclohexenone production may have a role in the persistence of mycorrhizal structures (Walter *et al.* 2010), since mutant plants (with reduced C_{13} cyclohexenone production) are associated with an increased amount of dead and degenerating mycorrhizal structures (Floss *et al.* 2008).

Aside from these apocarotenoids implicated in plant-AMF signalling, there are also indications that AMF colonisation may contribute to plant defences. AMF-induced changes to plant secondary chemistry can increase plant resistance to below-ground antagonists such as parasitic plants (Li *et al.* 2012) and plant parasitic nematodes (Rodriguez-Echeverria *et al.* 2009). Furthermore, plant interactions with above-ground herbivores can be affected by AMF (van der Putten *et al.* 2001, Hartley and Gange 2009, Koricheva *et al.* 2009), although the outcome may vary with AMF species identity, herbivore diet breadth and/or feeding mode (Koricheva *et al.* 2009). Only a few studies have examined the impact of AMF on the chemical protection of above-ground tissues, moreover by targeting specific chemical groups these were limited in their power to detect induced chemical responses (Bennett *et al.* 2009, de Deyn *et al.* 2009, Eftekhari *et al.* 2012). Consequently, much remains to be discovered about the potential mechanisms by which AMF colonisation of plant roots can affect above-ground interactions (Gange *et al.* 2012).

A more meticulous, yet not widely applied, approach to quantifying the plant-AMF interaction is to examine changes to the plant metabolome following AMF colonisation. Schliemann *et al.* (2008a), using such a metabolomic approach, showed that primary (e.g. amino acids and fatty acids) and secondary (e.g. apocarotenoids) metabolites differed between *Medicago truncatula* L. individuals with and without AMF colonisation. A similar metabolomic approach revealed that AMF colonisation of *Lotus japonicas* L. altered the levels of several metabolite classes; mature leaves were most affected presumably due to competition with AMF as an alternative carbon sink (Fester *et al.* 2011). Hitherto, there has been no metabolomic investigation into

the concomitant above- and below-ground changes in plant secondary chemistry following AMF colonisation.

Ragwort (*Senecio jacobaea* L.) is a good model to study the plant-AMF chemical interaction. It is known to be an AMF host, with colonisation rates between 4-40% (Gange *et al.* 2002, Reidinger *et al.* 2012). Moreover, the roots are the site of synthesis of pyrrolizidine alkaloids (PAs) (Hartmann *et al.* 1989) - the principle group of chemical defences against herbivory - making it ideal to ascertain the effects of AMF colonisation on plant secondary metabolism. Indeed, the above-ground concentration of the PA jacoline is known to be correlated negatively with the percentage of root colonised by AMF (Reidinger *et al.* 2012). Hitherto, the effect of AMF on root concentrations of PAs has not been studied. By combining an untargeted metabolomic approach with a factorial experiment, this study aimed to test the simultaneous effect of AMF (*Glomus intraradices* Smith & Schenck) colonisation on the growth and secondary chemistry of ragwort roots and leaves. Specifically, this study addressed two questions. Firstly, does AMF colonisation of ragwort elicit the same apocarotenoid (e.g. increased levels of strigolactones, C_{14} polyenes and C_{13} cyclohexenones) changes observed in the roots of other plant taxa? Secondly, does AMF colonisation induce plant chemical defences (e.g. PAs) below and above ground?

4.3. Methods

4.3.1. Arbuscular mycorrhizal fungi(AMF) study species

Glomus intraradices is an AMF species belonging to the phylum Glomeromycota. It is a generalist species, which colonises a wide range of host plants and is consequently commonly used in laboratory studies (Parniske 2008). After germinating, the fungal spore forms a specialised hyphal organ called an appressorium, which penetrates and colonises the intracellular space of the hosts roots (Strack *et al.* 2003). Like all AMF species, *G.intraradices* forms fungal structures called arbuscules inside plant cell walls. Arbuscules are highly branched to maximise the surface area for the exchange of nutrients between fungi and plant. Plant roots colonised by AMF contain arbuscules at all stages of development because they senesce and turnover 4-10 days after formation (Sanders *et al.* 1977). AMF can also form extraradical mycelia to tap into nutrient rich patches of soil (Hodge *et al.* 2010). In the latter stages of colonisation, lipid-rich storage vesicles are formed at the ends of intracellular hyphae (Strack *et al.* 2003).

4.3.2. Ragwort microcosms and experimental treatments

Thirty-one microcosms were created comprising a 1.7L plastic pot filled with a growth medium comprising 1:1 mixture of silver sand:Terragreen® (an attapulgite clay; Turf-Pro Ltd, UK) and bone meal (0.25g/L^{-1}, as a source of phosphorous available only to AMF to encourage the development of a plant-AMF association). Prior to use, all growth media was double-autoclaved (2 x 75 minutes at 121°C) to greatly reduce and standardise the existing fungal and microbial communities. Replicate microcosms were randomly assigned to live AMF (n=16) and control (n=15) treatments. Each replicate in the live AMF treatment was inoculated with 50g (dry weight) of granular *G.intraradices* (PlantWorks, UK). To account for the input of organic material introduced with the AMF inoculate, those replicates assigned to the control treatment had 50g of double autoclaved, and thus killed, granular *G.intraradices* inoculate added. After mixing the growth media, all microcosms were flushed to saturation with water twice, aiming to remove the pulse of nutrients released following sterilisation (Troelstra *et al.* 2001). To re-establish the microbial community destroyed by autoclaving the AMF inoculate, control microcosms received a microbial wash prepared by washing the mycorrhizal inoculum (Karasawa *et al.* 2012). This wash was obtained by mixing the granular AMF inoculate destined for control replicates with reverse osmosis water prior to autoclaving. This mixture was then

filtered (Whatmann, Number 1) overnight at 4°C and 100ml was applied to each control replicate. To account for any differences caused by the addition of water with the microbe wash in control treatments, 100ml of deionised water was applied to the AMF treated microcosms.

Ragwort plants used in the microcosms were sourced from seeds collected (October 2008) from a single plant on the University of Sussex campus (Grid Ref: TQ 348 098). Prior to their use in this experiment (June 2011), seeds were dried at ambient temperature and stored with silica gel at 4°C. Eight days before creating the microcosms (20/06/2011), seeds were surface sterilised in a 5% bleach solution and germinated on double autoclaved vermiculite. Following the establishment of the soil treatments, six seedlings were transferred to each microcosm and after two weeks thinned so that only one seedling remained per microcosm. Each microcosm received a weekly dose of 50ml of half-strength Rorison's solution (Hewitt 1966), but with the plant-available phosphate removed to encourage AMF colonisation. The experiment ran for 10 weeks in a greenhouse maintained at 15-25°C with supplementary lighting (400W, high pressure sodium lamps) on a 16:8 L:D photoperiod. Microcosms were watered with tap water *ad libitum*.

4.3.3. Plant measures and harvesting

Plants were harvested after 10 weeks in treatment and the number of leaves, rosette width, largest leaf length and largest leaf width (together used to calculate largest leaf area) were recorded. All microcosms were destructively harvested (5-6/09/2011) in a random order across treatments to provide samples for metabolomic analysis and AMF quantification (below). From each replicate three new leaves (fully mature closest to the centre of the rosette) and two old leaves (closest to the edge of the rosette with no visible signs of senescence) were excised, weighed (g) and immediately snap frozen in liquid nitrogen to halt enzymatic processes. These samples were then wrapped in tin foil and kept on dry ice until they could be moved to a -80°C freezer. The remaining leaf rosette was removed and weighed to obtain a wet weight (g). It was then dried at 60°C for 72 hours to obtain an above-ground dry weight (g). Water content in shoots was calculated as follows: (fresh weight-dry weight)/(fresh weight) *100.

To quantify ragwort root biomass the roots of each plant were shaken free of substrate, hand-washed for 13 minutes, patted dry with paper towels and weighed to obtain a total root fresh

weight (g). Two representative root samples (each ~10% of the total root mass) were then taken for plant metabolomic analysis (snap frozen and stored at 80°C until analysed, see Section 4.3.5) and measurement of AMF colonisation (stored at 4°C until processed, see Section 4.3.4). The remaining root material was weighed to obtain a wet weight (g) and then dried at 60°C for 72 hours to obtain a below-ground dry weight (g). Water content in roots was calculated in the same way as for shoots.

4.3.4. AMF colonisation of roots

A quarter of the root sub-sample (~10% of the total root mass) taken for AMF analysis was randomly selected to quantify the percentage root length colonised (RLC) by AMF structures. Root colonisation by AMF was estimated in control and treated plants following a method modified from Vierheilig *et al.* (1998). The roots were cleared of pigmentation by immersion overnight in a 10% potassium hydroxide (KOH) solution. They were then rinsed with water and placed for an hour in a 1% hydrochloric acid (HCl) solution to remove all KOH, thus halting the clearing process before sample degradation. AMF structures (arbuscules and vesicles) were stained for one hour with a 1% HCl solution containing a few drops of dark blue Parker Quink Ink (Parker; Boston, USA). Twenty root sections per plant were slide-mounted and the presence or absence of AMF structures were recorded for a minimum of 100 root intersections using a compound microscope (x200 magnification) (McGonigle *et al.* 1990). Percentage RLC for total AMF colonisation (intersections containing vesicles, arbuscules or both) was calculated for each plant as follows: (intersections containing AMF structures/total number of intersections examined) *100.

4.3.5. Metabolomic profiling of AMF-plant interactions

4.3.5.1. Chemicals and standards

Centrifuge Anopore VectaSpin Micro filters (0.2µl pore size, 2ml volume) were purchased from Whatmann (United Kingdom). All of the remaining equipment and chemicals used in the extraction process were purchased from the suppliers listed in Chapter 3. The external standards used were prepared and used to monitor mass spectrometer (MS) performance as described previously in Chapter 2. Internal standards were used to monitor extraction efficiency and prepared as described in Chapter 3. Here, each sample received two internal standards, 12µl of E2-d_4-S solution (10ng/µl) and 24µl of P-d_4 solution (1ng/µl).

4.3.5.2. Solvent extractions

Plant material was extracted using broadly the same method of double solvent extraction as described in Chapter 2. Differences are outlined below. The second extraction solvent was 80% methanol, to ensure extraction of polar metabolites such as sugars. For each sample 0.15g ± 0.01g of plant material was extracted. The internal standard (IS) solutions were added to the plant material during the first solvent extraction prior to vortexing and storing in the freezer. A 1.5ml aliquot of each extract (totalling 3ml) was evaporated down, resuspended in 160µl of methanol:water (3:1), centrifuged (five minutes) and the supernatent filtered through an Phenomenex protein precipitation plate. This filtrate was then stored in an amber HPLC vial at -80°C until analysed.

4.3.5.3. UPLC-TOF MS conditions

The injection volumes of plant extracts analysed was 20µl, and in positive ESI an additional analysis of a 0.5µl injection of root extracts was undertaken. This allowed the large metabolite signals of PAs to be examined in the low volume injections and small metabolite signals to be measured in the high volume injections. The UPLC column and conditions used to analyse samples were identical to that described in Chapter 3. Metabolites were detected using a Micromass TOF-MS system (Waters, Manchester, UK). MS conditions and lockmass were identical to those previously described (Chapter 2), with the exception of the details outlined below. TOF penning pressures ranged from 4.63×10^{-7} to 4.83×10^{-7}. Capillary voltage ranged from 2.40-2.71 in positive mode and was -2.91 in negative mode. In positive mode, the cone voltage was set at 36V, and the multiplier voltage was set at 654V. In negative mode the cone and multiplier voltage were set at 35V and 550V respectively. Desolvation N_2 gas flow was set at 401L h^{-1} for both ionisation modes.

4.3.5.4. Monitoring UPLC-TOFMS performance using composite samples

Composite samples, appropriate to the plant material being analysed, were run periodically to ensure that the MS instrument was running consistently. Root and shoot composite extracts were prepared by using 500µl of the appropriate extracts from every plant replicate to form a composite sample and 3ml of this composite extract was evaporated down to dryness and resuspended in 160µl of 3:1 methanol:water. While analysing root extracts 8µl of the

composite was injected every six samples, for leaf extracts it was 10µl every six samples. Composite samples were included in the statistical analysis of the profiles and examined using PCA modelling to investigate the analytical performance of the MS during analysis of the plant replicates.

4.3.5.5. Analysis of data sets from UPLC-TOFMS analyses of plant extracts

Datasets were examined to ensure the IS was present and aligned in all samples. Metabolomic profiles were aligned, binned and processed using MarkerLynx V 4.1, (see Chapter 3). Using SIMCA-P multivariate analysis software (Umetrics UK Ltd, Windsor, UK), the data sets were pareto-scaled, log-transformed and modelled using PCA, PLS-DA and OPLS-DA analyses (see Chapter 2). Biochemical markers potentially associated with the plant signalling of, or defence response to, AMF colonisation were extracted from 'S'-plots and quantified as outlined in Chapter 2. To quantify the complex mixtures of PAs in the extracts, the chromatograms collected in positive ESI were manually searched, and the observed signals were quantified using peak integration software (Chapter 2).

4.3.5.6. Structural analysis of biochemical markers associated with *G. intraradices* colonisation

Concentrated composite samples were prepared to aid in the structural analysis of the biochemical markers. All remaining roots were pooled, totalling approximately 15g of plant material. Three samples (0.15g ± 0.01g) were taken from the pooled material and extracted as above (Section 4.3.4.2.). All extracts from these samples (9ml) were evaporated down and resuspended in 240µl of methanol:water (3:1), resulting in a sample twice as concentrated as those used for profiling. Structural information and accurate mass measurements were obtained using Q-TOFMSMS CID and a UPLC-NanoSpray system as described in Chapter 2.

4.3.6. Statistical analysis

Statistical analysis of plant biometrics, biomass, biochemical markers and AMF colonisation were performed in SPSS V11. Where the residuals of the plant and AMF data were normally distributed with homogeneity of variance (either before or following transformations) one-way ANOVA was used, otherwise a non-parametric Mann-Whitney U test was used. Adjusted weight was calculated to account for a statistically significant difference in water content both

above and below ground as follows: (total fresh weight/100)*water content. Shoot:root ratios (adjusted below-ground dry weight (g)/adjusted above-ground dry weight (g)) were calculated using these adjusted weight values. Concentration differences for both metabolites and PAs were compared between treatment groups using t-tests when the assumptions of normality (Kolmogorov-Smirnov tests) and equality of variances (Levene's test) were met. If the assumptions for parametric testing could not be satisfied, either before or following transformations, the non-parametric Mann-Whitney test was used. Bonferroni corrections were applied to all tests for differences in metabolite concentrations. The AMF colonisation (percentage RLC) between treatments was also compared with a Mann-Whitney U test. The association between metabolite markers of AMF colonisation and colonisation levels (percentage RLC) were investigated using Spearman rank-order correlations.

4.4. Results

4.4.1. AMF colonisation and plant parameters

The AMF treatment was successful, and the percentage root length colonised (RLC) differed significantly between *G. intraradices* treated plants and controls (Mann-Whitney U test: z = 4.761; P < 0.001). Average percent RLC was 0.86% (range 0-3.36%) and 15.79% (3.70-30.36%) in control and *G. intraradices* treated plants, respectively. Shoot and root water content were higher in controls than in *G. intraradices* treated plants (Table 4.1., Figure 4.2.). All other plant parameters measured were unaffected by *G. intraradices* colonisation (Table 4.1.).

Table 4.1. Summary of plant performance parameters between ragwort colonised by AMF and controls recorded at harvest (10 weeks growth). Data are means (±S.E.) and the test statistic is the F-ratio (one-way ANOVA) or the Z statistic* (Mann-Whitney U tests). Significant results (P<0.05) are displayed in **bold**. All weight and shoot:root ratio data had been adjusted prior to analysis to account for a significant difference in root and shoot water content.

Plant measure	Control	With AMF	Test	P-value
Number of leaves	16.0 (±0.90)	18.0 (±1.35)	-0.835*	0.423
Rosette width (mm)	245.87	244.25	0.012	0.914
Largest leaf length (mm)	132.87	132.38	-0.158*	0.892
Largest leaf width (mm)	49.47 (±2.28)	52.63 (±2.50)	0.866	0.360
Largest leaf area (mm)	6586.00	6955.19	0.555	0.462
Shoot water content (%)	**88.62 (±0.50)**	**82.37 (±0.54)**	**6.623**	**0.015**
Root water content (%)	**88.62 (±0.28)**	**87.64 (±0.25)**	**13.032**	**0.001**
Adjusted shoot weight (g)	10.79 (±0.63)	11.50 (±0.34)	1.008	0.324
Adjusted root weight (g)	7.76 (±0.69)	8.31 (±0.52)	0.412	0.526
Adjusted total weight (g)	18.55 (±1.22)	19.81 (±0.75)	0.793	0.381
Shoot:root ratio	0.71 (±0.69)	0.72 (±0.04)	0.040	0.842

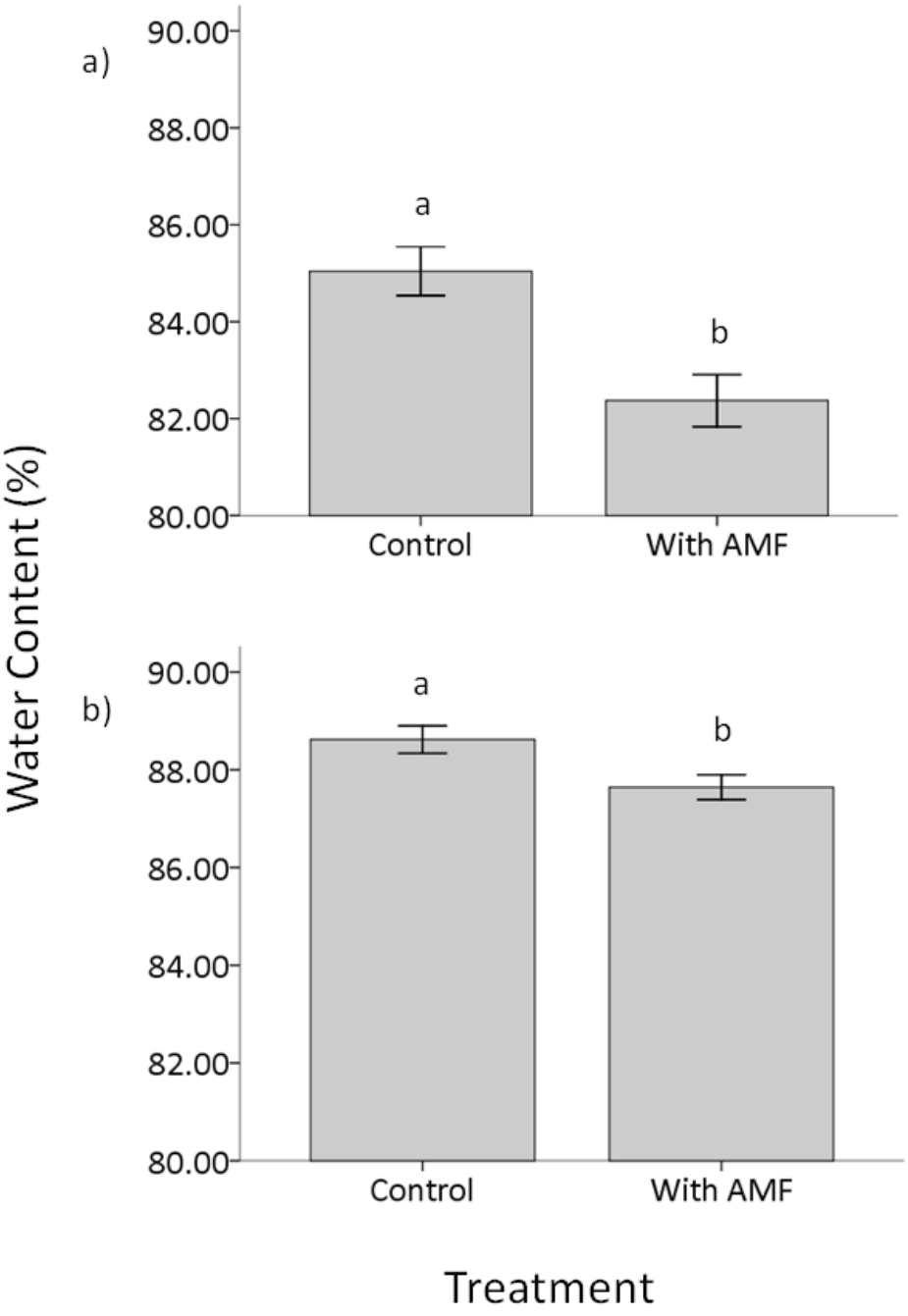

Figure 4.2. Mean (±S.E.) differences in a) shoot (F = 6.623; d.f. = 30; P = 0.015) and b) root (F = 13.032; d.f. = 30; P = 0.001) water content between AMF treated and control ragwort plants at harvest (10 weeks in treatment).

4.4.2. Root responses

4.4.2.1. Multivariate modelling of root profiles

Root samples of ragwort from *G. intraradices* treated plants and controls were analysed by UPLC-TOFMS in both positive and negative ESI. Preliminary analysis of both datasets revealed no outliers (as defined in Chapter 2) in the dataset and all 31 replicates and composite samples (negative: n=5, positive n=6) were included in the PCA. MS performance was consistent throughout the positive ESI analytical run, as indicated by the composite samples being tightly grouped (Figure 4.3.a). PCA revealed no apparent clustering of samples between the two treatment groups in positive mode (Figure 4.3.a), and the percentage variation explained by the model was low (R^2X = 0.156; Q^2 =0.038). The composite samples examined in negative ESI MS mode grouped well, barring a single outlier. This outlier represented the first composite sample analysed, and indicated that MS performance may have been more consistent after the UPLC had finished equilibrating after analysis of the first few samples. PCA of the negative mode dataset revealed some separation between control and AMF treated plants, although the model only explained a small amount of the variation within the dataset (R^2X = 0.126; Q^2 = -0.007) (Figure 4.3.b).

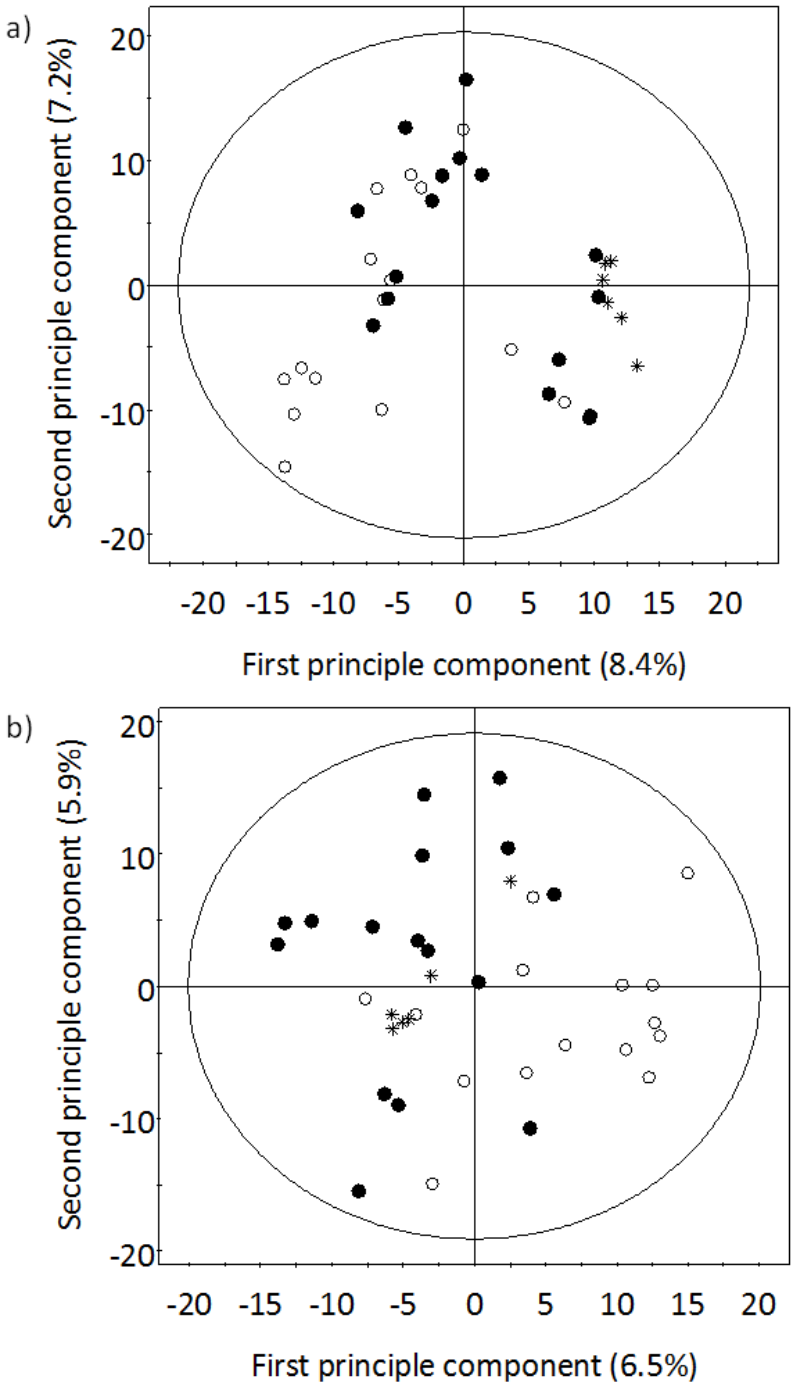

Figure 4.3. Principle component analysis (PCA) score plots of the chemical profiles of roots from *Glomus intradices* treated plants, controls and composite samples. Profiling datasets were from a) positive and b) negative ESI MS modes. Open circles represent control ragwort plants and closed circles are those plants in the *Glomus intraradices* treatment. Asterisks represent composite samples analysed throughout the UPLC-TOFMS run and used to monitor analytical performance of the MS. The percentages of explained variation (R^2X) modelled by the first two principle components are displayed on the axes.

A supervised analysis of the root datasets using OPLS-DA revealed that both datasets (positive or negative ESI modes) resulted in models that explained a large amount of the variation (for both OPLS-DA models the total R^2Y for the predictive component was > 0.984) (Table 4.2.). In addition, both positive and negative models had good predictability (Q^2 > 0.481) and the metabolite profiles of *G. intraradices* colonised and control plants were clearly separated indicating a shift in secondary chemistry between treatment groups (Figure 4.4.). A number of discriminatory metabolites (represented by the retention times and MS signals) driving this separation between treatment classes were extracted from both models using the 'S'-plots. Thirty-two metabolites increased in concentration with *G. intraradices* colonisation (Table 4.3., S4.1. & S4.2.) as determined by Mann Whitney U tests (after Bonferroni adjusted P-value threshold: positive mode: $P < 5.20 \times 10^{-7}$; negative mode: $P < 5.01 \times 10^{-7}$).

Table 4.2. Outline of the parameters of all OPLS-DA models. R^2Y is a measure of the variability of the data explained by the model and Q^2 indicates the predictability of the model. Only the models based on the root profiling data produced reliable markers.

Plant material	Mode	R^2Y	Q^2
Roots	Positive	0.984	0.481
	Negative	0.990	0.528
New leaves	Positive	0.674	0.115
	Negative	0.986	-0.0837
Old leaves	Positive	0.989	0.431
	Negative	1.000	0.302

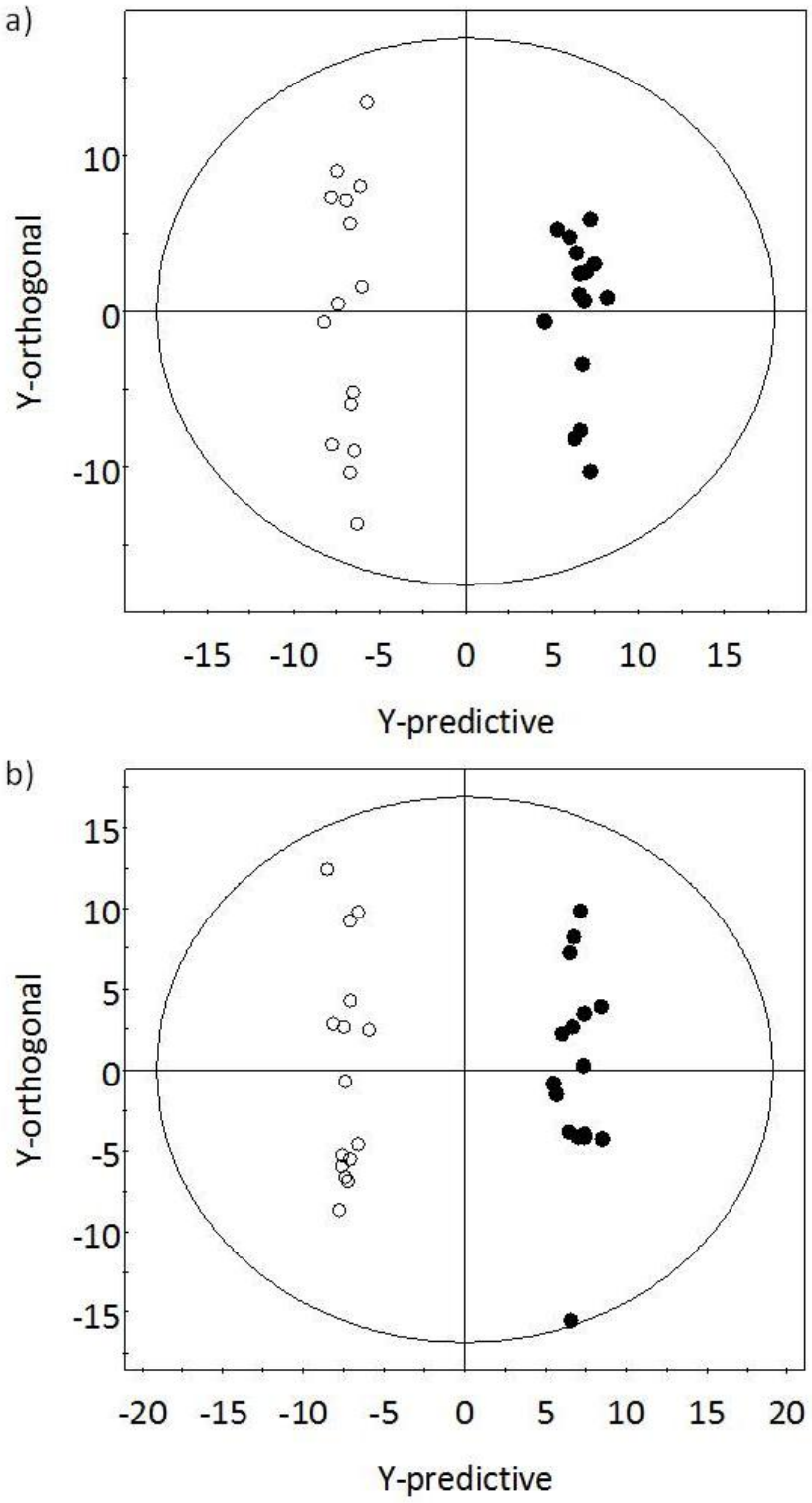

Figure 4.4. Orthogonal partial least squares- discriminate analysis (OPLS-DA) score plots of the chemical profile of *Glomus intradices* treated and control roots in a) positive and b) negative ESI. Open circles represent control ragwort plants and closed circles are those plants in the *Glomus intraradices* treatment.

Table 4.3. Metabolites identified in the roots of ragwort colonised with the AMF *Glomus intraradices*. Fold change indicates the concentration (determined in 20µl injections and are equivalent to 14.061mg of fresh root) increase in roots colonised with AMF when compared to the concentrations observed in control plants. *Indicates that LOD values were used to calculate fold changes, this occurred when concentrations of a metabolite in control plants was below levels that could be detected. P-values marked with a ^ are from t-tests, unmarked P-values are from Mann-Whitney U tests.

Metabolite number	Observed ion (*m/z*)	UPLC-TOFMS r.t.	Putative formula	Theoretical mass of ion	Δ PPM	*m/z* of additional ions and fragments	Formula of ion	Putative identity	Fold change	P-value
1	389.2177	6.37	$C_{19}H_{33}O_8$	389.2175	0.5	411.1995	$C_{19}H_{32}O_8Na$	13-hydroxyblumenol C glycoside $[M+H]^+$	1151.19	6.65×10^{-9}
						227.1647	$C_{13}H_{23}O_3$			
						209.1543	$C_{13}H_{21}O_2$			
						191.1440	$C_{13}H_{19}O$			
						173.1330	$C_{13}H_{17}$			
						163.1484	$C_{12}H_{19}$			
						149.0940	$C_{10}H_{13}O$			
1	387.2018	6.37	$C_{19}H_{33}O_8$	387.2018	-0.3	433.2072	$C_{20}H_{34}O_{10}$	13-hydroxyblumenol C glycoside $[M-H]^-$	746.61*	6.65×10^{-9}
2	373.2228	7.23	$C_{19}H_{33}O_7$	373.2226	0.5	211.1698	$C_{13}H_{23}O_2$	Blumenol C glycoside $[M+H]^+$	8065.78	6.65×10^{-9}
						193.1591	$C_{13}H_{21}O$			
						175.1487	$C_{13}H_{19}$			
						135.1175	$C_{10}H_{15}$			
3	547.2389	7.30	$C_{25}H_{39}O_{13}$	547.2391	-0.4	429.2125	$C_{21}H_{33}O_9$	Blumenol C glycosyl-galacturonide $[M-H]^-$	1553.27	6.65×10^{-9}
						209.1542	$C_{13}H_{21}O_2$			
						175.0243	$C_6H_7O_6$			

Table 4.3. continued...

Metabolite number	Observed ion (*m/z*)	UPLC-TOFMS r.t.	Putative formula	Theoretical mass of ion	Δ PPM	*m/z* of additional ions and fragments	Formula of ion	Putative identity	Fold change	P-value
4	475.2182	7.55	$C_{22}H_{35}O_{11}$	475.2179	0.6	227.1647	$C_{13}H_{23}O_3$	13-hydroxyblumenol C malonylglycoside $[M+H]^+$	489.66*	2.99×10^{-7}
						209.1543	$C_{13}H_{21}O_2$			
						191.1440	$C_{13}H_{19}O$			
						173.1330	$C_{13}H_{17}$			
						163.1484	$C_{12}H_{19}$			
						149.0940	$C_{10}H_{13}O$			
5	373.2222	8.20	$C_{19}H_{33}O_7$	373.2226	-1.1	395.2046	$C_{19}H_{32}O_7Na$	Blumenol C glycoside $[M+H]^+$	5032.03	6.65×10^{-9}
						211.1698	$C_{13}H_{23}O_2$			
						193.1591	$C_{13}H_{21}O$			
						175.1487	$C_{13}H_{19}$			
						135.1175	$C_{10}H_{15}$			
						109.1012	C_8H_{13}			
						95.0821	C_7H_{11}			
6	635.2551	8.24	$C_{28}H_{43}O_{16}$	635.2551	0.0	657.2363	$C_{28}H_{42}O_{16}Na$	Blumenol C malonylglycosyl-galacturonide $[M+H]^+$	3101.31	6.65×10^{-9}
						595.2023	$C_{28}H_{35}O_{14}$			
						459.2230	$C_{22}H_{35}O_{10}$			
						423.2014	$C_{22}H_{31}O_8$			
						211.1698	$C_{13}H_{23}O_2$			
						193.1592	$C_{13}H_{21}O$			
						175.1489	$C_{13}H_{19}$			
						135.1174	$C_{10}H_{15}$			
						109.1021	C_8H_{13}			

Table 4.3. continued...

Metabolite number	Observed ion (*m/z*)	UPLC-TOFMS r.t.	Putative formula	Theoretical mass of ion	Δ PPM	*m/z* of additional ions and fragments	Formula of ion	Putative identity	Fold change	P-value
6	633.2396	8.24	$C_{28}H_{41}O_{16}$	633.2395	0.2	655.2216 589.2495 529.2285 371.2072 161.0447	$C_{28}H_{40}O_{16}Na$ $C_{27}H_{41}O_{14}$ $C_{25}H_{37}O_{12}$ $C_{19}H_{31}O_7$ $C_6H_9O_5$	Blumenol C malonylglycosyl-galacturonide $[M-H]^-$	250.35	6.65×10^{-9}
7	459.2232	9.38	$C_{22}H_{35}O_{10}$	459.2230	0.5	481.2050 437.2149 211.1698 193.1592 175.1487 135.1174 109.1020	$C_{22}H_{34}O_{10}Na$ $C_{21}H_{34}O_8Na$ $C_{13}H_{23}O_2$ $C_{13}H_{21}O$ $C_{13}H_{19}$ $C_{10}H_{15}$ C_8H_{13}	Blumenol C malonylglycoside $[M+H]^+$	1109.15	6.65×10^{-9}
8	494.3247	14.20	$C_{24}H_{29}NO_7P$	494.3247	0.0	476.3141 311.2856 184.0739	$C_{24}H_{27}NO_6P$ $C_{19}H_{35}O_3$ $C_5H_{15}NO_4P$	Hexadecenoyl-glycero-phosphocholine $[M+H]^+$	7.86	6.69×10^{-8}^

4.4.2.2. Metabolites associated with *Glomus intraradices* colonisation

None of the discriminatory metabolites associated with *G.intraradices* colonisation were identified as PA metabolites. Therefore, PA concentrations analysed in the UPLC-TOFMS chromatograms of the root extracts were manually quantified. This revealed 19 potential PA signals in the metabolomic profiles of roots (Table S4.3.), of which six appeared to increase in concentrations following AMF treatment. Following a Bonferroni correction (threshold: $P < 5.20 \times 10^{-7}$) to account for the false discovery rate, none of the PAs in root extracts significantly differed in concentration between the control and AMF colonised plants.

Of the 32 metabolites associated with *G. intraradices* colonisation, eight were assigned putative identities (see below and Table 4.3.); the remaining unidentified markers (n=24) are outlined in Tables S4.1. and S4.2. Seven of the identified metabolite signals were conjugates of C_{13} cyclohexenones apocarotenoids (blumenols) (first question). Concentrations of all blumenol apocarotenoids were positively associated with increasing percentage RLC by *G. intraradices* (Spearman correlation coefficient range 0.776-0.902, $P < 2.95 \times 10^{-7}$ in each case, see Table 4.4.). Of those blumenols identified, two were common to both positive and negative ESI modes, which left seven different structures (Table 4.3.). All metabolites were present as their molecular ions, which were $[M+H]^+$ or $[M-H]^-$ in positive or negative ESI respectively. In positive ESI, some metabolites were also present as the sodium adduct of the molecular ion.

Table 4.4. Spearman rank-order correlations (n = 31) between the concentration (determined in 20µl injections and are equivalent to 14.061mg of fresh root) of different apocarotenoid metabolite markers measured in ragwort roots, and colonisation by *Glomus intraradices* (percentage root length colonised).

Metabolite number	Putative identity	Ionisation mode	UPLC-TOFMS r.t.	Correlation coefficient	P-value
1	13-hydroxyblumenol C glycoside $[M+H]^+$	positive	6.37	0.852	1.16×10^{-9}
1	13-hydroxyblumenol C glycoside $[M-H]^-$	negative	6.37	0.825	1.10×10^{-8}
2	Blumenol C glycoside $[M+H]^+$	positive	7.23	0.902	4.33×10^{-12}
3	Blumenol C glycosyl-galacturonide $[M-H]^-$	negative	7.30	0.828	9.37×10^{-9}
4	13-hydroxyblumenol C malonylglycoside $[M+H]^+$	positive	7.55	0.841	3.21×10^{-9}
5	Blumenol C glycoside $[M+H]^+$	positive	8.20	0.844	2.41×10^{-9}
6	Blumenol C malonylglycosyl-galacturonide $[M+H]^+$	positive	8.24	0.832	6.39×10^{-9}
6	Blumenol C malonylglycosyl-galacturonide $[M-H]^-$	negative	8.24	0.776	2.95×10^{-7}
7	Blumenol C malonylglycoside $[M+H]^+$	positive	9.38	0.855	9.36×10^{-10}

Metabolites 2 and 5 (Table 4.3.) were identified as glucoside conjugates of blumenol C, with the same molecular ion and fragmentation patterns but with different retention times. Fragmentation gave rise to an ion corresponding to the aglycone $C_{13}H_{23}O$ (*m/z* 211.1698) indicating loss of a hexose moiety *(m/z* 162, $C_6H_{10}O_5$) from the parent ion. Further fragmentation of the blumenol C ring resulted in the following ions which were ± 5ppm of the calculated *m/z* of 193.1591 ($C_{11}H_{21}O$) and 175.1487 ($C_{11}H_{19}$), and which have been previously reported for this structure (Schliemann *et al.* 2006, Schliemann *et al.* 2008b). In addition, this study observed an additional fragment which was ± 5ppm of the calculated *m/z* of 135.1175 ($C_{10}H_{15}$) (see Figure 4.5.a & d). Further fragmentation of Metabolite 5 resulted in ions consistent with loss of the propyl side chain. Therefore, Metabolites 2 and 5 were identified as steroisomers of Blumenol C glycoside with different structures or configurations of the hexose moiety (Figure 4.6.). Without further chemical analysis using nuclear magnetic resonance spectroscopy (NMR) the exact nature of the hexose conjugates could not be determined. Metabolite 7 was identified as blumenol C conjugated with malonylglycoside (Table 4.6., Figure 4.6.). This structure was determined by the observation of a loss of the malonyglycoside moiety (*m/z* 248, $C_9H_{12}O_8$) from the parent ion, and fragmentation consistent with the blumenol C aglycone structure (Table 4.3.).

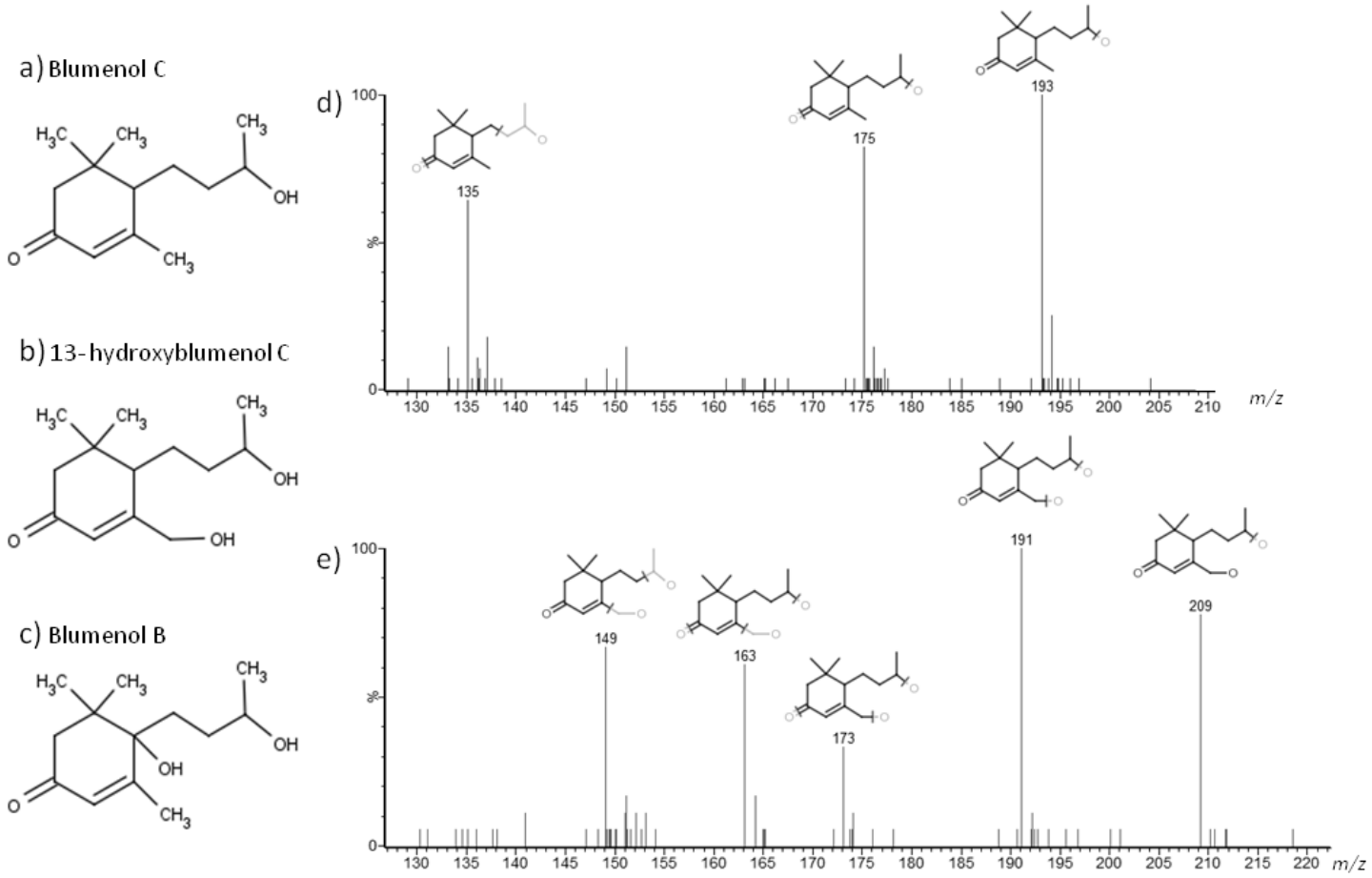

Figure 4.5. Structures of a) blumenol C and b) 13-hydroxyblumenol C and c) blumenol B. The characteristic fragment pattern associated with the structures of d) blumenol C and e) 13-hydroxyblumenol C. Spectra were recorded using QTOFMS CID fragmentation in positive ESI.

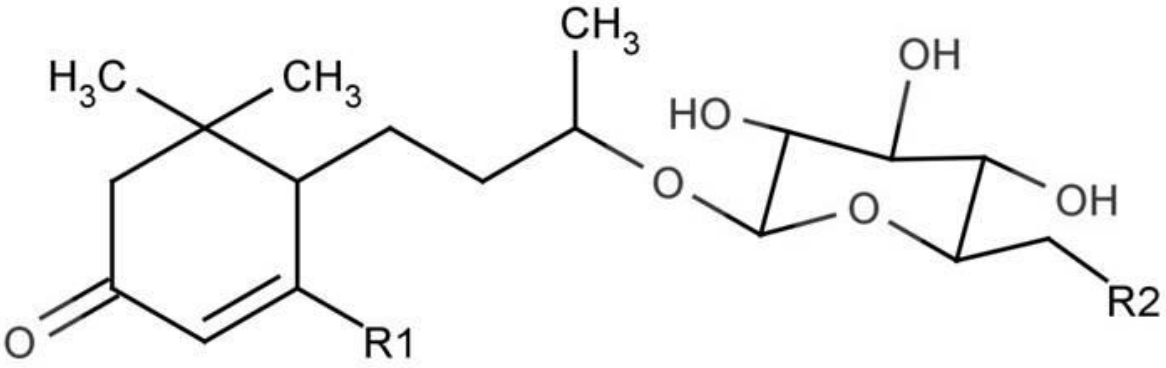

Metabolite	R1	R2
1	$-CH_2OH$	-OH
2	$-CH_3$	-OH
3	$-CH_3$	$-C_6H_9O_7$
4	$-CH_2OH$	$-OCOCH_2CO_2H$
5	$-CH_3$	-OH
6	$-CH_3$	$-OCOCH_2CO-C_6H_9O_7$
7	$-CH_3$	$-OCOCH_2CO_2H$

Figure 4.6. Structure scheme of the identified blumenol apocarotenoids associated with *Glomus intraradices* colonisation of ragwort.

Metabolite 6 was identified as blumenol C malonylglycosylgalacturonide, a unique metabolite hitherto unreported (Table 4.3., Figure 4.6.). Metabolite 6 was detected as the same metabolite, with the same retention time, in both positive and negative ESI modes (Figure 4.6.). Fragmentation of the molecular ion in positive mode resulted in a fragment of m/z 459.2230 which was ± 5ppm of the calculated *m/z* 459.2230 and corresponded to an elemental composition $C_{22}H_{35}O_{10}$. The 459 ion corresponded to the loss of $C_6H_8O_6$ from the parent ion and indicated the loss of a conjugate of the elemental composition $C_6H_{10}O_7$ (galacturonic acid) assuming loss of a water molecule during conjugation. Further fragmentation gave rise to ions corresponding to the unconjugated blumenol C ring (*m/z*: 211.1698, elemental composition: $C_{13}H_{23}O_2$), which indicated that Metabolite 6 was also conjugated to a malonylglycoside group ($C_9H_{12}O_8$). The order of conjugate loss demonstrated that the galacturonic acid was probably conjugated to the glycosylmalonyl group. The fragmentation pattern observed in negative ESI, along with their elemental composition, agreed with the structure identified from the positive ESI data. A key fragment of m/z 371.2072 corresponded to loss of malonyl galacturonide from blumenol C glycoside, further supporting conjugation of the galacturonide moiety to the malonyl group (Table 4.3.). Further analytical work would be required to confirm the position of the galacturonic acid on the glycoside structure.

Another hitherto unseen metabolite was Metabolite 3, which was identified as blumenol C glycosylgalacturonide and detected in negative ESI mode (Table 4.3., Figure 4.6.). Fragmentation of the molecular ion resulted in a fragment ± 5ppm of the calculated *m/z* 175.0243 ($C_6H_7O_6$) which represented a conjugate with the elemental composition $C_6H_{10}O_7$ (galacturonic acid) assuming loss of a water molecule during conjugation. Further fragmentation of the molecular ion gave rise to ions corresponding to the unconjugated blumenol C ring (*m/*z: 209.1542, elemental composition: $C_{13}H_{21}O_2$), which indicated that metabolite 3 was also conjugated with a glycoside group ($C_6H_{11}O_5$) assuming the loss of a hydroxyl group during conjugation. The order of conjugate loss suggested that the galacturonic acid was conjugated to the glycosyl group.

A second group of conjugated blumenols were identified that contained an aglycone composition of $C_{13}H_{23}O_3$, and these were Metabolites 1 and 4 (Table 4.3.). Fragmentation of Metabolite 1 in positive ESI mode gave rise to an ion which was ± 5ppm of the calculated *m/z* of 227.1647 and corresponded to a $C_{13}H_{23}O_3$ blumenol ring structure. The loss of *m/z* 162 ($C_6H_{10}O_5$) from the parent ion indicated that the structure was a glycoside conjugate. Further fragmentation of the aglycone structure resulted in ions that were ± 5ppm of the calculated

m/z of 209.1543 ($C_{13}H_{21}O_2$) and 191.1440 ($C_{13}H_{19}O$) that were consistent with previous reports for this structure (Schliemann *et al.* 2006, Schliemann *et al.* 2008b). Three additional fragment ions of the aglycone structure were present which were ± 5ppm of the calculated *m/z* of 173.1330 ($C_{13}H_{17}$) 163.1484 ($C_{12}H_{19}$) and 149.0940 ($C_{10}H_{13}O$). The fragment of *m/z* 163.1484 ($C_{12}H_{19}$) corresponded to the loss of CH_2OH from the aglycone structure and indicated that the aglycone was 13-hydroxyblumenol C rather than a blumenol B type structure (see Figures 4.5.b, c, and e). Metabolite 1 was also observed in negative ESI, where the calculated empirical formula was also consistent with the identified structure of 13-hydroxyblumenol C glycoside (Figure 4.6.). Metabolite 4 was identified as 13-hydroxyblumenol C malonylglycoside. This was determined by the loss of *m/z* 248 ($C_9H_{12}O_8$) from the parent ion leaving the aglycone 13-hydroxyblumenol C (*m/z*: 277.1647, elemental composition: $C_{13}H_{23}O_2$) (Table 4.3., Figure 4.6.).

The remaining identified metabolite was not an apocarotenoid, and Metabolite 8 was identified as the lysophospholipid hexadecenoyl-glycerophosphocholine. Fragmentation of the parent ion of Metabolite 8 in positive ESI mode gave rise to an ion which was ± 5ppm of the calculated *m/z* of 476.3141 and corresponded to the loss of a water molecule. Further fragmentation of the metabolite resulted in ions that were ± 5ppm of the calculated *m/z* 311.2856 ($C_{19}H_{35}O_3$) and 184.0739 ($C_5H_{15}NO_4P$) that corresponded to the chain and head of the hexadecenoyl-glycerophosphocholine structure respectively.

4.4.3. Shoot responses

4.4.3.1. Multivariate modelling of shoot profiles

Extracts of new and old leaves from ragwort plants colonised with AMF or from controls were profiled by UPLC-TOFMS. PCA modelling revealed no outliers (as defined in Chapter 2) within the positive ESI dataset; whereas six (two new leaf extracts, one control and one colonised by *G. intraradices*; four old leaf extracts, three controls and one *G. intraradices* colonised plants) outliers were detected in the negative ESI dataset and were subsequently excluded from analysis. The PCA model diagnostics for both the positive and negative data were poor (positive ESI: $R^2X = 0.283$, $Q^2 = 0.213$; negative ESI: $R^2X = 0.262$, $Q^2 = 0.216$). PCA revealed a tight clustering of all composite samples, demonstrating consistent MS performance throughout the analytical run in both positive (Figure 4.7.a) and negative (Figure 4.7.b) ESI. In both positive and negative ESI, PCA models clearly differentiated between old and new leaves

tissues along the first principle component axis. There was no differentiation of leaf tissues in the PCA according to AMF colonisation of plants (Figure 4.7.).

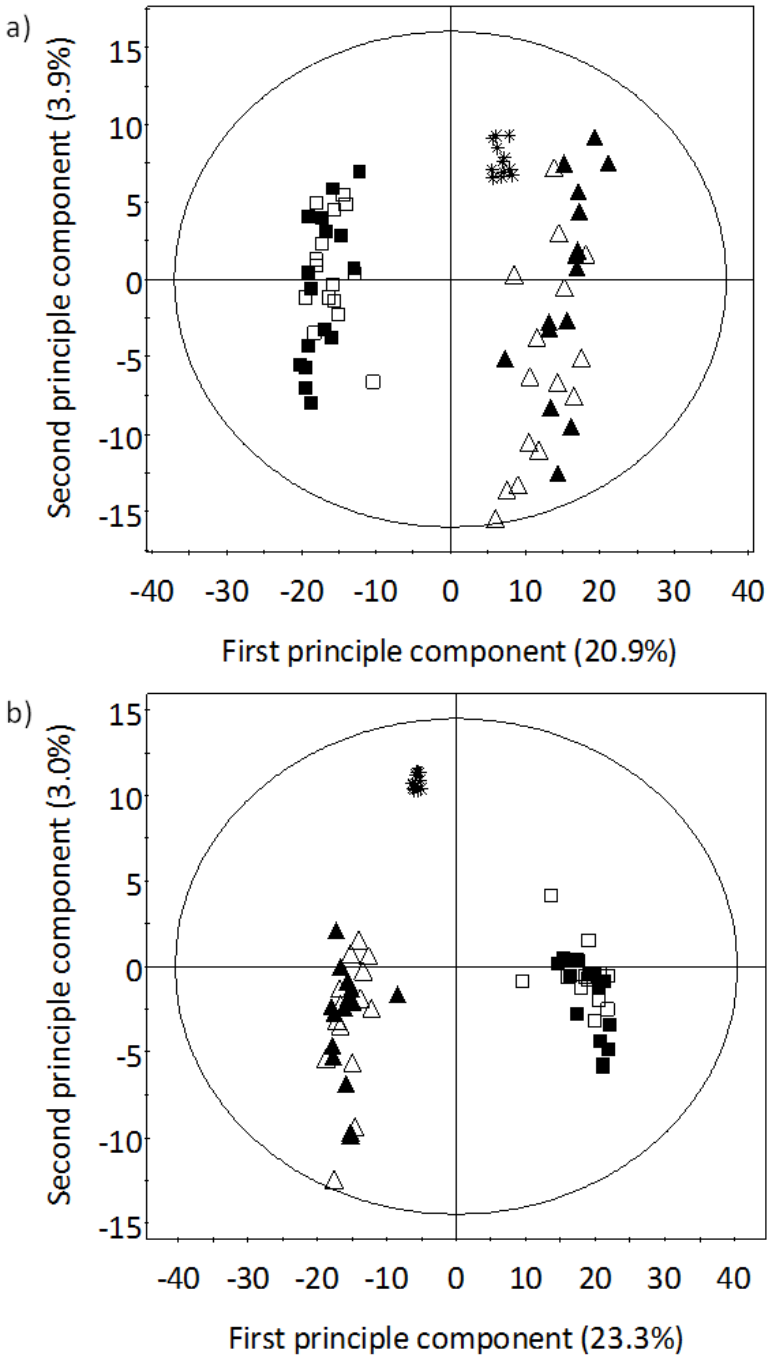

Figure 4.7. Principle component analysis (PCA) score plots of the chemical profiles of leaves from *Glomus intradices* treated ragwort plants, controls and composite samples. Profiling datasets were from a) positive and b) negative ESI MS modes. Open symbols represent control ragwort plants and closed symbols are those plants in the *G. intraradices* treatment. Triangles represent new leaves and squares old leaves. Asterisks represent composite samples analysed throughout the UPLC-TOFMS run and used to monitor analytical performance of the MS. The percentages of explained variation (R^2X) modelled by the first two principle components are displayed on the axes.

The datasets were further analysed using PLS-DA, and these models of the dataset from positive ESI analysis had good predictability (Q^2 = 0.657) and a high degree of explained variation (total R^2Y = 0.986 for six latent variables) (Figure 4.8.a). The first latent variable separated old and new leaves and accounted for 22.4% of the explained variation. The second distinguished between those plants with and without AMF but only explained 2.5% of the variation in the dataset. PLS-DA of shoot chemistry recorded in negative ESI results in reasonable models (R^2Y = 0.624, Q^2Y = 0.361, 2 latent variables). Again, the first latent variable reveals a separation between old and new leaves and explains 24.9% of the variation in the dataset (Figure 4.8.b). The second latent variable separates between plants with and without AMF, especially between old leaves; but again this latent variable explained only a small amount of variation (2.2%) in the data.

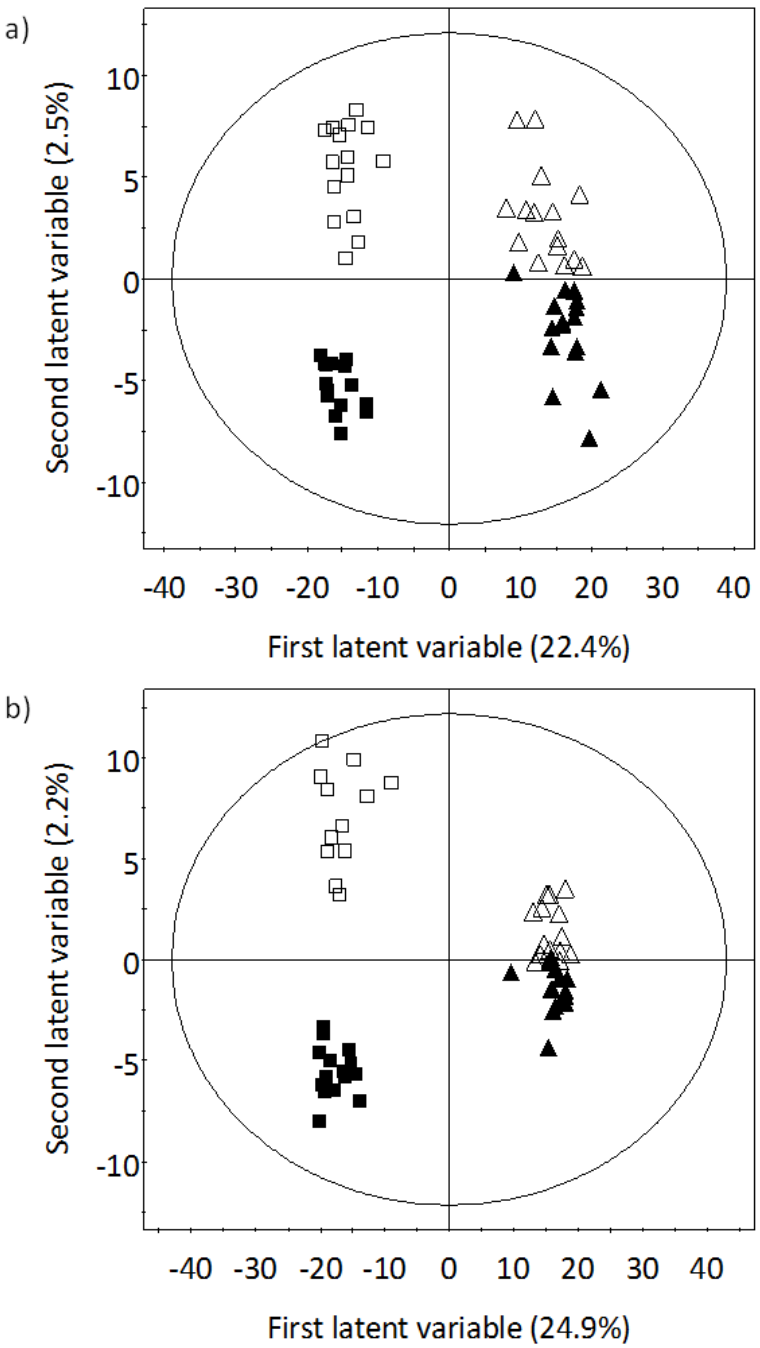

Figure 4.8. Partial least squared-discriminate analysis (PLS-DA) score plots of the chemical profiles of leaves from control ragwort plants and those colonised with *Glomus intradices*. Profiling datasets were from a) positive and b) negative ESI MS modes. Open symbols represent control ragwort plants and closed symbols are those plants in the *G. intraradices* treatment. Triangles represent new leaves and squares old leaves. The percentages of explained variation (R^2Y) modelled by the first two latent variables are displayed on the axes.

Models revealed that the datasets with the highest predictability were associated with the profiles of old leaves from the different treatment groups (Table 4.2.). Examination of the 'S'-plots of these models did not, however, result in the detection of discriminatory shoot chemicals associated with *G. intraradices* colonisation of ragwort. This result suggested that if differences in some metabolites had occurred in the leaves as a result of AMF colonisation, then the concentration differences were too low or inconsistent to be detected using these analytical methods. The PAs analysed in the UPLC-TOFMS chromatograms of shoots (second question) were also manually quantified to determine whether their concentrations altered with AMF colonisation. While 17 PA structures were detected in the shoots (Table S4.4.), there were no significant differences in concentrations between treatment groups after applying Bonferroni corrections ($P < 6.06 \times 10^{-7}$).

4.5. Discussion

This study details for the first time the concomitant metabolomic assessment of the effect of AMF colonisation on the secondary chemistry of host plant tissues above- and below-ground. The first question of this study was to assess whether AMF-induced changes in concentrations of apocarotenoids involved in chemical signalling mirrored those in other plant taxa. Seven blumenol structures were identified in AMF colonised root tissues and of those two were novel and hitherto unreported. The second question investigated was to examine if AMF colonisation induced ragwort chemical defences (principally PAs) both above and below ground. After Bonferroni correction, no changes in PA concentrations were observed in root or shoot tissues. Indeed, AMF colonisation did not elicit any above-ground metabolomic differences in shoot tissues. Of the 25 additional metabolites that increased in AMF colonised root tissues, one was identified as a lysophospholipid suggesting AMF-induced changes in fatty acid metabolism.

Despite minimal differences in the plant morphometric parameters, multivariate modelling of the root metabolome revealed 32 significant metabolomic changes following AMF colonisation. Of the discriminatory metabolites examined, seven were blumenol apocarotenoids with a C_{13} cyclohexenone structure. Blumenols are known to be associated with AMF colonisation of root tissues (Strack and Fester 2006). The concentrations of each blumenol apocarotenoid was positively related to *G. intraradices* colonisation, in accordance with other studies (Maier *et al.* 2000, Schliemann *et al.* 2008a). Two of the blumenols observed in this study were conjugated with a sugar and galacturonic acid moiety, a combination that has hitherto never been reported. These metabolites may not have been discovered if a targeted approach was undertaken, demonstrating one of the benefits of adopting a metabolomic approach. The precise signalling role of blumenol apocarotenoids in the AMF-plant relationship is unknown, but it has been suggested to play a part in the maintenance of the mutualistic association (Walter *et al.* 2010). Species specific C_{13} cyclohexenone apocarotenoids have been observed in a range of plant taxa *M. truncatula* (Schliemann *et al.* 2008a), *Zea mays* L. (Fester *et al.* 2002), *Hordeum vulgare* L. (Peipp *et al.* 1997), *L. japonicus* (Fester *et al.* 2005), *Ornithogalum umbellatum* L. (Schliemann *et al.* 2006) and *Lycopersicon esculentum* L. (Maier *et al.* 2000). Between-species differences in the parent blumenol structure and the nature of their conjugates have been observed (Strack and Fester 2006). The novel blumenol structures observed in this study could represent the formation of chemical signals highly specific to the particular plant-AMF interaction (Strack and Fester

2006). It could be that a mechanism of species recognition exists between the AMF and its host, as observed in the interactions between plants and nitrogen fixing bacteria (Perret *et al.* 2000). The production of species specific blumenols could provide such a mechanism of species recognition. It cannot, however, be ruled out that the occurrence of species-specific blumenols is as a result of a limited number of untargeted investigations that examine the AMF-plant interaction.

An additional chemical change reported in roots colonised by AMF is the accumulation of C_{14} polyene apocarotenoids (Fester *et al.* 2002). The cleavage pattern of the C_{40} carotenoid precursor suggests that the concentration of C_{14} polyenes should be half that of C_{13} cyclohexenones (Schwartz *et al.* 2001). No C_{14} polyenes were observed in this study. The detection of C_{14} polyene apocarotenoids in roots is often associated with a yellowing of roots (Klingner *et al.* 1995a), and this was not observed in the current study either. This is consistent with other plant species that similarly do not demonstrate a change in root colour or produce C_{14} polyene apocarotenoids with AMF colonisation (Klingner *et al.* 1995b).

AMF colonisation can have a negative effect on generalist below-ground herbivores such as parasitic nematodes (Li *et al.* 2006, Rodriguez-Echeverria *et al.* 2009) and beetle larvae (Gange *et al.* 1994), but a positive effect on the larvae of specialist weevils that feed below ground (Currie *et al.* 2011). These results suggest a role for AMF conveyed tolerance of herbivory via changes to secondary chemicals, since overall generalist herbivores are more susceptible then specialists are to defensive plant secondary chemistry (e.g. Lankau 2007, Roslin and Salminen 2008). In this study ragwort root and shoot PAs were not affected by *G. intraradices* colonisation (after Bonferroni correction). As root and shoot PAs are known to change with root damage (Hol *et al.* 2004), and root PAs respond to infection with plant parasitic nematodes (Chapter 3) it seems likely that *G. intraradices* is indeed perceived as a mutualist by its ragwort host. The lack of leaf PA variation in the current study is in direct contrast to the findings of Reidinger *et al.* (2012), who found ragwort leaf concentrations of both total PAs and jacoline to be correlated negatively with AMF colonisation. The differences in the results of the two studies could be accounted for using one or a combination of explanations. Firstly, AMF species identity is an important determinant for the outcome of AMF-plant interactions (Helgason *et al.* 2007). The identity of the AMF species colonising the ragwort plants in the field study of Reidinger *et al.* (2012) was not recorded. It is likely that the identity of the AMF species colonising the ragwort plants of the field study conducted by Reidinger *et al.* (2012) were different to the species used in the current study and could account for the differences between the studies. Secondly, ragwort genotype is important in determining the PA response

to damage below-ground (Hol *et al.* 2004). Significant variation in genotype has been observed both between and within ragwort populations (Witte *et al.* 1992, Macel *et al.* 2004). Genotype variation could explain the differences observed between the results of this study and Reidinger *et al.* (2012), as plant genotype in both experiments is unknown. Finally, while reducing the false discovery rate, applying a Bonferroni can incorrectly fail to reject the null hypothesis of no statistical difference (type II error) (Benjamini *et al.* 2001). It could be that the conservative Bonferroni correction term used in this study masked any differences in PA concentrations.

The absence of PA differences above ground as a result of AMF colonisation mirrored the lack of difference in all measured aspects of above-ground ragwort chemistry using UPLC-TOFMS. This result suggested that if differences in some metabolites had occurred in the leaves as a result of AMF colonisation, then the concentrations differences were too low or inconsistent to be detected using these analytical methods. While there are no detectable differences in shoot profiles as a result of AMF colonisation, the results of this chapter have demonstrated that leaf age has a significant influence on metabolomic profile (as in Chapter 2). Fester *et al.* (2011) employed a GC-MS metabolomic approach to examine the effect of *Glomus mossae* on the above-ground metabolome of *L. japonicus*. They detected significant changes in metabolome, specifically organic and amino acids, as a result of AMF colonisation (Fester *et al.* 2011). While an excellent tool to analyse secondary metabolites, the main focus of the current study, LC-MS is not as effective as GC-MS when examining primary metabolites (Macel *et al.* 2010). It could be that the above-ground chemical repercussions of *G. intraradices* colonisation in ragwort are driven by a change in primary metabolism and were thus missed in the current study. This problem is also observed when targeted analyses of the above-ground chemical effects of AMF are undertaken, commonly different patterns are observed depending on the chemical groups analysed (e.g. Copetta *et al.* 2006, Toussaint *et al.* 2007). Future work examining the effect of AMF should ideally utilise a mixture of approaches, so that coverage of both primary and secondary plant metabolism is maximised (Hagel and Facchini 2008).

The lack of difference observed in shoots could suggest that any AMF-conveyed resistance to above-ground herbivores is due to an increased ability of a host plant to mobilise defences once attacked (Pozo and Azcon-Aguilar 2007). This 'priming' of plant tissues at a genetic level is an efficient method of protecting plant material as metabolomic costs are relatively low (Conrath *et al.* 2002), and previous studies have demonstrated that AMF colonisation results in above-ground changes in gene expression (Taylor and Harrier 2003). If plants were 'primed' then no differences in constitutive plant defence would be expected. It would only be after

above-ground attack that any differences in above-ground chemistry would be predicted, caused by a larger induction of defences conveyed by AMF. Few studies have examined the effect of AMF on the induction of defences, and those that do report mixed effects (Bennett *et al.* 2009, Fontana *et al.* 2009, Kempel *et al.* 2010) possibly explained by differences among species (Gange *et al.* 2012) or, the methods used to measure induction. Kempel *et al.* (2010) examined AMF mediated induction in a number of species, including ragwort, and found increased induction in AMF colonised plants at the expense of growth. As such the mechanisms involved in AMF priming of ragwort remain undetermined because caterpillar performance was used to measure induction (Kempel *et al.* 2010). Future work should attempt to determine if priming is the mechanism that provides AMF-conveyed resistance; this could be achieved by examining the induced responses of AMF-colonised plants exposed to above-ground herbivores and comparing them to the induction of plants not colonised by AMF.

In addition to the increased concentrations of the seven blumenols already discussed, the concentration of the lysophospholipid, hexadecenoyl-glycerophosphocholine was increased in roots colonised by AMF. An increase in the concentration of lysophospholipids could be caused by two processes. First, it could be due to alterations in fatty acid metabolism. The cleavage of phospholipids results in the release of fatty acids and a lysophospholipid. Secondly, it could be due to an increase in the synthesis of the lysophospholipid itself. While previous studies have not detected changes in the concentrations of pysophospholipids as a result of AMF colonisation, they have observed changes in the concentrations of fatty acids (Schliemann *et al.* 2008a, Fester *et al.* 2011). This suggested that AMF colonisation affects fatty acid metabolism. Schliemann *et al.* (2008a) find increased amounts of some fungus-specific fatty acids, in addition to increased concentrations of the plant derived fatty acids, palmitvaccenic and vaccenic acid. The observed changes in fatty acid and lysophospholipid concentrations could be explained by two processes that occur in the roots of plants colonised by AMF. First, AMF linked changes in fatty acid metabolism are associated with the proliferation of plastids that contain fatty acids in their membranes (Lohse *et al.* 2005). Secondly, it could be that the formation of arbuscule structures, specifically the expansion of the plant plasma membrane to create the periarbuscular membrane (Toth and Miller 1984), was responsible for the observed increase in fatty acid associated with AMF colonisation of roots. In their metabolomic assessment of the AMF-induced changes of shoot tissues Fester *et al.* (2011) observed a decrease in the concentrations of the fatty acid octadecanoic acid in sink leaves, perhaps caused by competition with mycorrhizal root tissues as a carbon sink. Despite

the observation of increased concentrations of hexadecenoyl-glycerophosphocholine in the roots of the present study, no concomitant decrease in shoot concentrations were found.

In the current study, 24 discriminatory metabolites observed in roots colonised by AMF remained unidentified. The likely elemental composition and, where applicable, fragmentation pattern of these unidentified metabolites rules out the structures of all apocarotenoids: C_{14} polyenes, blumenols, or strigolactones. Phenolic metabolites are a group of secondary chemicals commonly suggested when the role of secondary chemistry in the AMF-plant relationship is considered (Morandi 1996). Although not essential for the development of the AMF-plant relationship (Becard *et al.* 1995), some studies have suggested a role for flavonoids, a class of phenolic metabolites, in the dialogue between AMF and its plant host (Guenoune *et al.* 2001, Larose *et al.* 2002, Schliemann *et al.* 2008a). However, the likely elemental composition of the unidentified metabolites demonstrated that they could not be flavonoids either. Instead, the information obtained from the unidentified metabolites suggests a series of very similar monosaccharide and disaccharide conjugates of metabolites with very similar structures that are true unknowns and not present in plant metabolite databases. There is a clear need for future work to determine the identity of these unknown metabolites, as without this information their role in the AMF-plant interaction cannot be determined.

In summary, this study showed the AMF species *G. intraradices* caused metabolomic changes in the roots of colonised plants. As a result of adopting a metabolomic approach, it was detected that two novel blumenol apocarotenoids were induced as a result of AMF colonisation. It is suggested that *G. intraradices* is considered a mutualist of ragwort on the basis that this study found no evidence of induction of the main group of defence metabolites of ragwort, PAs, in either below- or above-ground tissues. AMF colonisation of roots did not elicit concomitant chemical changes above ground. In roots, increased concentrations of a lysophospholipid were associated with AMF colonisation, suggesting an AMF-induced increase in fatty acid metabolism. Other root chemical changes were associated with AMF colonisation, but without structural identification their role in the AMF-plant relationship cannot be determined. When attempting to disentangle the effects of AMF on herbivore performance, future experiments should examine AMF as a primer of tissues, ideally using techniques that allow the concomitant observation of primary and secondary metabolites.

4.6. Supplementary Material

Table S4.1. Unidentified metabolites in the roots of ragwort colonised with the AMF *Glomus intraradices* observed using UPLC-TOFMS in positive ESI MS mode. Fold change indicates the concentration (determined in 20µl injections and are equivalent to 14.061mg of fresh root) increase in roots colonised with AMF when compared to the concentrations observed in control plants. P-values marked with a ^ are from t-tests, unmarked P-values are from Mann-Whitney U tests.

Observed ion (*m/z*)	UPLC-TOFMS r.t.	Putative formula	Theoretical mass of ion	Δ PPM	*m/z* of additional ions and fragments	Formula of ions	Fold change	P-value
513.1584	7.53	$C_{21}H_{30}O_{13}Na$	513.1584	0.0	365.1576	$C_{17}H_{26}O_7Na$	8.73	4.42×10^{-7}^
					351.1056	$C_{15}H_{20}O_8Na$		
					307.1158	$C_{14}H_{20}O_6Na$		
					203.1072	$C_{13}H_{15}O_2$		
541.2261	8.40	$C_{24}H_{38}O_{12}Na$	541.2261	0.0	-	-	31.10	4.46×10^{-7}
375.1658	9.33	$C_{17}H_{27}O_9$	375.1655	0.5	397.1465	$C_{17}H_{26}O_9Na$	11.84	6.65×10^{-9}
					392.1921	$C_{17}H_{30}NO_9$		
					357.1549	$C_{17}H_{25}O_8$		
					353.1591	$C_{16}H_{26}O_7Na$		
					311.1478	$C_{14}H_{24}O_6Na$		
					293.1367	$C_{14}H_{22}O_5Na$		
					249.1465	$C_{13}H_{22}O_3Na$		
					235.1328	$C_{14}H_{19}O_3$		
					231.1388	$C_{13}H_{20}O_2Na$		
357.1544	9.36	$C_{17}H_{25}O_8$	357.1549	-1.4	253.1440	$C_{14}H_{21}O_4$	5.89	4.66×10^{-8}
					235.1334	$C_{14}H_{19}O_3$		
207.1022	9.45	$C_{12}H_{15}O_3$	207.1021	0.5			2.67	2.99×10^{-7}

Table S4.1. continued...

Observed ion (*m/z*)	UPLC-TOFMS r.t.	Putative formula	Theoretical mass of ion	Δ PPM	*m/z* of additional ions and fragments	Formula of ions	Fold change	P-value
329.1238	9.46	$C_{15}H_{21}O_8$	329.1236	0.6	679.2238	$C_{30}H_{40}O_{16}Na$	8.48	1.26×10^{-7}
					351.1052	$C_{15}H_{20}O_8Na$		
					346.1506	$C_{15}H_{24}NO_8$		
					307.1159	$C_{14}H_{20}O_6Na$		
					265.1051	$C_{12}H_{18}O_5Na$		
465.1373	9.91	$C_{20}H_{26}O_{11}Na$	465.1373	0.0	460.1819	$C_{20}H_{30}NO_{11}$	3630.75	2.99×10^{-7}
					421.1475	$C_{19}H_{26}O_9Na$		
					379.1369	$C_{17}H_{24}O_8Na$		
					248.0770	$C_9H_{14}NO_7$		
					231.0505	$C_9H_{11}O_7$		
					216.0762	$C_{11}H_{13}O_3Na$		
					195.1021	$C_{11}H_{15}O_3$		
					145.0501	$C_6H_9O_4$		
					127.0395	$C_6H_7O_3$		
499.0796	9.92	$C_{13}H_{23}O_{20}$	499.0783	2.6	-	-	5391.43	6.65×10^{-9}
611.1956	10.74	$C_{26}H_{36}O_{15}Na$	611.1952	0.7	606.2398	$C_{26}H_{40}NO_{15}$	13.18	3.15×10^{-11}^
					567.2054	$C_{25}H_{36}O_{13}Na$		
					525.1948	$C_{23}H_{34}O_{12}Na$		
					363.1420	$C_{17}H_{24}O_7Na$		
					323.1495	$C_{17}H_{23}O_6$		
					289.0536	$C_9H_{14}O_9Na$		
					201.0916	$C_{13}H_{13}O_2$		
645.1353	10.74	$C_{29}H_{31}O_{13}NaCl$	645.1351	0.3	-	-	11.69	6.65×10^{-9}

Table S4.1. continued...

Observed ion (*m/z*)	UPLC-TOFMS r.t.	Putative formula	Theoretical mass of ion	Δ PPM	*m/z* of additional ions and fragments	Formula of ions	Fold change	P-value
985.4650	10.99	$C_{48}H_{73}O_{21}$	985.4644	0.6	737.3951 719.4000 497.1101 479.1021 249.0610 231.0499	$C_{35}H_{61}O_{16}$ $C_{39}H_{59}O_{12}$ $C_{16}H_{26}O_{16}Na$ $C_{16}H_{24}O_{15}Na$ $C_9H_{13}O_8$ $C_9H_{11}O_7$	37995.23	6.65×10^{-9}
452.2778	14.16	$C_{21}H_{43}NO_7P$	452.2777	0.2	-	-	10.40	2.49×10^{-7}^
462.3026	15.43	$C_{30}H_{40}NO_3$	462.3008	3.9	-	-	4.48	7.40×10^{-10}^

Table S4.2. Unidentified metabolites in the roots of ragwort colonised with the AMF *Glomus intraradices* observed using UPLC-TOFMS in negative ESI MS mode. Fold change indicates the concentration increase(determined in 20µl injections and are equivalent to 14.061mg of fresh root) in roots colonised with AMF when compared to the concentrations observed in control plants. P-values marked with a ^ are from t-tests, unmarked P-values are from Mann-Whitney U tests.

Observed ion (*m/z*)	UPLC-TOFMS r.t.	Putative formula	Theoretical mass of ion	Δ PPM	*m/z* of additional ions and fragments	Formula of ions	Fold change	P-value
403.1986	5.82	$C_{19}H_{31}O_9$	403.1968	4.5	449.2023	$C_{20}H_{33}O_{11}$	12.72	2.99×10^{-7}
429.2120	7.66	$C_{21}H_{33}O_9$	429.2125	-1.2	473.2023	$C_{22}H_{33}O_{11}$	113.79	4.66×10^{-8}
					215.0919	$C_{10}H_{15}O_5$		
					197.0814	$C_{10}H_{13}O_4$		
					171.1021	$C_9H_{15}O_3$		
					153.0916	$C_9H_{13}O_2$		
287.1490	8.38	$C_{14}H_{23}O_6$	287.1495	-1.7	269.1389	$C_{14}H_{21}O_5$	23.87	6.65×10^{-9}
					227.1283	$C_{12}H_{19}O_4$		
					209.1178	$C_{12}H_{17}O_3$		
373.1497	9.42	$C_{17}H_{25}O_9$	373.1499	0.0	769.2889	$C_{34}H_{50}O_{18}Na$	11.06	4.05×10^{-10}^
					351.1417	$C_{16}H_{24}O_7Na$		
					329.1600	$C_{16}H_{25}O_7$		
					287.1496	$C_{14}H_{23}O_6$		
					269.1391	$C_{14}H_{21}O_5$		
					225.1490	$C_{13}H_{21}O_3$		
943.4476	9.46	$C_{53}H_{67}O_{15}$	943.4480	-0.4	-	-	22.41	1.33×10^{-8}

Table S4.2. continued...

Observed ion (*m/z*)	UPLC-TOFMS r.t.	Putative formula	Theoretical mass of ion	Δ PPM	*m/z* of additional ions and fragments	Formula of ions	Fold change	P-value
715.2816	9.87	$C_{33}H_{47}O_{17}$	715.2813	0.4	671.2917	$C_{32}H_{47}O_{15}$	588.15	6.65×10^{-9}
397.1493	10.00	$C_{19}H_{25}O_9$	397.1499	-1.5	193.0867 178.0633	$C_{11}H_{13}O_3$ $C_{10}H_{10}O_3$	339.34	6.65×10^{-9}
927.3853	10.00	$C_{44}H_{63}O_{21}$	927.3862	-1.0	373.1862 261.0763	$C_{18}H_{29}O_8$ $C_{14}H_{13}O_5$	100.50	6.65×10^{-9}
383.1338	10.17	$C_{18}H_{23}O_9$	383.1342	-1.0	179.0714	$C_{10}H_{11}O_3$	1108.49	8.04×10^{-6}
281.0870	10.83	$C_{10}H_{17}O_9$	281.0873	-1.1	-	-	19.85	8.19×10^{-14}^
983.4483	11.03	$C_{48}H_{71}O_{21}$	983.4488	-0.5	895.4691 793.4373 733.4163 631.3846 203.0556	$C_{46}H_{71}O_{17}$ $C_{42}H_{65}O_{14}$ $C_{40}H_{61}O_{12}$ $C_{36}H_{55}O_9$ $C_8H_{11}O_6$	13095.74	6.65×10^{-9}

Table S4.3. Pyrrolizidine alkaloid (PA) signals observed in the root profiles of ragwort plants, as observed in profiles recorded in positive ESI UPLC-TOFMS. Average relative concentrations (±S.E.) are displayed for plants colonised by the AMF *Glomus intraradices* (n=16) and a controlled comparison (n=15). Concentrations measured using the response observed in 0.5µl injections, equivalent to 0.352mg of fresh root, are indicated by a ^, all other concentrations represent the response observed in the 20µl injections and are equivalent to 14.061mg of fresh root. When the PA response was saturated the C_{13} and O_{18} isotope responses of the PA were used for quantification, these are indicated by [a] and [b] respectively. Unmarked P-values are from t-tests, and P-values marked with a ~ are from Mann-Whitney U tests. None of the differences between treatment groups were significantly different after Bonferroni correction ($P < 5.01 \times 10^{-7}$).

Theoretical mass of ion	Putative formula	UPLC-TOFMS r.t.	Control	With AM fungi	P-value
334.1654	$C_{18}H_{23}NO_5$	6.00	49.68 (±5.25)	59.23 (±5.27)	0.210 ^
336.1811	$C_{18}H_{25}NO_5$	6.86	211.74 (±17.74)	289.77 (±21.63)	9.73×10^{-3} ^
350.1604	$C_{18}H_{23}NO_6$	6.34	220.46 (±27.68)	223.17 (±21.56)	0.874 ^[a]
		9.01	24.49 (±3.16)	38.56 (±6.16)	0.021
352.1760	$C_{18}H_{25}NO_6$	4.89	23.67 (±8.69)	52.01 (±14.23)	0.089 [a]
		5.82	76.05 (±11.29)	55.27 (±5.43)	0.216~
		6.13	327.92 (±23.93)	303.77 (±17.87)	0.711
		6.99	48.78 (±2.53)	52.99 (±2.36)	0.018 ^[a]
		7.16	108.80 (±4.23)	112.95 (±3.52)	0.128 ^[b]
366.1553	$C_{18}H_{23}NO_7$	4.29	193.17 (±46.09)	174.39 (±31.43)	0.736
		4.98	126.02 (±33.77)	141.86 (±39.54)	0.764
368.1709	$C_{18}H_{25}NO_7$	5.24	45.92 (±6.71)	65.17 (±10.15)	3.12×10^{-3} ^
		5.62	93.77 (±20.24)	119.31 (±18.84)	0.363 [a]
		6.39	550.52 (±54.41)	530.79 (±38.62)	0.767
370.1866	$C_{18}H_{27}NO_7$	5.94	24.04 (±2.17)	25.76 (±2.82)	0.636 ^
376.1760	$C_{20}H_{25}NO_6$	9.55	118.49 (±12.14)	118.41 (±14.33)	0.992 [a]
386.1815	$C_{18}H_{27}NO_8$	3.68	34.57 (±9.85)	105.59 (±15.96)	8.36×10^{-4}
392.1709	$C_{20}H_{25}NO_7$	9.77	196.45 (±26.17)	193.98 (±31.42)	0.902 ^[a]
404.1476	$C_{18}H_{26}NO_7Cl$	5.22	39.32 (±9.73)	122.20 (±13.49)	3.13×10^{-5}

Table S4.4. Pyrrolizidine alkaloid (PA) signals observed in the old and new leaves of ragwort, as observed in profiles recorded in positive ESI UPLC-TOFMS. Average relative concentrations (±S.E.) are displayed for plants colonised by the AMF *Glomus intraradices* (n=16) and a controlled comparison (n=15). All concentrations were measured using the response observed in 20µl injections, equivalent to 14.061mg of fresh shoots. When the PA response was saturated the C_{13} isotope response of the PA was used for quantification, these are indicated by [a]. The differences between treatment groups were tested using t-tests; no differences in PAs were significant after Bonferroni correction ($P < 6.06x10^{-7}$).

Theoretical mass of ion	Putative formula	UPLC-TOFMS r.t.	New leaves			Old leaves		
			Control	With AM fungi	P-value	Control	With AM fungi	P-value
334.1654	$C_{18}H_{23}NO_5$	6.00	110.88 (±11.94)	103.09 (±12.12)	0.651	39.17 (±7.19)	47.39 (±10.71)	0.534
336.1811	$C_{18}H_{25}NO_5$	6.86	213.19 (±34.58)	168.48 (±25.98)	0.306	54.80 (±11.81)	84.24 (±17.81)	0.185
350.1604	$C_{18}H_{23}NO_6$	4.10	20.03 (±6.35)	16.58 (±5.32)	0.679	29.30 (±12.06)	64.64 (±18.37)	0.071
		6.34	741.29 (±75.54)	762.90 (±83.49)	0.850 [a]	135.413 (±33.37)	198.64 (±51.75)	0.320 [a]
		9.05	71.44 (±18.23)	40.13 (±12.30)	0.334	11.31 (±5.59)	7.49 (±2.11)	0.518
352.1760	$C_{18}H_{25}NO_6$	4.90	114.44 (±54.71)	140.08 (±61.72)	0.759	769.00 (±351.01)	1758.03 (±475.37)	0.109
		5.42	20.33 (±5.59)	15.35 (±3.10)	0.435	4.49 (±1.96)	1.30 (±0.59)	0.045
		6.26	132.18 (±14.37)	129.80 (±11.25)	0.897	40.73 (±8.19)	46.87 (±9.71)	0.634
		7.01	854.30 (±170.44)	680.76 (±117.86)	0.404 [a]	168.16 (±48.79)	238.58 (±60.38)	0.376 [a]
366.1553	$C_{18}H_{23}NO_7$	4.28	467.80 (±59.05)	469.97 (±77.10)	0.982	30.99 (±5.22)	29.87 (±5.50)	0.884
		4.97	119.74 (±33.15)	138.241 (±34.48)	0.702 [a]	26.45 (±10.95)	20.96 (±7.90)	0.684
		6.79	76.86 (±19.58)	144.612 (±33.81)	0.099	11.81 (±4.89)	23.26 (±6.57)	0.177
368.1709	$C_{18}H_{25}NO_7$	5.25	326.42 (±93.82)	763.88 (±212.03)	0.074 [a]	72.96 (±20.04)	171.609 (±33.74)	0.049 [a]
		5.65	181.91 (±50.13)	158.44 (±30.30)	0.687 [a]	155.56 (±80.86)	86.70 (±24.66)	0.687
		6.40	33.43 (±5.53)	28.66 (±3.42)	0.462	34.36 (±3.67)	33.02 (±5.57)	0.844
386.1815	$C_{18}H_{27}NO_8$	3.69	24.66 (±8.62)	59.63 (±18.07)	0.098	23.14 (±6.27)	66.22 (±12.90)	0.025
404.1476	$C_{18}H_{26}NO_7Cl$	5.24	11.43 (±3.82)	27.65 (±3.82)	0.011	17.80 (±4.96)	47.72 (±9.54)	0.025

Chapter 5. General discussion

One of the aims of this thesis was to test the application of a UPLC-TOFMS metabolomic approach to ragwort (*Senecio jacobaea* L.) tissues. This was achieved by characterising the variation in the secondary metabolites of the above-ground tissues of ragwort collected in the field. Then using an experimental approach, the changes in the ragwort metabolome caused by below-ground interactions with an antagonistic herbivorous nematode (*Pratylenchus penetrans* (Cobb, 1917) Filipjev & Schuurmans Stekhoven, 1941) and a mutualist arbuscular mycorrhizal fungi (AMF) (*Glomus intraradices* Smith & Schenck) were investigated in above- and below-ground tissues. Ragwort was chosen as the study species because the main group of ragwort defensive secondary metabolites (PAs) are synthesised in the roots and subsequently translocated to areas of the plant attacked by herbivores. This ragwort response to herbivory meant that it was an ideal focal plant to study how the interactions between plant roots and below-ground mutualists or antagonists could influence the wider plant metabolome. This provides a potential chemical mechanism for the interaction between spatially separated organisms linked by a shared host-plant.

The studies outlined in this thesis were the first to apply metabolomics to the study of interactions between the above- and belowground secondary chemistry of plants. The study outlined in Chapter 3 was the first to use a metabolomic approach to detect changes in plant secondary metabolism as a result of infection by a migratory endoparasitic nematode. Previous studies that have examined the effect of nematodes (Hofmann et al. 2010, Baldacci-Cresp et al. 2012) and AMF (Schliemann et al. 2008a, Fester et al. 2011) on the plant metabolome have considered roots or shoots in isolation. By examining both roots and shoots concomitantly, these studies have demonstrated that changes induced in roots in response to antagonist (Chapter 3) and mutualist (Chapter 4) organisms had no implications for the secondary chemistry of aboveground tissues. Another important benefit of adopting a more holistic metabolomic approach is the discovery of novel metabolites that are previously unreported. The discovery of two novel structures in ragwort suggests a potential mechanism for species recognition between plants and fungi (Chapter 4). In this chapter the key findings and overarching themes of this thesis are discussed in a wider context.

5.1. Metabolomic responses of ragwort to soil biotic agents

Changes in the metabolomic profiles of ragwort roots were observed as a result of infection with migratory endoparasitic nematodes (Chapter 3) and colonisation by AMF (Chapter 4). The defensive role of ragwort PAs was confirmed by this study. Colonisation by AMF did not affect root PA concentrations whereas nematode herbivory did induce an elevation of root PA concentrations, specifically retrorsine N-oxide and another suspected alkaloid previously unseen in ragwort. These were the only PAs that changed as a result of nematode herbivory out of a total of 17 PAs detected in the ragwort roots in this study. This result was in accordance with Hol *et al.* (2004) who demonstrated that artificial damage of ragwort roots, aiming to simulate herbivory resulted in increased in total PA concentration driven by increased amounts of one PA (seneciphylline). Previous studies have shown that PAs have differential effects on organisms depending on the identity and chemical structure of individual PAs (Macel et al. 2005, Thoden et al. 2009a). Indeed, this mirrors interactions between herbivores and other classes of plant metabolites. For example, subtle differences in the glucosinolate profile of *Barbarea vulgaris* R. Br. - driven by the concentration of one metabolite glucobarbarin - were shown to affect the pupal biomass of the cabbage root fly (*Delia radicum* L.) markedly (van Leur *et al.* 2008). These subtle changes in the concentrations of specific PAs and glucosinolates demonstrate that coarser quantification of metabolites (e.g. total concentrations of metabolite classes) are insufficient to examine fully the interactions between plants and other organisms. Furthermore, multivariate analysis of the ragwort metabolome revealed a number of other metabolites induced by nematode herbivory or AMF colonisation (Chapters 3 & 4). The induced metabolites differed depending on the identity of the soil organism with mainly flavonoids (Chapter 3) and C_{13} cyclohexenones (Chapter 4) being induced in roots as a consequence of nematode herbivory and AMF colonisation, respectively. None of the identified metabolites were shared between those plants colonised by AMF and infected with nematodes. This suggests that ragwort, like other plant species (Reymond *et al.* 2000, Walling 2000, Ali and Agrawal 2012), can tailor chemical responses to the identity of the soil biotic agent.

In the last 20 years, it has been recognised that below-ground and above-ground insect herbivores interact with each other through induced metabolite changes in a shared host plant (Gange and Brown 1989, van der Putten *et al.* 2001, Wardle *et al.* 2004, de Deyn and van der Putten 2005, van Dam and Heil 2011). It has been demonstrated that mechanical damage of ragwort roots induced changes in shoot PA composition and concentration (Hol *et al.* 2004). However in this thesis, no above-ground differences in ragwort shoot PAs were observed as a

result of *P. penetrans* (Chapter 3) infection and *G. intraradices* (Chapter 4) colonisation. One of the advantages of adopting an unbiased metabolomic approach is the concomitant examination of the suite of metabolite classes in the plant metabolome (Fiehn 2002). In addition to PAs, this approach allows many metabolite classes to be observed in the leaves of ragwort including flavonoids, steroids, fatty acids, C_{13} cyclohexenones and phospholipids (Chapter 2). Despite this, no differences in shoot metabolome were detected as a result of the below-ground treatments (Chapters 3 & 4). While unexpected, one interpretation is that the increased concentrations of below-ground metabolites (Chapters 3 & 4) does not incur a cost to the plant, such as a reduction in the maintenance of above-ground defences. Alternatively, it could be that a plant's ability to respond to above-ground interactions could be affected by its interactions with below-ground organisms. By the 'priming' of plant tissues at a genetic level metabolomic costs of defences are reduced (Conrath *et al.* 2002). Therefore, plants are able to quickly mobilise defences once attacked (Pozo and Azcon-Aguilar 2007). Plant 'priming' could not be ruled out by the experiments outlined in Chapters 3 and 4. 'Priming' would not be detected without the application of an above-ground herbivore.

This lack of below-ground induction of above-ground secondary metabolism could be a result of issues arising from the analytical platform used. The first possibility to consider concerns whether a UPLC-TOFMS metabolomic approach was sensitive enough to detect secondary chemical changes in leaves. The consistent ability of this technique to discriminate between old and new leaf material (Chapters 2 & 4) suggest that technical limitations do not provide an explanation. Secondly, the technique used to examine a metabolome inherently introduces bias into an analysis (Macel *et al.* 2010). LC-MS analyses are preferable when examining secondary plant metabolism (Allwood and Goodacre 2010), but are not as suited to the analysis of primary metabolism as GC-MS techniques (Hagel and Facchini 2008). It could be that, as in other study systems (Gange and Brown 1989, Bezemer *et al.* 2005), above-ground induced changes in primary metabolism mediate the interactions between below- and above-ground organisms. Such changes in ragwort primary metabolism, if they occurred, would not have been detected using the UPLC-TOFMS approach used throughout this thesis. Finally, it could be that these results reflect a genuine lack of induction in the leaf metabolome as a result of below-ground interactions. Determining which explanation(s) apply in this case should be the focus of further work (Section 5.4. below).

5.2. Temporal influences on plant interactions

The temporal dimension needs to be considered in understanding the outcomes of plant interactions with other organisms. For example, time of arrival can have a significant influence on the outcomes of biotic interactions (Blossey and Hunt-Joshi 2003, Soler *et al.* 2012). *Spodoptera frugiperda* (Smith, 1797) have a negative effect on the colonisation of the root herbivore *Diabrotica virgifera virgifera* LeConte, 1868 when they arrive first on maize (*Zea mays* L.) (Erb *et al.* 2011), whereas, when the root herbivore feeds on the plant first subsequent feeding by *S. frugiperda* has no effect on *D. virgifera virgifera* colonisation (Erb *et al.* 2011). This study, by including a temporal element in the experimental design, provided a novel insight into the interaction between ragwort and the nematode herbivore *P. penetrans* (Chapter 3). By harvesting sequentially, the induction and subsequent waning of ragwort defences in response to *P. penetrans* infection was observed. Seven days post-infection a total of 16 metabolites, including the PA retrorsine N-oxide, were induced as a result of nematode herbivory. In the subsequent harvest (28 days post-infection) only seven metabolites were induced and no differences in retrorsine N-oxide were observed. If a temporal dimension had not been considered in this study (Chapter 3), then a subtlety (e.g. early induction of the PA retrorsine N-oxide) in this plant-nematode interaction would have been overlooked and the subsequent conclusions altered (e.g. without the earlier harvest, it would have been concluded that nematode herbivory does not induce PAs). This finding was in agreement with studies that have examined the interaction between plants and migratory endoparasitic nematodes at a genetic level (Kyndt *et al.* 2012).

A temporal element has been used in some other metabolomic examinations of plant responses to environmental peturbation (Kaplan *et al.* 2004, Schliemann *et al.* 2008a, Depuydt *et al.* 2009, Parker *et al.* 2009). For example, in *Arabidopsis thaliana* L. Heynh. clear metabolomic separations were observed over time after exposure to extreme temperatures (4°C and 40°C) (Kaplan *et al.* 2004). Through a metabolomic analysis over six time points they were able to examine the timing (early, intermediate and late) and longevity (sustained and transient) of the plant responses to temperature regimes (Kaplan *et al.* 2004). The metabolomic analysis of the early harvest allowed salicylic acid to be putatively identified as the signalling molecule involved in the response of *A. thaliana* to temperature stress (Kaplan *et al.* 2004). Metabolomic analysis of subsequent time points allowed the consequences of receiving this signal to be observed, including increased concentrations of some amino acids and sugars (Kaplan *et al.* 2004). In addition, through the temporal examination of plant interactions with biotic organisms using a metabolomic approach, new insights in to

metabolomic pathways can be determined. For example, precursor metabolites and their products can be concomitantly observed using metabolomic approaches. By detecting changes in the concentrations of both precusor and product metabolites, Hartley *et al.* (2012) were able to conclude that the jasmonic acid pathway was involved in the interaction between thistles (*Cirsium arvense* (L.) Scop.) and the endophytic fungi *Chaetomium cochlioides* (Wallr.) S. Hughs, (1958). Thus, by adding an extra dimension to metabolomic studies extra information about the pathways involved in plant interactions with other organisms can be elucidated.

5.3. Metabolomics as a tool to study plant interactions

All three chapters of this thesis have demonstrated that metabolomics is an excellent tool to study the interactions between plants and other organisms. Adopting a metabolomic approach allowed new insights in to the interactions between ragwort and biotic organisms to be observed. Hitherto the majority of studies that investigated the effect of other interactions on the metabolite defences of ragwort considered PAs solely (for example de Boer 1999, Joosten *et al.* 2009, Reidinger *et al.* 2012). The metabolomic approach used here allowed, in addition to PA content, within-plant variation of steroids, flavonoids, C_{13} cyclohexenones, phospholipids and hydroxy fatty acids to be concomitantly examined (Chapters 2-4). Other than PAs, only a few secondary metabolites (phenylpropanoids, flavonoids and benzoquinoids) have previously been reported in the leaves of ragwort (Kirk *et al.* 2005, Nuringtyas *et al.* 2012). Moreover, the non-PA secondary metabolites of ragwort flowers and roots had never been examined prior to the studies outlined in this thesis. In addition, a metabolomic approach provided a more rigorous test of defence theories. One of the main predictions of Optimal Defence Theory (ODT) is that those tissue of high physiological or fitness value to the plant should be the most defended (McKey 1974). In this study, approximately two thirds of the metabolites (e.g. hydroxy fatty acids and most PAs) identified follow the allocation patterns predicted by ODT (Chapter 2). Whereas the remaining third of identified metabolites, including metabolites with a known role in plant defence (a PA and chlorogenic acid), did not follow the predictions made (Chapter 2). This finding suggested some limitations to the theory or a non-defensive role for these metabolites in ragwort. In Chapter 3, it was demonstrated that flavonoids were induced as a result of *P. penetrans* infection, and a targeted PA approach would not have detected this. In addition, by adopting a metabolomic approach, variations in a previously unreported alkaloid were also detected in ragwort as a result of nematode

herbivory (Chapter 3). In response to AMF colonisation, increased concentrations of previously unreported C_{13} cyclohexenones conjugated with sugar and galactose moieties were identified (Chapter 4). The identification of previously unknown metabolites is one of the main advantages of adopting an unbiased metabolomic approach.

The analyses in this study used a Bonferroni correction term to reduce the false discovery rate (Type I error) associated with multiple statistical testing, a necessary approach when handling metabolomic datasets (Broadhurst and Kell 2006). The use of the Bonferroni correction is a very conservative method that while reducing the false discovery rate can incorrectly fail to reject the null hypothesis of no statistical difference (Type II error) (Benjamini *et al.* 2001). It is possible that by not applying a Bonferroni correction term changes in many other metabolite concentrations could have been detected in response to nematode herbivory or AMF colonisation. For example, the concentrations of one PA (*m/z*: 352.1760, r.t.: 4.40) in roots infected by *P. penetrans* was half that detected in the roots of control plants (Chapter 3). These changes, although not significant after the application of a conservative Bonferroni correction term, may represent biologically relevant changes. An alternative approach would have been to apply either a Benjamini and Hochberg, or Benjamini and Lui correction. These methods also control the occurrence of Type I errors, but introduce fewer Type II errors when compared with Bonferroni adjustment (Benjamini *et al.* 2001). Nonetheless, large differences in metabolite concentrations were observed throughout this thesis even after applying the rigorous Bonferroni approach. Additional challenges associated with the use of metabolomics as a tool to study plant interactions, specifically problems relating to the identification of metabolites, are discussed in Section 5.4.

5.4. Further work and knowledge gaps

In addition to the future directions already suggested in this discussion, the findings presented highlight some technical problems associated with adopting a metabolomic approach and some future research areas. Further metabolite identification would have strengthened the conclusions of the experimental chapters in this thesis. Across all data chapters, approximately one in four metabolites of interest were identified. Identifying all the metabolites detected is a problem common to metabolomic studies (e.g. Desbrosses *et al.* 2005, Sanchez *et al.* 2008, Baldacci-Cresp *et al.* 2012). For example, Sanchez *et al.* (2008) identified one third of the metabolites that increased as a result of acclimatisation of *Lotus*

japonicus L. to soil salinity. Metabolite identification is a bottleneck common to metabolomic analyses regardless of analytical platform (Hagel and Facchini 2008). This is a particular problem when identifying metabolites of plant origin that are numerous and can be conjugated to a variety of sugars. Metabolite identification should become easier with the improvement of the online databases and increased availability of authenticated standards, however progress is still slow in this area (Fiehn 2002).

Chapters 3 and 4 of this thesis used microcosms in a laboratory based experimental approach to examine the interactions between ragwort and soil biotic agents. Adopting a laboratory approach allows variability that could be caused by environmental conditions to be reduced. By reducing variation within a dataset, the mechanisms underpinning plant interactions with other biotic organisms can be examined (Verhoef 1996). It may not, however, provide reliable data that can be scaled up to represent real world situations (Carpenter 1996). Ideally, the experiments outlined in chapters three and four would be replicated in the field. It could be that some of the metabolite changes induced in the laboratory, are too small and variable to be detected in the field using a metabolomic approach. This is especially true when examining the interaction between plants and migratory endoparasitic nematodes, the changes in metabolite profile were subtle and represented small changes in metabolite concentrations (Chapter 3). The results of the laboratory experiments outlined in this thesis could be used to guide targeted analyses of key metabolites expected to vary in the field as a result of the interaction with soil organisms. For example, targeted LC-MSMS analyses could be used to profile and quantify flavonoids in root tissues when examining the interaction between plants and *P. penetrans*.

The experiments reported in Chapters 3 and 4 examine pair-wise interactions between two organisms. This is not a realistic representation of nature where plants are the centre of a network of complex species interactions. Increasing the complexity of the soil community could influence the outcomes of the interactions studied. For example, it has been shown that AMF colonisation can negatively affect the population density of herbivorous nematodes (Pinochet *et al.* 1995, Jaizme-Vega *et al.* 1997, Elsen *et al.* 2003, Rodriguez-Echeverria *et al.* 2009). As mentioned above, future experiments should ensure that they are designed so that they can examine priming as well as changes in primary and secondary metabolism. For example, in this study system, by adding an above-ground herbivore and examining the subsequent plant response, priming could be examined. To ensure subtle changes in primary and secondary metabolism were measured GC-MS and LC-MS techniques should be used. It has been shown that plant-mediated interactions between organisms in below-ground

systems can have implications for higher trophic levels (Soler *et al.* 2007a), with repercussions for community composition (de Deyn and van der Putten 2005). In future, it would be interesting to consider the wider effects that changes in plant chemistry, induced by soil biotic agents, have at higher trophic levels below ground.

5.5. Concluding remarks

The findings presented in this thesis emphasise the power of the metabolomic approach when studying plant interactions with biotic organisms. As well as observing variations in PAs, by adopting a metabolomic approach variations in metabolite classes hitherto previously unreported in ragwort were detected. No evidence of above-ground changes in secondary metabolism was detected as a result of the interactions with an antagonist (*P. penetrans*) or a mutualist (*G. intraradices*). This demonstrated that induced changes in secondary chemistry below ground are not at the expense of above-ground defences or other processes governed by secondary metabolites. The identification of the metabolites induced as a result of the interactions with soil biota examined in this thesis is an important area for further research if the effects of these below-ground interactions on other organisms are to be determined. The results demonstrate the need of further studies to include further levels of complexity both above and below ground. Such studies should analyse a wide range of metabolites to allow the mechanisms of plant interactions with biotic organisms to be elucidated.

References

Acedo, J. R. and R. A. Rohde. 1971. Histochemical rootpathology of *Brassica oleracea capitata* L. infected by *Pratylenchus penetrans* (Cobb) Filipjev and Schuurmans Stekhoven (Nematoda: Tylenchidea). Journal of Nematology **3**:62-68.

Adler, F. R. and R. Karban. 1994. Defended fortresses or moving targets? Another model of inducible defences inspired by military metaphors. American Naturalist **144**:813-832.

Adler, L. S. 2000. The ecological significance of toxic nectar. Oikos **91**:409-420.

Adler, L. S. and R. E. Irwin. 2012. Nectar alkaloids decrease pollination and female reproduction in a native plant. Oecologia **168**:1033-1041.

Agrawal, A. A. and R. Karban. 1999. Why induced defenses may be favored over constitutive strategies in plants. Pages 45-61 *in* R. Tollrian and C. D. Harvell, editors. The Ecology and Evolution of Inducible Defenses. Princeton University Press, Princeton, U.S.A.

Agrawal, A. A., G. Petschenka, R. A. Bingham, M. G. Weber, and S. Rasmann. 2012. Toxic cardenolides: chemical ecology and coevolution of specialized plant-herbivore interactions. New Phytologist **194**:28-45.

Akiyama, K., K. Matsuzaki, and H. Hayashi. 2005. Plant sesquiterpenes induce hyphal branching in arbuscular mycorrhizal fungi. Nature **435**:824-827.

Alborn, H. T., T. C. J. Turlings, T. H. Jones, G. Stenhagen, J. H. Loughrin, and J. H. Tumlinson. 1997. An elicitor of plant volatiles from beet armyworm oral secretion. Science **276**:945-949.

Ali, J. G. and A. A. Agrawal. 2012. Specialist versus generalist insect herbivores and plant defense. Trends in Plant Science **17**:293-302.

Ali, J. G., H. T. Alborn, and L. L. Stelinski. 2010. Subterranean herbivore-induced volatiles released by citrus roots upon feeding by *Diaprepes abbreviatus* recruit entomopathogenic nematodes. Journal of Chemical Ecology **36**:361-368.

Allwood, J. W. and R. Goodacre. 2010. An introduction to liquid chromatography-mass spectrometry instrumentation applied in plant metabolomic analyses. Phytochemical Analysis **21**:33-47.

Anderson, P. and J. Agrell. 2005. Within-plant variation in induced defence in developing leaves of cotton plants. Oecologia **144**:427-434.

Anon. 2004. Code of Practice on How to Prevent the Spread of Ragwort. Department for Environment, Food and Rural Affairs, UK.

Aplin, R. T., M. H. Benn, and Rothschi.M. 1968. Poisonous alkaloids in body tissues of cinnabar moth (*Callimorpha jacobaeae* L). Nature **219**:747-&.

Arany, A. M., T. J. de Jong, H. K. Kim, N. M. van Dam, Y. H. Choi, R. Verpoorte, and E. van der Meijden. 2008. Glucosinolates and other metabolites in the leaves of *Arabidopsis thaliana* from natural populations and their effects on a generalist and a specialist herbivore. Chemoecology **18**:65-71.

Aratchige, N. S., I. Lesna, and M. W. Sabelis. 2004. Below-ground plant parts emit herbivore-induced volatiles: olfactory responses of a predatory mite to tulip bulbs infested by rust mites. Experimental and Applied Acarology **33**:21-30.

Ardrey, R. E. 2003. Liquid Chromatography-Mass Spectrometry: an introduction. John Wiley & Sons, Ltd, Chichester, UK.

Bago, B., P. E. Pfeffer, and Y. Shachar-Hill. 2000. Carbon metabolism and transport in arbuscular mycorrhizas. Plant Physiology **124**:949-957.

Bais, H. P., B. Prithiviraj, A. K. Jha, F. M. Ausubel, and J. M. Vivanco. 2005. Mediation of pathogen resistance by exudation of antimicrobials from roots. Nature **434**:217-221.

Bais, H. P., T. L. Weir, L. G. Perry, S. Gilroy, and J. M. Vivanco. 2006. The role of root exudates in rhizosphere interations with plants and other organisms. Annual Review of Plant Biology **57**:233-266.

Baldacci-Cresp, F., C. Chang, M. Maucourt, C. Deborde, J. Hopkins, P. Lecomte, S. Bernillon, R. Brouquisse, A. Moing, P. Abad, D. Herouart, A. Puppo, B. Favery, and P. Frendo. 2012. (Homo)glutathione deficiency impairs root-knot nematode development in *Medicago truncatula*. Plos Pathogens **8**:e1002471.

Baldridge, G. D., N. R. O'Neill, and D. A. Samac. 1998. Alfalfa (*Medicago sativa* L.) resistance to the root-lesion nematode, *Pratylenchus penetrans*: defense-response gene mRNA and isoflavonoid phytoalexin levels in roots. Plant Molecular Biology **38**:999-1010.

Ballizany, W. L., R. W. Hofmann, M. Z. Z. Jahufer, and B. A. Barrett. 2012. Multivariate associations of flavonoid and biomass accumulation in white clover (*Trifolium repens*) under drought. Functional Plant Biology **39**:167-177.

Banos, L., M. Duenas, A. M. Carvalho, I. Ferreira, and C. Santos-Buelga. 2012. Characterization of phenolic compounds in flowers of wild medicinal plants from Northeastern Portugal. Food and Chemical Toxicology **50**:1576-1582.

Bardgett, R. D., D. A. Wardle, and G. W. Yeates. 1998. Linking above-ground and below-ground interactions: how plant responses to foliar herbivory influence soil organisms. Soil Biology & Biochemistry **30**:1867-1878.

Barton, K. E. and J. Koricheva. 2010. The ontogeny of plant defense and herbivory: characterizing general patterns using meta-analysis. American Naturalist **175**:481-493.

Beales, K. A., S. M. Colegate, and J. A. Edgar. 2003. Experiences with the quantitative trace analysis of pyrrolizidine alkaloids using GCMS and LCMS. Pages 453-458 *in* T. Acamovic, C. S. Stewart, and T. W. Pennycott, editors. Poisonous Plants and Related Toxins. Wallingford, CABI Publishing.

Becard, G., L. P. Taylor, D. D. Douds, P. E. Pfeffer, and L. W. Doner. 1995. Flavanoids are not necessary plant signal compounds in arbuscular mycorrhizal symbioses. Molecular Plant-Microbe Interactions **8**:252-258.

Bede, J. C., R. O. Musser, G. W. Felton, and K. L. Korth. 2006. Caterpillar herbivory and salivary enzymes decrease transcript levels of *Medicago truncatula* genes encoding early enzymes in terpenoid biosynthesis. Plant Molecular Biology **60**:519-531.

Begum, S., A. Wahab, B. S. Siddiqui, and F. Qamar. 2000. Nematicidal constituents of the aerial parts of *Lantana camara*. Journal of Natural Products **63**:765-767.

Belsky, A. J. 1986. Does herbivory benefit plants - a review of the evidence. American Naturalist **127**:870-892.

Benjamini, Y., D. Drai, G. Elmer, N. Kafkafi, and I. Golani. 2001. Controlling the false discovery rate in behavior genetics research. Behavioural Brain Research **125**:279-284.

Bennett, A. E., J. D. Bever, and M. D. Bowers. 2009. Arbuscular mycorrhizal fungal species suppress inducible plant responses and alter defensive strategies following herbivory. Oecologia **160**:771-779.

Beuerle, T., C. Theuring, N. Klewer, S. Schulz, and T. Hartmann. 2007. Absolute configuration of the creatonotines and callimorphines, two classes of arctiid-specific pyrrolizidine alkaloids. Insect Biochemistry and Molecular Biology **37**:80-89.

Bezemer, T. M., G. B. de Deyn, T. M. Bossinga, N. M. van Dam, J. A. Harvey, and W. H. van der Putten. 2005. Soil community composition drives aboveground plant-herbivore-parasitoid interactions. Ecology Letters **8**:652-661.

Bezemer, T. M., J. A. Harvey, G. A. Kowalchuk, H. Korpershoek, and W. H. van der Putten. 2006. Interplay between *Senecio jacobaea* and plant, soil, and aboveground insect community composition. Ecology **87**:2002-2013.

Bezemer, T. M. and N. M. van Dam. 2005. Linking aboveground and belowground interactions via induced plant defenses. Trends in Ecology & Evolution **20**:617-624.

Bezemer, T. M., R. Wagenaar, N. M. van Dam, and F. L. Wackers. 2003. Interactions between above- and belowground insect herbivores as mediated by the plant defense system. Oikos **101**:555-562.

Blossey, B. and T. R. Hunt-Joshi. 2003. Belowground herbivory by insects: influence on plants and aboveground herbivores. Annual Review of Entomology **48**:521-547.

Blüthgen, N. and A. Metzner. 2007. Contrasting leaf age preferences of specialist and generalist stick insects (*Phasmida*). Oikos **116**:1853-1862.

Boege, K. and R. J. Marquis. 2005. Facing herbivory as you grow up: the ontogeny of resistance in plants. Trends in Ecology & Evolution **20**:441-448.

Bonsall, M. B., E. van der Meijden, and M. J. Crawley. 2003. Contrasting dynamics in the same plant-herbivore interaction. Proceedings of the National Academy of Sciences of the United States of America **100**:14932-14936.

Boppre, M., S. M. Colegate, and J. A. Edgar. 2005. Pyrrolizidine alkaloids of *Echium vulgare* honey found in pure pollen. Journal of Agricultural and Food Chemistry **53**:594-600.

Bowers, M. D. and G. M. Puttick. 1986. Fate of ingested iridoid glycosides in Lepidopteran herbivores. Journal of Chemical Ecology **12**:169-178.

Brinkman, E. P., J. A. van Veen, and W. H. van der Putten. 2004. Endoparasitic nematodes reduce multiplication of ectoparasitic nematodes, but do not prevent growth reduction of *Ammophila arenaria* (L.) Link (marram grass). Applied Soil Ecology **27**:65-75.

Broadhurst, D. I. and D. B. Kell. 2006. Statistical strategies for avoiding false discoveries in metabolomics and related experiments. Metabolomics **2**:171-196.

Brown, P. D., J. G. Tokuhisa, M. Reichelt, and J. Gershenzon. 2003. Variation of glucosinolate accumulation among different organs and developmental stages of *Arabidopsis thaliana*. Phytochemistry **62**:471-481.

Buskov, S., B. Serra, E. Rosa, H. Sorensen, and J. C. Sorensen. 2002. Effects of intact glucosinolates and products produced from glucosinolates in myrosinase-catalyzed hydrolysis on the potato cyst nematode (*Globodera rostochiensis* cv. Woll). Journal of Agricultural and Food Chemistry **50**:690-695.

Bylesjo, M., M. Rantalainen, O. Cloarec, J. K. Nicholson, E. Holmes, and J. Trygg. 2006. OPLS discriminant analysis: combining the strengths of PLS-DA and SIMCA classification. Journal of Chemometrics **20**:341-351.

Caetano-Anollés, G., D. K. Crist-Estes, and W. D. Bauer. 1988. Chemotaxis of *Rhizobium meliloti* to the plant flavone luteolin requires functional nodulation genes. Journal of Bacteriology **170**:3164-3169.

Cameron, E. 1935. A study of the natural control of ragwort (*Senecio jacobaea* L.). Journal of Ecology **23**:265-322.

Candrian, U., J. Luthy, P. Schmid, C. Schlatter, and E. Gallasz. 1984. Stability of pyrrolizidine alkaloids in hay and silage. Journal of Agricultural and Food Chemistry **32**:935-937.

Cao, Y., S. M. Colegate, and J. A. Edgar. 2008. Safety assessment of food and herbal products containing hepatotoxic pyrrolizidine alkaloids: interlaboratory consistency and the importance of N-oxide determination. Phytochemical Analysis **19**:526-533.

Care, D. A., J. R. Crush, S. Hardwick, S. N. Nichols, and L. Ouyang. 2000. Interactions between clover root weevil and clover root type. New Zealand Plant Protection **53**:420-424.

Carpenter, S. R. 1996. Microcosm experiments have limited relevance for community and ecosystem ecology. Ecology **77**:677-680.

Castillo, P. and N. Vovlas. 2007. *Pratylenchus* (Nematoda: Pratylenchidae): Diagnosis, biology, pathogenicity and management. Koninklijke Brill NV, Leiden, The Netherlands.

Cates, R. G. 1980. Feeding patterns of monophagous, oligophagous, and polyphagous insect herbivores - the effect of resource abundance and plant chemistry Oecologia **46**:22-31.

Chang-Hung, C. 1999. Roles of allelopathy in plant biodiversity and sustainable agriculture. Critical Reviews in Plant Sciences **18**:609-636.

Cheeke, P. R. and M. L. Pierson-Goeger. 1983. Toxicity of *Senecio jacobaea* and pyrrolizidine alkaloids in various laboratory animals and avian species. Toxicology Letters **18**:343-349.

Chen, K., W. Ohmura, S. Doi, and M. Aoyama. 2004. Termite feeding deterrent from Japanese larch wood. Bioresource Technology **95**:129-134.

Chitwood, D. J. 2002. Phytochemical based strategies for nematode control. Annual Review of Phytopathology **40**:221-249.

Clark, R. T., R. B. MacCurdy, J. K. Jung, J. E. Shaff, S. R. McCouch, D. J. Aneshansley, and L. V. Kochian. 2011. Three-dimensional root phenotyping with a novel imaging and software platform. Plant Physiology **156**:455-465.

Clay, K., S. Marks, and G. P. Cheplick. 1993. Effects of insect herbivory and fungal endophyte infection on competitive interactions among grasses. Ecology **74**:1767-1777.

Clifford, M. N. 2000. Chlorogenic acids and other cinnamates - nature, occurrence, dietary burden, absorption and metabolism. Journal of the Science of Food and Agriculture **80**:1033-1043.

Colazza, S., J. S. McElfresh, and J. G. Millar. 2004. Identification of volatile synomones, induced by *Nezara viridula* feeding and oviposition on bean spp., that attract the egg parasitoid *Trissolcus basalis*. Journal of Chemical Ecology **30**:945-964.

Colebatch, G., G. Desbrosses, T. Ott, L. Krusell, O. Montanari, S. Kloska, J. Kopka, and M. K. Udvardi. 2004. Global changes in transcription orchestrate metabolic differentiation during symbiotic nitrogen fixation in *Lotus japonicus*. Plant Journal **39**:487-512.

Colegate, S. M., J. A. Edgar, A. M. Knill, and S. T. Lee. 2005. Solid-phase extraction and HPLC-MS profiling of pyrrolizidine alkaloids and their N-oxides: a case study of *Echium plantagineum*. Phytochemical Analysis **16**:108-119.

Coley, P. D., J. P. Bryant, and F. S. Chapin. 1985. Resource availability and plant antiherbivore defence. Science **230**:895-899.

Collingborn, F. M. B., S. R. Gowen, and I. Mueller-Harvey. 2000. Investigations into the biochemical basis for nematode resistance in roots of three *Musa* cultivars in response to *Radopholus similis* infection. Journal of Agricultural and Food Chemistry **48**:5297-5301.

Conrath, U., C. M. J. Pieterse, and B. Mauch-Mani. 2002. Priming in plant-pathogen interactions. Trends in Plant Science **7**:210-216.

Copetta, A., G. Lingua, and G. Berta. 2006. Effects of three AM fungi on growth, distribution of glandular hairs, and essential oil production in *Ocimum basilicum* L. var. Genovese. Mycorrhiza **16**:485-494.

Crawley, M. J. and M. P. Gillman. 1989. Population dynamics of cinnabar moth and ragwort in grassland. Journal of Animal Ecology **58**:1035-1050.

Crawley, M. J. and M. Nachapong. 1984. Facultative defenses and specialist herbivores - cinnabar moth (*Tyria jacobaeae*) on the regrowth foliage of ragwort (*Senecio jacobaea*). Ecological Entomology **9**:389-393.

Crews, C., F. Berthiller, and R. Krska. 2010. Update on analytical methods for toxic pyrrolizidine alkaloids. Analytical and Bioanalytical Chemistry **396**:327-338.

Crews, C., M. Driffield, F. Berthiller, and R. Krska. 2009. Loss of pyrrolizidine alkaloids on decomposition of ragwort (*Senecio jacobaea*) as measured by LC-TOF-MS. Journal of Agricultural and Food Chemistry **57**:3669-3673.

Currie, A. F., P. J. Murray, and A. C. Gange. 2011. Is a specialist root-feeding insect affected by arbuscular mycorrhizal fungi? Applied Soil Ecology **47**:77-83.

Cyr, H. and M. L. Pace. 1993. Magnitude and patterns of herbivory in aquatic and terrestrial ecosystems. Nature **361**:148-150.

da Silva, C. D., A. A. Bolzan, and B. M. Heinzmann. 2006. Pyrrolizidine alkaloids from *Senecio* species. Quimica Nova **29**:1047-1053.

de Boer, N. J. 1999. Pyrrolizidine alkaloid distribution in *Senecio jacobaea* rosettes minimises losses to generalist feeding. Entomologia Experimentalis Et Applicata **91**:169-173.

de Deyn, G. B., A. Biere, W. H. van der Putten, R. Wagenaar, and J. N. Klironomos. 2009. Chemical defense, mycorrhizal colonization and growth responses in *Plantago lanceolata* L. Oecologia **160**:433-442.

de Deyn, G. B., C. E. Raaijmakers, H. R. Zoomer, M. P. Berg, P. C. de Ruiter, H. A. Verhoef, T. M. Bezemer, and W. H. van der Putten. 2003. Soil invertebrate fauna enhances grassland succession and diversity. Nature **422**:711-713.

de Deyn, G. B. and W. H. van der Putten. 2005. Linking aboveground and belowground diversity. Trends in Ecology & Evolution **20**:625-633.

Delphia, C. M., M. C. Mescher, G. W. Felton, and C. M. De Moraes. 2006. The role of insect-derived cues in eliciting indirect plant defenses in tobacco, *Nicotiana tabacum*. Plant signaling & behavior **1**:243-250.

Dempster, J. P. 1982. The ecology of the cinnabar moth, *Tyria jacobaeae* L. (Lepidoptera, Arctiidae). Advances in Ecological Research **12**:1-36.

Depuydt, S., S. Trenkamp, A. R. Fernie, S. Elftieh, J.-P. Renou, M. Vuylsteke, M. Holsters, and D. Vereecke. 2009. An integrated genomics approach to define niche establishment by *Rhodococcus fascians*. Plant Physiology **149**:1366-1386.

Desbrosses, G. G., J. Kopka, and M. K. Udvardi. 2005. *Lotus japonicus* metabolic profiling. Development of gas chromatography-mass spectrometry resources for the study of plant-microbe interactions. Plant Physiology **137**:1302-1318.

Dicke, M., R. M. P. van Poecke, and J. G. de Boer. 2003. Inducible indirect defence of plants: from mechanisms to ecological functions. Basic and Applied Ecology **4**:27-42.

Dinan, L. 1995. A strategy for the identification of ecdysteroid receptor agonists and antagonists from plants. European Journal of Entomology **92**:271-283.

Dinan, L. 2009. The Karlson Lecture. Phytoecdysteroids: what use are they? Archives of Insect Biochemistry and Physiology **72**:126-141.

Dobler, S., W. Haberer, L. Witte, and T. Hartmann. 2000. Selective sequestration of pyrrolizidine alkaloids from diverse host plants by *Longitarsus* flea beetles. Journal of Chemical Ecology **26**:1281-1298.

Dolzhenko, Y., C. M. Bertea, A. Occhipinti, S. Bossi, and M. E. Maffei. 2010. UV-B modulates the interplay between terpenoids and flavonoids in peppermint (*Mentha x piperita* L.). Journal of Photochemistry and Photobiology B-Biology **100**:67-75.

Doss, R. P., J. E. Oliver, W. M. Proebsting, S. W. Potter, S. R. Kuy, S. L. Clement, R. T. Williamson, J. R. Carney, and E. D. DeVilbiss. 2000. Bruchins: Insect-derived plant regulators that stimulate neoplasm formation. Proceedings of the National Academy of Sciences of the United States of America **97**:6218-6223.

Edens, R. M., S. C. Anand, and R. I. Bolla. 1995. Enzymes of the phenylpropanoid pathway in soybean infected with *Meloidogyne incognita* or *Heterodera glycines*. Journal of Nematology **27**:292-303.

Edgar, J. A., C. C. J. Culvenor, P. A. Cockrum, L. W. Smith, and M. Rothschild. 1980. Callimorphine - identification and synthesis of the cinnabar moth metabolite. Tetrahedron Letters **21**:1383-1384.

Eftekhari, M., M. Alizadeh, and P. Ebrahimi. 2012. Evaluation of the total phenolics and quercetin content of foliage in mycorrhizal grape (*Vitis vinifera* L.) varieties and effect of postharvest drying on quercetin yield. Industrial Crops and Products **38**:160-165.

Ehmke, A., K. Vonborstel, and T. Hartmann. 1988. Alkaloid N-oxides as transport and vacuolar storage compounds of pyrrolizidine alkaloids in *Senecio vulgaris* L. Planta **176**:83-90.

Elsen, A., S. Declerck, and D. De Waele. 2003. Use of root organ cultures to investigate the interaction between Glomus intraradices and Pratylenchus coffeae. Applied and Environmental Microbiology **69**:4308-4311.

Endara, M. J. and P. D. Coley. 2011. The resource availability hypothesis revisited: a meta-analysis. Functional Ecology **25**:389-398.

Epstein, E. 1972. Biochemical changes in terminal root galls caused by an ectoparasitic nematode, *Longidorus africanus* - phenols, carbohydrates and cytokinins. Journal of Nematology **4**:246-250.

Epstein, E. 1974. Biochemical changes in terminal root galls caused by an ectoparasitic nematode, *Longidorus africanus* - nucleic acids. Journal of Nematology **6**:48-52.

Epstein, E. and E. Cohn. 1971. Biochemical changes in terminal root galls caused by an ectoparasitic nematode, *Longidorus africanus* - amino acids. Journal of Nematology **3**:334-340.

Erb, M., C. A. M. Robert, B. E. Hibbard, and T. C. J. Turlings. 2011. Sequence of arrival determines plant-mediated interactions between herbivores. Journal of Ecology **99**:7-15.

Fahey, J. W., A. T. Zalcmann, and P. Talalay. 2001. The chemical diversity and distribution of glucosinolates and isothiocyanates among plants. Phytochemistry **56**:5-51.

Feeny, P. 1976. Plant apparency and chemical defence. Pages 1-40 *in* J. W. Wallace and R. L. Mansell, editors. Recent Advances in Phytochemistry. Plenum Press, New York, U.S.A.

Felton, G. W., K. K. Donato, R. M. Broadway, and S. S. Duffey. 1992. Impact of oxidized plant phenolics on the nutritional quality of dietary-protein to a Noctuid herbivore, *Spodoptera exigua*. Journal of Insect Physiology **38**:277-285.

Fester, T., I. Fetzer, S. Buchert, R. Lucas, M. C. Rillig, and C. Haertig. 2011. Towards a systemic metabolic signature of the arbuscular mycorrhizal interaction. Oecologia **167**:913-924.

Fester, T., B. Hause, D. Schmidt, K. Halfmann, J. Schmidt, V. Wray, G. Hanse, and D. Strack. 2002. Occurrence and localization of apocarotenoids in arbuscular mycorrhizal plant roots. Plant and Cell Physiology **43**:256-265.

Fester, T., V. Wray, M. Nimtz, and D. Strack. 2005. Is stimulation of carotenoid biosynthesis in arbuscular mycorrhizal roots a general phenomenon? Phytochemistry **66**:1781-1786.

Fiehn, O. 2002. Metabolomics - the link between genotypes and phenotypes. Plant Molecular Biology **48**:155-171.

Floss, D. S., B. Hause, P. R. Lange, H. Kuester, D. Strack, and M. H. Walter. 2008. Knock-down of the MEP pathway isogene 1-deoxy-D-xylulose 5-phosphate synthase 2 inhibits formation of arbuscular mycorrhiza-induced apocarotenoids, and abolishes normal expression of mycorrhiza-specific plant marker genes. Plant Journal **56**:86-100.

Fontana, A., M. Reichelt, S. Hempel, J. Gershenzon, and S. B. Unsicker. 2009. The effects of arbuscular mycorrhizal fungi on direct and indirect defense metabolites of *Plantago lanceolata* L. Journal of Chemical Ecology **35**:833-843.

Friedman, P. A. and R. A. Rohde. 1976. Phenol levels in leaves of tomato cultivars infected with *Pratylenchus penetrans*. Journal of Nematology **8**:285-285.

Fuller, V. L., C. J. Lilley, and P. E. Urwin. 2008. Nematode resistance. New Phytologist **180**:27-44.

Gange, A. C., E. Bower, and V. K. Brown. 2002. Differential effects of insect herbivory on arbuscular mycorrhizal colonization. Oecologia **131**:103-112.

Gange, A. C. and V. K. Brown. 1989. Effects of root herbivory by an insect on a foliar-feeding species, mediated through changes in the host plant. Oecologia **81**:38-42.

Gange, A. C., V. K. Brown, and G. S. Sinclair. 1994. Reduction of black vine weevil larval growth by vesicular-arbuscular mycorrhizal infection. Entomologia Experimentalis Et Applicata **70**:115-119.

Gange, A. C., R. Eschen, and V. Schroeder. 2012. The soil microbial community and plant foliar defences against insects. Pages 170-189 *in* G. R. Iason, M. Dicke, and S. E. Hartley, editors. The Ecology of Plant Secondary Metabolites: From Genes to Global Processes. Cambridge University Press, New York, U.S.A.

Gershenzon, J., A. Fontana, M. Burow, U. Wittstock, and J. Degenhardt. 2012. Mixtures of plant secondary metabolites: metabolic origins and ecological benefits. Pages 56-77 *in* G. R.

Iason, M. Dicke, and S. E. Hartley, editors. The Ecology of Plant Secondary Metabolites. Cambridge University Press, New York, U.S.A.

Givskov, M., R. DeNys, M. Manefield, L. Gram, R. Maximilien, L. Eberl, S. Molin, P. D. Steinberg, and S. Kjelleberg. 1996. Eukaryotic interference with homoserine lactone-mediated prokaryotic signaling. Journal of Bacteriology **178**:6618-6622.

Gols, R., C. Veenemans, R. P. J. Potting, H. M. Smid, M. Dicke, J. A. Harvey, and T. Bukovinszky. 2012. Variation in the specificity of plant volatiles and their use by a specialist and a generalist parasitoid. Animal Behaviour **83**:1231-1242.

Goodger, J. Q. D., R. M. Gleadow, and I. E. Woodrow. 2006. Growth cost and ontogenetic expression patterns of defence in cyanogenic *Eucalyptus* spp. Trees-Structure and Function **20**:757-765.

Grayer, R. J. and J. B. Harborne. 1994. A survey of antifungal compounds from higher-plants, 1982-1993. Phytochemistry **37**:19-42.

Guenoune, D., S. Galili, D. A. Phillips, H. Volpin, I. Chet, Y. Okon, and Y. Kapulnik. 2001. The defense response elicited by the pathogen *Rhizoctonia solani* is suppressed by colonization of the AM-fungus *Glomus intraradices*. Plant Science **160**:925-932.

Guo, X. S., L. M. Ding, R. J. Long, B. Qi, Z. H. Shang, Y. P. Wang, and X. Y. Cheng. 2012. Changes of chemical composition to high altitude results in *Kobresia littledalei* growing in alpine meadows with high feeding values for herbivores. Animal Feed Science and Technology **173**:186-193.

Gutbrodt, B., K. Mody, R. Wittwer, and S. Dorn. 2011. Within-plant distribution of induced resistance in apple seedlings: rapid acropetal and delayed basipetal responses. Planta **233**:1199-1207.

Haddad, N. M., G. M. Crutsinger, K. Gross, J. Haarstad, and D. Tilman. 2011. Plant diversity and the stability of foodwebs. Ecology Letters **14**:42-46.

Hagel, J. M. and P. J. Facchini. 2008. Plant metabolomics: analytical platforms and integration with functional genomics. Phytochemical Review **7**:479-497.

Halket, J. M., D. Waterman, A. M. Przyborowska, R. K. P. Patel, P. D. Fraser, and P. M. Bramley. 2005. Chemical derivatization and mass spectral libraries in metabolic profiling by GC/MS and LC/MS/MS. Journal of Experimental Botany **56**:219-243.

Halkier, B. A. and J. Gershenzon. 2006. Biology and biochemistry of glucosinolates. Annual Review of Plant Biology **57**:303-333.

Hall, R. D. 2006. Plant metabolomics: from holistic hope, to hype, to hot topic. New Phytologist **169**:453-468.

Hanley, M. E., B. B. Lamont, M. M. Fairbanks, and C. M. Rafferty. 2007. Plant structural traits and their role in anti-herbivore defence. Perspectives in Plant Ecology Evolution and Systematics **8**:157-178.

Haribal, M. and P. Feeny. 2003. Combined roles of contact stimulant and deterrents in assessment of host-plant quality by ovipositing zebra swallowtail butterflies. Journal of Chemical Ecology **29**:653-670.

Harper, J. L. and W. A. Wood. 1957. *Senecio jacobaea* L. Journal of Ecology **45**:617-637.

Harrison, S. and C. D. Thomas. 1991. Patchiness and spatial pattern in the insect community on ragwort *Senecio jacobaea*. Oikos **62**:5-12.

Hartley, S. E., R. Eschen, J. M. Horwood, L. A. Robinson, and E. M. Hill. 2012. Plant secondary metabolites and the interactions between plants and other organisms: the potential of a metabolomic approach.*in* G. R. Iason, M. Dicke, and S. E. Hartley, editors. The Ecology of Plant Secondary Metabolites: From Genes to Global Processes. Cambridge University Press, New York, U.S.A.

Hartley, S. E. and A. C. Gange. 2009. Impacts of plant symbiotic fungi on insect herbivores: mutualism in a multitrophic context. Annual Review of Entomology **54**:323-342.

Hartmann, T. and B. Dierich. 1998. Chemical diversity and variation of pyrrolizidine alkaloids of the senecionine type: biological need or coincidence? Planta **206**:443-451.

Hartmann, T., A. Ehmke, U. Eilert, K. Vonborstel, and C. Theuring. 1989. Sites of synthesis, translocation and accumulation of pyrrolizidine alkaloid N-oxides in *Senecio vulgaris* L. Planta **177**:98-107.

Hartmann, T. and G. Toppel. 1987. Senecionine N-oxide, the primary product of pyrrolizidine alkaloid biosynthesis in root cultures of *Senecio vulgaris*. Phytochemistry **26**:1639-1643.

Hartmann, T. and M. Zimmer. 1986. Organ-specific distribution and accumulation of pyrrolizidine alkaloids during the life-history of two annual *Senecio* species. Journal of Plant Physiology **122**:67-80.

Heasley, B. 2012. Chemical synthesis of the cardiotonic steroid glycosides and related natural products. Chemistry-a European Journal **18**:3092-3120.

Helgason, T., J. M. Merryweather, J. P. W. Young, and A. H. Fitter. 2007. Specificity and resilience in the arbuscular mycorrhizal fungi of a natural woodland community. Journal of Ecology **95**:623-630.

Hewitt, E. J. 1966. Sand and Water Culture Methods Used in the Study of Plant Nutrition. 2nd edition. CAB, Farnham Royal, U.K.

Hilker, M. and T. Meiners. 2006. Early herbivore alert: Insect eggs induce plant defense. Journal of Chemical Ecology **32**:1379-1397.

Hilker, M., C. Stein, R. Schroder, M. Varama, and R. Mumm. 2005. Insect egg deposition induces defence responses in *Pinus sylvestris*: characterisation of the elicitor. Journal of Experimental Biology **208**:1849-1854.

Hiltpold, I. and T. C. J. Turlings. 2012. Manipulation of chemically mediated interactions in agricultural soils to enhance the control of crop pests and to improve crop yield. Journal of Chemical Ecology **38**:641-650.

Hodge, A., C. D. Campbell, and A. H. Fitter. 2001. An arbuscular mycorrhizal fungus accelerates decomposition and acquires nitrogen directly from organic material. Nature **413**:297-299.

Hodge, A., T. Helgason, and A. H. Fitter. 2010. Nutritional ecology of arbuscular mycorrhizal fungi. Fungal Ecology **3**:267-273.

Hofmann, J., A. E. N. El Ashry, S. Anwar, A. Erban, J. Kopka, and F. Grundler. 2010. Metabolic profiling reveals local and systemic responses of host plants to nematode parasitism. Plant Journal **62**:1058-1071.

Hol, W. H. G. 2011. The effect of nutrients on pyrrolizidine alkaloids in *Senecio* plants and their interactions with herbivores and pathogens. Phytochemistry Reviews **10**:119-126.

Hol, W. H. G., M. Macel, J. A. van Veen, and E. van der Meijden. 2004. Root damage and aboveground herbivory change concentration and composition of pyrrolizidine alkaloids of *Senecio jacobaea*. Basic and Applied Ecology **5**:253-260.

Hol, W. H. G. and J. A. van Veen. 2002. Pyrrolizidine alkaloids from *Senecio jacobaea* affect fungal growth. Journal of Chemical Ecology **28**:1763-1772.

Hol, W. H. G., K. Vrieling, and J. A. van Veen. 2003. Nutrients decrease pyrrolizidine alkaloid concentrations in *Senecio jacobaea*. New Phytologist **158**:175-181.

Horiuchi, J., B. Prithiviraj, H. P. Bais, B. A. Kimball, and J. M. Vivanco. 2005. Soil nematodes mediate positive interactions between legume plants and rhizobium bacteria. Planta **222**:848-857.

Hou, C. T. and R. J. Forman. 2000. Growth inhibition of plant pathogenic fungi by hydroxy fatty acids. Journal of Industrial Microbiology & Biotechnology **24**:275-276.

Irwin, R. E., J. L. Bronstein, J. S. Manson, and L. Richardson. 2010. Nectar Robbing: Ecological and Evolutionary Perspectives. Annual Review of Ecology, Evolution and Systematics **41**:271-292.

Islam, Z. and M. J. Crawley. 1983. Compensation and regrowth in ragwort (*Senecio jacobaea*) attacked by cinnabar moth (*Tyria jacobaeae*). Journal of Ecology **71**:829-843.

Jacobsen, O. W. 1992. Factors affecting selection of nitrogen-fertilized grassland areas by breeding wigeon *Anas penelope*. Ornis Scandinavica **23**:121-131.

Jahnke, S., M. I. Menzel, D. van Dusschoten, G. W. Roeb, J. Buhler, S. Minwuyelet, P. Blumler, V. M. Temperton, T. Hombach, M. Streun, S. Beer, M. Khodaverdi, K. Ziemons, H. H. Coenen, and U. Schurr. 2009. Combined MRI-PET dissects dynamic changes in plant structures and functions. Plant Journal **59**:634-644.

Jaizme-Vega, M. C., P. Tenoury, J. Pinochet, and M. Jaumot. 1997. Interactions between the root-knot nematode Meloidogyne incognita and Glomus mosseae in banana. Plant and Soil **196**:27-35.

Jansen, J. J., J. W. Allwood, E. Marsden-Edwards, W. H. van der Putten, R. Goodacre, and N. M. van Dam. 2009. Metabolomic analysis of the interaction between plants and herbivores. Metabolomics **5**:150-161.

Janzen, D. H. 1977. Why don't ants visit flowers? Biotropica **9**:252-252.

Javot, H., N. Pumplin, and M. J. Harrison. 2007. Phosphate in the arbuscular mycorrhizal symbiosis: transport properties and regulatory roles. Plant Cell and Environment **30**:310-322.

Johns, R., D. T. Quiring, R. Lapointe, and C. J. Lucarotti. 2009. Foliage-age mixing within balsam fir increases the fitness of a generalist caterpillar. Ecological Entomology **34**:624-631.

Johnson, A. E. 1978. Tolerance of cattle to tansy ragwort (*Senecio jacobaea*). American Journal of Veterinary Research **39**:1542-1544.

Johnson, A. E., R. J. Molyneux, and G. B. Merrill. 1985. Chemistry of toxic range plants - variation in pyrrolizidine alkaloid content of *Senecio*, *Amsinckia*, and *Crotalaria* species. Journal of Agricultural and Food Chemistry **33**:50-55.

Johnson, A. E. and R. A. Smart. 1983. Effects on cattle and their calves of tansy ragwort (*Senecio jacobaea*) fed in early gestation. American Journal of Veterinary Research **44**:1215-1219.

Johnson, M. T. J. 2011. Evolutionary ecology of plant defences against herbivores. Functional Ecology **25**:305-311.

Johnson, S. N., P. D. Hallett, T. L. Gillespie, and C. Halpin. 2010. Below-ground herbivory and root toughness: a potential model system using lignin-modified tobacco. Physiological Entomology **35**:186-191.

Johnson, S. N. and U. N. Nielsen. 2012. Foraging in the dark - chemically mediated host plant location by belowground insect herbivores. Journal of Chemical Ecology **38**:604-614.

Jones, D. L., C. Nguyen, and R. D. Finlay. 2009. Carbon flow in the rhizosphere: carbon trading at the soil-root interface. Plant and Soil **321**:5-33.

Joosten, L., D. Cheng, P. P. J. Mulder, K. Vrieling, J. A. van Veen, and P. G. L. Klinkhamer. 2011. The genotype dependent presence of pyrrolizidine alkaloids as tertiary amine in *Jacobaea vulgaris*. Phytochemistry **72**:214-222.

Joosten, L., P. P. J. Mulder, P. G. L. Klinkhamer, and J. A. van Veen. 2009. Soil-borne microorganisms and soil-type affect pyrrolizidine alkaloids in *Jacobaea vulgaris*. Plant and Soil **325**:133-143.

Joosten, L., P. P. J. Mulder, K. Vrieling, J. A. van Veen, and P. G. L. Klinkhamer. 2010. The analysis of pyrrolizidine alkaloids in *Jacobaea vulgaris*; a comparison of extraction and detection methods. Phytochemical Analysis **21**:197-204.

Joosten, L. and J. A. van Veen. 2011. Defensive properties of pyrrolizidine alkaloids against microorganisms. Phytochemistry Reviews **10**:127-136.

Joshi, J. and K. Vrieling. 2005. The enemy release and EICA hypothesis revisited: incorporating the fundamental difference between specialist and generalist herbivores. Ecology Letters **8**:704-714.

Kabouw, P., A. Biere, W. H. van der Putten, and N. M. van Dam. 2010. Intra-specific differences in root and shoot glucosinolate profiles among white cabbage (*Brassica oleracea* var. capitata) cultivars. Journal of Agricultural and Food Chemistry **58**:411-417.

Kahl, J., D. H. Siemens, R. J. Aerts, R. Gabler, F. Kuhnemann, C. A. Preston, and I. T. Baldwin. 2000. Herbivore-induced ethylene suppresses a direct defense but not a putative indirect defense against an adapted herbivore. Planta **210**:336-342.

Kaplan, F., J. Kopka, D. W. Haskell, W. Zhao, K. C. Schiller, N. Gatzke, D. Y. Sung, and C. L. Guy. 2004. Exploring the temperature-stress metabolome of *Arabidopsis*. Plant Physiology **136**:4159-4168.

Kaplan, I., R. Halitschke, A. Kessler, S. Sardanelli, and R. F. Denno. 2008. Constitutive and induced defenses to herbivory in above- and belowground plant tissues. Ecology **89**:392-406.

Karasawa, T., A. Hodge, and A. H. Fitter. 2012. Growth, respiration and nutrient acquisition by the arbuscular mycorrhizal fungus *Glomus mosseae* and its host plant *Plantago lanceolata* in cooled soil. Plant Cell and Environment **35**:819-828.

Karban, R. and J. H. Myers. 1989. Induced plant-responses to herbivory. Annual Review of Ecology and Systematics **20**:331-348.

Kempel, A., A. K. Schmidt, R. Brandl, and M. Schaedler. 2010. Support from the underground: Induced plant resistance depends on arbuscular mycorrhizal fungi. Functional Ecology **24**:293-300.

Kessler, A. and I. T. Baldwin. 2001. Defensive function of herbivore-induced plant volatile emissions in nature. Science **291**:2141-2144.

Kim, H. K., Y. H. Choi, and R. Verpoorte. 2011. NMR-based plant metabolomics: where do we stand, where do we go? Trends in Biotechnology **29**:267-275.

Kim, J., J. F. Tooker, D. S. Luthe, C. M. De Moraes, and G. W. Felton. 2012. Insect eggs can enhance wound response in plants: a study system of romato *Solanum lycopersicum* L. and *Helicoverpa zea* Boddie. Plos One **7**:e37420.

Kimball, B. A., J. H. Russell, and P. K. Ott. 2012. Phytochemical variation within a single plant species influences foraging behavior of deer. Oikos **121**:743-751.

Kirk, H., Y. H. Choi, H. K. Kim, R. Verpoorte, and E. van der Meijden. 2005. Comparing metabolomes: the chemical consequences of hybridization in plants. New Phytologist **167**:613-622.

Klingner, A., H. Bothe, V. Wray, and F. J. Marner. 1995a. Identification of a yellow pigment formed in maize roots upon mycorrhizal colonization. Phytochemistry **38**:53-55.

Klingner, A., B. Hundeshagen, H. Kernebeck, and H. Bothe. 1995b. Localization of the yellow pigment formed in roots of gramineous plant colonized by arbuscular fungi. Protoplasma **185**:50-57.

Koekemoer, M. J. and F. L. Warren. 1951. The *Senecio* alkaloids. 8. The occurrence and preparation of the N-oxides - an improved method of extraction of the *Senecio* alkaloids. Journal of the Chemical Society:66-68.

Koricheva, J. 1999. Interpreting phenotypic variation in plant allelochemistry: problems with the use of concentrations. Oecologia **119**:467-473.

Koricheva, J. 2002. Meta-analysis of sources of variation in fitness costs of plant antiherbivore defenses. Ecology **83**:176-190.

Koricheva, J., A. C. Gange, and T. Jones. 2009. Effects of mycorrhizal fungi on insect herbivores: a meta-analysis. Ecology **90**:2088-2097.

Kosslak, R. M., R. Bookland, J. Barkei, H. E. Paaren, and E. R. Appelbaum. 1987. Induction of *Bradyrhizobium japonicum* common nod genes by isoflavones isolated from *Glycine max*. Proceedings of the National Academy of Sciences of the United States of America **84**:7428-7432.

Kosslak, R. M., R. S. Joshi, B. A. Bowen, H. E. Paaren, and E. R. Appelbaum. 1990. Strain-specific inhibition of NOD gene induction in *Bradyrhizobium japonicum* by flavanoid compounds. Applied and Environmental Microbiology **56**:1333-1341.

Kostenko, O., T. F. J. van de Voorde, P. P. J. Mulder, W. H. van der Putten, and T. M. Bezemer. 2012. Legacy effects of aboveground-belowground interactions. Ecology Letters **15**:813-821.

Kowalchuk, G. A., W. H. G. Hol, and J. A. van Veen. 2006. Rhizosphere fungal communities are influenced by *Senecio jacobaea* pyrrolizidine alkaloid content and composition. Soil Biology & Biochemistry **38**:2852-2859.

Kunin, W. E. 1999. Patterns of herbivore incidence on experimental arrays and field populations of ragwort, *Senecio jacobaea*. Oikos **84**:515-525.

Kurppa, S. and T. C. Vrain. 1985. Penetration and feeding behaviour of *Pratylenchus penetrans* in strawberry roots. Revue de Nematologie **8**:273-276.

Kutywayo, V. and T. H. Been. 2006. Host status of six major weeds to *Meloidogyne chitwoodi* and *Pratylenchus penetrans*, including a preliminary field survey concerning other weeds. Nematology **8**:647-657.

Kyndt, T., K. Nahar, A. Haegeman, D. De Vleesschauwer, M. Hofte, and G. Gheysen. 2012. Comparing systemic defence-related gene expression changes upon migratory and sedentary nematode attack in rice. Plant Biology **14**:73-82.

Lajide, L., P. Escoubas, and J. Mizutani. 1996. Cyclohexadienones-insect growth inhibitors from the foliar surface and tissue extracts of *Senecio cannabifolius*. Experientia **52**:259-263.

Lambdon, P. W., M. Hassall, R. R. Boar, and R. Mithen. 2003. Asynchrony in the nitrogen and glucosinolate leaf-age profiles of *Brassica*: is this a defensive strategy against generalist herbivores? Agriculture Ecosystems & Environment **97**:205-214.

Langenheim, J. H. 1994. Higher plant terpenoids - a phytocentric overview of their ecological roles. Journal of Chemical Ecology **20**:1223-1280.

Lankau, R. A. 2007. Specialist and generalist herbivores exert opposing selection on a chemical defense. New Phytologist **175**:176-184.

Larose, G., R. Chenevert, P. Moutoglis, S. Gagne, Y. Piche, and H. Vierheilig. 2002. Flavonoid levels in roots of *Medicago sativa* are modulated by the developmental stage of the symbiosis and the root colonizing arbuscular mycorrhizal fungus. Journal of Plant Physiology **159**:1329-1339.

Lee, K. C., M. W. Cheuk, W. Chan, A. W. M. Lee, Z. Z. Zhao, Z. H. Jiang, and Z. W. Cai. 2006. Determination of glucosinolates in traditional Chinese herbs by high-performance liquid chromatography and electrospray ionization mass spectrometry. Analytical and Bioanalytical Chemistry **386**:2225-2232.

Leiss, K. A. 2011. Management practices for control of ragwort species. Phytochemistry Reviews **10**:153-163.

Leiss, K. A., Y. H. Choi, I. B. Abdel-Farid, R. Verpoorte, and P. G. L. Klinkhamer. 2009a. NMR metabolomics of thrips (*Frankliniella occidentalis*) resistance in *Senecio* hybrids. Journal of Chemical Ecology **35**:1-11.

Leiss, K. A., F. Maltese, Y. H. Choi, R. Verpoorte, and P. G. L. Klinkhamer. 2009b. Identification of chlorogenic acid as a resistance factor for thrips in chrysanthemum. Plant Physiology **150**:1567-1575.

Levin, D. A. 1973. Role of trichromes in plant defense. Quarterly Review of Biology **48**:3-15.

Li, A. R., S. E. Smith, F. A. Smith, and K. Y. Guan. 2012. Inoculation with arbuscular mycorrhizal fungi suppresses initiation of haustoria in the root hemiparasite *Pedicularis tricolor*. Annals of Botany **109**:1075-1080.

Li, H. Y., G. D. Yang, H. R. Shu, Y. T. Yang, B. X. Ye, I. Nishida, and C. C. Zheng. 2006. Colonization by the arbuscular mycorrhizal fungus *Glomus versiforme* induces a defense response against the root-knot nematode *Meloidogyne incognita* in the grapevine (*Vitis amurensis* Rupr.), which includes transcriptional activation of the class III chitinase gene VCH3. Plant and Cell Physiology **47**:154-163.

Liland, K. H. 2011. Multivariate methods in metabolomics - from pre-processing to dimension reduction and statistical analysis. Trac-Trends in Analytical Chemistry **30**:827-841.

Lin, G., K. Y. Zhou, X. G. Zhao, Z. T. Wang, and P. P. H. But. 1998. Determination of hepatotoxic pyrrolizidine alkaloids by on-line high performance liquid chromatography mass spectrometry with an electrospray interface. Rapid Communications in Mass Spectrometry **12**:1445-1456.

Lohmann, M., S. Scheu, and C. Muller. 2009. Decomposers and root feeders interactively affect plant defence in *Sinapis alba*. Oecologia **160**:289-298.

Lohse, S., W. Schliemann, C. Ammer, J. Kopka, D. Strack, and T. Fester. 2005. Organization and metabolism of plastids and mitochondria in arbuscular mycorrhizal roots of *Medicago truncatula*. Plant Physiology **139**:329-340.

Lopez-Raez, J. A., T. Charnikhova, I. Fernandez, H. Bouwmeester, and M. J. Pozo. 2011. Arbuscular mycorrhizal symbiosis decreases strigolactone production in tomato. Journal of Plant Physiology **168**:294-297.

Luthy, J., U. Zweifel, B. Karlhuber, and C. Schlatter. 1981. Pyrrolizidine alkaloids of *Senecio alpinus* L and their detection in feedingstuffs. Journal of Agricultural and Food Chemistry **29**:302-305.

Macel, M., M. Bruinsma, S. M. Dijkstra, T. Ooijendijk, H. M. Niemeyer, and P. G. L. Klinkhamer. 2005. Differences in effects of pyrrolizidine alkaloids on five generalist insect herbivore species. Journal of Chemical Ecology **31**:1493-1508.

Macel, M. and P. G. L. Klinkhamer. 2010. Chemotype of *Senecio jacobaea* affects damage by pathogens and insect herbivores in the field. Evolutionary Ecology **24**:237-250.

Macel, M., P. G. L. Klinkhamer, K. Vrieling, and E. van der Meijden. 2002. Diversity of pyrrolizidine alkaloids in *Senecio* species does not affect the specialist herbivore *Tyria jacobaeae*. Oecologia **133**:541-550.

Macel, M., N. M. van Dam, and J. J. B. Keurentjes. 2010. Metabolomics: the chemistry between ecology and genetics. Molecular Ecology Resources **10**:583-593.

Macel, M. and K. Vrieling. 2003. Pyrrolizidine alkaloids as oviposition stimulants for the cinnabar moth, *Tyria jacobaeae*. Journal of Chemical Ecology **29**:1435-1446.

Macel, M., K. Vrieling, and P. G. L. Klinkhamer. 2004. Variation in pyrrolizidine alkaloid patterns of *Senecio jacobaea*. Phytochemistry **65**:865-873.

Maier, W., H. Peipp, J. Schmidt, V. Wray, and D. Strack. 1995. Levels of a terpenoid glycoside (blumenin) and cell wall-bound phenolics in some cereal mycorrhizas. Plant Physiology **109**:465-470.

Maier, W., J. Schmidt, M. Nimtz, V. Wray, and D. Strack. 2000. Secondary products in mycorrhizal roots of tobacco and tomato. Phytochemistry **54**:473-479.

Marquis, R. J. 1984. Leaf herbivores decrease fitness of a tropical plant. Science **226**:537-539.

Masters, G. J. 1995. The impact of root herbivory on aphid performance - field and laboratory evidence. Acta Oecologica-International Journal of Ecology **16**:135-142.

Masters, G. J. and V. K. Brown. 1992. Plant-mediated interactions between two spatially separated insects. Functional Ecology **6**:175-179.

Masters, G. J., V. K. Brown, and A. C. Gange. 1993. Plant mediated interactions between aboveground and belowground insect herbivores. Oikos **66**:148-151.

Masters, G. J., T. H. Jones, and M. Rogers. 2001. Host-plant mediated effects of root herbivory on insect seed predators and their parasitoids. Oecologia **127**:246-250.

Mattiacci, L., M. Dicke, and M. A. Posthumus. 1995. Beta-glucosidase - An elicitor of herbivore-induced plant odor that attracts host-searching parasitic wasps Proceedings of the National Academy of Sciences of the United States of America **92**:2036-2040.

Mattocks, A. R. 1986. Chapter 2: Extraction, separation and analysis of pyrrolizidine alkaloids. Chemistry and Toxicology of Pyrrolizidine Alkaloids. Academic Press Inc., London.

Mattson, W. J. 1980. Herbivory in relation to plant nitrogen-content. Annual Review of Ecology and Systematics **11**:119-161.

McCall, A. C. and J. A. Fordyce. 2010. Can optimal defence theory be used to predict the distribution of plant chemical defences? Journal of Ecology **98**:985-992.

McEvoy, P. B. 1984. Dormancy and dispersal in dimorphic achenes of tansy ragwort, *Senecio jacobaea* L (Compositae). Oecologia **61**:160-168.

McEvoy, P. B., N. T. Rudd, C. S. Cox, and M. Huso. 1993. Disturbance, competition and herbivory effects on ragwort *Senecio jacobaea* populations. Ecological Monographs **63**:55-75.

McGonigle, T. P., M. H. Miller, D. G. Evans, G. L. Fairchild, and J. A. Swan. 1990. A new method which gives an objective measure of colonization of roots by vesicular-arbuscular mycorrhizal fungi. New Phytologist **115**:495-501.

McKey, D. 1974. Adaptive patterns in alkaloid physiology. American Naturalist **108**:305-320.

Meiners, T. and M. Hilker. 1997. Host location in *Oomyzus gallerucae* (Hymenoptera: Eulophidae), an egg parasitoid of the elm leaf beetle *Xanthogaleruca luteola* (Coleoptera: Chrysomelidae). Oecologia **112**:87-93.

Mendel, V. E., M. R. Witt, B. S. Gitchell, D. N. Gribble, Q. R. Rogers, H. J. Segall, and H. D. Knight. 1988. Pyrrolizidine alkaloid induced liver disease in horses - an early diagnosis. American Journal of Veterinary Research **49**:572-578.

Milewski, A. V., T. P. Young, and D. Madden. 1991. Thorns as induced defences - experimental evidence. Oecologia **86**:70-75.

Mirnezhad, M., R. R. Romero-Gonzalez, K. A. Leiss, Y. H. Choi, R. Verpoorte, and P. G. L. Klinkhamer. 2010. Metabolomic analysis of host plant resistance to thrips in wild and cultivated tomatoes. Phytochemical Analysis **21**:110-117.

Mitter, C., B. Farrell, and D. J. Futuyma. 1991. Phylogenetic studies of insect plant interaction - insights into the genesis of diversity. Trends in Ecology & Evolution **6**:290-293.

Moco, S., R. J. Bino, R. C. H. De Vos, and J. Vervoort. 2007. Metabolomics technologies and metabolite identification. Trac-Trends in Analytical Chemistry **26**:855-866.

Moran, N. A. and T. G. Whitham. 1990. Interspecific competition between root-feeding and leaf-galling aphids mediated by host-plant resistance. Ecology **71**:1050-1058.

Morandi, D. 1996. Occurrence of phytoalexins and phenolic compounds in endomycorrhizal interactions, and their potential role in biological control. Plant and Soil **185**:241-251.

Moreira, X., R. Zas, and L. Sampedro. 2012. Differential allocation of constitutive and induced chemical defenses in pine tree juveniles: A test of the optimal defense theory. Plos One **7**:e34006.

Myers, J. H. 1980. Is the insect or the plant the driving force in the cinnabar moth - tansy ragwort system. Oecologia **47**:16-21.

Narberhaus, I., C. Theuring, T. Hartmann, and S. Dobler. 2003. Uptake and metabolism of pyrrolizidine alkaloids in *Longitarsus* flea beetles (Coleoptera : Chrysomelidae) adapted and non-adapted to alkaloid-containing host plants. Journal of Comparative Physiology B-Biochemical Systemic and Environmental Physiology **173**:483-491.

Narberhaus, I., V. Zintgraf, and S. Dobler. 2005. Pyrrolizidine alkaloids on three trophic levels - evidence for toxic and deterrent effects on phytophages and predators. Chemoecology **15**:121-125.

Niggeweg, R., A. J. Michael, and C. Martin. 2004. Engineering plants with increased levels of the antioxidant chlorogenic acid. Nature Biotechnology **22**:746-754.

Nuringtyas, T. R., Y. H. Choi, R. Verpoorte, P. G. L. Klinkhamer, and K. A. Leiss. 2012. Differential tissue distribution of metabolites in *Jacobaea vulgaris*, *Jacobaea aquatica* and their crosses. Phytochemistry **78**:89-97.

Ohgushi, T. 2005. Indirect interaction webs: Herbivore-induced effects through trait change in plants. Annual Review of Ecology Evolution and Systematics **36**:81-105.

Ohnmeiss, T. E. and I. T. Baldwin. 2000. Optimal defense theory predicts the ontogeny of an induced nicotine defense. Ecology **81**:1765-1783.

Oliver, J. E., R. P. Doss, R. T. Williamson, J. R. Carney, and E. D. DeVilbiss. 2000. Bruchins-mitogenic 3-(hydroxypropanoyl) esters of long chain diols from weevils of the bruchidae. Tetrahedron **56**:7633-7641.

Oliver, S. G., M. K. Winson, D. B. Kell, and F. Baganz. 1998. Systematic functional analysis of the yeast genome. Trends in Biotechnology **16**:373-378.

Onyilagha, J. C., J. Lazorko, M. Y. Gruber, J. J. Soroka, and M. A. Erlandson. 2004. Effect of flavonoids on feeding preference and development of the crucifer pest *Mamestra configurata* Walker. Journal of Chemical Ecology **30**:109-124.

Oyekan, P. O., C. D. Blake, and J. E. Mitchell. 1972. Histopathology of pea roots axenically infected by *Pratylenchus penetrans*. Journal of Nematology **4**:32-35.

Palmer, T. M., M. L. Stanton, T. P. Young, J. R. Goheen, R. M. Pringle, and R. Karban. 2008. Breakdown of an ant-plant mutualism follows the loss of large herbivores from an African Savanna. Science **319**:192-195.

Pandya, S., P. Iyer, V. Gaitonde, T. Parekh, and A. Desai. 1999. Chemotaxis of rhizobium SP.S2 towards *Cajanus cajan* root exudate and its major components. Current Microbiology **38**:205-209.

Parker, C. E., S. Verma, K. B. Tomer, R. L. Reed, and D. R. Buhler. 1990. Determination of *Senecio* alkaloids by thermospray liquid-chromatography mass-spectrometry. Biomedical and Environmental Mass Spectrometry **19**:1-12.

Parker, D., M. Beckmann, H. Zubair, D. P. Enot, Z. Caracuel-Rios, D. P. Overy, S. Snowdon, N. J. Talbot, and J. Draper. 2009. Metabolomic analysis reveals a common pattern of metabolic re-programming during invasion of three host plant species by *Magnaporthe grisea*. Plant Journal **59**:723-737.

Parniske, M. 2008. Arbuscular mycorrhiza: the mother of plant root endosymbioses. Nature Reviews Microbiology **6**:763-775.

Pauli, G. F. 2001. qNMR - A versatile concept for the validation of natural product reference compounds. Phytochemical Analysis **12**:28-42.

Pawlak-Sprada, S., M. Stobiecki, and J. Deckert. 2011. Activation of phenylpropanoid pathway in legume plants exposed to heavy metals. Part II. Profiling of isoflavonoids and their glycoconjugates induced in roots of lupine (*Lupinus luteus*) seedlings treated with cadmium and lead. Acta Biochimica Polonica **58**:217-223.

Peipp, H., W. Maier, J. Schmidt, V. Wray, and D. Strack. 1997. Arbuscular mycorrhizal fungus-induced changes in the accumulation of secondary compounds in barley roots. Phytochemistry **44**:581-587.

Perret, X., C. Staehelin, and W. J. Broughton. 2000. Molecular basis of symbiotic promiscuity. Microbiology and Molecular Biology Reviews **64**:180-201.

Pichersky, E. and D. R. Gang. 2000. Genetics and biochemistry of secondary metabolites in plants: an evolutionary perspective. Trends in Plant Science **5**:439-445.

Pinochet, J., C. Calvet, A. Camprubi, and C. Fernandez. 1995. Growth and nutritional response of Nemared peach rootstock infected with *Pratylenchus vulnus* and the mycorrhizal fungus *Glomus mosseae*. Fundamental and Applied Nematology **18**:205-210.

Potter, K. J. B., J. E. Ireson, and G. R. Allen. 2004. Oviposition of the ragwort flea beetle, *Longitarsus flavicornis* (Stephens) (Coleoptera : Chrysomelidae), in relation to the phenology of ragwort, *Senecio jacobaea* L. (Asteraceae). Biological Control **30**:404-409.

Potter, M. J., V. A. Vanstone, K. A. Davies, J. A. Kirkegaard, and A. J. Rathjen. 1999. Reduced susceptibility of *Brassica napus* to *Pratylenchus neglectus* in plants with elevated root levels of 2-phenylethyl glucosinolate. Journal of Nematology **31**:291-298.

Pozo, M. J. and C. Azcon-Aguilar. 2007. Unraveling mycorrhiza-induced resistance. Current Opinion in Plant Biology **10**:393-398.

Praz, C. J., A. Mueller, and S. Dorn. 2008. Specialized bees fail to develop on non-host pollen: Do plants chemically protect their pollen? Ecology **89**:795-804.

Qi, X. Y., S. F. Wang, B. Wu, and H. B. Qu. 2009a. Determination of hepatotoxic pyrrolizidine alkaloids in *Gynura segetum* by MEKC. Chromatographia **70**:281-285.

Qi, X. Y., B. Wu, Y. Y. Cheng, and H. B. Qu. 2009b. Simultaneous characterization of pyrrolizidine alkaloids and N-oxides in *Gynura segetum* by liquid chromatography/ion trap mass spectrometry. Rapid Communications in Mass Spectrometry **23**:291-302.

Quintero, C. and M. D. Bowers. 2011. Plant induced defenses depend more on plant age than previous history of damage: implications for plant-herbivore interactions. Journal of Chemical Ecology **37**:992-1001.

Quintero, C. and M. D. Bowers. 2012. Changes in plant chemical defenses and nutritional quality as a function of ontogeny in *Plantago lanceolata* (Plantaginaceae). Oecologia **168**:471-481.

Rasmann, S. and A. A. Agrawal. 2008. In defense of roots: A research agenda for studying plant resistance to belowground herbivory. Plant Physiology **146**:875-880.

Rasmann, S., A. C. Erwin, R. Halitschke, and A. A. Agrawal. 2011. Direct and indirect root defences of milkweed (*Asclepias syriaca*): trophic cascades, trade-offs and novel methods for studying subterranean herbivory. Journal of Ecology **99**:16-25.

Rasmann, S., T. G. Kollner, J. Degenhardt, I. Hiltpold, S. Toepfer, U. Kuhlmann, J. Gershenzon, and T. C. J. Turlings. 2005. Recruitment of entomopathogenic nematodes by insect-damaged maize roots. Nature **434**:732-737.

Reidinger, S., R. Eschen, A. C. Gange, P. Finch, and T. M. Bezemer. 2012. Arbuscular mycorrhizal colonization, plant chemistry, and aboveground herbivory on *Senecio jacobaea*. Acta Oecologica-International Journal of Ecology **38**:8-16.

Reinhard, A., M. Janke, W. von der Ohe, M. Kempf, C. Theuring, T. Hartmann, P. Schreier, and T. Beuerle. 2009. Feeding deterrence and detrimental effects of pyrrolizidine alkaloids fed to Honey Bees (*Apis mellifera*). Journal of Chemical Ecology **35**:1086-1095.

Reymond, P., H. Weber, M. Damond, and E. E. Farmer. 2000. Differential gene expression in response to mechanical wounding and insect feeding in *Arabidopsis*. Plant Cell **12**:707-719.

Rhoades, D. F. and J. C. Bergdahl. 1981. Adaptive significance of toxic nectar. American Naturalist **117**:798-803.

Rhodes, D. F. and R. G. Cates. 1976. Toward a general theory of plant antiherbivore chemistry. Pages 168-213 *in* J. W. Wallace and R. L. Mansell, editors. Recent Advances in Phytochemistry. Plenum Press, New York, U.S.A.

Riely, B. K., J. M. Ane, R. V. Penmetsa, and D. R. Cook. 2004. Genetic and genomic analysis in model legumes bring Nod-factor signaling to center stage. Current Opinion in Plant Biology **7**:408-413.

Robert, C. A. M., N. Veyrat, G. Glauser, G. Marti, G. R. Doyen, N. Villard, M. D. P. Gaillard, T. G. Koellner, D. Giron, M. Body, B. A. Babst, R. A. Ferrieri, T. C. J. Turlings, and M. Erb. 2012. A specialist root herbivore exploits defensive metabolites to locate nutritious tissues. Ecology Letters **15**:55-64.

Roberts, P. D. and A. S. Pullin. 2007. The effectiveness of management interventions used to control ragwort species. Environmental Management **39**:691-706.

Rodriguez-Echeverria, S., E. de la Pena, M. Moens, H. Freitas, and W. H. van der Putten. 2009. Can root-feeders alter the composition of AMF communities? Experimental evidence from the dune grass *Ammophila arenaria*. Basic and Applied Ecology **10**:131-140.

Roeder, E. 1999. Analysis of pyrrolizidine alkaloids. Current Organic Chemistry **3**:557-576.

Rohde, R. A. 1972. Expression of resistance in plants to nematodes. Annual Review of Phytopathology **10**:233-252.

Rösemann, G. M. 2006. Analysis of pyrrolizidine alkaloids in *Crotalatia* species by HPLC-MS/MS in order to evaluate related food health risks. University of Pretoria.

Roslin, T. and J. P. Salminen. 2008. Specialization pays off: contrasting effects of two types of tannins on oak specialist and generalist moth species. Oikos **117**:1560-1568.

Ruiz-Sanchez, M., E. Armada, Y. Munoz, I. E. G. de Salamone, R. Aroca, J. M. Ruiz-Lozano, and R. Azcon. 2011. *Azospirillum* and arbuscular mycorrhizal colonization enhance rice

growth and physiological traits under well-watered and drought conditions. Journal of Plant Physiology **168**:1031-1037.

Sana, T. R., S. Fischer, G. Wohlgemuth, A. Katrekar, K. H. Jung, P. C. Ronald, and O. Fiehn. 2010. Metabolomic and transcriptomic analysis of the rice response to the bacterial blight pathogen *Xanthomonas oryzae* pv. oryzae. Metabolomics **6**:451-465.

Sanchez, D. H., M. R. Siahpoosh, U. Roessner, M. Udvardi, and J. Kopka. 2008. Plant metabolomics reveals conserved and divergent metabolic responses to salinity. Physiologia Plantarum **132**:209-219.

Sanders, F. E., P. B. Tinker, R. L. B. Black, and S. M. Palmerley. 1977. Development of endomycorrhizal root systems. 1. Spread of infection and growth-promoting effects with 4 species of vesicular-arbuscular endophyte. New Phytologist **78**:257-268.

Schafer, M., C. Fischer, S. Meldau, E. Seebald, R. Oelmuller, and I. T. Baldwin. 2011. Lipase activity in insect oral secretions mediates defense responses in *Arabidopsis*. Plant Physiology **156**:1520-1534.

Schaffner, U., K. Vrieling, and E. van der Meijden. 2003. Pyrrolizidine alkaloid content in *Senecio*: ontogeny and developmental constraints. Chemoecology **13**:39-46.

Schliemann, W., C. Ammer, and D. Strack. 2008a. Metabolite profiling of mycorrhizal roots of *Medicago truncatula*. Phytochemistry **69**:112-146.

Schliemann, W., B. Kolbe, J. Schmidt, M. Nimtz, and V. Wray. 2008b. Accumulation of apocarotenoids in mycorrhizal roots of leek (*Allium porrum*). Phytochemistry **69**:1680-1688.

Schliemann, W., J. Schmidt, M. Nimtz, V. Wray, T. Fester, and D. Strack. 2006. Accumulation of apocarotenoids in mycorrhizal roots of *Ornithogalum umbellatum*. Phytochemistry **67**:1196-1205.

Schmelz, E. A., M. J. Carroll, S. LeClere, S. M. Phipps, J. Meredith, P. S. Chourey, H. T. Alborn, and P. E. A. Teal. 2006. Fragments of ATP synthase mediate plant perception of insect attack. Proceedings of the National Academy of Sciences of the United States of America **103**:8894-8899.

Schmelz, E. A., R. J. Grebenok, D. W. Galbraith, and W. S. Bowers. 1999. Insect-induced synthesis of phytoecdysteroids in spinach, Spinacia oleracea. Journal of Chemical Ecology **25**:1739-1757.

Schmelz, E. A., R. J. Grebenok, T. E. Ohnmeiss, and W. S. Bowers. 2002. Interactions between *Spinacia oleracea* and *Bradysia impatiens*: A role for phytoecdysteroids. Archives of Insect Biochemistry and Physiology **51**:204-221.

Schroeder, F. C., M. L. del Campo, J. B. Grant, D. B. Weibel, S. R. Smedley, K. L. Bolton, J. Meinwald, and T. Eisner. 2006. Pinoresinol: A lignol of plant origin serving for defense in a caterpillar. Proceedings of the National Academy of Sciences of the United States of America **103**:15497-15501.

Schwartz, S. H., X. Q. Qin, and J. A. D. Zeevaart. 2001. Characterization of a novel carotenoid cleavage dioxygenase from plants. Journal of Biological Chemistry **276**:25208-25211.

Shapiro, A. M. and J. E. DeVay. 1987. Hypersensivity reaction of *Brassica nigra* L. (Cruciferae) kills eggs of *Pieris* butterflies (Lepidoptera, Pieridae). Oecologia **71**:631-632.

Sharma, S., S. Sharma, F. J. Kopisch-Obuch, T. Keil, E. Laubach, N. Stein, A. Graner, and C. Jung. 2011. QTL analysis of root-lesion nematode resistance in barley: 1. *Pratylenchus neglectus*. Theoretical and Applied Genetics **122**:1321-1330.

Smallegange, R. C., J. J. A. van Loon, S. E. Blatt, J. A. Harvey, N. Agerbirk, and M. Dicke. 2007. Flower vs. leaf feeding by *Pieris brassicae*: Glucosinolate-rich flower tissues are preferred and sustain higher growth rate. Journal of Chemical Ecology **33**:1831-1844.

Soler, R., T. M. Bezemer, A. M. Cortesero, W. H. van der Putten, L. E. M. Vet, and J. A. Harvey. 2007a. Impact of foliar herbivory on the development of a root-feeding insect and its parasitoid. Oecologia **152**:257-264.

Soler, R., T. M. Bezemer, W. H. van der Putten, L. E. M. Vet, and J. A. Harvey. 2005. Root herbivore effects on above-ground herbivore, parasitoid and hyperparasitoid performance via changes in plant quality. Journal of Animal Ecology **74**:1121-1130.

Soler, R., J. A. Harvey, and T. M. Bezemer. 2007b. Foraging efficiency of a parasitoid of a leaf herbivore is influenced by root herbivory on neighbouring plants. Functional Ecology **21**:969-974.

Soler, R., J. A. Harvey, A. F. D. Kamp, L. E. M. Vet, W. H. van der Putten, N. M. van Dam, J. F. Stuefer, R. Gols, C. A. Hordijk, and T. M. Bezemer. 2007c. Root herbivores influence the behaviour of an aboveground parasitoid through changes in plant-volatile signals. Oikos **116**:367-376.

Soler, R., W. H. Van der Putten, J. A. Harvey, L. E. M. Vet, M. Dicke, and T. M. Bezemer. 2012. Root herbivore effects on aboveground multitrophic interactions: patterns, processes and mechanisms. Journal of Chemical Ecology **38**:755-767.

Soriano, I. R., I. T. Riley, M. J. Potter, and W. S. Bowers. 2004. Phytoecdysteroids: A novel defense against plant-parasitic nematodes. Journal of Chemical Ecology **30**:1885-1899.

Stamp, N. 2003. Out of the quagmire of plant defense hypotheses. Quarterly Review of Biology **78**:23-55.

Steinbrenner, A. D., S. Gomez, S. Osorio, A. R. Fernie, and C. M. Orians. 2011. Herbivore-induced changes in tomato (*Solanum lycopersicum*) primary metabolism: A whole plant perspective. Journal of Chemical Ecology **37**:1294-1303.

Stephenson, A. G. 1982. Iridoid glycosides in the nectar of *Catalpa speciosa* are unpalatable to nectar thieves. Journal of Chemical Ecology **8**:1025-1034.

Strack, D. and T. Fester. 2006. Isoprenoid metabolism and plastid reorganization in arbuscular mycorrhizal roots. New Phytologist **172**:22-34.

Strack, D., T. Fester, B. Hause, W. Schliemann, and M. H. Walter. 2003. Arbuscular mycorrhiza: Biological, chemical, and molecular aspects. Journal of Chemical Ecology **29**:1955-1979.

Strauss, S. Y., R. E. Irwin, and V. M. Lambrix. 2004. Optimal defence theory and flower petal colour predict variation in the secondary chemistry of wild radish. Journal of Ecology **92**:132-141.

Sumner, L. W., P. Mendes, and R. A. Dixon. 2003. Plant metabolomics: large-scale phytochemistry in the functional genomics era. Phytochemistry **62**:817-836.

Suter, M., S. Siegrist-Maag, J. Connolly, and A. Luscher. 2007. Can the occurrence of *Senecio jacobaea* be influenced by management practice? Weed Research **47**:262-269.

Tamagnone, L., A. Merida, N. Stacey, K. Plaskitt, A. Parr, C. F. Chang, D. Lynn, J. M. Dow, K. Roberts, and C. Martin. 1998. Inhibition of phenolic acid metabolism results in precocious cell death and altered cell morphology in leaves of transgenic tobacco plants. Plant Cell **10**:1801-1816.

Taylor, J. and L. A. Harrier. 2003. Expression studies of plant genes differentially expressed in leaf and root tissues of tomato colonised by the arbuscular mycorrhizal fungus *Glomus mosseae*. Plant Molecular Biology **51**:619-629.

Teplitski, M. I., J. B. Robinson, and W. D. Bauer. 2000. Plants secrete substances that mimic bacterial N-acyl homoserine lactone signal activities and affect population density-dependant behavious in associated bacteria. The American Phytopathological Society **13**:637-648.

Thoden, T. C. and M. Boppre. 2010. Plants producing pyrrolizidine alkaloids: sustainable tools for nematode management? Nematology **12**:1-24.

Thoden, T. C., M. Boppre, and J. Hallmann. 2007. Pyrrolizidine alkaloids of *Chromoldena odorata* act as nematicidal agents and reduce infection of lettuce roots by *Meloidogyne incognita*. Nematology **9**:343-349.

Thoden, T. C., M. Boppre, and J. Hallmann. 2009a. Effects of pyrrolizidine alkaloids on the performance of plant-parasitic and free-living nematodes. Pest Management Science **65**:823-830.

Thoden, T. C., J. Hallmann, and M. Boppre. 2009b. Effects of plants containing pyrrolizidine alkaloids on the northern root-knot nematode *Meloidogyne hapla*. European Journal of Plant Pathology **123**:27-36.

Thoison, O., T. Sevenet, H. M. Niemeyer, and G. B. Russell. 2004. Insect antifeedant compounds from *Nothofagus dombeyi* and *N. pumilio*. Phytochemistry **65**:2173-2176.

Toppel, G., L. Witte, B. Riebesehl, K. von Borstel, and T. Hartmann. 1987. Alkaloid patterns and biosynthetic capacity of root cultures from some pyrrolizidine alkaloid producing *Senecio* species. Plant Cell Reports **6**:466-469.

Toth, R. and R. M. Miller. 1984. Dynamics of abuscule development and degeneration in a *Zea mays* mycorrhiza. American Journal of Botany **71**:449-460.

Toussaint, J. P., F. A. Smith, and S. E. Smith. 2007. Arbuscular mycorrhizal fungi can induce the production of phytochemicals in sweet basil irrespective of phosphorus nutrition. Mycorrhiza **17**:291-297.

Treutter, D. 2005. Significance of flavonoids in plant resistance and enhancement of their biosynthesis. Plant Biology **7**:581-591.

Troelstra, S. R., R. Wagenaar, W. Smant, and B. A. M. Peters. 2001. Interpretation of bioassays in the study of interactions between soil organisms and plants: involvement of nutrient factors. New Phytologist **150**:697-706.

Trygg, J. and S. Wold. 2002. Orthogonal projections to latent structures (O-PLS). Journal of Chemometrics **16**:119-128.

Turlings, T. C. J., P. J. McCall, H. T. Alborn, and J. H. Tumlinson. 1993. An elicitor in caterpillar oral secretions that induces corn seedlings to emit chemical signals attractive to parasitic wasps. Journal of Chemical Ecology **19**:411-425.

Turlings, T. C. J., J. H. Tumlinson, and W. J. Lewis. 1990. Exploitation of herbivore-induced plant odors by host-seeking parasitic wasps. Science **250**:1251-1253.

van Bezooijen, J. 2006. Methods and Techniques for Nematology, Department of Nematology, Plant Sciences, Wageningen University, Binnenhaven5 6709PD Wageningen, The Netherlands.

van Dam, N. M. 2009. Belowground herbivory and plant defenses. Annual Review of Ecology Evolution and Systematics **40**:373-391.

van Dam, N. M. 2012. Phytochemicals as mediators of aboveground-belowground interactions in plants. Pages 190-203 *in* G. R. Iason, M. Dicke, and S. E. Hartley, editors. The Ecology of Plant Secondary Metabolites: From Genes to Global Processes. Cambridge University Press, New York, U.S.A.

van Dam, N. M., K. Hadwich, and I. T. Baldwin. 2000. Induced responses in *Nicotiana attenuata* affect behavior and growth of the specialist herbivore *Manduca sexta*. Oecologia **122**:371-379.

van Dam, N. M., J. A. Harvey, F. L. Wackers, T. M. Bezemer, W. H. van der Putten, and L. E. M. Vet. 2003a. Interactions between aboveground and belowground induced responses against phytophages. Basic and Applied Ecology **4**:63-77.

van Dam, N. M. and M. Heil. 2011. Multitrophic interactions below and above ground: en route to the next level. Journal of Ecology **99**:77-88.

van Dam, N. M., C. E. Raaijmakers, and W. H. van der Putten. 2005. Root herbivory reduces growth and survival of the shoot feeding specialist *Pieris rapae* on *Brassica nigra*. Entomologia Experimentalis Et Applicata **115**:161-170.

van Dam, N. M., E. van der Meijden, and R. Verpoorte. 1993. Induced responses in three alkaloid-containing plant-species. Oecologia **95**:425-430.

van Dam, N. M., R. Verpoorte, and E. van der Meijden. 1994. Extreme differences in pyrrolizidine alkaloid levels between leaves of *Cynoglossum officinale*. Phytochemistry **37**:1013-1016.

van Dam, N. M. and K. Vrieling. 1994. Genetic-variation in constitutive and inducible pyrrolizidine alkaloid levels in *Cynoglossum officinale* L. Oecologia **99**:374-378.

van Dam, N. M., L. Witjes, and A. Svatos. 2003b. Interactions between aboveground and belowground induction of glucosinolates in two wild *Brassica* species. New Phytologist **161**:801-810.

van der Meijden, E., N. J. de Boer, and C. A. M. van der Veen-van Wijk. 2000. Pattern of storage and regrowth in ragwort. Evolutionary Ecology **14**:439-455.

van der Meijden, E., M. van Bemmelen, R. Kooi, and B. J. Post. 1984. Nutritional quality and chemical defense in the ragwort-cinnabar moth interaction. Journal of Animal Ecology **53**:443-453.

van der Meijden, E., A. M. van Zoelen, and L. L. Soldaat. 1989. Oviposition by the cinnabar moth, *Tyria jacobaeae*, in relation to nitrogen, sugars and alkaloids of ragwort, *Senecio jacobaea*. Oikos **54**:337-344.

van der Meijden, E., M. Wijn, and H. J. Verkaar. 1988. Defense and regrowth, alternative plant strategies in the struggle against herbivores. Oikos **51**:355-363.

van der Putten, W. H., L. E. M. Vet, J. A. Harvey, and F. L. Wackers. 2001. Linking above- and belowground multitrophic interactions of plants, herbivores, pathogens, and their antagonists. Trends in Ecology & Evolution **16**:547-554.

van Leur, H., C. E. Raaijmakers, and N. M. van Dam. 2008. Reciprocal interactions between the cabbage root fly (*Delia radicum*) and two glucosinolate phenotypes of *Barbarea vulgaris*. Entomologia Experimentalis Et Applicata **128**:312-322.

van Tol, R., A. T. C. van der Sommen, M. I. C. Boff, J. van Bezooijen, M. W. Sabelis, and P. H. Smits. 2001. Plants protect their roots by alerting the enemies of grubs. Ecology Letters **4**:292-294.

van Zoelen, A. M. and E. van der Meijden. 1991. Alkaloid concentration of different developmental stages of the cinnabar moth (*Tyria jacobaeae*). Entomologia Experimentalis Et Applicata **61**:291-294.

Verhoef, H. A. 1996. The role of soil microcosms in the study of ecosystem processes. Ecology **77**:685-690.

Vierheilig, H., A. P. Coughlan, U. Wyss, and Y. Piche. 1998. Ink and vinegar, a simple staining technique for arbuscular-mycorrhizal fungi. Applied and Environmental Microbiology **64**:5004-5007.

Vivas, A., A. Voros, B. Biro, J. M. Barea, J. M. Ruiz-Lozano, and R. Azcon. 2003. Beneficial effects of indigenous Cd-tolerant and Cd-sensitive *Glomus mosseae* associated with a Cd-adapted strain of Brevibacillus sp in improving plant tolerance to Cd contamination. Applied Soil Ecology **24**:177-186.

Vos, M., S. M. Berrocal, F. Karamaouna, L. Hemerik, and L. E. M. Vet. 2001. Plant-mediated indirect effects and the persistence of parasitoid-herbivore communities. Ecology Letters **4**:38-45.

Vovlas, N. and A. Troccoli. 1990. Histopathology of broad bean roots infected by the lesion nematode *Pratylenchus penetrans*. Nematologia Mediterranea **18**:239-242.

Vrieling, K. and N. J. de Boer. 1999. Host-plant choice and larval growth in the cinnabar moth: do pyrrolizidine alkaloids play a role? Entomologia Experimentalis Et Applicata **91**:251-257.

Vrieling, K. and S. Derridj. 2003. Pyrrolizidine alkaloids in and on the leaf surface of *Senecio jacobaea* L. Phytochemistry **64**:1223-1228.

Vrieling, K., H. Devos, and C. A. M. van Wijk. 1993. Genetic-analysis of the concentrations of pyrrolizidine alkaloids in *Senecio jacobaea*. Phytochemistry **32**:1141-1144.

Vrieling, K., W. Smit, and E. van der Meijden. 1991. Tritrophic Interactions between aphids (*Aphis jacobaeae* Schrank), ant species, *Tyria jacobaeae* L, and *Senecio jacobaea* L lead to maintenance of genetic-variation in pyrrolizidine alkaloid concentration. Oecologia **86**:177-182.

Vrieling, K. and C. A. M. van Wijk. 1994. Cost assessment of the production of pyrrolizidine alkaloids in Ragwort (*Senecio-jacobaea* L.). Oecologia **97**:541-546.

Wackers, F. L. and T. M. Bezemer. 2003. Root herbivory induces an above-ground indirect defence. Ecology Letters **6**:9-12.

Walling, L. L. 2000. The myriad plant responses to herbivores. Journal of Plant Growth Regulation **19**:195-216.

Walter, M. H., D. S. Floss, and D. Strack. 2010. Apocarotenoids: hormones, mycorrhizal metabolites and aroma volatiles. Planta **232**:1-17.

Walter, M. H. and D. Strack. 2011. Carotenoids and their cleavage products: Biosynthesis and functions. Natural Product Reports **28**:663-692.

Wardle, D. A. 1987. The ecology of ragwort (*Senecio jacobaea* L) - a review. New Zealand Journal of Ecology **10**:67-76.

Wardle, D. A. 2006. The influence of biotic interactions on soil biodiversity. Ecology Letters **9**:870-886.

Wardle, D. A., R. D. Bardgett, J. N. Klironomos, H. Setala, W. H. van der Putten, and D. H. Wall. 2004. Ecological linkages between aboveground and belowground biota. Science **304**:1629-1633.

Wardle, D. A., W. M. Williamson, G. W. Yeates, and K. I. Bonner. 2005. Trickle-down effects of aboveground trophic cascades on the soil food web. Oikos **111**:348-358.

Wenke, K., M. Kai, and B. Piechulla. 2010. Belowground volatiles facilitate interactions between plant roots and soil organisms. Planta **231**:499-506.

Widarto, H. T., E. Van der Meijden, A. W. M. Lefeber, C. Erkelens, H. K. Kim, Y. H. Choi, and R. Verpoorte. 2006. Metabolomic differentiation of *Brassica rapa* following herbivory by different insect instars using two-dimensional nuclear magnetic resonance spectroscopy. Journal of Chemical Ecology **32**:2417-2428.

Wiklund, S., E. Johansson, L. Sjostrom, E. J. Mellerowicz, U. Edlund, J. P. Shockcor, J. Gottfries, T. Moritz, and J. Trygg. 2008. Visualization of GC/TOF-MS-based metabolomics data for identification of biochemically interesting compounds using OPLS class models. Analytical Chemistry **80**:115-122.

Wilcox, A. and M. J. Crawley. 1988. The effects of host plant defoliation and fertilizer application on larval growth and oviposition behavior in cinnabar moth. Oecologia **76**:283-287.

Williams, K. J., S. P. Taylor, P. Bogacki, M. Pallotta, H. S. Bariana, and H. Wallwork. 2002. Mapping of the root lesion nematode (*Pratylenchus neglectus*) resistance gene Rlnn1 in wheat. Theoretical and Applied Genetics **104**:874-879.

Williamson, V. M. and C. A. Gleason. 2003. Plant-nematode interactions. Current Opinion in Plant Biology **6**:327-333.

Williamson, V. M. and A. Kumar. 2006. Nematode resistance in plants: the battle underground. Trends in Genetics **22**:396-403.

Windig, J. J. 1991. Life-cycle and abundance of *Longitarsus jacobaeae* (Col, Chrysomelidae), biocontrol agent of *Senecio jacobaea*. Entomophaga **36**:605-618.

Windig, J. J. 1993. Intensity of *Longitarsus jacobaeae* herbivory and mortality of *Senecio jacobaea*. Journal of Applied Ecology **30**:179-186.

Witte, L., L. Ernst, H. Adam, and T. Hartmann. 1992. Chemotypes of two pyrrolizidine alkaloid-containing *Senecio* species. Phytochemistry **31**:559-565.

Wittstock, U. and J. Gershenzon. 2002. Constitutive plant toxins and their role in defense against herbivores and pathogens. Current Opinion in Plant Biology **5**:300-307.

World Health Organisation. 1988. Environmental Health Criteria 80: Pyrrolizidine Alkaloids. Lightning Source UK Ltd., Milton Keynes.

Wu, J. Q. and I. T. Baldwin. 2010. New insights into plant responses to the attack from insect herbivores. Annual Review of Genetics **44**:1-24.

Wuilloud, J. C. A., S. R. Gratz, B. M. Gamble, and K. A. Wolnik. 2004. Simultaneous analysis of hepatotoxic pyrrolizidine alkaloids and N-oxides in comfrey root by LC-ion trap mass spectrometry. Analyst **129**:150-156.

Wurst, S. and W. H. van der Putten. 2007. Root herbivore identity matters in plant-mediated interactions between root and shoot herbivores. Basic and Applied Ecology **8**:491-499.

Wuyts, N., R. Swennen, and D. De Waele. 2006. Effects of plant phenylpropanoid pathway products and selected terpenoids and alkaloids on the behaviour of the plant-parasitic nematodes *Radopholus similis*, *Pratylenchus penetrans* and *Meloidogyne incognita*. Nematology **8**:89-101.

Yamawo, A., N. Suzuki, J. Tagawa, and Y. Hada. 2012. Leaf ageing promotes the shift in defence tactics in *Mallotus japonicus* from direct to indirect defence. Journal of Ecology **100**:802-809.

Young, T. P., M. L. Stanton, and C. E. Christian. 2003. Effects of natural and simulated herbivory on spine lengths of *Acacia* drepanolobium in Kenya. Oikos **101**:171-179.

Yu, L. J., Y. Xu, H. T. Feng, and S. F. Y. Li. 2005. Separation and determination of toxic pyrrolizidine alkaloids in traditional Chinese herbal medicines by micellar electrokinetic chromatography with organic modifier. Electrophoresis **26**:3397-3404.

Zangerl, A. R. 1986. Leaf value and optimal defense in *Pastinaca-sativa* L. (Umbelliferae). American Midland Naturalist **116**:432-436.

Zangerl, A. R. and C. E. Rutledge. 1996. The probability of attack and patterns of constitutive and induced defense: A test of optimal defense theory. American Naturalist **147**:599-608.

Zinov'eva, S. V., N. I. Vasyukova, and O. L. Ozeretskovskaya. 2004. Biochemical aspects of plant interactions with phytoparasitic nematodes: A review. Applied Biochemistry and Microbiology **40**:111-119.

Zlatanov, M. D., M. J. Angelova-Romova, G. A. Antova, R. D. Dimitrova, S. M. Momchilova, and B. M. Nikolova-Damyanova. 2009. Variations in fatty acids, phospholipids and sterols during the seed development of a high oleic sunflower variety. Journal of the American Oil Chemists Society **86**:867-875.

Zunke, U. 1990. Observations on the invasion and endoparasitic behaviour of the root lesion nematode *Pratylenchus penetrans*. Journal of Nematology **22**:309-320.

Zvereva, E. L. and M. V. Kozlov. 2012. Sources of variation in plant responses to belowground insect herbivory: a meta-analysis. Oecologia **169**:441-452.

Appendix one

This is a placeholder for the following co-authored publication. The full book chapter cannot be displayed here due to copyright restrictions.

Hartley, S. E., Eschen, R., Horwood, J. M., Robinson, L. A. & Hill, E. M. 2012. Plant secondary metabolites and the interactions between plants and other organisms: the potential of a metabolomic approach. *In:* IASON, G. R., DICKE, M. & HARTLEY, S. E. (eds.) *The Ecology of Plant Secondary Metabolites: From Genes to Global Processes.* New York, U.S.A.: Cambridge University Press.